HERE COMES THE SUN

Improving local use of electricity generated by rooftop photovoltaic systems

HERE COMES THE SUN
Improving local use of electricity generated by rooftop photovoltaic systems

Geert Litjens
Copernicus Institute of Sustainable Development, Utrecht University

This research was carried out as part of the research programme “Transitioning to a More Sustainable Energy System” (Grant No. 022.004.023), which was funded by the Netherlands Organisation for Scientific Research (NWO).

ISBN: 978-90-8672-087-3
Print: Ridderprint BV
Cover design: Sander Smits

HERE COMES THE SUN

Improving local use of electricity generated by rooftop photovoltaic systems

DAAR IS DE ZON

Verbetering van lokaal gebruik van elektriciteit opgewekt uit dakgebonden fotovoltaïsche systemen

(met een samenvatting in het Nederlands)

Proefschrift

ter verkrijging van de graad van doctor aan de Universiteit Utrecht op gezag van de rector magnificus, prof.dr. H.R.B.M. Kummeling, ingevolge het besluit van het college voor promoties in het openbaar te verdedigen op vrijdag 14 december 2018 des middags te 12.45 uur

door

Gerhard Bernardus Marinus Antonius Litjens

geboren op 15 juni 1987 te Druten

Promotoren: Prof. dr. E. Worrell
Prof. dr. W.G.J.H.M. van Sark

To our future

Voor onze toekomst

Summary

Photovoltaic (PV) systems installed on buildings will be playing a major role in providing renewable energy and support the transition to a sustainable energy system. Rooftop PV systems will be mainly connected to the low voltage grid. Typically, these grids are not designed to accommodate large scale decentralized PV electricity production. This calls for research to effectively and efficiently integrate electricity generated by rooftop PV systems in our energy system. One of the possibilities for more integration of PV in the energy system is increasing the amount of directly consumed energy and consequently reducing feed-in PV power peaks to the electricity grid. Chapter 1 describes the PV power integration issues and possible solutions in more detail and presents the research aims of this thesis.

The main objective of this thesis is the assessment of technical, economic and environmental benefits that can be obtained from the local use of energy generated by rooftop PV systems. The technical benefits include enhancing PV self-consumption and reducing PV feed-in peak power to the grid. This PV self-consumption is affected by the PV system design, electricity consumption patterns and energy technology used in the building, for example by using heat pumps. This thesis focussed on PV systems installed on residential and commercial buildings located in the Netherlands.

Chapter 2 assessed the impact of the orientation of PV modules on the self-consumption and self-sufficiency, taking into account electricity consumption and PV generation. Residential systems showed the highest self-consumption when oriented to 212° module azimuth (about wind direction southwest) and 26° tilt. Commercial systems should be positioned to 188° azimuth with 17° tilt to enhance self-consumption. However, the added self-consumption is limited to a few percent compared to a south oriented system with a module tilt of 37°. Also, optimal orientations for economic revenues are presented for 9 scenarios using historical Dutch and German power market prices.

Energy from PV systems can be temporary stored using battery energy storage systems. These systems can reduce the feed-in PV peak power while enhancing self-consumption. Forecasting methods of energy production and energy consumption of buildings are required to store PV power optimally. Several forecasting methods combined with a battery control algorithm were developed, assessed and presented in chapter 3. Predictive control strategies are capable to improve self-consumption, as well as reduce potential curtailment losses. It was

found that residential electricity consumption should be forecasted using average electricity consumption of the previous seven days. Commercial electricity consumption can be forecasted by using the historical demand of the previous weekday. PV production forecasts with modelled clear-sky radiation data can be best used as input for battery control strategies to reduce the PV peak power to the grid.

Using battery energy storage systems for self-consumption enhancement is currently not economically feasible. To improve the economics, battery systems should be used for multiple applications. Chapter 4 assessed the combination of using battery storage for self-consumption enhancement and provision of frequency restoration reserves. These reserves are required to maintain the imbalance between electricity production and consumption. As a result of combing these applications, revenues of storage systems would increase while self-consumption increased with 26%. Prioritizing provision of frequency restoration reserves over self-consumption enhancement resulted in even higher revenues, but resulted in a minor increase of 3% in self-consumption.

Ground source heat pumps (GSHP) are one of the options to replace gas-based heating systems and potentially reduce greenhouse gas emissions. Chapter 5 assessed the combination of PV, battery storage and GSHP systems. The technological, economic and environmental performance of this combination was evaluated for 16 dwellings. PV produced energy could provide around 19% of the GSHP demand. Battery energy storage systems increased this to 29%. Moreover, battery systems could reduce the peak demand of dwellings by 45%, which reduces the impact of GSHP on the low voltage grid. Avoided life cycle GHG emissions for dwellings with a ground source heat pump were calculated to be 42 tCO_2-eq on average and combined with a PV system 73 tCO_2-eq on average. Despite this large emission reduction, investment in GSHP systems is not attractive for many dwellings. Higher natural gas tariffs, carbon taxing or larger investment subsidies are required to increase the economic feasibility.

Self-consumption and GHG emission reduction potential on a neighbourhood scale were assessed in chapter 6. A model framework was developed to evaluate these using four PV rooftop utilization scenarios, battery storage systems and with future energy demand of light-duty electric vehicle demand. Spatial mapping was used to visualize the difference between 88 neighbourhoods in the city of Utrecht, the Netherlands. Self-consumption was between 34% and 100% for the neighbourhoods and is mainly influenced by the rooftop space availability. Electric vehicles could increase this with 12% and battery storage with 25%. Avoided life cycle GHG emissions were on average 17 tCO_2-eq per dwelling. The large variation in results between neighbourhoods indicates that area dependent

investments and supporting policies could improve PV power integration in cities.

Results from chapter 2 to chapter 6 were combined and compared using similar metrics in chapter 7. Furthermore, the impact of PV orientation on the self-consumption, feed-in power and economic payback times was assessed in more detail. The overarching evaluation of results provided new insights regarding PV power integration. This has resulted in the key conclusions and recommendations of this thesis, mentioned in chapter 8.

The following key conclusions were drawn. About 33% of the PV generated energy of residential systems can be directly consumed by dwellings. This is 44% for commercial buildings. Stationary battery energy storage can charge surplus PV electricity and therefore increase self-consumption. A 1 kWh storage capacity per MWh of annual electricity consumption increases self-consumption by 23% for residential buildings and by 22% for commercial buildings. Only 4% of PV electricity during the systems lifetime is lost when a feed-in limit of 0.5 kW per kWp is imposed. This can be reduced to 0.2% using a 1 kWh storage capacity for each MWh of annual demand. Discounted payback times for PV systems are around 10 years for residential systems and 12 years for commercial systems. Dwellings with a PV capacity of 1 kWp for each MWh of annual demand contribute with about 17 tCO_2-eq to avoided life cycle greenhouse gas emissions.

Recommendations for policy makers to support the growth of PV systems on buildings were given for both short and medium term perspectives. Policies for the next five years should financially support PV systems larger than a 1 kWp per MWh annual electricity demand. When additional PV capacity is limited by the grid capacity, a feed-in limitation of 0.5 kW per kWp of PV is advisable to implement. Beyond 5 years, policies should provide rules and guidelines to enable new value streams from grid services provided by third parties. Also, a dynamic tax tariff based on marginal emissions factors could enable emission reduction by battery energy storage systems. Future research should focus on how storage and electrification can enable more variable renewable energy in our energy system. Therefore, methods to define dynamic electricity tariff structures and to assess the environmental impact of energy storage must be further developed.

Samenvatting

Fotovoltaïsche (PV) systemen op gebouwen zullen een steeds groter deel van de duurzame energie gaan opwekken in de toekomst. Deze dakgebonden PV-systemen zijn nodig om het huidige energiesysteem te transformeren naar een duurzaam systeem. De PV-systemen worden voornamelijk aangesloten op de laagspanningsnetten. De meeste van deze netten zijn niet ontworpen om grootschalige decentrale elektriciteit van PV-systemen te verwerken. Daarom is onderzoek om elektriciteit van dakgebonden PV-systemen effectief en efficiënt te integreren in ons energiesysteem noodzakelijk. Eén van de mogelijkheden om de integratie van PV-energie te bevorderen is om het lokale gebruik van deze energie te verhogen. Hiermee kan ook het piekvermogen dat wordt ingevoed in het elektriciteitsnet worden verlaagd. Hoofdstuk 1 beschrijft de integratieproblemen en mogelijke oplossingen voor elektriciteit uit dakgebonden PV-systemen. Ook worden de onderzoekdoelstellingen van dit proefschrift hier gepresenteerd.

Het hoofddoel van dit proefschrift betreft onderzoek naar de technische, economische en milieu voordelen die behaald kunnen worden door het lokale gebruik van energie uit dakgebonden PV-systemen. Onder technische mogelijkheden vallen het verhogen van het eigen verbruik van energie uit PV-systemen en het verlagen van het PV-piekvermogen dat wordt ingevoed op het elektriciteitsnet. Het aandeel eigenverbruik wordt beïnvloed door het ontwerp van het PV-systeem en het energieverbruikspatroon van het gebouw. Ook kan een andere energietechnologie gebruikt worden om het eigen gebruik te veranderen, bijvoorbeeld het gebruik van een warmtepomp. Dit proefschrift focust op PV-systemen geïnstalleerd op residentiële en commerciële gebouwen in Nederland.

In hoofdstuk 2 is de invloed van de oriëntatie van PV-modules op het eigenverbruik en de zelfvoorzieningsgraad onderzocht. PV-modules op residentiële gebouwen halen het hoogste eigenverbruik wanneer ze geplaatst worden onder een oriëntatie van 212° azimut (windrichting zuidwesten) en een hellingshoek van 26°. PV-modules op commerciële gebouwen realiseren het hoogste eigenverbruik met een azimut van 188° en een hellingshoek van 17°. Het toegevoegde eigenverbruik door het gebruik van deze oriëntaties is echter beperkt tot een paar procent vergeleken met een zuidelijk georiënteerd systeem met een hellingshoek van 37°. Ook zijn er optimale oriëntaties vanuit economisch oogpunt bepaald voor 9 scenario's. Deze scenario's gebruiken historische groothandelsprijzen van de Nederlandse en de Duitse elektriciteitsmarkt.

Elektriciteit uit PV-systemen kan tijdelijk worden opgeslagen in batterijsystemen, en daardoor kan het PV-piekvermogen dat wordt ingevoed op het elektriciteitsnet verlagen. Tevens zorgen batterijen er voor dat de bijdrage van eigenverbruik wordt verhoogd. Voorspellingsmethodes die PV-energie productie en energieconsumptie van gebouwen voorspellen zijn nodig om zodoende een overschot van elektriciteit optimaal te kunnen opslaan in batterijen. In hoofdstuk 3 zijn voorspellingsmethodes met batterijcontrolestrategieën ontwikkeld en geanalyseerd. Deze methodes zijn in staat om de PV-piekproductie op te slaan en daardoor eventuele afregelverliezen te reduceren. Afregelverliezen ontstaan door het terugregelen van het PV-vermogen. Het elektriciteitsverbruik van woningen kan het beste worden voorspeld door het gemiddelde verbruik van de afgelopen zeven dagen te nemen. Voor het voorspellen van commerciële elektriciteitsverbruik kan men het beste gebruik maken van de historische energievraag van de vorige weekdag. Voorspellingen voor elektriciteit uit PV-systemen zijn nodig om het PV-piekvermogen op te slaan in batterijen zodat een lager piekvermogen wordt gevoed aan het elektriciteitsnet. Hiervoor kan als beste een voorspelling op basis van de gemodelleerde zonne-instraling bij een onbewolkte hemel worden gebruikt.

Momenteel is het economisch niet aantrekkelijk om batterijen te gebruiken voor het verhogen van eigenverbruik. Verbetering is mogelijk als batterijsystemen voor diverse toepassingen tegelijk worden gebruikt. In hoofdstuk 4 is het gebruik van een batterij voor het verhogen van eigenverbruik onderzocht, in combinatie met het leveren van regelvermogen aan het elektriciteitsnetwerk. Dit regelvermogen is nodig om een onbalans tussen vraag en aanbod te compenseren. Door het combineren van deze toepassingen kunnen de inkomsten voor batterijen verhoogd worden, terwijl de bijdrage van eigenverbruik stijgt met 26%. Wanneer een batterijcontrolestrategie prioriteit geeft aan het beschikbaar stellen van de opslagcapaciteit voor regelvermogen zullen deze inkomsten meer groeien. Deze strategie zal wel ten koste gaan van het aandeel eigenverbruik, dat nog maar zal toenemen met 3%.

Grondgebonden warmtepompen zijn één van de opties om verwarmingssystemen op aardgas te vervangen en de uitstoot van broeikasgassen te verlagen. In hoofdstuk 5 is de combinatie van PV-systemen met batterijen en grondgebonden warmtepompen onderzocht. De technologische, economische en milieu-impact van deze combinatie is geëvalueerd voor 16 woningen. 19% van de elektriciteitsvraag van een warmtepomp kan worden voorzien door het directe gebruik van PV-energie. Batterijopslagsystemen kunnen dit aandeel eigenverbruik verhogen tot 29%. Ook kunnen deze batterijen de piekvraag van woningen met 45% verlagen. Dit zorgt voor een lagere impact van grondgebonden warmtepompen op

het laagspanningsnet. Woningen met een grondgebonden warmtepomp zorgen voor een gemiddelde reducering in broeikasgasemissies van 42 tCO_2-eq gedurende de levenscyclus van de warmtepomp. Als een PV-systeem wordt toegevoegd aan de woning loopt dit op tot een gemiddelde reductie van 73 tCO_2-eq. Ondanks deze hoge vermeden emissies is het voor veel woningen nu niet economisch aantrekkelijk om te investeren in grondgebonden warmtepompen; Om dit wel aantrekkelijk te maken zijn hogere aardgastarieven, CO_2 belastingen of investeringssubsidies nodig.

In hoofdstuk 6 is het eigenverbruik van PV-systemen en het reductiepotentieel van broeikasgasemissies onderzocht voor woningen en op buurtniveau. Er is een model ontwikkeld om het PV-potentieel op daken te bepalen voor 4 dak benuttingsscenario's. Ook de invloed van batterijopslagsystemen en de toekomstige energievraag voor elektrische auto's is onderzocht. Middels grafische kaartweergaves zijn de resultaten inzichtelijk gemaakt voor 88 buurten in de stad Utrecht. Het eigenverbruik per buurt ligt tussen de 34% en 100%, en is voornamelijk afhankelijk van het beschikbare dakoppervlak. Elektrische auto's kunnen het aandeel eigenverbruik verhogen met 12% en batterijen met 25%. De vermeden broeikasgasemissies over de levenscyclus zijn gemiddeld 17 tCO_2-eq per woning. De resultaten laten grote variatie zien tussen de verschillende buurten. Dit geeft aan dat als investeringen en ondersteunend beleid gebiedsafhankelijk zijn, dit de integratie van opgewekte energie uit PV-systemen in steden kan verbeteren.

De resultaten van hoofdstuk 2 tot en met 6 zijn samengevoegd en vergeleken in hoofstuk 7. Daarnaast is de invloed van de oriëntatie van PV-systemen op het eigenverbruik, het PV-piekvermogen naar het elektriciteitsnet en de economische terugverdientijden geanalyseerd. Deze evaluatie van de resultaten hebben nieuwe inzichten opgeleverd betreffende de integratie van PV-energie. Dit heeft geleid tot de belangrijkste conclusies en aanbevelingen van dit proefschrift, zoals beschreven in hoofdstuk 8.

De belangrijkste conclusies zijn alsvolgt: Ongeveer 33% van de energie uit PV-systemen op daken van residentiële gebouwen kan direct worden gebruikt. Voor commerciële gebouwen is dit zelfs 44%. Overtollige PV-energie kan worden opgeslagen in batterijopslagsystemen om het eigenverbruik te verhogen. Zo kan een opslagcapaciteit van 1 kWh per MWh jaarlijks elektriciteitsverbruik het eigenverbruik verhogen met 23% voor residentiële en met 22% voor commerciële gebouwen. Als teruglevering kan worden beperkt tot een vermogen van 0,5 kW per kWp geïnstalleerd PV-vermogen, dan gaat slechts 4% van de totaal opgewekte PV-energie verloren. Dit verlies kan worden verlaagd tot 0,2% met behulp van een batterijopslagcapaciteit van 1 kWh per MWh jaarlijks elektriciteitsverbruik.

De verdisconteerde terugverdientijd voor PV-systemen is rond de 10 jaar voor residentiële systemen en rond de 12 jaar voor commerciële systemen. Woningen met een PV-systeemcapaciteit van 1 kWp per MWh jaarlijks elektriciteitsverbruik zorgen voor gemiddeld 17 tCO_2-eq vermeden broeikasgasemissies gedurende de levenscyclus.

Om de groei van PV-systemen op gebouwen door te zetten zijn er de volgende aanbevelingen voor beleidsmakers, op zowel korte als lange termijn voorgesteld: Voor de komende vijf jaar is het belangrijk dat PV-systemen groter dan 1 kWp per MWh jaarlijks elektriciteitsverbruik worden ondersteund met extra financiële steun. Als de PV-capaciteit wordt beperkt door de netcapaciteit, dan is het zeer raadzaam om een beperking van 0,5 kW per kWp PV-capaciteit op het terugleververmogen in te voeren. Beleid voor 5 jaar vanaf nu dient regels en richtlijnen te bevatten om vergoeding mogelijk te maken voor netdiensten en services uitgevoerd door derden. Een dynamisch belastingtarief op basis van de marginale emissiefactoren kan zorgen dat energieopslagsystemen meer emissies reduceren. Daarvoor zullen nieuwe methodes nodig zijn om dynamische elektriciteitstariefstructuren vast te stellenen die milieu-impact van energieopslag te beoordelen.

Contents

Summary **vii**

Samenvatting **xi**

Nomenclature **xvii**

1 Introduction **1**
- 1.1 Motivation . . . 2
- 1.2 Integrating PV power in the electricity grid . . . 4
- 1.3 The need for electrification and energy storage . . . 7
- 1.4 Thesis objectives and outline . . . 8
- 1.5 Thesis outline . . . 10

2 Influence of PV orientation **13**
- 2.1 Introduction . . . 15
- 2.2 Methods . . . 17
- 2.3 Optimal orientation without self-consumption . . . 23
- 2.4 Maximize self-consumption . . . 25
- 2.5 Minimize curtailed energy under feed-in limitations . . . 27
- 2.6 Maximize revenue . . . 29
- 2.7 Temporal influences . . . 35
- 2.8 Discussion . . . 39
- 2.9 Conclusion . . . 41

3 Forecasting methods for PV-battery systems **43**
- 3.1 Introduction . . . 45
- 3.2 Methods . . . 48
- 3.3 Results . . . 59
- 3.4 Sensitivity analysis . . . 65
- 3.5 Discussion . . . 76
- 3.6 Conclusion . . . 79

4 FRR provision by PV-battery systems **81**
- 4.1 Introduction . . . 83
- 4.2 Methods . . . 85
- 4.3 Technical assessment . . . 97
- 4.4 Economic assessment . . . 102
- 4.5 Sensitivity analysis . . . 106
- 4.6 Discussion . . . 113
- 4.7 Conclusion . . . 116

5 Combing GSHP with PV-battery systems **117**
5.1 Introduction . . . 119
5.2 Method . . . 122
5.3 Results . . . 131
5.4 Sensitivity analysis . . . 137
5.5 Discussion . . . 139
5.6 Conclusion . . . 142
Appendices . . . 143

6 Spatio-temporal model for PV integration **161**
6.1 Introduction . . . 163
6.2 Methods . . . 165
6.3 Results . . . 175
6.4 Sensitivity analysis . . . 184
6.5 Discussion . . . 189
6.6 Conclusion . . . 191

7 Synthesis of the main findings **193**
7.1 Synthesis framework . . . 194
7.2 On improving PV self-consumption and self-sufficiency . . . 194
7.3 On reducing feed-in peak power . . . 200
7.4 On realizing economic benefits . . . 205
7.5 On realizing GHG emission reductions . . . 214

8 Conclusions and recommendations **217**
8.1 Research context . . . 218
8.2 Key conclusions . . . 218
8.3 Recommendations for policy makers . . . 220
8.4 Recommendations for further research . . . 222

9 Conclusies en aanbevelingen **225**
9.1 Onderzoek context . . . 226
9.2 Belangrijkste conclusies . . . 226
9.3 Aanbevelingen voor beleidsmakers . . . 228
9.4 Aanbevelingen voor verder onderzoek . . . 231

Bibliography **233**

Acknowledgement / Dankwoord **249**

About the Author **253**

Nomenclature

Abbreviations

AC	alternating current
AR	added revenue
ASC	added self-consumption
BAG	basisregistratie adressen en gebouwen
BESS	battery energy storage systems
BOS	balance of system
CAE	cumulative avoided emissions
CBS	centraal bureau voor de statistiek (Statistics Netherlands)
CCF	cumulative cash flow
CEC	California Energy Commission
CF	cash flow
CGB	condensing gas boiler
CLR	curtailment loss ratio
CO_2	carbon dioxide
CO_2-eq	carbon dioxide equivalent
COP	coefficient of performances
DC	direct current
DEM	digital elevation model
DHW	domestic hot water
DOD	depth of discharge
DPBP	discounted payback period
DSO	distribution system operator
EFE	emission factor electricity
EPAR	export peak to average ratio
EPC	engineering procurement construction
EV	electric vehicle
FCE	full cycle equivalents
FCR	frequency containment reserves
FIL	feed-in limit
FRR	frequency restoration reserves
FRRSR	frequency restoration reserve storage ratio
GHG	greenhouse gas
GHGPBP	greenhouse payback period
GIS	geographic information system
GSHP	ground source heat pump

HHV	higher heating value
IPAR	import peak to average ratio
IRR	internal rate of return
MAPE	mean absolute percentage error
NG	natural gas
nMBE	normalized mean bias error
NPV	net present value
nRMSE	normalized root mean square error
O&M	operation and maintenance
PBP	payback period
PC6	postal code 6
PI	profitability index
POA	plane of array
PR	performance ratio
PSCN	prioritize self-consumption over providing negative FRR only
PV	photovoltaics
RCE	reduced curtailed energy
RER	relative electricity revenue
SCCR	self-consumption contribution rate
SCR	self-consumption ratio
SOC	state of charge
SPR	sales to purchase ratio
SRR	storage revenue ratio
SSR	self-sufficiency ratio
SUR	storage use rate
TF	temporal fraction
TSO	transmission system operator
VRE	variable renewable energy

Battery storage dispatch strategies and forecasting methods

D-PD	demand pattern using previous day
D-PW	demand pattern using average of previous week
D-PWD	demand pattern using previous weekday
FRRO	FRR provision only
PC	predictive control
PFRR	prioritize FRR provision over self-consumption
PFRRN	prioritize providing only negative FRR over self-consumption
PSC	prioritize self-consumption over FRR provision
PV-CS	PV pattern using clear-sky radiation
PV-PD	PV pattern using previous day

PV-PW	PV pattern using average of previous week
PV-WX	PV pattern using weather prediction data
RC	real-time control
SCO	self-consumption only

Symbols & notations

ΔP	difference between PV production and electricity demand	[W]
Δt	time step of 5 min	
$\Delta E_{\text{B pot}}$	battery charge or discharge energy potential	[Wh]
ΔE_{B}	battery charge or discharge energy	[Wh]
π_{cons}	consumption tariff	[€/Wh]
$\pi_{\text{feed-in}}$	feed-in tariff	[€/Wh]
π_{neg}	price for negative FRR provision	[€/Wh]
π_{ng}	natural gas price	[€/GJ]
π_{pos}	price for positive FRR provision	[€/Wh]
AR_{TF}	temporal fraction of added revenue	[%]
ASC_{TF}	temporal fraction of the added self-consumption	[%]
$C_{\text{reduction}}$	cost reduction of actual system to reference system	[%]
CF_{Elec}	cash flow from electricity	[€]
CF_{FRR}	cash flow from frequency restoration reserves provision	[€]
CF_{NG}	cash flow from natural gas	[€]
$CF_{\text{PV,export}}$	cash flow from exported PV electricity	[€]
CF_{SC}	cash flow from self-consumption	[€]
CF_{SE}	cash flow from sold electricity to the grid	[€]
D_{BESS}	battery storage capacity degradation	[%]
$E_{\text{B, t}}$	battery state of charge	[Wh]
$E_{\text{B cur}}$	current battery state of charge	[Wh]
$E_{\text{B max}}$	maximum battery state of charge	[Wh]
$E_{\text{B min}}$	minimum battery state of charge	[Wh]
$E_{\text{B REL}}$	battery SOC reserved to charge PV peak	[Wh]
$E_{\text{B res pot}}$	potential battery storage capacity reserved	[Wh]
$E_{\text{B res}}$	storage state of charge reserved	[Wh]
$E_{\text{B RIL}}$	battery SOC reserved to discharge peak demand	[Wh]
$E_{\text{buy PV-B}}$	electricity bought with a PV-battery system	[Wh]
$E_{\text{buy PV}}$	electricity bought with a PV system	[Wh]
E_{CE}	curtailed energy	[Wh]
E_{demand}	electricity demand	[Wh]
$E_{\text{FIL loss}}$	lost PV energy due to feed-in limitation	[Wh]
E_{Lim}	energy fed back to the grid without a feed-in limitation	[Wh]
$E_{\text{No lim}}$	energy fed back to the grid with a feed-in limitation	[Wh]

E_{PV}	PV produced energy	[Wh]
E_{RIE}	reduced imported energy	[Wh]
E_{SC}	self-consumed energy	[Wh]
$E_{\text{sell PV-B}}$	electricity sold with a PV-battery system	[Wh]
$E_{\text{sell PV}}$	electricity sold with a PV system	[Wh]
E_{SE}	sold energy	[Wh]
GHG_{actual}	life cycle GHG emissions from actual system	[CO_2-eq]
$GHG_{\text{avoided,ex}}$	avoided emis. excluding emissions of manufacturing	[CO_2-eq]
GHG_{avoided}	avoided life cycle GHG emissions	[CO_2-eq]
GHG_{dwelling}	life cycle GHG emissions from a dwelling perspective	[CO_2-eq]
$GHG_{\text{E export}}$	emissions associated with exporting energy	[CO_2-eq]
$GHG_{\text{E import}}$	emissions associated with importing energy	[CO_2-eq]
$GHG_{\text{mfg BESS}}$	emissions from manufacturing a battery storage system	[CO_2-eq]
$GHG_{\text{mfg HS}}$	emissions from manufacturing a heating system	[CO_2-eq]
$GHG_{\text{mfg PV}}$	emissions from manufacturing a PV system	[CO_2-eq]
$GHG_{\text{mfg actual}}$	emissions from manufacturing the actual system	[CO_2-eq]
$GHG_{\text{mfg ref}}$	emissions from manufacturing the reference system	[CO_2-eq]
GHG_{mfg}	emissions from manufacturing the total system	[CO_2-eq]
$GHG_{\text{neighb.}}$	life cycle GHG emis. from a neighbourhood perspective	[CO_2-eq]
$GHG_{\text{reduction}}$	reduction of life cycle GHG emissions	[%]
$GHG_{\text{reference}}$	life cycle GHG emissions from the reference system	[CO_2-eq]
GHG_{system}	life cycle GHG emissions from an elec. sys. perspective	[CO_2-eq]
$I_{\text{B BOS}}$	battery balance of system cost	[€]
$I_{\text{B EPC}}$	battery engineering procurement construction cost	[€]
$I_{\text{B store}}$	battery energy storage system cost	[€]
I_{BESS}	battery energy storage system investment cost	[€]
I_{HS}	heating system investment cost	[€]
I_{PV}	PV system investment cost	[€]
I_{total}	total system investment cost	[€]
NPV_{actual}	net present value of the actual system	[€]
$NPV_{\text{reference}}$	net present value of the reference system	[€]
$O\&M_{\text{BESS}}$	operation and maintenance cost battery system	[€]
$O\&M_{\text{HS}}$	operation and maintenance cost heating system	[€]
$O\&M_{\text{PV}}$	operation and maintenance cost PV system	[€]
P_{actual}	actual power of PV yield or demand	[W]
$P_{\text{B charge}}$	power charged to the battery	[W]
$P_{\text{B discharge}}$	power discharged from the battery	[W]
$P_{\text{B from PV}}$	PV power used to charge the BESS	[W]
$P_{\text{B inv max}}$	battery inverter rating	[W]

$P_{\text{B inv}}$	battery inverter load	[W]
$P_{\text{B pot}}$	battery load potential	[W]
$P_{\text{B pre}}$	pre-charged or pre-discharged power	[W]
$P_{\text{B res}}$	battery charge capacity reserved	[W]
P_{B}	battery load	[W]
$P_{\text{D FC}}$	forecasted electricity demand	[W]
$P_{\text{demand GSHP}}$	power demand from GSHP	[W]
P_{demand}	power demand	[W]
$P_{\text{direct SC}}$	direct self-consumed PV power	[W]
P_{EL}	power export limit	[W]
P_{FC}	forecasted power of PV yield or demand	[W]
$P_{\text{FIL FC}}$	forecasted feed-in power exceeding the feed-in limited	[W]
$P_{\text{FIL loss}}$	power loss due to the feed-in limit	[W]
P_{FIL}	power feed-in limit	[W]
P_{G}	load from or to the grid	[W]
P_{IL}	power import limit	[W]
P_{Lim}	power exported under a feed-in limit	[W]
P_{neg}	power provided for negative FRR	[W]
P_{pos}	power provided for positive FRR	[W]
$P_{\text{PV FC}}$	forecasted PV production	[W]
$P_{\text{PV neighb.}}$	used PV power from an neighbourhood perspective	[W]
$P_{\text{PV system}}$	used PV power from an elec. sys. perspective	[W]
P_{PV}	PV produced power	[W]
P_{R}	residual power flow	[W]
R_{BESS}	battery energy storage system revenues	[€]
R_{SC}	revenue from self-consumption	[€]
R_{SE}	revenue from sold electricity	[€]
R_{tot}	total revenue of a PV system	[€]
RCE_{TF}	temporal fraction of reduced curtailed energy	[%]
t	time step	
T_{TF}	temporal fraction subsets	
Δ_{se}	difference in performance indicator	[%]

1

Introduction

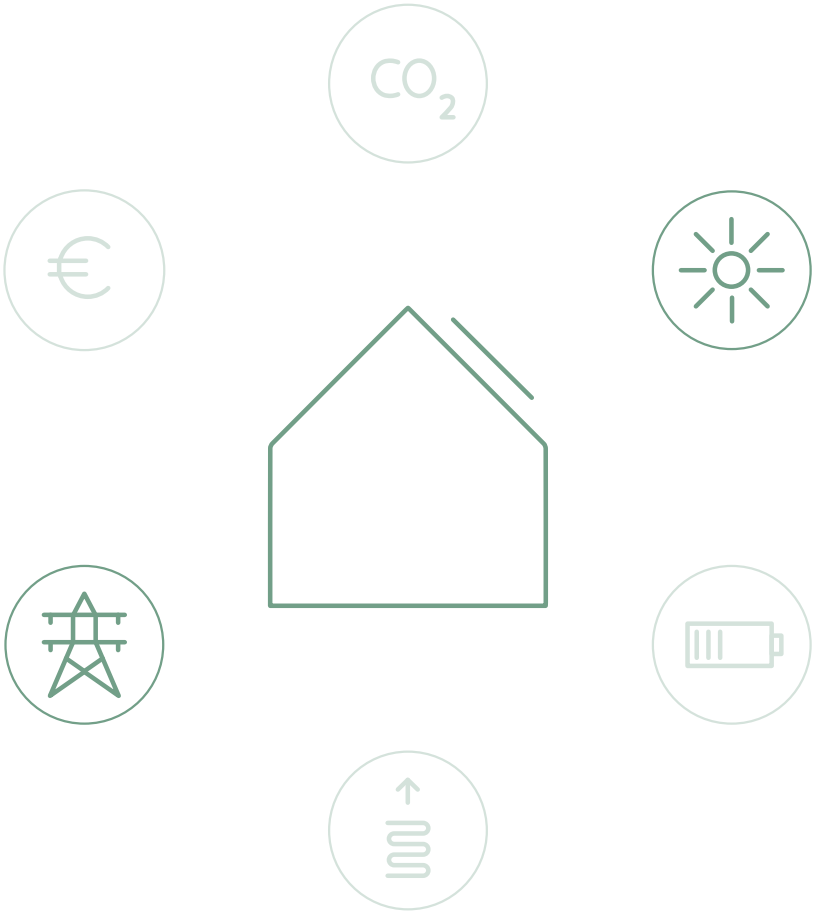

1.1 Motivation

One of the biggest challenges for humanity in the 21st century is to handle climate change. Climate change has already a major impact on ecosystems and will extremely likely cause irreversible global impacts[1]. Since the 1950s, increasing global temperatures, rising sea level, and larger variations in temperature and precipitations have been observed. The main driver of climate change is the increase of anthropogenic greenhouse gas (GHG) emissions. At this moment, the largest share of greenhouse gas emissions (25%) are caused by the use of fossil fuels for electricity and heat production[1]. Around half of this electricity and heat is used within buildings.

In 2015, 195 counties signed the Paris Agreement to reduce global GHG emissions and limit global temperature rise. This agreement confirmed to limit global temperature rise to "well below 2°C", and to pursue efforts to limit this to 1.5°C[2]. Consequently, global GHG emissions should be reduced with 41% to 72% by 2050 and even further with 118% by 2100, relative to 2010. Firm actions from all countries must be taken to realize these ambitions, and political barriers have to be overcome[3] A fundamental change in our energy systems must happen, and a shift from fossil based energy resources to 100% renewable based energy sources is indispensable

1.1.1 Photovoltaic systems

Photovoltaic (PV) solar energy conversion is one of the most promising technologies for renewable electricity generation[4]. A PV system consists of PV cells that are grouped together in modules which are operated by inverters. These systems convert solar irradiation to electricity with a conversion efficiency mainly depending on the cell structure and material[5]. Around 90% of installed PV worldwide consist of crystalline silicon solar cells, with efficiencies between 14% and 24.1%[6]. Most PV systems are grid connected systems which produce alternating current (AC). This AC power must have a frequency and voltage complying with the electricity networks they are connected with.

PV systems are modular and therefore their size can vary between a few kWp to GWp. PV systems are generally classified based on market segments: residential, commercial and utility-scale systems. Residential PV systems are small scale systems, up to a capacity of 15 kWp and mostly installed on residential roofs. Commercial PV systems are larger systems and installed on commercial roofs. These systems vary in capacity, up to a few MWp. Utility-scale systems are ground mounted systems with sizes from a few to hundreds of MWp. Clearly, electricity generation of PV systems can be classified as centralized as well decentralized.

1.1.2 PV development and future projections

Currently, PV systems are the fastest growing power generation source deployed. The global historical growth of and contribution to the electricity production by PV systems is shown in Fig. 1.1. Also, historical data of five selected countries is shown. By the end of 2017, about 390 GWp of PV was installed worldwide. The global PV installed capacity showed and exponential growth. While China has the largest PV installed capacity today, PV in Germany has the largest share in electricity production on an annual basis. The Netherlands has an installed capacity of 2.6 GWp which contributes to 2% of the Dutch electricity production. PV electricity cost is very much depended on location and market conditions. For example, levelized costs of electricity for PV systems in Germany are between €37 per MWh for utility scale systems to €115 per MWh for small scale residential systems[11]. Presently, the lowest levelized cost of electricity bid is €23.4 per MWh for a 300 MWp tender in Saudi Arabia[12].

Most energy transition scenarios underestimated the historical growth of global cumulative PV capacity. The rapid growth is a result of additional policy support for PV, steep technological learning and increasing cost of competitive technologies[4]. Feed-in policies for PV electricity resulted in way more PV capacity installations than expected. Moreover, PV system cost have decreased with an annual learning rate of 20%[13]. Also, other low carbon technologies such as nuclear fission show an increase of cost[14]. Therefore, investments shifted towards alternatives technologies, such as PV or wind energy. Short term projections indicate that the 1 TWp milestone of global installed PV capacity is expected

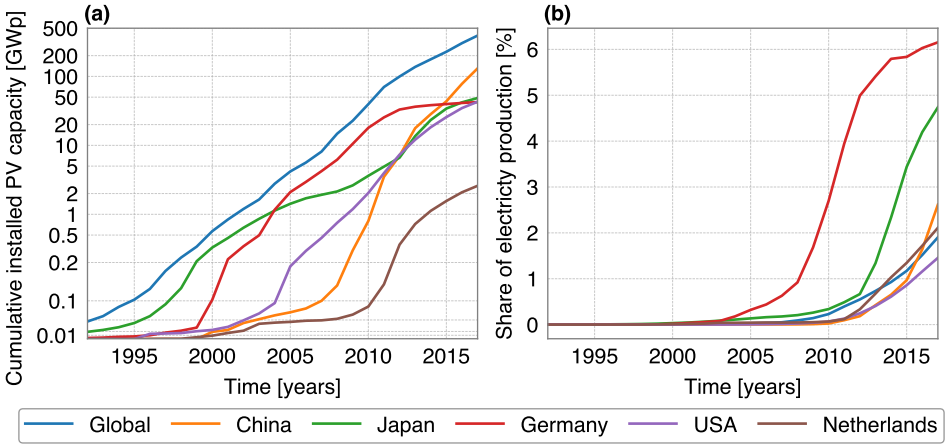

Figure 1.1 · Historical development of PV installed capacity (a) and share of electricity production by PV (b) from 1992 until 2017. Note, the cumulative installed PV capacity is shown using a log scale. Data sources[7–10]

by 2023[12]. On the longer term, projection of installed PV capacities display a larger range depending on the energy transition scenarios[15]. The total installed PV capacity in 2050 is estimated between 12 and 23 TWp globally. PV could then be the major electricity supply technology with a share up to 50% globally[4].

In 2017, 95% of PV systems installed in the Netherlands was placed on buildings, of which around half was placed on residential dwellings[16]. This is quite high for the Netherlands, since only 31% of the PV is installed on rooftops globally[12]. Also, in Germany more than half of the PV systems are located on buildings, mainly due to supporting policies for residential users. Projections for future scenarios show that a larger share of PV systems will be integrated in the building. These building integrated PV systems will cover the unused space of rooftop and facades[17]. Projections for the Dutch market for PV installed on buildings show that a capacity of 25 GWp can be expected by 2030 and over 90 GWp by 2050. Furthermore, 45 GWp of ground mounted systems and 69 GWp of floating PV systems are projected by 2050[18].

1.2 Integrating PV power in the electricity grid

The electricity grid structure in Europe can be classified in three main levels, based on the voltages used: low, medium and high voltage grids. Low and medium voltage grids are used to distribute electricity to consumers, whereas high voltage grids are used for transportation of electricity over large distances. These different grids are connected with each other using transformers located in substations. Residential and commercial buildings are connected with power cables to transformers.

The current electricity system is designed from a perspective of central generation capacities connected to high voltage grids. However, PV systems are mainly connected to low and medium voltage grids. In Germany, 57% of the PV capacity was connected to a low voltage grid and 32% of the PV capacity to a medium voltage grid in 2015[19]. These low and medium voltage grids are typically designed on the expected peak demand within the grid, instead of the peak production from PV. With an evenly spread distribution of PV systems over the Dutch rooftops, 16 GWp of PV can be installed without any additional measures[20]. However, additional integration challenges occur when more than 16 GWp of PV is installed or in areas with already a higher concentration of PV systems.

Three main issues occur when a significantly amount of PV capacity is installed on a low voltage grid[21]. First of all, reverse power flows occur in the distribution systems which often results in voltage rises at the feed-in point. Secondly, these reverse power flows could cause power flows from the distribution system to

the transmission system, which could lead to problems of enhanced aging at the substation level[22]. Thirdly, the grid stability in terms of frequency and voltage could be disrupted. The frequency should ideally be 50 Hz for the synchronous grid of continental Europe. This grid frequency depends on the match between electricity supply and demand. If the supply is larger than demand, then the frequency increases. The opposite occurs when supply is lower than demand. Maintaining frequency between 49.8 and 50.2 Hz is vital for the connected devices and the transportation infrastructure of the electricity system[23].

1.2.1 PV integration measures for the low voltage grid

Measures for technical integration of PV power in the electricity grid can be separated into two groups: grid-side measures and PV system side measures. Grid-side measures include all measures from the distribution grid side. Reliable operation of the distribution grid is the responsibility of Distribution System Operators (DSOs) and therefore grid side measures are undertaken by the DSO. PV system side measures include options that are taken before PV power is feed into the grid, and are undertaken by either the DSO, or the PV system owner.

Grid-side measures

Various technical options are available for the DSO to reduce grid congestion, maintain the voltage range and keep the grid reliable[19]. These can be separated into static and dynamic measures. Static measures expand the hosting capacity of the local grid by making permanent changes in the infrastructure. Dynamic measures increase the hosting capacity by regulating grid properties.

Several static measures can be undertaken to increase the capacity of the low voltage grid. First, the transformer which connects the low voltage grid with the medium voltage grid can be replaced or upgraded to a higher capacity. Secondly, the existing local grid can be segmented into two grids. An additional transformer is used to connect this new grid with the medium voltage grid. Then, new parallel cables can be placed next to existing cables or existing cables are replaced with thicker cables.

For dynamic measures manual or automatic operating equipment are used to regulate the voltage within the local grid. This can be achieved by adjusting the voltage ratio, which is the ratio of the voltage of the medium voltage grid divided by the voltage of the low voltage grid. This voltage ratio can be increased to maintain the voltage on the low voltage grid and thus more PV power can be injected in the grid. Automatic voltage regulators can be installed in the transformers to dynamically adjust the voltage ratio. This also requires active control of the medium voltage grid by the DSO.

PV system side measures

Two main measures from the PV inverter side can be used to support more PV capacity in the low voltage grid. These are reactive feed-in power provision and reduction of the feed-in power. PV inverters can provide reactive power to lower the voltage with a few percent at the connection point to the grid. This results in lower voltage fluctuations within the local grid. The impact that a PV inverter can have depends on the length of the feeder multiplied with the rated active power of the inverter[24]. Most PV inverters are capable of providing reactive power. Furthermore, the reactive power provision results in larger currents, which increases the local grid losses. Different reactive power provision control strategies are available for inverters[25].

The second option is to reduce the feed-in power from the PV system and therefore maintain the quality of the grid. This can be implemented using a feed-in limit (FIL). In Germany, feed-in limits can be seen as an alternative to grid expansion measures for the high and medium voltage grid[26]. The total PV yield that cannot be fed back to the grid depends on the FIL. Annual load duration curves for optimal oriented PV systems with 9 different feed-in limits are shown in Fig. 1.2. Power >90% of rated PV capacity is produced in only 32 hours in the year. Only 0.06% of the total annual energy is produced is above this 90%. Also, with a FIL of 0.5 kW per kWp, 86 % of PV electricity can still be exported. The remaining energy should be self-consumed or be stored in a battery, or otherwise this energy cannot be generated by the PV system. Communication between the PV inverter and a smart electricity meter is required to maintain a feed-in limit.

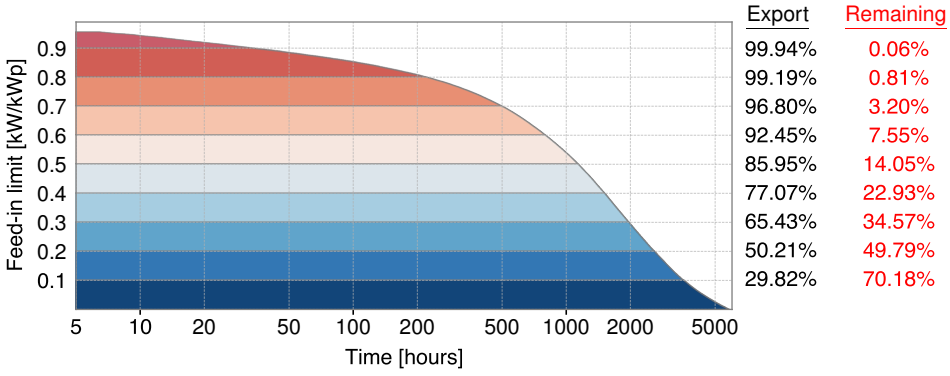

Figure 1.2 · Annual load duration curves of PV exported to the grid for 9 feed-in limitations. Note that the hours on the horizontal axis are shown with a log scale. The percentage of PV electricity production that can be exported to the grid and the percentage of energy that remains (in red) are shown on the right side of the plot. The PV yield was modelled with an orientation of 185 ° surface azimuth, a 36° tilt, a high performance ratio of 91% and with weather data of The Netherlands from 2010 until 2016. Remaining PV yield model steps are similar as described in section 3.2.1.

1.3 The need for electrification and energy storage

PV electricity production is limited to certain moments in time due to daily and seasonal variation in irradiance. In the Netherlands, PV systems have an annual specific yield of around 900 kWh per kWp which corresponds to a capacity factor of 10%[27]. The hourly load for 2017 was between 7.5 GW and 18.6 GW with an average of 13.1 GW[28]. When PV power generation surpasses these loads, measures need to be taken to keep the electricity grid running.

1.3.1 Electrification of heating and transport

A large share of global energy is used for heat production and transport[1]. Currently, fossil based fuels are used to provide this demand. Part of this energy consumption can be decarbonized using electricity from renewable electricity sources. Subsequently, a larger share of renewable energy sources can be installed within the current energy system[29]. Heating can be electrified by using heat pump technologies. This technology can be deployed to generate heat from electricity, for central and decentral applications. Electrification of transport, especially light-duty vehicles, is also one of the solutions to reduce the global GHG emissions and to increase the share of variable renewable energy (VRE) sources. VRE sources can only generate electricity when their natural resources are available and are therefore non-dispatchable sources of electricity. Charing electric vehicles (EVs) on moments with surplus renewable energy generation will allow for a larger share of VRE sources in the electricity system.

Moreover, a shift from gasoline cars to electric vehicles reduces air pollution and thus improves the air quality[30]. The global stock of battery electric vehicles increased tenfold from around 0.2 million in 2013 to 2 million in 2017[31]. Growth projections for 2030 show a global EV stock between 100 and 200 million cars[31]. Also, the number of EVs in the Netherlands is increasing rapidly, with around 30,000 battery electric vehicles in July 2018[32].

Both electrification of heating and transport adds additional flexibility to the electricity system by providing demand response services[33]. Yet, a low carbon intensity of the electricity mix is a must to successfully reduce emissions[34]. Thus, electrification of heating and transport is an important and realistic solution to incorporate more variable PV generated electricity and reduce GHG emissions.

1.3.2 Energy storage

Dispatchable thermal power plants provide the majority of the global electricity demand. A shift from these dispatchable plants to non-dispatchable VRE sources requires solutions to balance electricity supply with demand, for example storage. Excess electricity from PV, wind turbines or other VRE can be stored and

used on later moments. In this case, storage improves the availability and therefore the degree of dispatchability of these sources. Moreover, VRE sources have a higher uncertainty and variability of production which influences the stability of the electricity network. As a result, storage is seen as a requirement in a system where VRE sources are a major source of energy[35].

Various storage technologies exist to incorporate renewable energy and help to keep the grid stable[36]. Currently, pumped hydro storage represents around 97% of the global installed storage capacity[37]. However, this technology has geographical restrictions limiting the deployment potential in certain areas. Also, EV batteries can be used as storage for surplus electricity, but bidirectional charging technology are required for EVs and charging stations. Stationary battery energy storage systems (BESS) is a modular technology and can be easily implemented on both central and decentral level in the electricity system. Furthermore, this technology can be used for multiple applications due to fast response times and is therefore seen as a multi-purpose technology[38].

In 2017, around 11 GWh of stationary BESS capacity is installed globally[37]. The main primary use cases of these BESS are frequency regulation, reserve provision and shifting electricity use[37]. Also, cost of BESS are dropping and are expected to continue due to the large potential of deployment in the future[39]. Projections for 2030 show that 56% of the BESS systems are coupled with PV systems, which represent an installed storage capacity between 79 to 198 GWh. This range mainly depends on the installed storage capacity per kWp of PV capacity, which could range between 1.2 kWh per kWp and 2 kWh per kWp[37]. The major role for these storage capacities is to shift energy demand and increase self-consumption of PV electricity. Knowledge of electricity consumption profiles, PV production profiles, and battery control strategies is required for an optimal use of PV with storage.

1.4 Thesis objectives and outline

It is evident that PV systems installed on buildings will play an important role in the energy transition. Future projections for the Netherlands show a large increase in PV capacity installed on buildings, upto 25 GWp by 2030[18]. These will be mainly connected to the low voltage grid and call for research on integration measures of PV systems. The previous sections have given a general overview of technical requirements and solutions to incorporate more PV electricity in the energy system. However, the optimal measures to support integration of PV systems in the low voltage grid are very case specific. The impact of grid-side measures mainly depends on the expected PV capacity to be installed and connected

to the low voltage grid, the current topology of the grid and the remaining lifetime of grid components. Grid-side measures costs are paid by the DSO and thus socialised to all their customers.

Limiting the PV feed-in shows a greater potential to quickly increase the PV system capacity without an investment in grid infrastructure and expansion. PV self-consumption lowers the feed-in power to the electricity grid and results in lower grid electricity losses. Also, it can be increased by local production of heat or when local EVs are charged. Moreover, PV peak power can be reduced using smart EV charging. Energy storage will increase self-consumption to higher levels and can be controlled to reduce the PV peak power. Moreover, energy storage can be used for a range of applications to support the electricity network and subsequently integration of other VRE sources[40]. Consequently, these options allow for more installed PV capacity in the energy system. These PV system side measures show many benefits compared to grid system side measures. Therefore this thesis focus is on integration measures from the PV system side, with emphasis on local electrification and energy storage.

Demand side management of small residential applications to improve the self-consumption were not considered in this thesis. Previous research shows households have a relative low economic incentive to increase PV self-consumption, caused by the small difference in consumption and feed-in tariffs[41,42].

1.4.1 Research questions

This thesis focusses on exploring benefits of using locally PV power, produced with rooftop systems. The main research question of this thesis is:

What technical, economic and environmental benefits can be obtained from the local use of electricity generated by rooftop PV systems?

The main question is divided into the following sub questions:

Q 1. How can PV self-consumption and self-sufficiency be improved?

Q 2. How can PV feed-in peak power be reduced?

Q 3. What economic benefits can be realized?

Q 4. What GHG emission reductions can be realized?

The first and second sub questions quantify the impact of the local use of PV electricity. The third and fourth sub questions assess the impact of side benefits which can be realized.

The emphasis is on PV systems situated on residential and commercial buildings and located in the Netherlands. These questions will be addressed for these buildings categories in the remaining chapters of this thesis, see Table 1.1. Main results from chapter 2 to chapter 6 are combined per sub question in chapter 7. Final conclusions and recommendations concerning the main question are given in chapter 8.

1.5 Thesis outline

Chapter 2 assesses the impact of the orientation of a PV system on PV self-consumption for 48 residential and 42 commercial buildings. Measured electricity consumption patterns of these buildings are combined with 10,761 PV yield time series, each with a different orientation. Furthermore, the impact of the exported peak power and potential revenues are evaluated. These revenues of the systems are assessed for 9 scenarios and include Dutch and German market prices. Optimal orientations are determined using high resolution data (5 min) for a 7 year period (2010 -2016). Also, the impact of flat roof east-west systems is quantified.

Chapter 3 presents a simple method to forecast PV and demand patterns and uses this as input for a BESS control strategy. The strategies are developed to enhance PV self-consumption while reducing PV peak power. Four methods to forecast PV and three methods to forecast electricity demand of residential and commercial buildings are developed. These methods are used to generate 14 battery control strategies. The performance of these control strategies are analysed using three indicators: self-consumption, curtailment losses and storage revenues. Electricity consumption patterns of 48 residential and 42 commercial buildings are used. A sensitivity analysis is performed on the input conditions of the PV and storage system parameters. Findings of this analysis give better insight in the behaviour of the control strategies.

Table 1.1 · Overview of chapters and involving research questions.

Chapter	Q 1.	Q 2.	Q 3.	Q 4.
2. Influence of PV orientation	•	•	•	
3. Forecasting methods for PV-battery systems	•	•	•	
4. FRR provision by PV-battery systems	•		•	
5. Combing GSHP with PV-battery systems	•	•	•	•
6. Spatio-temporal model for PV integration	•			•
7. Synthesis of the main findings	•	•	•	•

Chapter 4 assesses the impact of using stationary BESS systems for multiple applications namely enhancement of self-consumption and provision of frequency restoration reserves (FRR). Six battery storage strategies are developed and assessed for 48 residential and 42 commercial buildings. Four technical performance indicators and five economic performance indicators are evaluated. A tornado graph is used to display the impact of 15 system parameters on the economic profitability of the storage strategies. Moreover, a sensitivity analysis is conducted on the impact of market prices and on the impact of BESS degradation parameters. An estimation of the FRR market participation by PV-battery storage systems is also provided.

Chapter 5 assesses the combination of ground source heat pumps (GSHP) with PV and battery energy storage. The PV self-consumption, peak reduction, economic benefits and life cycle emissions for 16 residential buildings is assessed. Consumption patterns of households with a GSHP and PV production patterns are used, both measured over a 2-year period. A new battery control strategy is developed to enhance self-consumption, while reducing both PV peak and demand peak. The system costs, revenues and life cycle emissions are assessed for 5 different combinations and over a 30-year lifetime. Furthermore, a sensitivity study on the input parameters will give several recommendations to improve the economics of GSHP systems with and without PV and storage.

Chapter 6 presents a model framework to assess the PV self-consumption and GHG emission reductions potential on a city scale. This framework includes the impact of storage and future electric vehicle demand with smart charging. The model demonstrates this impact for 88 neighbourhoods in the city of Utrecht in the Netherlands. Spatial mapping is used to show the difference in self-consumption potential and emissions reduction potential between neighbourhoods. A sensitivity analysis on PV rooftop utilization rate provides insights in the potential of PV self-consumption, storage and emission reductions.

Chapter 7 compares the main findings from chapter 2 to 6 and gives answers to the four sub questions. The questions are answered for three relative PV system capacities and for both residential and commercial systems. Also, a new scenario is added in which PV and storage systems would be installed in 5 years.

Chapter 8 provides an answer to the main question and provides final conclusions. It also provides short and medium term recommendations for policy makers and recommendations for future research.

2

Influence of PV orientation

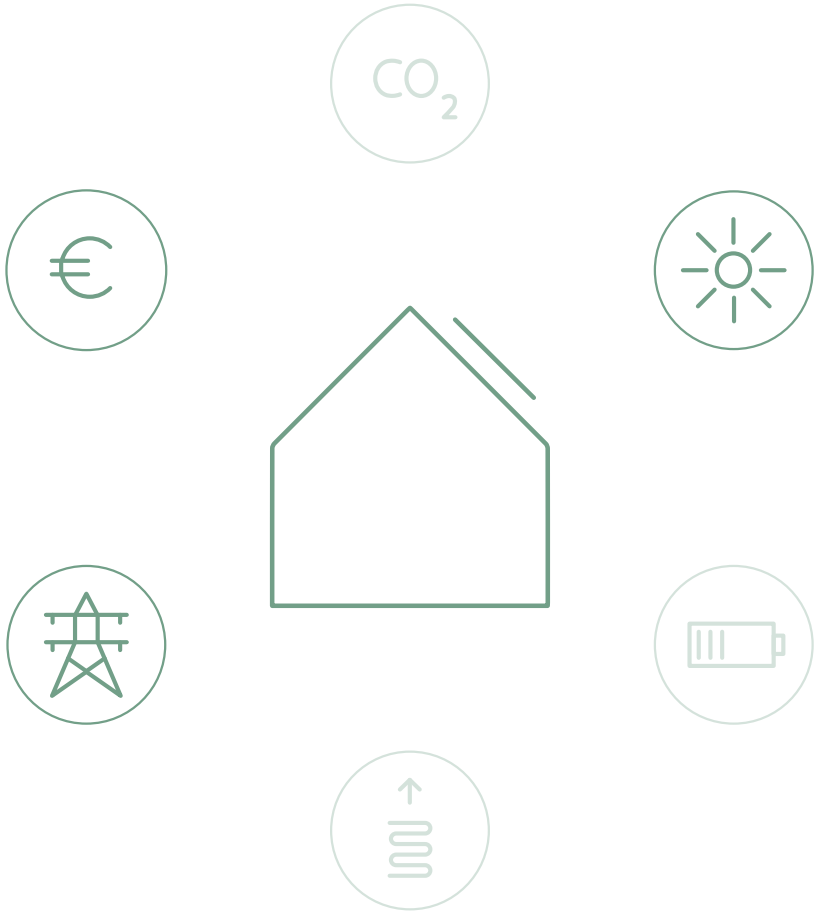

This chapter is based on the publication: G.B.M.A. Litjens, E. Worrell and W.G.J.H.M. van Sark. "Influence of demand patterns on the optimal orientation of photovoltaic systems". in: *Solar Energy* **155** (2017), pp. 1002-1014. DOI:10.1016/j.solener.2017.07.006

Abstract

Photovoltaic (PV) systems are usually orientated to maximize annual energy yield. This may not optimize other system indicators, specifically: direct consumption of self-generated PV power, reduced feed-in power and annual revenue. Also, these indicators are influenced by the energy demand of a building in relation to the PV system size. Therefore, we evaluate how demand patterns influence the optimal PV orientation for self-consumption, feed-in power and revenue. Historical Dutch demand patterns of 48 residential and 42 commercial buildings were used. We combined Dutch and German electricity prices from day-ahead markets with different ratios of electricity sales to purchase prices. Differences between demand patterns caused large variations in optimal PV orientations. On average, PV self-consumption is maximized for residential systems with an azimuth of 212° and a tilt of 26°. Commercial PV systems have an average of 188° azimuth and 17° tilt. Self-consumption can be increased 4.6% for residential systems and 2.6% for commercial systems, by optimizing orientation for self-consumption rather than for energy production. Curtailment losses are significant reduced by decreasing the module tilt angles. Optimizing for revenue can increase annual revenue of PV systems with 5.0% for certain demand patterns and pricing scenarios. The ratio of sales to purchase electricity price has a larger influence on the economically optimal orientation for residential systems than for commercial systems. Differences between Dutch and German market prices have minor effects on PV orientation. Analysed demand patterns significantly affect optimal PV orientation. Therefore, we recommend that optimal PV orientation should not only be based on maximizing energy production, but also on expected demand patterns and market prices.

2.1 Introduction

Commonly, PV (photovoltaic) modules are oriented to maximize their annual generated electricity. A variety of methods have been developed to determine this orientation[43–46]. However, the economic value of rooftop PV generated electricity varies for time intervals shorter than one year. This value of grid-connected PV systems is influenced by electricity markets, policy regulations and the electricity consumption pattern of the PV yield producer. This consumption is typically the electricity demand of a building on which the PV system is installed.

The current increase of installed PV capacity results in larger fluctuations of time-dependent value. In addition, the maximum feed-in power is expected to become more and more regulated with an increasing share of variable renewable sources in the electricity generation mix. Consequently, self-consumption of PV energy (or PV self-consumption) is supported by new policies in many European countries[47]. Thus, PV orientation should not only be based on maximizing energy production, but also on expected demand patterns and market prices.

Feed-in limitations set restrictions to the maximum power flow that can be exported back to the electricity grid, and are typically given as a ratio of the maximum installed PV capacity. Consequently, high injection peaks of PV power on the local electricity grid are avoided which lowers grid disturbances. For example, currently in Germany, PV-battery systems that limit the power fed back to the grid to 0.5 kW/kWp of the PV installed capacity can apply for financial support[48]. PV generated energy that is not exported nor used is lost, and is usually defined as curtailment losses.

Previous studies mainly focused on effects of PV orientation by comparing maximized energy yield and revenue. Economical optimization of PV orientation could increase annual revenue up to 4%, with module azimuth angles ranging from 178° to 223° azimuth in the Northern hemisphere[49]. Another study showed optimal azimuth angles between 200° to 223° for Austin, TX, USA[50]. A difference of 10° azimuth between a flat rate pricing regime and a spot market price regime was presented for Ottawa, Canada[51]. A different study including Ottawa, showed an increase in revenue of 19% for an azimuth of 234° and a tilt of 41° for a peak-dependent tariff[52]. The economically optimal PV orientation from an electricity system perspective was examined for Germany and Austrian regions. For a total installed PV capacity of 70 GWp, an optimal azimuth of 165° was presented[53].

Only a few studies were found that included consumer demand patterns. A German study combined 74 residential demand patterns with a 1 kWh battery storage size and different PV system sizes[54]. PV systems with 0.5 kWp installed

capacity for each MWh annual consumption were found to have an averaged optimal orientations around 185° azimuth and 36° tilt. Systems with 2 kWp installed PV capacity for each kWh storage were found to have 200° azimuth and 22° tilt. In addition, variance in optimal PV orientations is lower for smaller systems than larger systems. Another study investigated electricity bill savings of PV systems, using 215 residential demand patterns from California, USA. It was found that south-west facing PV systems had a slightly higher bill saving, <5%, compared to south facing PV systems[55]. PV self-consumption of apartments and detached houses in Sweden can be increased by respectively 2% and 3% through optimizing the PV orientation[56]. An west oriented PV system showed a higher share of directly consumed energy than east oriented systems for a residential Germany demand pattern[57].

A study including residential demand for and time-of-use tariffs from Las Vegas, USA, showed an economical optimal orientation of 220° azimuth. A large part of residential electricity demand was cooling load in the afternoon, due to the desert climate. Consequently, a significant drop in peak demand due to PV generation was observed[58]. However, for locations with a relatively large heating demand, especially in winter months, there was no significant drop of peak demand related to PV production observed.[59]. Demand patterns that had relative more load during morning and evening hours benefit from PV systems with a relatively lower tilt angle[60].

Little is known about how demand patterns influence the optimal PV orientation for self-consumption, feed-in power flows, and revenues. Therefore it is not clear to what extent self-consumption or revenue can be increased by optimizing PV orientation, leading to suboptimal revenues.

With this paper, we aim to determine the influence and sensitivity of demand patterns on the optimal PV system orientation for self-consumption, curtailed energy under feed-in limitations, and PV revenue. Demand patterns of 48 residential and 42 commercial buildings in combination with historical Dutch and German electricity market data were used. We present new insights on PV system design that help the PV market to maximize PV self-consumption and revenues. Furthermore, increased PV self-consumption leads to reduced grid losses and therefore potential energy savings and reduced CO_2 emissions from backup power generation.

2.2 Methods

A model was developed and written in Python to determine the optimal orientation for each PV system. Demand patterns were combined with pricing patterns and a range of PV orientation to find optimal PV orientations for three aims:

- Maximize self-consumption
- Minimize curtailed energy under feed-in limitations
- Maximize added revenue

For each optimization aim, indicators were defined which describe influences of demand patterns on optimal PV orientation. Used indicators were annually evaluated by patterns with a 5 min interval. Furthermore, PV module azimuth was varied from 75° till 285° and module tilt from 0° till 50°. Both angles were varied with 1° steps, resulting in 10,761 different orientations analysed. Each orientation has corresponding indicators. The optimization function selects the maximum or minimum indicators and the affiliated PV orientation for each demand pattern. Details about used PV model, demand patterns and price patterns are provided in section 2.2.5.

2.2.1 Self-consumption indicators

Three indicators were used to analyse the effect of PV system orientation on PV self-consumption of residential and commercial systems; self-consumption ratio (SCR), self-sufficiency ratio (SSR), and added self-consumption (ASC). SCR, SSR are quantified for a certain corresponding PV orientation. ASC quantifies the difference in self-consumption caused by a change from optimal orientation for energy production to optimal orientation for maximized self-consumption. The optimal orientation for energy production is commonly used as ideal orientation and therefore a good reference to evaluate.

Self-consumed power ($P_{\text{direct SC}}$) is the amount of PV power (P_{PV}) that is directly consumed by the electricity demand of a building. (P_{demand}). Self-consumption ratio specifies the share of PV yield that is directly consumed. This is calculated by dividing self-consumed energy (E_{SC}) with total produced energy (E_{PV}), see Eq. (2.1). Total self-consumption was calculated by the sum of self-consumed power of each 5 min(Δt) interval between time step t=1 and t_{end}.

$$P_{\text{direct SC}} = \begin{cases} P_{\text{PV}} & \text{if } P_{\text{PV}} < P_{\text{demand}} \\ P_{\text{demand}} & \text{if } P_{\text{PV}} \geq P_{\text{demand}} \end{cases} \tag{2.1a}$$

$$E_{\text{SC}} = \sum_{t=1}^{t_{\text{end}}} P_{\text{direct SC,t}} \cdot \Delta t \tag{2.1b}$$

$$E_{\text{PV}} = \sum_{t=1}^{t_{\text{end}}} P_{\text{PV,t}} \cdot \Delta t \tag{2.1c}$$

$$\text{SCR} = \frac{E_{\text{SC}}}{E_{\text{PV}}} \tag{2.1d}$$

Self-sufficiency ratio indicates the share of building demand directly covered by PV yield, and is defined as the ratio between self-consumed energy (E_{SC}) and total consumed energy (E_{demand}) on annual basis, see Eq. (2.2).

$$E_{\text{demand}} = \sum_{t=1}^{t_{\text{end}}} P_{\text{demand,t}} \cdot \Delta t \tag{2.2a}$$

$$\text{SSR} = \frac{E_{\text{SC}}}{E_{\text{demand}}} \tag{2.2b}$$

Added self-consumption indicates relative change between the maximum self-consumption ($E_{\text{SC Max(SC)}}$) which is obtained from the orientation that maximize the annual self-consumption, and the self-consumption obtained for a PV orientation that maximizes energy production ($E_{\text{SC Max(PV)}}$) in percentage, see Eq. (2.3).

$$\text{ASC} = \frac{E_{\text{SC Max(SC)}} - E_{\text{SC Max(PV)}}}{E_{\text{SC Max(PV)}}} \tag{2.3}$$

2.2.2 Curtailed energy indicators

Two indicators were used to quantify the effect of PV orientation on the curtailed energy under feed-in limitations. The annual amount of lost energy is quantified with the curtailment loss ratio (CLR). This is the share of energy lost due to a feed-in limitation (E_{lim}) from energy that could be fed back without a feed-in limitations ($E_{\text{No lim}}$). The total energy fed back due under a feed-in limitation is the sum of power under (P_{lim}). This power is restricted by a feed-in limitation (P_{FIL}). The curtailed energy (E_{CE}) is defined as the difference between the maximum annual energy that is fed back to the grid without a feed in limitation ($E_{\text{No lim Max}(E_{\text{No lim}})}$) and with a feed-in limitation (E_{Lim}). CLR was calculated by dividing the curtailed energy with the produced PV energy, see Eq. (2.4).

$$P_{\text{Lim}} = \begin{cases} P_{\text{PV}} - P_{\text{demand}} & \text{if } P_{\text{PV}} - P_{\text{demand}} \leq P_{\text{Lim}} \\ P_{\text{Lim}} & \text{if } P_{\text{PV}} - P_{\text{demand}} > P_{\text{FIL}} \end{cases} \tag{2.4a}$$

$$E_{\text{No lim}} = \sum_{t=1}^{t_{\text{end}}} P_{\text{PV}} - P_{\text{demand}}, t \cdot \Delta t \tag{2.4b}$$

$$E_{\text{Lim}} = \sum_{t=1}^{t_{\text{end}}} P_{\text{Lim,t}} \cdot \Delta t \tag{2.4c}$$

$$E_{\text{CE}} = E_{\text{No lim Max}(E_{\text{No lim}})} - E_{\text{Lim}} \tag{2.4d}$$

$$\text{CLR} = \frac{E_{\text{CE}}}{E_{\text{PV}}} \tag{2.4e}$$

The share of curtailed energy that can be fed back to the grid due to the change in orientation from maximizing annual energy production to minimize curtailed energy is defined by the reduced curtailed energy (RCE). This is the relative change between the minimized curtailed energy ($E_{\text{CE Min(CE)}}$) and the curtailed energy under an orientation that maximizes energy production ($E_{\text{CE Max(PV)}}$) in absolute percentage, see Eq. (2.5).

$$\text{RCE} = \frac{E_{\text{CE Min(CE)}} - E_{\text{CE Max(PV)}}}{E_{\text{CE Max(PV)}}} \cdot -1 \tag{2.5}$$

2.2.3 Added revenue indicators

Total revenue of a PV system (R_{tot}) is the sum of revenue from self-consumed energy (R_{SC}) and revenue from sold electricity to the grid (R_{SE}), see Eq. (2.6). This depends power to the grid (P_{G}), on the price of electricity bought from (π_{buy}) and on the price of sold electricity (π_{sell}) to the grid. Revenues were analysed with fixed tariffs that have a constant price value throughout a year and with time-of-use tariffs that vary for each hour of the year. Added revenue (AR) shows the change between the revenue for an orientation with maximum energy production ($R_{\text{tot Max(PV)}}$) and an orientation with maximum revenue ($R_{\text{tot Max}(\text{R}_{\text{tot}})}$).

$$R_{\text{SC}} = P_{\text{direct SC}} \cdot \pi_{\text{buy}} \tag{2.6a}$$

$$R_{\text{SE}} = \begin{cases} P_{\text{G}} \cdot \pi_{\text{sell}} & \text{if } P_{\text{PV}} > P_{\text{demand}} \\ 0 & \text{if } P_{\text{PV}} \leq P_{\text{demand}} \end{cases} \tag{2.6b}$$

$$R_{\text{tot}} = \sum_{t=1}^{t_{\text{end}}} (R_{\text{SC,t}} + R_{\text{SE,t}}) \cdot \Delta t \tag{2.6c}$$

$$\text{AR} = \frac{R_{\text{tot Max}(\text{R}_{\text{tot}})} - R_{\text{tot Max(PV)}}}{R_{\text{tot Max(PV)}}} \tag{2.6d}$$

Taxes or grid network operator costs induce a difference between the price of electricity sold from and bought to the grid. The effect of this difference was examined using the sales to purchase ratio (SPR) and is given in Eq. (2.7).

$$\mathrm{SPR} = \frac{\pi_{\mathrm{sell}}}{\pi_{\mathrm{buy}}} \tag{2.7}$$

2.2.4 Temporal contribution

Contributions of hour of the day and month of the year on annual ASC, RCE and AR values were analysed and defined as temporal fraction (TF). $\mathrm{ASC_{TF}}$, $\mathrm{RCE_{TF}}$ and $\mathrm{AR_{TF}}$ were calculated according to Eq. (2.8) , Eq. (2.9) and Eq. (2.10) respectively. Subsets for each temporal factor were defined as $\mathrm{T_{TF}}$ and each parameter was calculated for a subset time $t \in T_{\mathrm{TF}}$. The temporal indicators of the corresponding maximum (Max) annual optimal orientation were selected. For example, $E_{\mathrm{SC,TF,Max(SC)}}$ is the self-consumption for a certain temporal fraction, under the orientation that maximizes the annual self-consumption.

$$E_{\mathrm{SC,TF}} = \sum_{t \in T_{\mathrm{TF}}} P_{\mathrm{direct\,SC,t}} \cdot \Delta t \tag{2.8a}$$

$$\mathrm{ASC_{TF}} = \frac{E_{\mathrm{SC,TF,Max(SC)}} - E_{\mathrm{SC,TF,Max(PV)}}}{E_{\mathrm{SC\,Max(PV)}}} \tag{2.8b}$$

$$E_{\mathrm{No\,lim,TF}} = \sum_{t \in T_{\mathrm{TF}}} P_{\mathrm{PV,t}} - P_{\mathrm{demand,t}} \cdot \Delta t \tag{2.9a}$$

$$E_{\mathrm{Lim,TF}} = \sum_{t \in T_{\mathrm{TF}}} P_{\mathrm{Lim,t}} \cdot \Delta t \tag{2.9b}$$

$$E_{\mathrm{CE,TF}} = E_{\mathrm{No\,lim,TF\,Max}(E_{\mathrm{No\,lim,TF}})} - E_{\mathrm{Lim,TF}} \tag{2.9c}$$

$$\mathrm{RCE_{TF}} = \frac{E_{\mathrm{CE,TF,Min(CE)}} - E_{\mathrm{CE,TF,Max(PV)}}}{E_{\mathrm{CE\,Max(PV)}}} \cdot -1 \tag{2.9d}$$

$$R_{\mathrm{tot,TF}} = \sum_{t \in T_{\mathrm{TF}}} (R_{\mathrm{SC,t}} + R_{\mathrm{SE,t}}) \cdot \Delta t \tag{2.10a}$$

$$\mathrm{AR_{tot,TF}} = \frac{R_{\mathrm{tot,TF,Max(R)}} - R_{\mathrm{TF,Max(PV)}}}{R_{\mathrm{tot\,Max(PV)}}} \tag{2.10b}$$

An overview of acronyms used in this study with corresponding indicators and equations is shown in Table 2.1.

Table 2.1 · Overview of acronyms with corresponding indicators and equations.

Acronyms	Indicator	Equation
SCR	Self-consumption ratio	2.1
SSR	Self-sufficiency ratio	2.2
ASC	Added self-consumption	2.3
CLR	Curtailment loss ratio	2.4
RCE	Reduced curtailed energy	2.5
AR	Added revenue	2.6
SPR	Sales to purchase ratio	2.7
TF	Temporal fraction	2.8 & 2.10

2.2.5 Input data

Three kinds of patterns were required for our analysis; PV yield, electricity demand and wholesale electricity price patterns. PV yield patterns, containing AC power, were modelled through the open source package PVLIB (v0.4.5)[61]. This package provides validated atmospheric functions and PV system performance models. Solar radiation, ambient temperature, dew point temperature, wind speed and pressure were measured in De Bilt, the Netherlands, (latitude: 52.11°, longitude: 5.18°). Measurement interval of radiation was 10 min and for other weather parameters one hour. All weather parameters were linearly interpolated to a 5 min interval and used as model input. In addition, specifications of the Sanyo HIP-225HDE1 module and the Enphase Energy M210 inverter were used[62,63]. This PV module has a relatively small temperature dependency, decreasing the influence of temperature within the results. Azimuth angles were varied from 75° till 285° and tilt angles from 0° till 50° tilt angles, with 1° steps.

Demand patterns of 48 households, with different dwelling types, were derived from measurements by a Dutch distribution system operator between 2012 and 2014 and are openly available[64]. These residential patterns have an interval of 15 min and are valid for 2013. Commercial electricity demand patterns were measured at 42 commercial buildings, mainly offices, on a 15 min interval in the Netherlands in 2013.

No demand data from 2010 till 2012 and from 2014 till 2016 were available. Hence, data of 2013 was used to model demand patterns of these absent years. Weekdays of these missing years were matched with weekdays of 2013, and leap days of 2012 and 2016 were filled with the last day of February 2013. Both residential and commercial patterns were linearly interpolated to a 5 min interval, matching the time interval of the PV yield pattern.

We normalized residential and commercial patterns to an annual consumption of 1 MWh. This allows comparison of the demand patterns variability. The influence of each individual demand pattern was visualized using violin plots[65].

This type of graphical representation extends the regular box-whisker plot with a full smoothed histogram of the values. This gives a quick indication of the distribution of results obtained from each demand pattern. In addition, mean values of the distributions were indicated using solid lines and 25% and 75% percentiles were indicated by dotted lines. Distributions of hour of the day and monthly electricity demand from residential and commercial buildings are shown in a violin plot in Fig. 2.1.

Dutch and German hourly electricity wholesale price patterns from 2010 till 2016 were obtained from the day-ahead action of EPEX SPOT markets. The Power NL market price was used as Dutch market price, and the Physical Electricity Index price as German market price. The electricity price patterns were resampled to a 5 min interval using zero-order hold interpolation, matching the PV yield and demand patterns.

Market prices for 2016 and hourly difference between Dutch and German prices are shown in Fig. 2.2. The difference between German and Dutch prices influences the optimal PV orientation and added revenues. Hence, we included both price patterns in our analyses, leading to a better understanding of market price influence. An overview of measured and modelled input patterns used is given in Table 2.2.

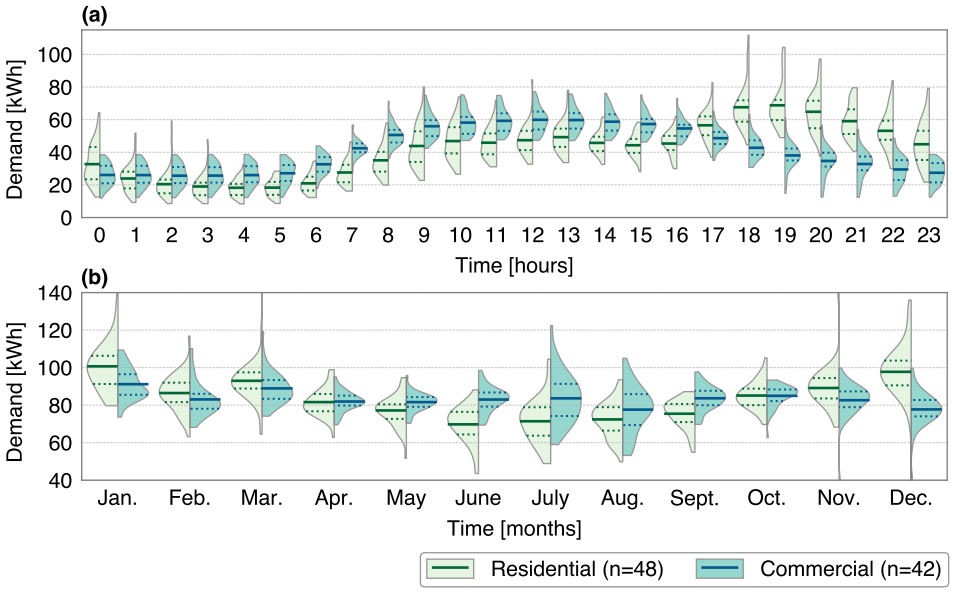

Figure 2.1 · Hour of the day (a) and monthly (b) electricity demand shown using violin plots. Residential demand is shown on the left part of the violin and commercial on the right part of the violin. The demand patterns were normalized to an annual energy consumption of 1 MWh. Mean values of the distributions are marked by dashed lines and 25% and 75% percentiles are marked by dotted lines.

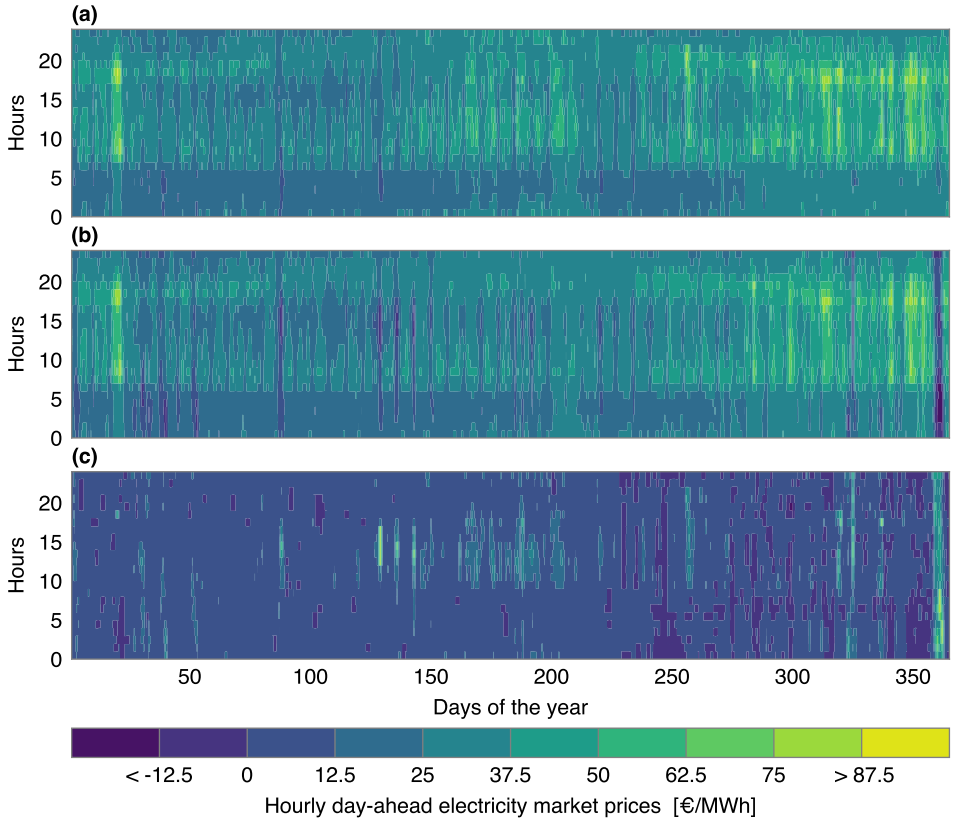

Figure 2.2 · Hourly Dutch (a), German (b) and difference in (Dutch-German (c)) day-ahead electricity market prices from 2016.

Table 2.2 · Overview of input timeseries used for this study.

Pattern	Amount	Measured	Modelled
PV yield	10761	-	2010 until 2014
Residential buildings	48	2013	2010 until 2012 & 2014 until 2016
Commercial buildings	42	2013	2010 until 2012 & 2014 until 2016
Dutch market prices	1	2010 until 2016	-
German market prices	1	2010 until 2016	-

2.3 Optimal orientation without self-consumption

Optimal orientations to maximize energy production and maximize profit without self-consumption are shown using Dutch and German market prices in Table 2.3. Also, the corresponding annual yield and added revenues are given for each year.

The optimal PV orientations to maximize energy production show a large range of annual differences. Optimal module azimuths are ranging from 181° to 188°, and tilt angles from 33° to 38°. It can be noted that the optimal azimuth

Table 2.3 · Optimal orientations to maximize energy production and optimal orientation to maximize revenue without self-consumption. Corresponding annual yield (AC output) is given for a PV system of 1 kWp. Added revenue values are given for the optimal orientations to maximize revenue.

Year	Max PV yield		Dutch market prices		German market prices	
	orientations [°] azimuth , tilt	E_{PV} [kWh]	orientations [°] azimuth , tilt	AR [%]	orientations [°] azimuth , tilt	AR [%]
2010	187 , 33	1046	180 , 33	0.12	179 , 33	0.13
2011	188 , 38	1078	184 , 37	0.05	184 , 37	0.05
2012	187 , 35	1010	184 , 36	0.02	184 , 36	0.04
2013	183 , 35	1027	178 , 35	0.06	176 , 37	0.14
2014	182 , 35	1068	179 , 37	0.05	178 , 36	0.04
2015	187 , 36	1111	182 , 35	0.08	184 , 36	0.02
2016	181 , 37	1086	177 , 38	0.06	177 , 39	0.10
Mean	185 , 36	1061	181 , 36	0.06	180 , 36	0.07

is located 1° to 8° from the south orientation. Clearing of clouds appears more in afternoon hours than morning hours, resulting in larger share of radiation in the afternoon. Annual PV yield production varied between 1010 kWh/kWp and 1111 kWh/kWp

Optimize PV orientation for market prices, without self-consumption, shows module azimuths from 177° to 184° for Dutch market prices and from 176° to 184° for German market prices. These orientations are between ≈3° and 8° lower than the optimal azimuth for maximum energy production. Module tilt angles are almost similar as found for maximum energy production. Small difference in optimal orientations between Dutch prices and German prices are shown, with maximum difference in azimuth of 2°. The maximum difference in module tilt is 1°. Furthermore, there is no clear annual relation between PV orientations and the electricity market prices of countries researched. A higher azimuth angle for Dutch than German prices is observed for 2010, 2013 and 2014, yet in 2015 the opposite is seen.

Additional revenues due to the change from an orientation to maximize energy production to an orientation to maximize revenues are between 0.02% and 0.14%. Added revenues increases with a larger difference in maximize energy production orientation and maximizing revenue orientation. Differences between Dutch AR and German AR are ranging from -0.08% to +0.06 %. Furthermore, mean optimal orientations and added revenues are almost similar for Dutch and German market prices.

2.4 Maximize self-consumption

Optimal PV orientations for maximized PV self-consumption, SSR and ASC of six different PV system sizes are illustrated using violin plots in Fig. 2.3. The influence of the residential and commercial demand patterns is shown in the distribution. The left part of the violin plot provides the distribution of results obtained from residential systems. Results of commercial systems are shown on the right part of the violin. Note that PV system sizes, indicated on the horizontal-axis, are not equally dispersed. Demand data were normalized to an annual energy consumption of 1 MWh and data of 2016 were used. Mean values of the distributions are indicated by dotted lines.

Note that a relative PV system size of 1 kWp for each MWh of annual energy consumption is commonly installed in the Netherlands, since this will approximately fulfil the annual demand. PV systems sizes smaller than 1 kWp per MWh of annual consumption are installed when there are space limitations. PV systems >1 kWp per MWh of annual consumption are normally not installed, but included in this analysis for a better understanding of the effect of demand patterns on PV orientation.

2.4.1 Optimal orientation for self-consumption

The optimal orientations to maximize self-consumption are closer to the optimal orientation to maximize energy production for smaller systems than larger systems. The latter orientation already results in a larger share of self-consumption, and lower export to the electricity grid, for these smaller systems. Therefore, the share of self-consumed energy that can be added due to optimizing the orientation is relatively small. Consequently, the influence of individual demand patterns on the self-consumption is lower, resulting in a slighter distribution range for smaller systems.

Larger PV systems have a relatively lower share of self-consumed energy at the optimal orientation to maximize energy production than the optimal orientation for self-consumption. Relatively more energy is produced and directly consumed in morning and evening hours. Consequently, the influence of individual demand patterns on the orientation increases as well for larger systems. Residential patterns have a higher volatility during the day than commercial patterns, see Fig. 2.1. Consequently, the orientation distribution for systems <1 kWp for each MWh of annual consumption have a broader range for residential than commercial systems, whereas for larger PV systems the opposite holds.

Azimuth angles for optimal energy production are between 181° to 188°, see Table 2.3. Residential systems show higher azimuth angles, whereas commercial systems have similar azimuth angles. The peak demand of residential buildings

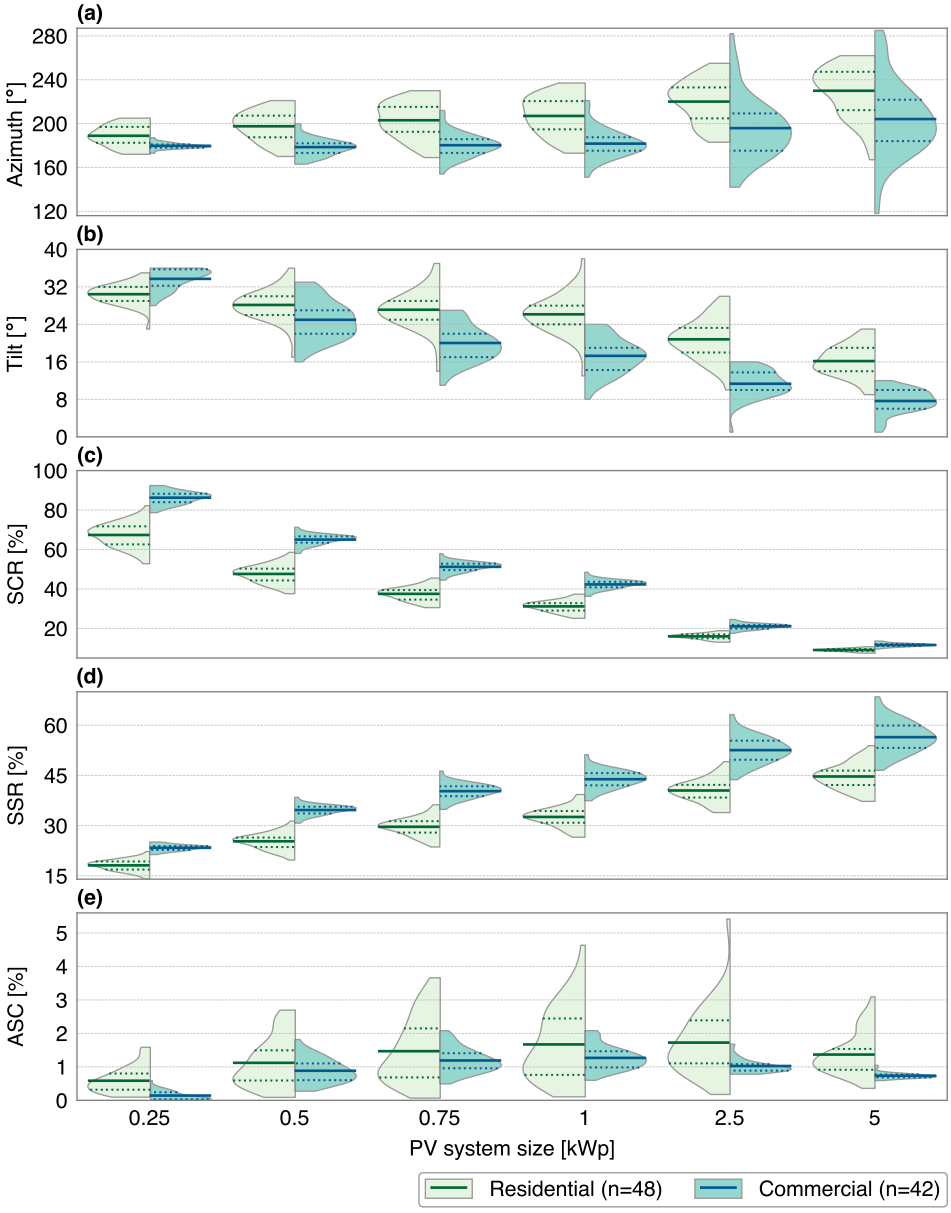

Figure 2.3 · Optimal orientation for annually maximized self-consumed energy (a & b), corresponding self-consumption ratio(c), self-sufficiency ratio(d) and added self-consumption (e) shown using violin plots. Distributions of residential systems (left part of the violin) and commercial systems (right part of the violin) are shown for six PV system sizes. Demand patterns were normalized to an annual energy consumption of 1 MWh and data of 2016 was used. Mean values of the distributions are marked by solid lines, and 25% and 75% percentiles are indicated by dotted lines.

is during late afternoon, whereas commercial buildings have a peak at noon, see Fig. 2.1. Consequently, the mean azimuth angles for residential systems are oriented south-west and for commercial systems oriented south.

Mean azimuth for residential systems increases with larger relative PV system size, while commercial systems show a small decrease. The optimal tilt decreases with an increasing PV system size, especially for commercial PV systems. A lower tilt angle results in a broader but lower daily PV profile, since energy is produced for a larger range of solar azimuth angles. This leads to higher self-consumption for commercial systems. Furthermore, the distribution ranges of optimal tilt angles are similar for commercial and residential systems, indicating comparable influences of demand patterns on the tilt.

2.4.2 Effect on self-consumption

SCR decreases with larger PV system size and is larger for commercial than residential systems. Commercial systems show a higher SCR because of a better match between PV production and energy demand. The SCR distribution ranges decreases with larger PV systems, indicating a reduced influence of the PV pattern on PV self-consumption. Also, the SSR is larger for commercial than residential systems and increases with PV system size. Contradictory to SCR, the SSR shows an increased distribution spread with larger PV systems, related to the relatively increased influence of the individual demand pattern.

ASC for commercial is smaller than for residential systems, showing that optimal PV orientation of commercial systems is closer to the optimal orientation for maximizing energy yield. Consequently, ASC distribution range is considerable larger for residential than commercial systems. In addition, ASC increases with PV system size, peaks at 2.5 kWp, and decreases for 5 kWp. Thus larger PV systems will increase SSR, but decrease ASC. Annual SCR and SSR are around 10% point higher for commercial systems than residential systems. Furthermore, the average ASC is larger for residential systems than commercial systems, for all investigated PV system sizes.

2.5 Minimize curtailed energy under feed-in limitations

Optimal PV orientations to minimize the curtailed energy were analysed for a 1 kWp PV system per MWh annual energy consumption with feed-in limitations from 0.1 till 0.7 kW/kWp. Distributions of these optimal orientations, and corresponding CLR and RCE are shown in Fig. 2.4. The CLR and RCE were calculated with an annual yield of 1086 kWh/kWp, derived from the optimal orientation for energy generation for 2016 (181° azimuth and 37° tilt).

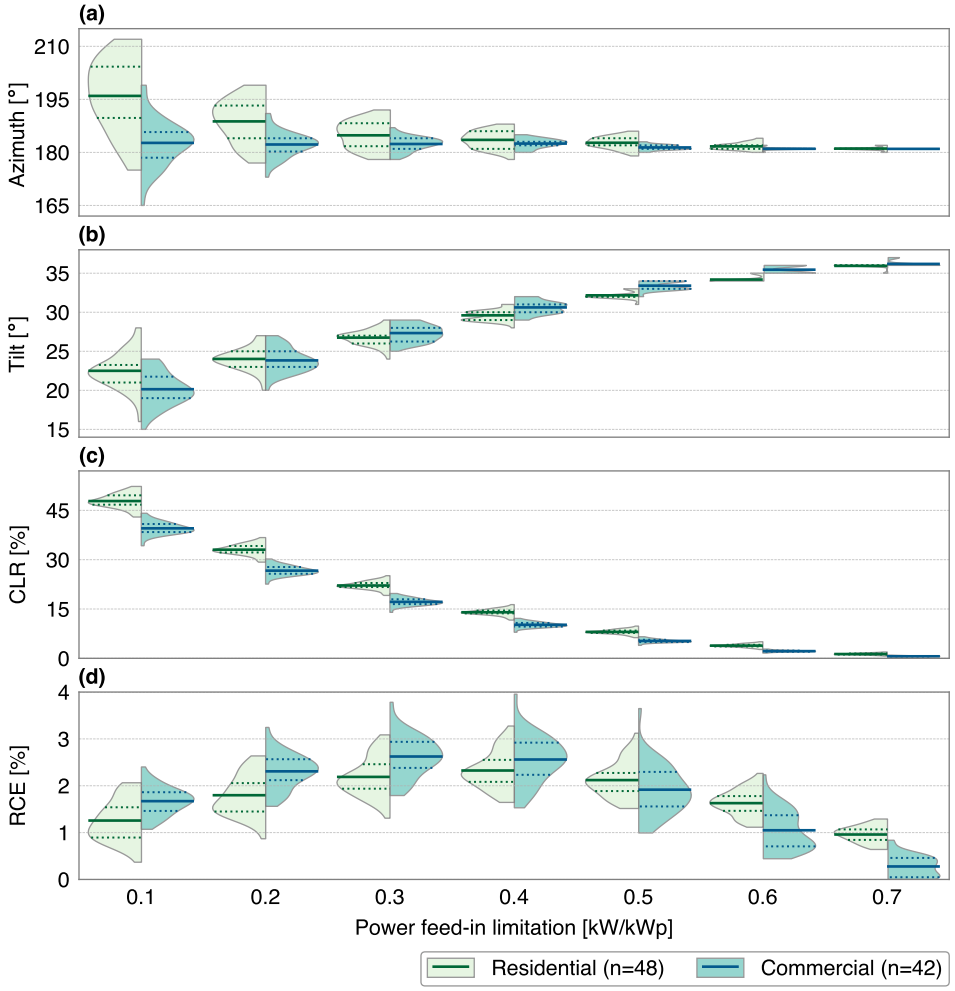

Figure 2.4 · Optimal orientation for annually minimized curtailed energy (a & b), corresponding curtailment loss ratios (c) and reduced curtailed energy (d) shown using violin plots. Distributions of residential systems (left) and commercial systems (right) are shown for seven power feed-in limitations. Demand patterns were normalized to an annual energy consumption of 1 MWh. Mean values of the distributions are marked by solid lines, and 25% and 75% percentiles are indicated by dotted lines.

With a strict feed-in limitation (0.1 kW/kWp), the optimal orientation to minimize curtailment losses is adjacent to the optimal orientation for maximizing annual energy production for commercial systems. Residential systems show a larger difference. With an enlarged feed-in limitation (towards 0.1 kW/kWp), most energy that is produced during noon time cannot be fed back to the grid. Subsequently, optimal PV orientation converges towards an orientation that increases PV self-consumption for low power demand. This is achieved by reducing

the tilt angle of the PV modules, thus flatten the PV yield profile and increase self-consumption in the early morning and late afternoon.

With a relaxed feed-in limitation (towards 0.6 kW/kWp), more energy can be fed-back to the grid. Thus, the optimal orientations converge towards the optimal orientation for energy production for both residential and commercial PV systems. Moreover, the influence of demand patterns on the optimal orientation decreases with reduced feed-in limitations. Consequently, the distribution range of optimal orientation is decreasing as well. Curtailment losses are larger for residential than for commercial PV systems and are reduced to a few percent for feed-in limitations of 0.7 kW/kWp.

Annual RCE is increasing till a limit of 0.3 and afterwards decreasing. A strict feed-in limitation of 0.1 kW/kWp has already a relative high curtailed energy loss under the optimal orientation for energy production, compared to a feed-in limitation of 0.3 kW/kWp. Consequently, the influence of changing the orientation to reduce curtailed energy losses is larger with an increase of feed-in limitation to 0.3 kW/kWp. A relaxed feed-in limitation of 0.7 kW/kWp has a relative low curtailed energy loss under the optimal orientation for energy production. Therefore, the change of curtailed energy losses by shifting the orientation is decreasing.

Annual reduced curtailed energy for feed-in limitations <0.3 is larger for commercial systems than residential systems, whereas for limitations >0.4 the opposite is seen. The benefit of optimizing PV orientation for RCE is larger for residential than commercial systems, and the RCE is below 4% for all patterns and feed-in limitations. A feed-in limitation of 0.5 kW/kWp has an averaged optimal PV orientation of 183° azimuth and 32° tilt for residential systems, and 181° azimuth and 33° tilt for commercial systems. This shows that reducing the tilt angle, compared to the orientation that maximizes energy yield, reduces the curtailed energy losses.

2.6 Maximize revenue

2.6.1 Fixed prices

Influences of price patterns with a constant price for a 1 kWp system are shown on the distribution plot of Fig. 2.5. Sold electricity has no economic value with a SPR of zero, thus maximizing self-consumption is most beneficial. Therefore, distribution of PV systems with different sizes and a SPR of zero are similar as in Fig. 2.3. Distributions for a SPR of 1 show optimal orientations for maximizing PV production.

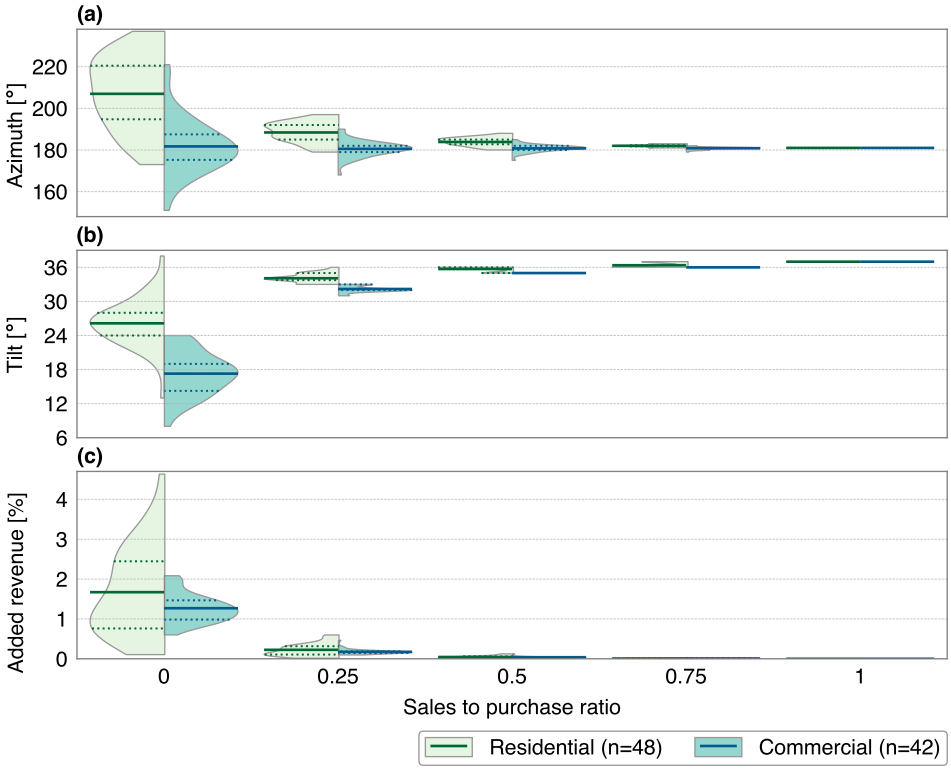

Figure 2.5 · Optimal orientation for maximized system revenue (a & b) and corresponding added revenue (c) shown using violin plots. Distributions of residential systems (left) and commercial systems (right) are shown for five fixed tariff pricing patterns. Demand patterns were normalized to an annual energy consumption of 1 MWh and data of 2016 was used. Mean values of the distributions are marked by solid lines, and 25% and 75% percentiles are indicated by dotted lines.

Both PV orientations of residential and commercial PV systems converge towards the optimal orientation for maximizing PV yield. Influence of variation between demand patterns is decreasing with an increase in SPR. Furthermore, added revenue of SPR >0.5 is very limited with values below 0.1%. Overall, the added revenue of PV systems is decreasing with exponential behaviour from ≈1.7% for residential systems and from ≈1.3% for commercial systems towards zero with larger sales to purchase ratios.

2.6.2 Time dependent market prices

Distributions of optimal orientations for time dependent pricing patterns for 7 years are presented in Fig. 2.6. The right seven distributions show results using Dutch prices and the left seven results using German prices, both for a PV system size of 1 kWp and a SPR of 0. A SPR of 0 is chosen to show the orientations for maximizing the value of self-consumed energy. The value of sold electricity is zero

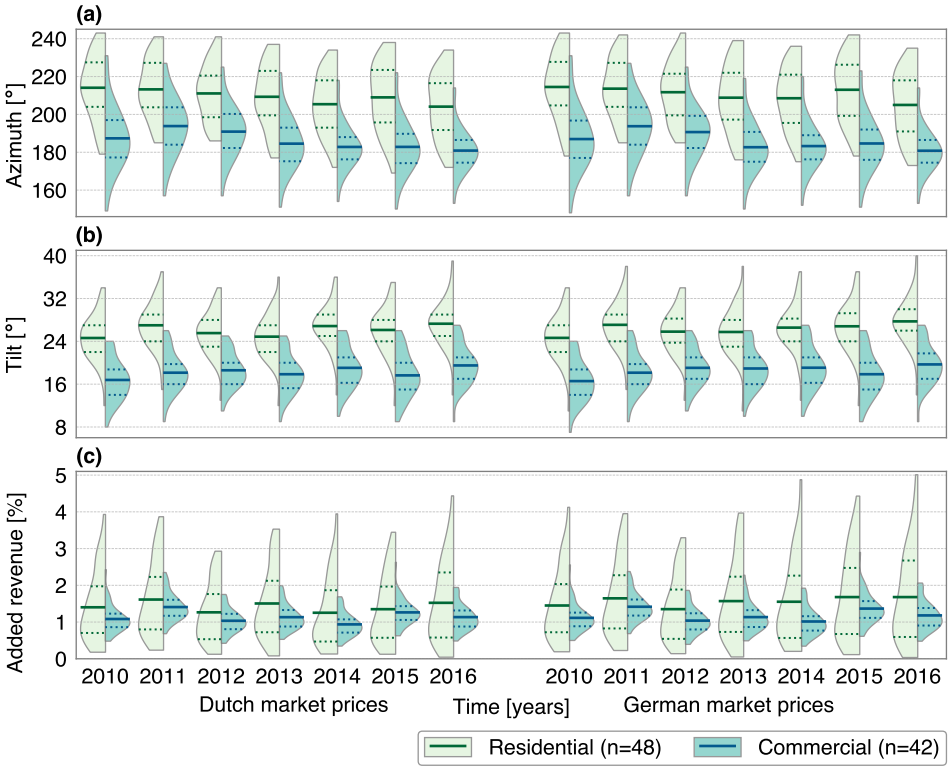

Figure 2.6 · Optimal orientation for maximized system revenue (a & b) and corresponding added revenue (c) shown using violin plots. Distributions of residential systems (left) and commercial systems (right) are for two markets and seven years. Results are shown for a PV system size of 1 kWp, a SPR of 0 and demand patterns were normalized to 1 MWh of annual energy consumption. Mean values of the distributions are marked by solid lines, and 25% and 75% percentiles are indicated by dotted lines.

with an SPR of 0. Thus, PV self-consumption on moments with a relatively higher electricity price is more valuable than PV self-consumption on moment with a relatively low electricity price. German market prices have a larger variance in prices between the early morning hours and afternoon hours than Dutch market prices, which influences the optimal orientation. This is especially visible for 2014 and 2015, shown by the difference in optimal azimuth angle. Residential systems show ≈3° higher azimuth angles for German prices than Dutch prices.

The average annual azimuth angles varied between 204° and 214° for residential systems, indicating a significant influence of each year on the optimal azimuth. The average optimal tilt angle varies between 24° and 28°. Furthermore, the distribution range for residential systems is larger than the range show for maximizing self-consumption, see Fig. 2.3. Commercial systems have average annual azimuth angles between 180° and 194° and tilt angle between 17° and 20°.

The range of annual difference between azimuths is larger for commercial than residential systems. The optimal orientation for commercial systems is closer to the orientations presented for the electricity markets without self-consumption (see Table 2.3) than residential systems. Hence, the influence of the annual variation in market prices is larger on commercial than residential systems.

There is a small correlation between the orientations for the electricity markets without self-consumption and including self-consumption. Relative high azimuth angles for maximizing profit with self-consumptions were found for 2011 and 2012 for Dutch market prices, and for 2011, 2012 and 2015 for German market prices. Residential and commercial systems show for these years a higher azimuth angle than the seven years average azimuth angle.

Mean tilt angles of residential and commercial systems are always lower than the optimal tilt angles for scenarios without self-consumption, see Table 2.3. Commercial systems show lower tilt angles than residential systems. A lower tilt angle results in a lower, but broader, daily PV yield. Hence, more moments in time have PV energy production, which increases the self-consumption for commercial systems.

The larger variance in market prices results in slightly more benefits for German prices than the Dutch prices. Average annual added revenue for residential systems is between 1.3% and 1.6% for Dutch prices and between 1.4 % and 1.7% for German prices. Commercial systems show benefits between 1.0% and 1.4% for both markets.

2.6.3 Comparison of nine scenarios

Optimal orientations to maximize added revenue for nine different scenarios is presented in Table 2.4. The scenarios are created by varying the price patterns and SPR for residential and commercial systems. The price patterns were varied between fixed price patterns and time-of-use price patterns (Dutch and German market prices). SPR were varied between 0, 0.5 and 1, therefore representing minimum and maximum values of energy fed back to the grid. A 1 kWp PV system was used with annual data from 2010 till 2016. Corresponding added self-consumption is presented in the last column.

Residential PV systems with an SPR of 0 show a large range in azimuth and tilt angles. This range indicates a large variance among the demand patterns. Differences in values between the R1 and the R4 scenario are small due to the low variance of the Dutch price pattern. The R1, R4 and R7 scenarios show the largest range of optimal orientations with azimuth angles from 169° till 247° and tilt angles from 11° till 40°. Largest revenues are observed for scenarios with an SPR of 0.

Table 2.4 · Comparison of optimal orientation to maximize revenue for 9 different scenarios. Residential system scenarios are indicated by a R, commercial with a C. Values are for a PV system of 1 kWp, an annual consumption of 1 MWh and for each year between 2010 till 2016.

Scenario	Price patterns	SPR	Azimuth [°]			Tilt [°]			Maximized AR [%]			Corresponding ASC [%]		
			Mean	Range		Mean	Range		Mean	Range		Mean	Range	
R1	Fixed	0	212	172	247	25.8	11.0	38.0	1.56	0.09	4.63	1.56	0.09	4.63
R2	Fixed	0.5	188	180	196	34.4	31.0	37.0	0.04	0.00	0.15	0.35	0.00	1.29
R3	Fixed	1	185	181	188	35.6	33.0	38.0	0.00	0.00	0.00	0.00	0.00	0.00
R4	Dutch	0	209	169	243	26.0	12.0	39.0	1.42	0.04	4.44	1.55	0.07	4.62
R5	Dutch	0.5	184	176	191	34.7	32.0	38.0	0.03	0.00	0.13	0.07	-0.22	0.59
R6	Dutch	1	182	177	187	35.5	33.0	38.0	0.04	0.00	0.12	-0.18	-0.82	0.19
R7	German	0	211	173	243	26.3	11.0	40.0	1.56	0.03	5.01	1.55	0.06	4.62
R8	German	0.5	184	176	193	35.0	31.0	39.0	0.03	0.00	0.14	0.08	-0.30	0.86
R9	German	1	182	176	187	35.8	32.0	39.0	0.04	0.00	0.13	-0.20	-0.82	0.15
C1	Fixed	0	188	148	237	17.2	7.0	26.0	1.22	0.38	2.57	1.22	0.38	2.57
C2	Fixed	0.5	185	175	192	33.6	30.0	36.0	0.04	0.01	0.19	0.25	0.07	1.02
C3	Fixed	1	185	181	188	35.6	33.0	38.0	0.00	0.00	0.00	0.00	0.00	0.00
C4	Dutch	0	186	149	231	18.2	8.0	27.0	1.14	0.35	2.63	1.21	0.37	2.57
C5	Dutch	0.5	181	172	188	34.0	31.0	37.0	0.08	0.00	0.43	0.21	-0.03	1.40
C6	Dutch	1	181	175	186	35.3	32.0	37.0	0.06	0.00	0.22	0.06	-0.37	0.92
C7	German	0	186	148	231	18.5	7.0	27.0	1.18	0.34	2.89	1.21	0.37	2.57
C8	German	0.5	181	169	189	34.2	31.0	37.0	0.08	0.00	0.47	0.19	-0.06	1.48
C9	German	1	180	173	186	35.4	32.0	39.0	0.06	0.01	0.23	0.04	-0.38	1.10

Commercial systems have lower mean azimuth angles in almost all pricing scenarios compared to residential systems. Especially, optimal orientation values for fixed pricing scenarios are closer to the maximum orientation for energy generation. Also, mean AR values from fixed pricing scenarios are lower for commercial systems. In SPR 0 scenarios, Dutch and German market price show higher mean AR values for residential systems than commercial systems.

The influence of market prices is larger in the SPR 0.5 and 1 scenarios. Consequently, the difference in mean AR between residential and commercial systems is smaller. Also, in the SPR 0.5 and 1 scenarios, the AR for commercial systems is larger than residential systems. Commercial systems have comparable AR values as shown for maximized revenue without self-consumption, see Table 2.3. Residential and commercial systems show small differences in optimal orientations between scenarios with German market prices and Dutch market prices.

SPR 0 scenarios show a larger range of corresponding ASC and a higher mean ASC for residential than commercial systems. However, the opposite is seen for the scenarios with time dependent market prices and a SPR of 1. These scenarios even show negative corresponding ASC values for residential systems, indicating a conflict in orientation between maximizing revenue and maximizing self-consumption. Optimal orientations for maximizing revenue are closer to orientations that maximize self-consumption for commercial systems than for residential systems. Consequently, the larger difference between these orientation results in lower corresponding ASC values for residential systems. Especially, the R6 and R9 scenario have respectively mean ASC values of -0.18% and -0.20%, with maximum self-consumption losses up to -0.82%.

2.6.4 East-West orientation

A common PV system design on flat roofs is the dual-tilt (or east-west) design. This reduces wind load on PV modules, decreases shading losses and increases the amount of PV modules that can be placed on a roof. This setup requires an azimuth difference of 180° between the first (m1) and second (m2) module and can have a tilt from 10° to 15° for both modules. The optimal azimuth angles for this setup, combined with a tilt angle of 13° for both modules, for each scenario, is presented in Table 2.5.

Mean optimal orientation for residential PV systems is in all scenarios between 91° and 94° for the panel oriented eastwards. Commercial PV systems have lower azimuth values, with mean values between 85° and 91°. Furthermore, the difference between scenario C7 and C8 is comparable to the result that includes optimal tilt, see Table 2.4.

Table 2.5 · Comparison of optimal orientation to maximize revenue for 9 different scenarios with a dual-tilt PV system design. The PV modules are placed under a tilt angle of 13°. Residential system scenarios are indicated by R, commercial by a C. The values are for a PV system size of 1 kWp, an annual consumption of 1 MWh and for each year between 2010 till 2016. The range presents the minimum and maximum value of the first module.

Scenario	Price pattern	SPR	Azimuth [°]	
			Mean (m1 , m2)	Range (m1)
R1	Fixed	0	94 , 274	75 105
R2	Fixed	0.5	91 , 271	83 97
R3	Fixed	1	90 , 270	85 94
R4	Dutch	0	91 , 271	75 105
R5	Dutch	0.5	92 , 272	84 100
R6	Dutch	1	92 , 272	86 97
R7	German	0	91 , 271	75 105
R8	German	0.5	91 , 271	84 99
R9	German	1	91 , 271	86 96
C1	Fixed	0	89 , 269	75 105
C2	Fixed	0.5	89 , 269	82 95
C3	Fixed	1	90 , 270	85 94
C4	Dutch	0	85 , 265	75 105
C5	Dutch	0.5	89 , 269	80 97
C6	Dutch	1	91 , 271	85 96
C7	German	0	85 , 265	75 105
C8	German	0.5	89 , 269	81 96
C9	German	1	90 , 270	85 95

2.7 Temporal influences

We analysed the hourly contribution and monthly contribution of added self-consumption, reduced curtailed energy and added revenue of 2016. The contributions of ASC were determined using the orientation found for maximizing self-consumption annually, see Fig. 2.3. Contributions of RCE were analysed using the orientations found to minimize the annual energy curtailed and a feed-in limitation of 0.5 kW/kWp was used. Contributions of AR were determined using the orientations found for maximizing annual revenue for the Dutch market. The analysis was conducted for a PV system size of 1 kWp and demand patterns were normalized to an annual energy consumption of 1 MWh. Added revenues were calculated with a SPR of 0.5 and with Dutch market prices from 2016. The orientation was kept constant over the year for each system.

2.7.1 Hour of the day contribution

Hour of the day contributions are shown in Fig. 2.7. Residential PV systems have negative ASC values between 6.00 and 9.00, due to the optimal module azimuth for self-consumption of 212°. Subsequently, ASC is increasing in the afternoon and positive in evening hours. Commercial PV systems show a relatively constant ASC value during the day. Furthermore, the distribution range increases in morning and evening hours, especially for residential systems. This is a result of the larger distribution of residential demand, especially shown in the afternoon.

Reduced curtailed energy distributions for a feed-in limitation of 0.5 kW/kWp clearly indicate the hours for in which losses and benefits are gained by minimizing the curtailed energy. PV peak production occurs more in the afternoon than

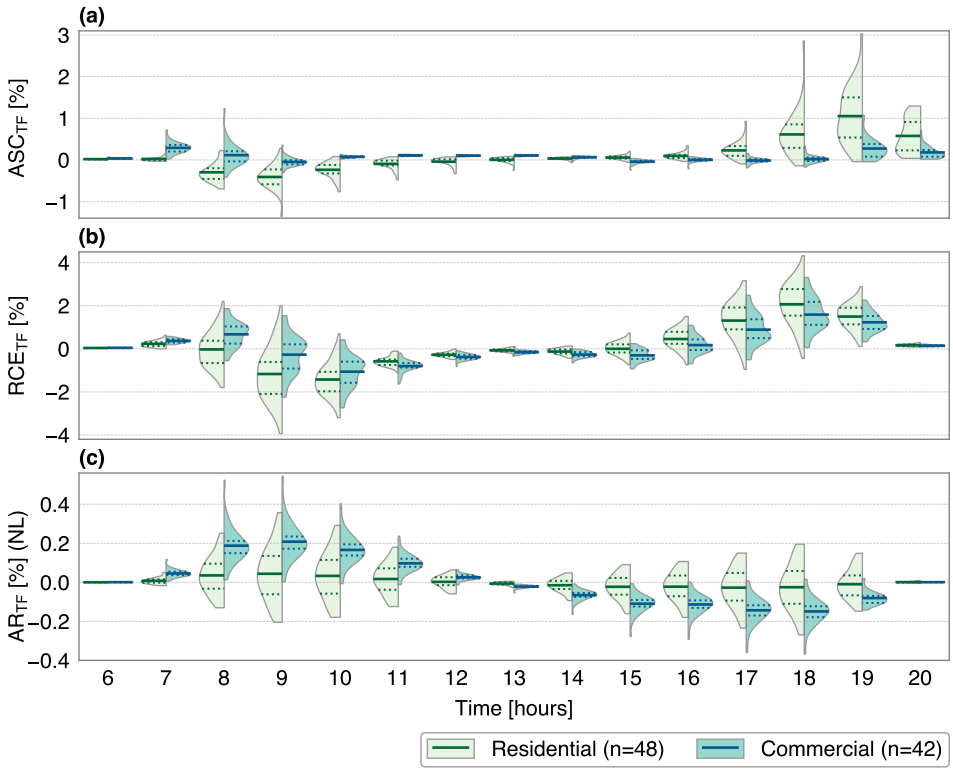

Figure 2.7 · Hour of the day contribution for added self-consumption (a) reduced curtailed energy (b) and added revenue for the Dutch prices (c) shown using violin plots. Distributions of residential systems (left) and commercial systems (right) are for a PV system size of 1 kWp and for 2016. Demand patterns were normalized to an annual energy consumption of 1 MWh. Reduced curtailed energy was calculated with a feed-in limitation of 0.5 kW/kWp and added revenue was calculated with a SPR of 0.5 and the year 2016. Mean values of the distributions are marked by solid lines, and 25% and 75% percentiles are indicated by dotted lines.

in the morning hours thus more PV energy is curtailed within these hours. Therefore, the effect of optimizing on curtailed energy is positive in the afternoon, yet negative in morning hours. Lower RCE fractions are shown for residential systems than commercial systems in morning hours and the opposite is seen in the afternoon hours. Residential systems have a higher optimal azimuth angle for RCE compared to commercial systems. Hence, less PV energy is produced in the morning hours, resulting in lower RCE values.

AR distributions of the Dutch market prices show on average a constant value for residential systems, but a variance for commercial systems. Residential systems have a higher optimal module azimuth than commercial systems. Hence, residential systems produce less PV energy and have lower added revenue in the morning. More energy is produced by residential than commercial systems in the afternoon, resulting in larger benefits for residential systems. AR distributions using German market prices show a similar daily pattern as shown with Dutch prices, and are therefore not shown here.

2.7.2 Monthly contribution

Monthly contributions are visualized with the distribution plot of Fig. 2.8. ASC distributions show negative values for the first, second month, and last three months of the year for both residential and commercial PV systems. These months have an optimal tilt angle higher than the annual optimal tilt angle for self-consumption, resulting in a relative loss of self-consumption, especially for residential systems. Yet, ASC values are positive from April until September, with averages of ≈0.3% for commercial and ≈0.5% for residential PV systems. Thus, the lost self-consumption from winter months is overcompensated by the gain from summer months. Also, a large distribution range is shown for higher absolute ASC values, especially for residential systems.

Monthly contributions of RCE show only positive mean average values for April till August. These months have a higher share of PV power production which excesses the feed-in limitation. The lower optimum tilt angle for RCE, compared to the optimum tilt angle for energy production results in a broader but lower daily PV profile. Therefore less energy has to be curtailed, which is especially visible for these months. Residential and commercial systems show a similar pattern over the year which is comparable with the ASC pattern. Monthly AR contribution using Dutch and German market prices shows very small variation over 2016, with all values between -0.11% and +0.12%. Positive values are shown in summer months and negative values in winter months. However, German market prices have positive AR contributions in winter months, and negative in summer months, especially for residential systems. German market prices were

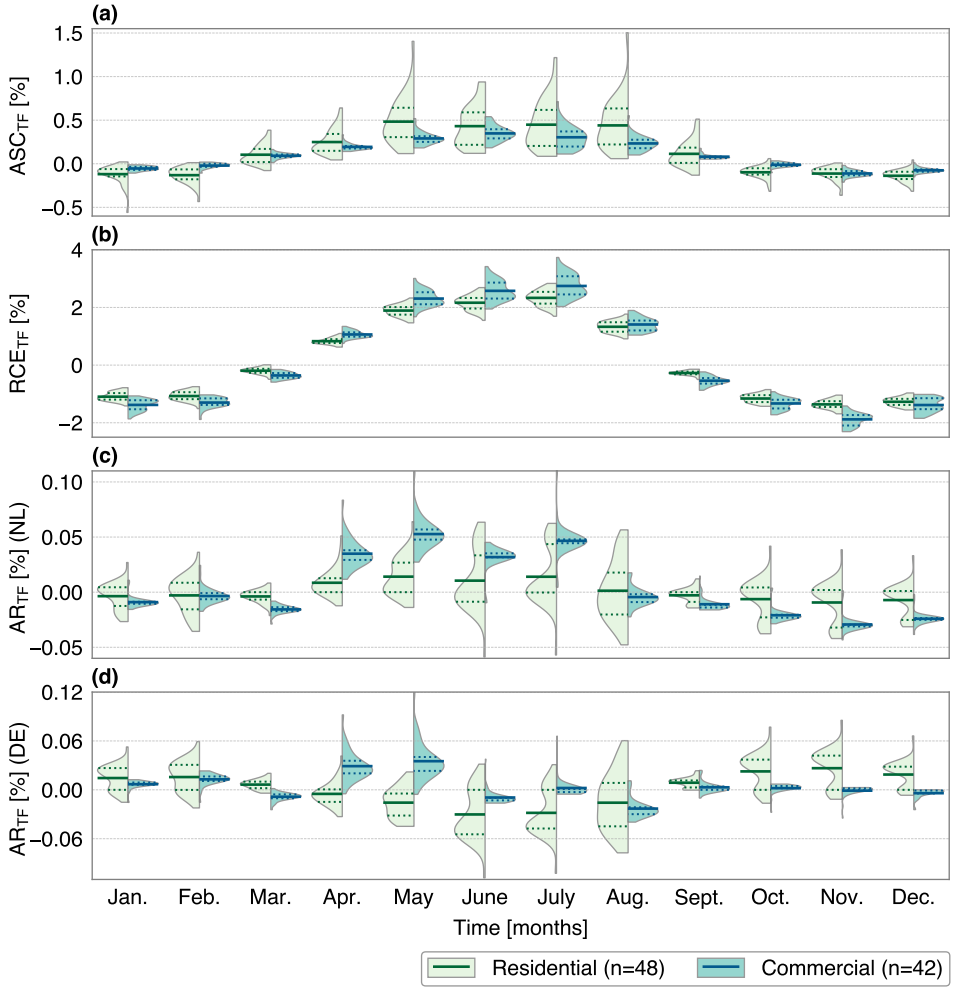

Figure 2.8 · Monthly contribution for added self-consumption (a) reduced curtailed energy (b) and added revenue for the Dutch prices (c) and German prices (d) shown using violin plots. Distributions of residential systems (left) and commercial systems (right) are shown for similar assumptions as used for Fig. 2.7. Mean values of the distributions are marked by solid lines, and 25% and 75% percentiles are indicated by dotted lines.

relative lower than Dutch market prices for these periods, resulting in a lower benefit from self-consumption.

Market prices in April and May were relatively low between the 11th and 15th hour of the day. Thus, the value of self-consumed energy during the day increased. Between these hours, self-consumption for residential systems is lower than commercial systems. Consequently, April and May showed larger added revenues for commercial systems than residential systems.

2.8 Discussion

In this research, we presented different optimal orientations, depending on optimization goal, demand patterns, PV system size and electricity prices. Clear trends are observed between the various optimization goals. Maximizing self-consumption is profitable with fixed prices, especially when there is no income from electricity fed to the grid. Reduced curtailed energy due to optimizing PV system orientation is 2.1 % for residential and 1.9% for commercial systems, for a feed-in limitation of 0.5 kW/kWp. Optimizing orientation to maximize profit is interesting for time-of-use tariffs especially when a large difference between the sales and purchase prices is present.

Results on the influence of PV systems size and demand patterns on the optimal PV orientation are comparable with previous studies that included German demand patterns[54,57]. Also, results from the German market are similar to a study including German and Austrian markets[53]. Other results shown in this paper are different from results of previous studies due to different markets[50–52].

Our study did not account for the obvious limitation of pre-defined building characteristics. Optimizing the PV orientation is only possible for buildings with flat roofs. The orientation for most PV systems depends on the roof orientation of a building. In the Netherlands, most residential buildings have a pitched roof, yet most commercial buildings have flat roofs available, enabling optimized orientation. Also, a change in orientation could lower the maximum power output of a PV system. Consequently, potential smaller inverters can be used for these systems. These inverters could reduce PV system costs, leading to additional benefits that are not included in our study.

2.8.1 Data limitations

Our research has several limitations that could affect the findings. Residential and commercial load is influenced by weather conditions, mainly by temperature[66]. Only measured demand data of 2013 was used, therefore results of other years are influenced by this effect. The difference between the mean optimal orientation values of 2013 and the mean orientations values of other years (2010 till 2012 & 2014 till 2016) were analysed for nine scenarios and shown in Table 2.6.

Residential and commercial systems show similar difference in mean azimuth, ranging between ≈-4.8° and ≈-1.9°. Differences in optimal tilt are significant lower for both residential and commercial systems, between ≈-0.16° and ≈+0.09°. The difference in optimal orientation between the measured year and modelled years is smaller than the range in optimal orientation observed, see Table 2.4. Therefore, we suggest that the influence of the individual demand pattern on the optimal orientation is larger than the influence of weather.

Table 2.6 · Difference between mean orientation values of 2013 with mean values of other years (2010 till 2012 & 2014 till 2016) for residential (Res.) and commercial (Com.) systems for nine scenarios, previously explained in section 2.6.4.

Scenario	Price pattern	SPR	Δ Azimuth [°]		Δ Tilt [°]	
			Res.	Com.	Res.	Com.
1	Fixed	0	-0.59	-1.90	-0.16	0.03
2	Fixed	0.5	-2.30	-2.34	-0.16	-0.15
3	Fixed	1	-2.33	-2.33	-0.10	-0.10
4	Dutch	0	-0.17	-1.89	-0.19	-0.06
5	Dutch	0.5	-2.69	-2.48	-0.13	-0.14
6	Dutch	1	-2.67	-2.65	-0.09	-0.13
7	German	0	-2.23	-4.02	-0.10	0.08
8	German	0.5	-4.58	-4.31	0.05	0.02
9	German	1	-4.75	-4.62	0.04	0.09

The measurement interval of demand patterns was 15 min, resulting in a more smoothed pattern than the actual pattern. The PV yield pattern is smoothed out by 10 min, therefore missing high PV power peaks caused by cloud enhancement. As a result, the overlap of the PV pattern with the demand pattern changes, which leads to slightly different results. However, a previous study found that relative errors were below 6% when using 15 min data to calculate PV self-consumption[67]. In addition, irradiance and demand patterns were measured for locations in the Netherlands, however our results could be used for other locations that show similarity in irradiance and demand patterns. A study for other countries with different irradiance and demand patterns is recommended for further research. Also, we modelled PV patterns without additional losses. In the built environment shade losses could occur, resulting in lower production in morning and evening hours.

2.8.2 Future trends

We used historical demand patterns, whereas future residential and commercial demand could shift due to increasing electrification by heat pumps and electric vehicles. Especially electric vehicles are expected to shift the peak demand for residential buildings to the evening, when residents arrive home and charge their electric vehicle. As a result, west oriented PV systems can increase their revenue even more. On the other hand, charging of electric cars can also increase energy demand of commercial buildings. When employees charge their electric vehicles in the morning hours, east oriented PV systems could be more beneficial for self-consumption. Alternatively, electric vehicle using charging algorithms aimed at optimizing PV self-consumption have been suggested[68].

PV systems combined with energy storage change the optimal orientation, depending on the battery storage size and algorithm. With sufficient battery capacity, the optimal orientation for maximizing energy production will be more beneficial, as found in a previous study[54,69]. However, additional energy loss occurs due to charging and discharging of the battery, resulting in a lower efficiency of the total system.Demand side management applications could shift the load towards moments with high solar irradiance, therefore influencing the optimal orientation. Also, electricity price signals can influence the electricity time-of-use for residential and commercial buildings. The effect of energy storage, demand side management and price signals on the optimal orientation from a system perspective is unknown. Therefore, we recommended investigating the optimal PV orientation with demand patterns including these opportunities.

It is expected that electricity market prices become more volatile with an increasing share of renewables. An increase of PV production during day time will lead to decrease of market prices, causing more benefits for east and west oriented PV systems. This is already visible from differences between the results using Dutch and German market prices. German market prices are influenced by a larger share of renewables compared to Dutch market prices. Therefore, lower prices are observed during moments when a larger share of electricity is produced from renewables. Furthermore, the difference in market design and limited interconnector capacity between the Dutch and German electricity markets affects the results. Yet, this could change in the future by integrating markets and increasing interconnection capacity, resulting in smaller differences between these two markets.

2.9 Conclusion

We combined 48 residential and 42 commercial demand patterns with different PV system capacities, feed-in power limits and market prices to determine the optimal PV orientation for seven individual years. Annual values for self-consumption, curtailed energy and revenues under the optimal orientation were compared with an orientation that maximizes annual energy production. Furthermore, nine different pricing scenarios were compared on the optimal orientation for maximizing added revenue. Our findings show a clear relation between PV orientation, demand pattern and electricity prices.

Commercial systems have relative more energy consumption during noon, whereas residential systems during the evening. Consequently, residential systems have a higher average azimuth angle for optimizing self-consumption compared to maximizing energy yield, whereas commercial systems have a similar

average azimuth angle. Maximizing self-consumption can be achieved with an azimuth of 212° and a tilt of 26° for residential and 188° azimuth and 17° tilt for a commercial PV systems. Maximum increase in self-consumption found for residential systems was 4.6% and commercial systems 2.6%.

A significant impact of reducing curtailment losses of the PV orientation was observed, dependent on the feed-in limit. A lower module tilt angle flattens the PV yield profile which decreases the curtailment loss. Annual curtailed energy losses can be reduced with ≈2.1% for residential and ≈1.9% for commercial systems, under a feed-in limitation of 0.5 kW/kWp.

A small difference among optimal orientation for maximizing added revenue was found between Dutch and German market prices. Azimuth angles for German market prices are ±1° different than Dutch market prices. Variances concerning tilt angles between these two markets are of the same order. Therefore, similar added revenue for Dutch as for German market prices was found. Low sales to purchase ratios lead to a higher influence of demand patterns, resulting in a larger variance of optimal orientations.

The maximum revenue for PV systems can be increased up to 5.0% for certain demand patterns and scenarios. Also, orientations that were maximized for revenue showed negative ASC values, indicating a conflict between optimizing orientation for maximizing self-consumption or optimizing for maximizing revenue. Nevertheless, this shows that a loss of self-consumption could be beneficial.

Analysing the contribution of three different temporal factors provided useful insight in the obtained results. Hour of the day analysis indicated that increasing self-consumption occurs in the evening hours for residential systems. Curtailed energy is reduced significantly around noon as a result of a lower module tilt angle. Furthermore, a small monthly variation was found for added revenue.

Including PV, demand and market price patterns gave a better insight on the optimal PV orientations. Especially, the variance between investigated demand patterns largely affects the orientation. To conclude, we advise that decisions related to the orientation of PV systems should not only focus on maximizing energy production, but also include expected demand patterns and market prices.

Acknowledgements

This work is part of the research programme Transitioning to a More Sustainable Energy System (Grant No. 022.004.023), which is financed by the Netherlands Organisation for Scientific Research (NWO). We are grateful to Hubert Spruijt of Senfal, Liander N.V. and the Royal Netherlands Meteorological Institute for providing data.

3

Forecasting methods for PV-battery systems

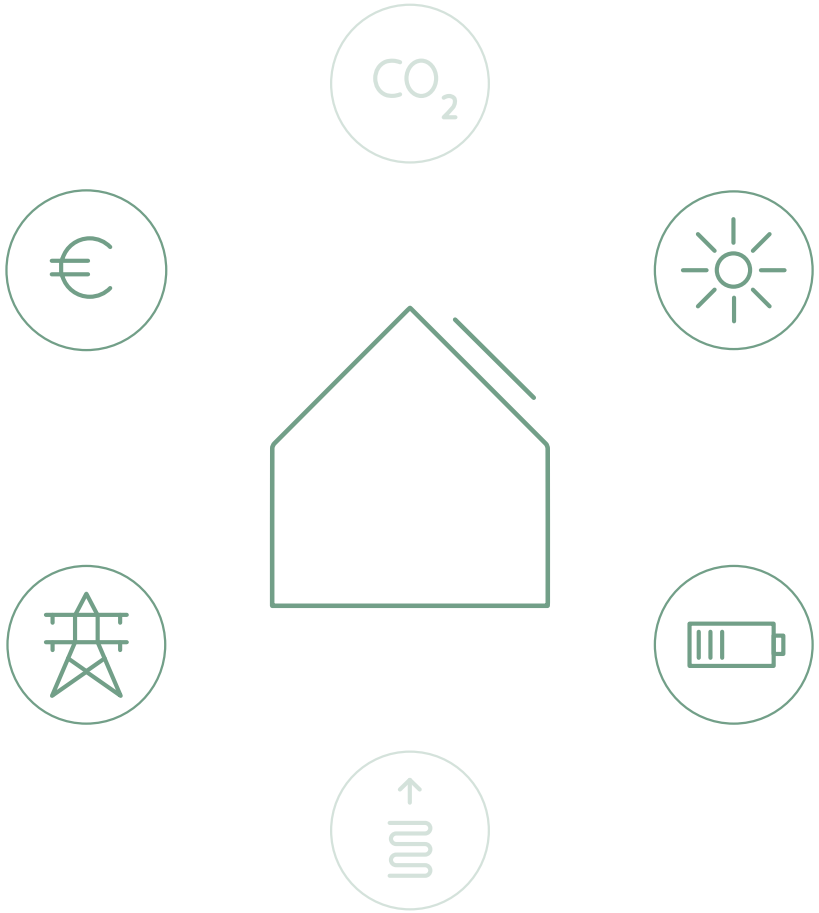

This chapter is based on the publication: G.B.M.A. Litjens, E. Worrell and W.G.J.H.M. van Sark. "Assessment of forecasting methods on performance of photovoltaic-battery systems". in: *Applied Energy* **211** (2018), pp. 358-373. DOI:10.1016/j.apenergy.2018.03.154

Abstract

Photovoltaic (PV) systems are increasingly deployed on buildings in urban areas, causing additional power flows and frequency fluctuation on the low voltage electricity grid. Control strategies for PV-battery energy storage systems (BESS) assist in reducing power flows to the grid and improve the self-consumption of PV generated electricity. Therefore, these control strategies require accurate forecasts of PV electricity production and electricity consumption. We developed and assessed relatively simple forecasting methods using 5 min resolution data, to predict the PV yield and to forecast electricity consumption for one year. We used these forecasts with a predictive control strategy to increase PV self-consumption, decrease curtailment losses and improve BESS revenues. Electricity demand patterns of 48 residential and 42 commercial Dutch buildings were used. PV yield forecast methods that uses predicted weather data shows the lowest forecast error. The best performing forecast method for predicting energy consumption of residential buildings requires historical energy consumption data of the previous seven days. Commercial systems require historical energy consumption of the previous weekday. Significant reduction in curtailment losses is achieved using predictive control strategies, especially in combination when clear-sky radiation data is used to forecast PV yield. Similar self-consumption ratios were found for predictive control as for real-time control. This indicates that reduction of curtailment loss can be combined while maintaining the level of PV self-consumption. Revenues from battery storage are increased by forecast methods and are highly dependable on boundary condition of a PV-battery system, such as the feed-in limit (FIL) and the feed-in tariff. Therefore, we recommend customizing battery control strategies based on these system boundaries conditions to improve energy storage potential.

3.1 Introduction

Optimal integration of photovoltaics (PV) produced energy in the low voltage electricity grid supports cost effective transition towards a fully sustainable energy system. One way to enhance PV system integration is using battery energy storage systems (BESS). PV systems with batteries enable the use of PV produced energy at later moments. Subsequently, more locally produced energy is used and thus PV self-consumption increased. PV-battery systems can reduce the impact on low voltage electricity grids when using algorithms that properly reduce PV peak power. Consequently, investments in new cables and transformers can be deferred to later years, thus saving on necessary update investments. Higher PV self-consumption lower grid losses and potentially reduces CO_2 emissions from fossil-based backup power generation, especially when curtailment of PV energy is avoided[13]. Another important economic incentive for self-consumption is the absolute difference in consumption tariff and feed-in tariff. This difference indicates the economic value of the self-consumed electricity. Due to all these benefits, PV self-consumption is becoming a major incentive for continued PV market growth in urban areas[70]. Subsequently, policies supporting PV self-consumption are developed and implemented in multiple countries[47].

Feed-in limits (FIL) restrict the maximum power flow which is exported back to the electricity grid. These are usually given as a percentage of the installed PV system capacity. Therefore, high PV peak power is avoided on the local electricity grid which increases power quality in low voltage grid. Electricity from PV systems that is not exported nor used is lost, also known as curtailment losses. Consequently, financial support schemes are developed that support the storage of PV peak power. For instance, PV-battery systems in Germany can apply for financial support when the power flow back to the grid is limited to 0.5 kW for each kWp of installed PV capacity[48]. Furthermore, a lower feed-in power results in a lower grid connection and potentially a reduced grid connection fee. In choosing the best charging and discharging times, forecasts of PV electricity production and electricity consumption are essential. Therefore the curtailment losses will be reduced and the level of PV self-consumption can be maintained.

3.1.1 Literature review

Several studies examined forecasting methods for PV yield and electricity consumptions. A comprehensive overview of PV forecasting methods has been given in a recent review[71]. This study divided forecasting methods into probabilistic forecasting and deterministic forecasting. Most of these studies used historical measured data and/or weather data. For example, PV forecast methods have been developed that used power output of neighbouring PV systems[72]. Also,

various methods have been proposed to demand forecasting in a recent literature review, which made a division between statistical based and artificial intelligence based models[73]. Time-of-use models have been proposed to predict energy consumption based on the user and appliances within a building[74]. A limited amount of studies assess the influence of these forecasts on the performance of control strategies for PV-battery systems. A recent review found that control strategies using forecasting data with feed-in power limits showed manageable curtailment losses. These strategies are promising, especially when feed-in limitations are further reduced[75]. A study including a German residential demand profile has shown that 26% more PV capacity can be added to the grid by using PV-battery systems with persistence forecast algorithms[76]. A Swiss study assessed a control strategy that used forecasted PV power production under clear-sky conditions for residential systems. This strategy has a shown a similar performance in reducing curtailment losses as an exact PV forecast[77]. Also, control strategies using variable time horizons from historical PV production data have been proposed and assessed[78–82]. These control strategies used diverse methods to determine the optimal battery state for each time step. Moreover, Markov chain-based forecasting approaches have been suggested for optimizing battery control strategies[83].

The economic profitability of PV-battery systems depends on the aim of the used control strategy. Storage of PV electricity to mitigate over-voltage problems could be economically viable, if feed-in tariffs are higher than off-peak consumption tariffs[84]. However, considering that a large share of the consumption tariff consists of taxes, a feed-in tariff higher than a consumption tariff seems not plausible. Control strategies that included a minimization of dwell times for high battery state of charges (SOC) could improve battery life time[85]. For example, a strategy that only stored PV energy required to meet the energy demand for the following night could be used to achieve this aim[86]. Also, forecast based strategy reduced the electricity bill of German households especially when a feed-in limit is present[87].

The literature illustrates that performance of control strategies for BESS is directly influenced by the accuracy of the forecasted energy consumption of a building and PV production. Furthermore, a recent review study identified that the economic impact of forecasting has not been studied in depth. More knowledge on the influence of the combination of electricity demand and PV production forecast methods is required to understand its impact on the PV-battery system. The influence of combining forecast methods on performance of PV-battery systems with different energy demand patterns is not well known. Most studies use a limited number of residential demand patterns. Also, studies that assess the

performance of commercial PV-battery systems, for example for office buildings, were not found.

3.1.2 Research aim

The aim of this study is to assess the influence of PV and demand pattern forecasting methods on the performance of the PV-battery system, using a predictive control strategy. This strategy aims to reduce curtailment losses without reducing the self-consumption of the PV-battery system. Previous studies mainly used single or a few demand patterns to assess forecast methods. Our paper goes beyond these studies by using 48 residential and 42 commercial electricity consumption patterns from a full year (2013) to test our forecasting methods. We present the results in the form of distributions and statistics which give realistic prognoses.

Most studies asses the performance of PV-battery systems using a single forecast method, or assume a perfect forecast. Besides sophisticated models, for example Markov chain models or artificial neuron network, are commonly used to predict system behaviour. We aimed to develop simple statistical based forecasting methods to use in a battery control strategy. The developed methods are easily applied to real-time applications and require less computational power and data storage space. We believe this will increases the implementation potential over the more sophisticated models.

Four methods to predict the PV yield and three methods to forecast energy consumption of residential and commercial (office) buildings were developed and assessed. A novel battery capacity reservation algorithm was developed that uses forecasting data. This algorithm updates the battery capacity reservation based on the predicted demand and PV yield for each 5 min for each day. Moreover, it is not dependent on location or seasonal influences, therefore widely applicable. The sensitivity of used forecast methods on the PV-battery system performance is assessed for different PV sizes, battery storage and battery inverter ratings, feed-in limitations and electricity tariffs.

Our obtained results provide insights on PV and demand pattern forecasting impact on PV-battery systems, especially for locations in Western Europe. Large variety in modelled systems and our sensitivity study provides an overview of the variety of results. Especially, the direct comparison between residential and commercial systems shows the potential for each sector. This knowledge will help developers of BESS control algorithms to improve their products. Also, distribution system operators gain a better understanding of the impact of feed-in limit on the performance of PV-battery systems. This will help policy makers making better decisions on strategies to implementing PV-battery systems in urban areas.

The remainder of this paper is structured according to the following format. Section 6.2 explanation the used data, developed forecasting methods and battery control strategies, and battery performance indicators. Section 6.3 presents the results on the performance of the forecast methods and the battery control strategies. In Section 6.4 the sensitivity of the PV-battery system parameters were assessed. Section 6.5 discusses the results and provides recommendations for further research and implementation of the developed strategies. The paper closes with the key conclusion in section 6.6.

3.2 Methods

The explanation of the methodology consists of four parts. Subsection 4.2.1 describes the used PV yield and electricity consumption patterns. Subsection 4.2.2 explains the developed forecasting methods to predict the PV production and electricity consumption. Also the forecast error metrics are explained. Subsection 3.2.3 explains the used battery storage model and control strategies. Subsection 4.2.4 defines the indicators used to assess the impact of these forecast methods and battery control strategies on the performance of the PV-battery systems.

3.2.1 Real-time patterns

PV yield pattern

A PV yield pattern containing AC power was generated using the PVLIB (v0.5.0) model for De Bilt in the Netherlands (52.11N, 5.18E), which is the location of the Royal Netherlands Meteorological Institute (KNMI). The Python package PVLIB contains validated atmospheric functions and PV system performance models and is open source[61]. Solar radiation, ambient temperature, dew point temperature, wind speed and atmospheric pressure data was measured by the KNMI. The time interval of measurements was 10 min for radiation and one hour for the remaining weather parameters. All weather parameters were resampled to a 5 min interval using linearly interpolation. These parameters were used to model a PV pattern with a 5 min time step.

The PV yield pattern was modelled for a south oriented PV system (180° azimuth) with a module tilt of 35°. The PV system model used PV module parameters from the Sanyo HIP-225HDE1. This PV technology shows stable performance under varying Dutch weather conditions and has a relative low temperature coefficient[88]. The Enphase Energy M210 PV inverter with 95.5% California Energy Commission (CEC) efficiency was used to convert direct current (DC) power PV output to alternative current (AC) power. The maximum DC input power of

this inverter is lower than the maximum output of the module, thus the PV inverter is slightly underrated. But, a larger inverter will have a reduced efficiency at low DC power inputs. Considering the Dutch weather conditions with many cloudy days, this will result in lower PV power output. We estimated a 0.6 kWh or 0.07% additional power loss caused by the clipping of the DC module power. A 5% larger inverter decreases these clipping losses, yet the annual yield is lower with 0.3 kWh. The PV yield pattern was scaled to a performance ratio of 85%, which corresponds with good performing PV systems in the Netherlands[89]. The modelled PV system yield was 956 kWh/kW for 2013. The standby consumption of the inverter was 5.8 kWh, resulting in a net PV yield of 949 kWh/kWp. The PV pattern was linearly scaled to the PV system sizes used throughout this study.

Demand patterns

Residential demand patterns were derived from measurements conducted by a Dutch distribution system operator between 2012 and 2014, which are available online[64]. 48 residential demand patterns, with different dwelling types, were selected for 2013. Commercial electricity consumption of 42 buildings, mainly offices, was measured in 2013. The selected residential and commercial demand patterns have a data availability of 100% and were used in a previous study[90]. Both residential and commercial demand patterns were measured at 15 min time resolution. Subsequently, these patterns were linearly resampled to match the PV yield pattern. Hence, all used patterns have an interval of 5 min and cover the full year of 2013.

Fig. 2.1 presents the distribution of the annual electricity demand for each hour and each month of 2013 using violin plots. These plots combine a box-whisker plot with a kernel density plot, providing a quick indication of the distribution of a dataset[65]. The wider sections of a violin plot indicate a higher probability whereas the smaller parts show a lower probability of the value. The electricity consumption was normalized to an annual electricity consumption of 1MWh. Residential electricity consumption is lower during the afternoon but higher in the evening, compared to commercial energy consumption. The distribution range of residential consumption is larger in the evening hours, due to the greater variation in user behaviour. Monthly electricity consumption shows a larger variation for residential buildings than commercial buildings. Residential buildings are occupied less in the summer months due to longer daytimes and holidays, if compared to winter months. Also commercial systems show a reduced consumption in August and December, mainly due holidays. Heat demand of the buildings was not provided by electricity, therefore limiting the influence of temperature on the electricity consumption.

3.2.2 Forecasting methods

Forecasted PV and demand patterns were developed and assessed. These patterns should be available prior to the start of each day of the year to be useable for the predictive forecast strategies. Four methods were used to obtain the forecasted PV yield.

- Use the PV pattern of the previous day (PV-PD).
- Calculate the average PV pattern from the previous week (PV-PW).
- Use weather prediction data for the coming day to model the PV pattern (PV-WX).
- Use clear-sky radiation to model the PV pattern (PV-CS).

The average PV pattern from the previous weekdays was constructed by taking the mean of each 5 min of each day. For example, the value from time step 12.00 is the average of the values from this similar time step of the previous seven days. Forecasted weather parameters were obtained for the next 24 h with a 3 hour time step from the European Centre for Medium-Range Weather Forecasts for location De Bilt (Netherlands)[91]. This dataset contains all weather parameters required to model the PV yield pattern with the PV model and was linear interpolate to a time interval of 5 min. The clear-sky radiation was modelled using the Ineichen clear-sky model[92]. The remaining weather parameters for the clear-sky PV pattern were set as constant values. These constants are a temperature of 12°C, a dew point temperature of 12°C, windspeed of 1 m/s, and a pressure of 101,325 Pa. Forecasted demand patterns were generated using three methods, all requiring historically measured demand.

- Use the demand profile of the previous day (D-PD).
- Use the demand profile of the previous weekday or weekend day (D-PWD).
- Calculate the average profile from the previous seven days (D-PW).

The demand of the previous weekday or weekend day was found by selecting the demand pattern measured from exactly seven days ago. The average profile of the previous seven days was determined using a similar method as described for averaging the PV patterns for seven days.

Forecast performance indicators

The accuracy of forecasted PV yield and demand patterns related to actual patterns was assessed using three error metrics: normalized root mean square error (nRMSE), normalized mean bias error (nMBE) and mean absolute percentage error (MAPE). These are the most used metrics to evaluate forecasts[71]. The nRMSE and MAPE assess the magnitude and volatility of the difference between actual (P_{actual}) and forecasted pattern (P_{FC}). The nMBE evaluates if the forecast methods overestimate or an underestimate the generated power. The nRMSE and nMBE were normalized with the maximum power output from the actual forecast. The nRMSE, MAPE and nMBE are given in Eq. (3.1),Eq. (3.2) and Eq. (3.3) respectively, where n indicates the number of total time steps.

$$\text{nRMSE} = \frac{\sqrt{\frac{100\%}{n} \cdot \sum_{t=1}^{n} (P_{\text{FC,t}} - P_{\text{actual,t}})^2}}{\text{Max}(P_{\text{actual}})} \tag{3.1}$$

$$\text{MAPE} = \frac{100\%}{n} \sum_{t=1}^{n} \left| \frac{P_{\text{FC,t}} - P_{\text{actual,t}}}{\text{Max}(P_{\text{actual}})} \right| \tag{3.2}$$

$$\text{nMBE} = \frac{\frac{100\%}{n} \cdot \sum_{t=1}^{n} (P_{\text{FC,t}} - P_{\text{actual,t}})}{\text{Max}(P_{\text{actual}})} \tag{3.3}$$

3.2.3 Battery control strategies

Real-time and forecasted PV patterns were assessed using a PV-battery model. This model assessed two control strategies and was developed in Python (v3.5). The strategies were modelled for the residential and commercial systems for the year 2013. A model step of 5 min was selected to match the time steps of input patterns.

- Real-time control (RC). This strategy uses actual measured energy PV production and energy consumption to control the battery energy storage systems. No forecasts are required.
- Predictive control (PC). This strategy uses forecasted energy production and forecasted energy consumption to reduce the curtailment losses. A forecasted PV and demand pattern before the start of the day is required.

Two PV-battery systems architectures, AC-coupled and DC-coupled, are mainly used. In an AC-coupled system, the battery storage is connected with a battery inverter to the electricity grid. The PV array is connected with a PV inverter to the electricity grid and a conversion step from DC to AC power is required. If the battery is charged then the AC power is converted back to DC. An overview of the power flows within AC-coupled systems is shown in Fig. 3.1. In a DC-coupled system, the battery is connected directly to the PV system inverter, and no conversion to AC is needed. A charge controller is required to match the PV voltage output within the boundaries of the battery voltage input. In this study an AC-coupled lithium-based battery system is assumed. AC-coupled systems are suitable for retrofit existing PV systems with battery storage and therefore widely used in other studies[93].

The battery inverter converts the AC power to a DC power as input for the battery. The conversion efficiencies depend on the input power and were obtained from a battery inverter efficiency curve. This curve was constructed using efficiency parameters of the SMA Sunny Boy Storage inverter and has efficiency steps of 0.01%[94]. The modelled efficiency curve has a CEC inverter efficiency of 96.4%. A constant battery charging and discharging efficiency of 96% was assumed. This leads to a DC input to DC output efficiency of 92.2%, almost similar to the efficiency of a Tesla Powerwall[95]. The battery roundtrip efficiency from AC input to AC output is $\approx$ 0.85%. We assumed a BESS standby consumption of 0.1% of the battery inverter rating. A typical battery system is operated in a restricted SOC range due to safety reasons and to reduce aging. Consequently, the minimum state of charge (SOC_{min}) was set to 10% and the maximum SOC (SOC_{max}) to 90% of the battery storage capacity[85]. To keep the battery SOC within these constraints, the battery SOC in the first time step was set similarly as the minimum battery SOC. Hence, the battery was charged for 10% at the start of the year.

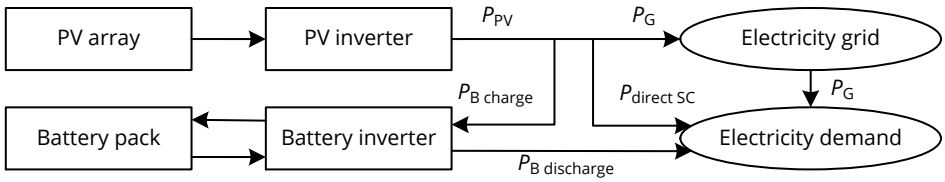

Figure 3.1 · Power flow diagram of an AC-coupled PV-battery system used in this study.

Real time control strategy

Charging and discharging of the battery storage, and the power flows to and from the grid for the real-time control strategy were modelled using Eqs. (3.5)-(3.9). The power flows and battery state of charge were modelled for each time step (t). The load potential ($P_{\mathrm{B\,pot}}$) depends on the difference between PV production (P_{PV}) and electricity demand (P_{demand}), see Eq. (3.4).

$$P_{\mathrm{B\,pot}} = P_{\mathrm{PV}} - P_{\mathrm{demand}} \tag{3.4}$$

The load potential that actually was charged or discharged is limited by the maximum AC output of the battery inverter ($P_{\mathrm{B\,inv\,max}}$). We assume that the maximum inverter charge power is identical to the maximum inverter discharge power, see Eq. (3.5).

$$P_{\mathrm{B\,pot}} = \begin{cases} P_{\mathrm{B\,pot}} & \text{if } |P_{\mathrm{B\,pot}}| < P_{\mathrm{B\,inv\,max}} \\ P_{\mathrm{B\,inv\,max}} & \text{if } |P_{\mathrm{B\,pot}}| \geq P_{\mathrm{B\,inv\,max}} \end{cases} \tag{3.5}$$

Next, the battery load was found using the charge (η_{charge}) and discharge ($\eta_{\mathrm{discharge}}$) efficiencies. These efficiencies are dependent on the corresponding charge and discharge power. A charge potential was found when PV production exceeds demands, and a discharge potential was found when demand exceeds PV production. Charged or discharged energy potential ($\Delta E_{\mathrm{B\,pot}}$) was found by multiplication of load potential with the used time interval (Δt) of 5 min, see Eq. (3.6).

$$\Delta E_{\mathrm{B\,pot}} = \begin{cases} P_{\mathrm{B\,pot}} \cdot \eta_{\mathrm{charge}} \cdot \Delta t & \text{if } P_{\mathrm{B\,pot}} > 0 \\ \dfrac{P_{\mathrm{B\,pot}}}{\eta_{\mathrm{discharge}}} \cdot \Delta t & \text{if } P_{\mathrm{B\,pot}} \leq 0 \end{cases} \tag{3.6}$$

Afterwards, the charged or discharged energy (ΔE_{B}) was determined. This depends on the current battery SOC ($E_{\mathrm{B,\,t}}$) and is limited by the minimum battery SOC ($E_{\mathrm{B\,min}}$) and maximum SOC ($E_{\mathrm{B\,max}}$), see Eq. (3.7).

$$\Delta E_{\mathrm{B}} = \begin{cases} \Delta E_{\mathrm{B\,pot}} & \text{if } E_{\mathrm{B,\,t}} + \Delta E_{\mathrm{B\,pot}} \geq E_{\mathrm{B\,min}} \\ \Delta E_{\mathrm{B\,pot}} & \text{if } E_{\mathrm{B,\,t}} + \Delta E_{\mathrm{B\,pot}} \leq E_{\mathrm{B\,max}} \\ E_{\mathrm{B,\,t}} - E_{\mathrm{B\,min}} & \text{if } E_{\mathrm{B,\,t}} + \Delta E_{\mathrm{B\,pot}} < E_{\mathrm{B\,min}} \\ E_{\mathrm{B\,max}} - E_{\mathrm{B,\,t}} & \text{if } E_{\mathrm{B,\,t}} + \Delta E_{\mathrm{B\,pot}} > E_{\mathrm{B\,max}} \end{cases} \tag{3.7}$$

Then, the battery state of charge ($E_{\mathrm{B,\,t+1}}$) used for the next time step was found by the summation of current SOC with the charged or discharged electricity. The actual battery load (P_{B}) and inverter load ($P_{\mathrm{B\,inv}}$) were calculated from

the charged or discharged energy, see Eq. (3.8).

$$E_{\mathrm{B,\,t+1}} = E_{\mathrm{B,\,t}} + \Delta E_{\mathrm{B}} \tag{3.8a}$$

$$P_{\mathrm{B}} = \frac{\Delta E_{\mathrm{B}}}{\Delta t} \tag{3.8b}$$

$$P_{\mathrm{B\,inv}} = \begin{cases} \dfrac{P_{\mathrm{B}}}{\eta_{\mathrm{charge}}} & \text{if } P_{\mathrm{B}} > 0 \\ P_{\mathrm{B}} \cdot \eta_{\mathrm{discharge}} & \text{if } P_{\mathrm{B}} \leq 0 \end{cases} \tag{3.8c}$$

Finally, the power to the grid was determined (P_{G}). First, the residual power (P_{R}) was calculated by subtracting the electricity consumption and battery load from the PV produced power. The power flow to the grid is limited by the feed-in limit (P_{FIL}). The difference in positive power flows between the residual power and the power to the grid is defined as the feed-in limit loss ($P_{\mathrm{FIL\,loss}}$), see Eq. (3.9).

$$P_{\mathrm{R}} = P_{\mathrm{PV}} - P_{\mathrm{demand}} - P_{\mathrm{B\,inv}} \tag{3.9a}$$

$$P_{\mathrm{G}} = \begin{cases} P_{\mathrm{R}} & \text{if } P_{\mathrm{R}} \leq P_{\mathrm{FIL}} \\ P_{\mathrm{FIL}} & \text{if } P_{\mathrm{R}} > P_{\mathrm{FIL}} \end{cases} \tag{3.9b}$$

$$P_{\mathrm{FIL\,loss}} = \begin{cases} P_{\mathrm{R}} - P_{\mathrm{G}} & \text{if } P_{\mathrm{R}} - P_{\mathrm{G}} > 0 \\ 0 & \text{if } P_{\mathrm{R}} - P_{\mathrm{G}} \leq 0 \end{cases} \tag{3.9c}$$

Predictive control strategy

The predictive control strategy aims to reduce the curtailment losses and maintain the level of self-consumption. Therefore, it reserves a battery storage capacity to charge PV power that exceeds the feed-in limit. This reserved capacity is deployed when the actual power fed back to the grid surpasses the feed-in limit. The reserved battery state of charge was calculated with Eq. (3.10) and Eq. (3.11).

The forecasted power that exceeds the feed-in limit ($P_{\mathrm{FIL\,FC}}$) was calculated by subtracting the forecasted electricity demand ($P_{\mathrm{D\,FC}}$) and power feed-in limit from the forecasted PV production. This was calculated in advance for each day, thus the forecasts should be available prior to the next day. The forecasted power that was charged with the battery ($P_{\mathrm{B\,res}}$), depends on the battery inverter rating and charge efficiency, see Eq. (3.10).

$$P_{\mathrm{FIL\,FC}} = P_{\mathrm{PV\,FC}} - P_{\mathrm{D\,FC}} - P_{\mathrm{FIL}} \tag{3.10a}$$

$$P_{\mathrm{B\,res}} = \begin{cases} 0 & \text{if } P_{\mathrm{FIL\,FC}} \leq 0 \\ P_{\mathrm{FIL\,FC}} & \text{if } 0 < P_{\mathrm{FIL\,FC}} < P_{\mathrm{B\,inv\,max}} \cdot \eta_{\mathrm{charge}} \\ P_{\mathrm{B\,inv\,max}} & \text{if } P_{\mathrm{FIL\,FC}} \geq P_{\mathrm{B\,inv\,max}} \cdot \eta_{\mathrm{charge}} \end{cases} \tag{3.10b}$$

A novel algorithm was developed to determine the reserved battery storage capacity ($E_{\mathrm{B\,res}}$) for each time step. The reserved battery capacity was found by the summation of reserved battery power from the start of a timeslot ($t = 1$) until the end of a timeslot ($t = end,\ timeslot$). The length of those timeslots varies between 5 min and 24 h, and decreases over the day. The first time step of the day (from 00:00 until 00:05) used a reserved battery capacity which was calculated for the next 24 h (from 00:00 until 00:00 the next day). The second timeslot used the battery capacity calculated for the next 23 h and 55 min (from 00:05 until 00:00 the next day). This was continued until the last timeslot of each day. Consequently, the reserved battery capacity was calculated for a declining time period for each next time step of the day. Furthermore, the reserved battery capacity was limited by the minimum and maximum battery SOC, see Eq. (3.11).

$$E_{\mathrm{B\,res\,pot}} = \sum_{t=1}^{t_{end,\,timeslot}} P_{\mathrm{B\,res\,t}} \cdot \Delta t \tag{3.11a}$$

$$E_{\mathrm{B\,res}} = \begin{cases} E_{\mathrm{B\,res\,pot}} & \text{if } E_{\mathrm{B\,res\,pot}} \leq E_{\mathrm{B\,max}} - E_{\mathrm{B\,min}} \\ 0 & \text{if } E_{\mathrm{B\,res\,pot}} > E_{\mathrm{B\,max}} - E_{\mathrm{B\,min}} \end{cases} \tag{3.11b}$$

The reserved battery storage capacity was subtracted from the maximum battery capacity to find the required battery SOC. This SOC was compared with the battery SOC of the next time step that was calculated from Eq. (3.8). If the required SOC was lower than the battery SOC of the next time step, then the battery was only charged with PV power that exceeded the feed-in limit. Otherwise, enough battery capacity is available to charge the difference between the PV production and electricity consumption. The new potential was calculated according Eq. (3.12), and was used to charge the battery according Eqs. (3.5)-(3.9).

$$P_{\mathrm{B\,pot}} = \begin{cases} P_{\mathrm{PV}} - P_{\mathrm{demand}} - P_{\mathrm{FIL}} & \text{if } E_{\mathrm{B\,max}} - E_{\mathrm{B\,res}} \leq E_{\mathrm{B,\,t+1}} \\ P_{\mathrm{PV}} - P_{\mathrm{demand}} & \text{if } E_{\mathrm{B\,max}} - E_{\mathrm{B\,res}} > E_{\mathrm{B,\,t+1}} \end{cases} \tag{3.12}$$

An example of the predictive control strategy for a residential PV-battery system is shown in Fig. 3.2. The predictive control strategy uses PV and demand forecasts (subplot a) to determine the surplus power (P_{top}). This predicted surplus power is used to determine a reserved battery storage capacity ($E_{\mathrm{B\,res}}$), shown in subplot (b). Charge of the battery storage during the day (subplot c) depends on the reserved battery capacity and the actual PV production and energy consumption.

More energy consumption is forecasted for 8$^{\mathrm{th}}$ of June than what was actually consumed for that day. Hence, the reserved battery capacity is underestimated for this day and therefore the battery charges excess PV energy in the early

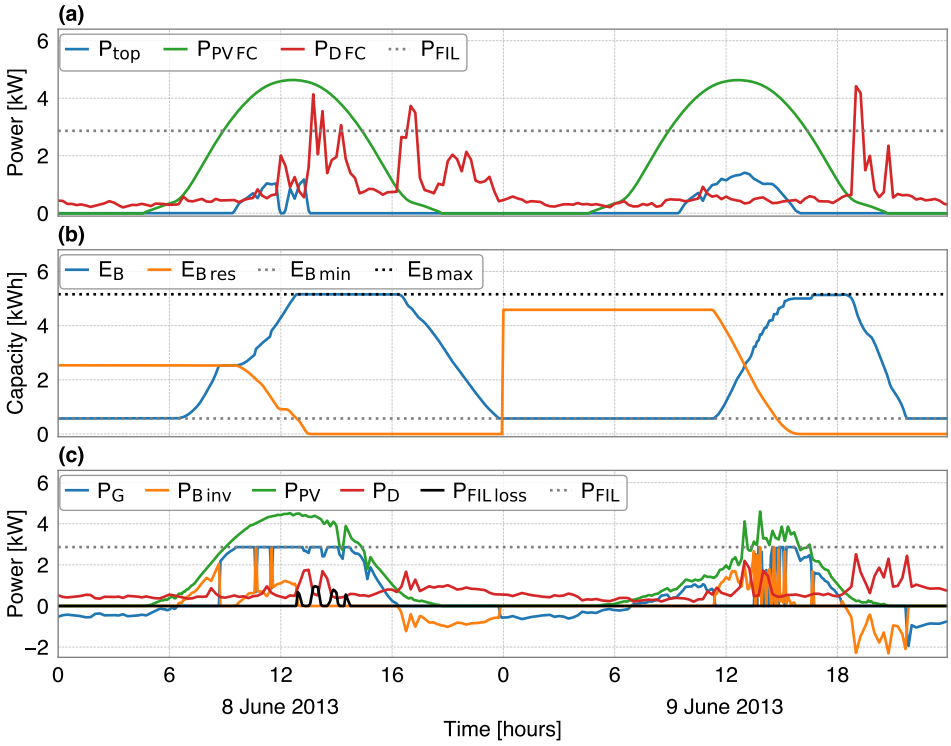

Figure 3.2 · Example of the predictive controls strategy operation of a residential PV-battery system for two days. The top graph (a) shows the PV forecast using PV-CS method and the demand forecast using D-PWD method. The middle graph (b) shows the reserved and actual battery state of charge. The bottom graph (c) displays the power flows to (positive) and from (negative) the electricity grid and the battery. Also the actual PV energy production, energy consumption and feed-in losses are shown. The annual consumption of this household is 5.73 MWh. Corresponding PV-battery system parameters used to this annual consumption are shown in Table 3.2.

morning hours. Consequently, the battery is fully charged at 13.00 and curtailment losses occur afterwards. The second day shows an overestimation of the demand forecast what results in a maximum battery capacity reservation for PV peak charging. The battery starts charging excess PV energy around 12:00 and the reserved battery capacity starts to decrease. The battery is fully charged around 16:30, and no curtailment losses occur on this day.

3.2.4 PV-battery performance indicators

The performance of control strategies with forecast methods on the PV-battery system was assessed using three annual indicators.

- Self-consumption ratio (SCR), which assess the share of direct consumed energy by the building or the battery storage system.
- Curtailment loss ratio (CLR), which indicates the share of energy lost due to a feed-in limit.
- Storage revenue ratio (SRR), which evaluates the financial gain generated by the energy that is stored in the battery relative to the revenue of a system without storage.

Self-consumption ratio is the share of energy self-consumed (E_{SC}) from the total energy produced (E_{PV}). Self-consumed power is the power directly consumed ($P_{direct\,SC}$) by the building added with the power used for battery charging ($P_{B\,charge}$). The annual self-consumed power is aggregated from the first time step of the year (t=1) until the last time step of the year (t_{end}), see Eq. (6.1).

$$P_{direct\,SC} = \begin{cases} P_{PV} & \text{if } P_{PV} < P_{demand} \\ P_{demand} & \text{if } P_{PV} \geq P_{demand} \end{cases} \tag{3.13a}$$

$$P_{B\,charge} = \begin{cases} P_{B\,inv} & \text{if } P_{B\,inv} > 0 \\ 0 & \text{if } P_{B\,inv} \leq 0 \end{cases} \tag{3.13b}$$

$$E_{PV} = \sum_{t=1}^{t_{end}} P_{PV,t} \cdot \Delta t \tag{3.13c}$$

$$E_{SC} = \sum_{t=1}^{t_{end}} (P_{direct\,SC,t} + P_{B\,charge,t}) \cdot \Delta t \tag{3.13d}$$

$$SCR = \frac{E_{SC}}{E_{PV}} \tag{3.13e}$$

Curtailment loss ratio is the share of lost PV produced energy, because it cannot be fed back to the electricity grid. The CLR is found by dividing the total feed-in lost ($E_{FIL\,loss}$) with the total produced PV energy, see Eq. (3.14).

$$E_{FIL\,loss} = \sum_{t=1}^{t_{end}} P_{FIL\,loss,t} \cdot \Delta t \tag{3.14a}$$

$$CLR = \frac{E_{FIL\,loss}}{E_{PV}} \tag{3.14b}$$

Two annual energy flows are required to calculate the value of a PV (or PV-battery) system: the reduced electricity imported from the grid and the sold electricity to the grid. The electricity import of a building decreases because of the self-consumption. This decrease was calculated for a PV and PV-battery system using the reduced imported electricity (E_{RIE}). This is the difference between the

electricity demand and the electricity imported from the grid. This imported electricity was converted to an absolute value. The sold electricity (E_{SE}) is the summation of the exported power over time, see Eq (3.15).

$$E_{RIE} = \Big(\sum_{t=1}^{t_{end}} P_{D,t} \cdot \Delta t\Big) - \Big|\Big(\sum_{t|P_{G,t}<0}^{t_{end}} P_{G,t} \cdot \Delta t\Big)\Big| \tag{3.15a}$$

$$E_{SE} = \sum_{t|P_{G,t}>0}^{t_{end}} P_{G,t} \cdot \Delta t \tag{3.15b}$$

Storage revenue ratio indicates the annual financial value of a PV-battery system compared to a PV system without storage. It is defined as the relative change between the relative electricity revenue (RER) of these two system types. The RER of the system consists of the value of the reduced electricity imported and the sold electricity. The value of the reduced imported electricity depends on the consumption tariff (π_{cons}) and the value of the sold electricity depends on the feed-in tariff ($\pi_{feed\text{-}in}$). These tariffs depend on electricity production costs, taxes and grid network operator costs. The consumption and feed-in tariff were assumed as constant over the examined time period. Besides, we used the RER in the numerator and denominator to calculate the SRR. Consequently, we can cancel the consumption and feed-in tariff and use a new term, namely the sales to purchase ratio (SPR). This is the ratio between the feed-in tariff and the consumption tariff. As a result, we can use a single factor to include the difference between the feed-in tariff and the consumption tariff. The SPR was included in the RER, which were calculated for a PV system (RER_{PV}), and a PV-battery systems ($RER_{PV\text{-}B}$). Finally, the SRR was determined according Eq. (3.16).

$$SPR = \frac{\pi_{feed\text{-}in}}{\pi_{cons}} \tag{3.16a}$$

$$RER = E_{RIE} + (E_{SE} \cdot SPR) \tag{3.16b}$$

$$SRR = \frac{RER_{PV\text{-}B} - RER_{PV}}{RER_{PV}} \tag{3.16c}$$

The quality of the forecast methods on the PV-battery performance indicators were assessed by comparing the results from using the exact forecast (FC exact) to results from a forecast scenario (FC scenario). A forecast scenario consists of a PV forecast method and demand forecast method. The difference in performance indicator (Δ_{se}) was calculated in percentage points (%p) for the SCR, CLR and SRR, according Eq. (3.17).

$$\Delta_{se} = \text{FC scenario} - \text{FC exact} \tag{3.17}$$

3.3 Results

3.3.1 Performance of forecasting methods

The forecasted PV and energy demand patterns were compared with the actual values using nRMSE, MAPE and nMBE. Annual errors for PV patterns forecast methods are presented in Table 3.1. PV yield forecasting with weather prediction data (PV-WX) has the lowest nRMSE and MAPE of respectively 11.4% and 5.5%. Highest errors were found for the PV yield forecasting method that used clear-sky radiation, which is indeed a worst case considering the typically cloudy weather in the Netherlands. This method show nRMSE and MAPE that is almost two times larger than for the PV-WX method.

A higher nRMSE but an almost similar MAPE are seen for the PV-PD method compared to the PV-PW method. Thus, the PV-PD method has a larger volatility of error, but the magnitude of errors for both methods is comparable. The lower volatility of the PV-PW method is clearly caused by averaging the historical PV production data of the previous seven days. The nMBE of PV-WX is close to zero, indicating that the PV energy production is neither under or overestimated. The PV-PW and PV-WX show negative values, indicating an underestimation of PV yield. The clear-sky method has a positive error and overestimates PV yield. This overestimation is around 10 times higher nMBE error than the errors observed with the PV-PD or PV-PW.

Errors of forecasted residential and commercial demand patterns are presented using violin plots in Fig. 3.3. Lowest average nRMSE from residential patterns are observed for the D-PW method, specifically 7.4%. Also, this method has the smallest distribution range, from 3.2% to 11.1%. Largest errors are seen for the D-PD method, with an average of 9.5% and a maximum of 14.7%. Commercial patterns show larger differences between the forecast methods. Lowest average nRMSE is observed for D-PWD patterns, specifically 9.1%. The D-PW method shows highest errors for commercial patterns, which is in contrast with the errors seen for residential systems.

MAPEs of the demand forecast methods show similar trends as seen for nRMSE. The nMBE shows values of zero for D-PD and D-PWD methods. These

Table 3.1 · Annual normalized RMSE, MAPE and normalized MBE values of the PV patterns forecasting methods, for 2013

Forecasted PV pattern	PV-PD	PV-PW	PV-WX	PV-CS
nRMSE [%]	16.98	14.98	11.35	20.64
MAPE [%]	7.79	7.82	5.51	10.51
nMBE [%]	-0.84	-0.88	-0.26	9.33

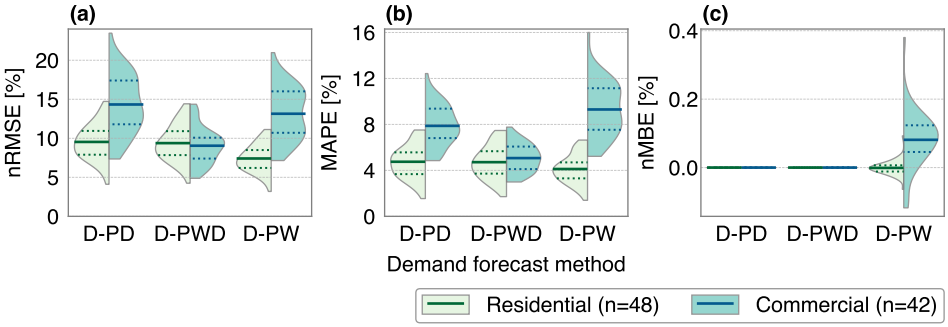

Figure 3.3 · Normalized RMSE (a), MAPE (b) and normalized MBE (c) of the demand forecast methods for residential patterns (left part of the violin) and commercial patterns (right part of the violin). Mean errors of the distributions are marked by solid lines, and 25% and 75% percentiles are indicated by dotted lines.

methods use data of the previous day, or previous weekday. Consequently, differences between the actual and the forecasted power are averaged out to zero over the full year. The D-PW method shows a minor impact on the nMBE, with an average overestimation of electricity consumption for commercial systems.

Moreover, the errors for commercial patterns are larger than for residential patterns, especially with the D-PD and D-PW method. Also, these methods have a far wider distribution range of errors than residential systems. This is related to larger differences of energy consumption between weekday and weekend days in commercial buildings than in residential buildings. Overall, residential demand forecast should include historical energy consumption of multiple days, whereas commercial demand only requires a single day.

3.3.2 Performance of control strategies

Real-time and predictive control strategies were assessed using performance indicators for residential and commercial PV-battery systems. The predictive control strategy has four PV forecast options and three electricity consumption forecasts options, resulting in twelve forecast options. Also, the assessment included the PC strategy using exact PV yield and exact electricity demand forecast. To sum up, one RC strategy and thirteen PC strategies were assessed.

The control strategies were assessed using similar PV-battery system parameters. All demand patterns were scaled to an annual consumption of 1 MWh, allowing us to compare patterns. Usually in the Netherlands, for each 1 MWh of annual energy consumption 1 kWp of PV is installed. This will almost fulfil the annual energy consumption. Hence, a PV system size of 1 kWp was chosen with a PV inverter of 1 kW. A battery storage size of 1 kWh for each MWh of electricity demand was chosen based on previous studies[69,93]. A battery inverter rating of

0.5 kW per kWh storage capacity was selected. This charge or discharge rate is quite common, for example with the Tesla Powerwall[95]. The feed-in limit was set to 0.5 kW per kWp installed PV capacity, based on the subsidy requirement for German PV-battery systems[48]. SRR was calculated using a sales to purchase ratio of 0.5. We assumed that the consumption tariff would be twice as high as the feed-in tariff due to the inclusion of taxation and network costs. An overview of default set of relative reference parameters is given in Table 3.2.

The influences of the fourteen options on SCR, CLR and SRR for the reference PV-battery systems are presented using violin plots in Fig. 3.4. Results from the RC strategy are shown in the most left violin plot. The second violin plot shows results from the PC strategy using exact forecasts. The remaining options present results of the PC strategy that uses all possible combinations of the PV and demand forecast methods.

Self-consumption ratio

Observed SCR are significantly higher in all strategies for commercial systems than for residential systems. Average residential SCR observed are between 56.6% and 57.6% under all control strategies. Commercial systems show a smaller variation in average between the control strategies, with values between 65.8% and 66.0%. Similar SCR are observed both in the RC strategy as the PC strategy, with exact forecasts. Also, PC strategy with PV pattern forecast based on weather prediction data (PV-WX) or based on the average values of last week (PV-PW) show nearly similar SCR. PC forecast using clear-sky radiation (PV-CS) show ≈0.9% point lower SCR for residential and ≈0.2% point lower SCR for commercial systems. Minor differences are observed between demand forecasting methods.

The distribution shape of commercial systems is significantly different than for residential systems. The difference between 25% and 75% percentile is ≈3.5% for residential systems and ≈2.8% for commercial systems. Yet, the total distribution range for residential patterns is ≈6% point larger than for commercial systems. A maximum SCR of 68.7% is observed for numerous commercial systems, whereas only a few residential systems show a SCR peak of 65%. This is caused by a bigger

Table 3.2 · Reference PV-battery system parameters.

Reference parameter	Value	Unit
Relative PV system size	1	$kWp_{pv}\ MWh_{demand}^{-1}$
Relative battery storage size	1	$kWh_{bess}\ MWh_{demand}^{-1}$
Relative battery inverter rating	0.5	$kW/kWh_{bess}\ MWh_{demand}^{-1}$
Relative feed-in limit	0.5	$kW/kWp_{pv}\ MWh_{demand}^{-1}$
Sales to purchase ratio	0.5	-

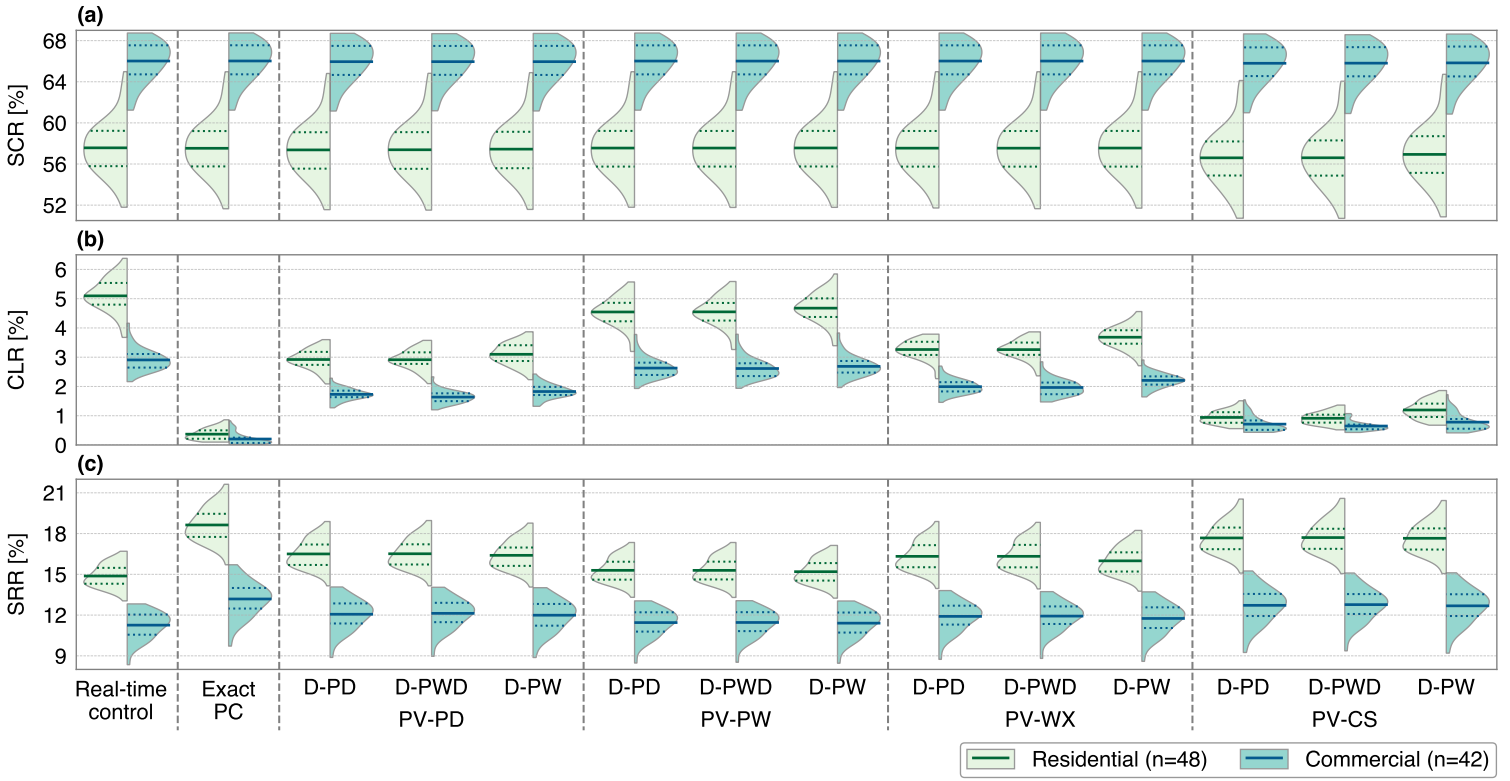

Figure 3.4 · Influence of control strategies on self-consumption ratio (a), curtailment loss ratio (b) and storage revenue ratio (c) for PV-battery systems using violin plots. Distributions are presented for residential systems (left) and commercial systems (right). The most left violin plots are results obtained using the real-time control strategy, while the others are obtained under the predictive control strategy. The top row of horizontal-axis labels are showing method to forecast demand, whereas the bottom row shows methods for PV energy forecasting. Used PV-battery system parameters are shown in Table 3.2. Mean values of the distributions are marked by solid lines, and 25% and 75% percentiles are indicated by dotted lines. Note, the results are clustered on PV forecast method for additional clarity.

difference in time-of-use of electricity from residential buildings than from commercial buildings, see Fig. 2.1. The latter have relative higher energy consumption at noon, on moments with larger shares of PV produced energy. Also, residential buildings have relatively lower energy consumption in summer months when compared to commercial buildings.

Curtailment loss ratio

Curtailment losses are significantly lower for all PC strategies than for the RC strategy. Average CLR of residential system decreases from 5.0% for RC strategy, to 0.4% for exact forecast. The PV-CS forecast method has lowest CLR from remaining PC strategies, specifically between 0.9% and 1.2%. The PV-CS forecast overestimates PV surplus production thus more battery capacity is reserved to store these peaks. For that reason, relatively more PV energy is stored and a lower CLR is realized. Yet, a lower SCR is obtained because the battery capacity is not fully utilized to improve self-consumption. The PV-PD, PV-PW and PV-WX underestimate PV peak production. Consequently, less battery capacity is reserved and a larger share of PV peak production cannot be stored, which results in higher CLR. However, these PV forecast methods have a higher SCR because a bigger share of battery capacity is used for self-consumption.

Commercial systems show an average CLR decrease from 2.9% for RC strategy to 0.2% for PC strategy with exact forecast. Residential systems have higher curtailment losses than commercial systems under all scenarios. Commercial buildings have higher energy consumption during daytime, which are moments when PV power generation occurs. Therefore, less excess PV power is curtailed in commercial systems than in residential systems. Subsequently, the difference in CLR between the RC strategy and PC strategies is larger for residential systems. The CLR distribution range is smaller for commercial systems than residential systems and is decreasing with lower curtailment ratios. Systems with a higher SCR have a lower CLR. This explains why the CLR distribution shape of commercial systems shows the opposite shape of the distributions seen for the SCR. The reduction in CLR is limited by the reserved battery storage capacity. The influence of the reserved battery storage limits the distribution range of the residential systems.

Storage revenue ratio

Higher SRRs are observed for all PC strategies compared to the RC strategy. Average SRR for residential systems are increased from 14.9% for RC strategy to 18.6% for PC strategy with exact forecast. Commercial PV-battery systems show a smaller increase from 11.3% to 13.2%. This increase in storage revenues are solely

caused by the reduction of the curtailment losses, which are larger for residential systems than for commercial systems. SRR distribution range for commercial system is larger than for residential systems. The distribution shape of the commercial systems is almost similar as seen with SCR, whereas residential systems show a different shape. Residential systems have higher curtailment losses, thus more value is created by reducing these losses. Consequently, the shape of the SRR distribution is influenced more by the CLR for residential systems than for commercial systems.

It is remarkable that the PC strategies that use the PV-CS forecast method show highest SRRs, but this forecast method has the largest nRMSE (see Table 3.1). The PV forecast method with the lowest forecast errors (PV-WX method) has lower SRRs. The PV-CS forecast method overestimates PV yield, whereas the PV-WX forecast underestimate this yield. In case of an underestimation of PV yield, not enough storage capacity is reserved and electricity is lost. In case of an overestimation of yield, sufficient storage capacity is available and no energy is lost. The underestimated yield of the PV-WX method has a lower error than the overestimated yield of the PV-CS method. Therefore a lower forecast error does not directly imply higher storage revenue.

Differences in average SRR related to the demand forecast method for PC strategies are relatively small. Furthermore, there is not a single demand forecast method that performs better for residential systems. However, the D-PWD forecast method shows the best performance for commercial systems. The difference in nRMSE between the forecasted residential demand patterns is considerably smaller than observed for commercial demand patterns, see Fig. 3.3. Subsequently, the influence of the demand forecast method is smaller for residential than for commercial systems.

Furthermore, the variation in PV energy production is much larger than variation in electricity consumption. Consequently, differences in nRMSE between the PV forecast methods are larger than the demand forecast methods. The difference between lowest and highest nRMSE forecast errors for the PV forecast method is 9.3% point. In contrast, this difference is 2.1% point for residential and 5.3% point for commercial demand forecasts. Thus, PV forecast methods have a larger influence than demand forecast methods.

3.4 Sensitivity analysis

The impact of PV-battery systems parameters on PV-battery performance indicators was assessed for six situations. The RC strategy and PC strategy with exact forecast were used to assess the absolute value of the indicator in percentage. Also, four forecast scenarios were assessed to provide insight in how much influence the forecast methods have on the PV-battery system performance. These four scenarios have each another PV-forecasting method. The demand forecast method with the lowest nRMSE was selected to predict electricity demand. These are the D-PW forecast method for residential systems and the D-PWD method for commercial systems. Performance indicators of these four scenarios were compared to performance indicators obtained with the PC strategy and using exact forecasts. Differences between the exact forecast and the four scenarios (Δ_{se}) are given in percentage points (%p). An overview of these scenarios used in this sensitivity study for residential and commercial systems is given in Table 3.3. The evaluated system parameters were varied while other parameters were kept constant, according to reference PV-battery system values, see Table 3.2.

3.4.1 PV system size

Relative PV system size influence on the performance indicators are presented in Fig. 3.5. The PV system size was varied with steps of 0.01 kWp. Results from the RC strategy and PC strategy with exact forecast are presented on the left graphs. Results of differences between the four scenarios and the exact forecast are shown on the right. The locations of the line markers represent the values of reference PV-battery system parameters.

RC strategy has almost similar SCR average values as the exact PC strategy. Residential SCR decreases more rapidly than for commercial systems when PV system size increases, as shown in Fig. 3.5 (a). The difference in SCR between residential and commercial systems increases until a relative PV system of 0.8 kWp, to a maximum of 8.8% point. Afterwards this difference reduces to 3.8% point for a 3 kWp relative PV system size. Small SCR differences are observed in the S-PW and S-WX scenarios, which states these have an almost similar performance

Table 3.3 · Overview of forecast scenarios for residential and commercial systems, assessed in the sensitivity analysis.

Scenario name	S-PD	S-PW	S-WX	S-CS
PV yield forecast	PV-PD	PV-PW	PV-WX	PV-CS
Residential demand forecast	D-PW	D-PW	D-PW	D-PW
Commercial demand forecast	D-PWD	D-PWD	D-PWD	D-PWD

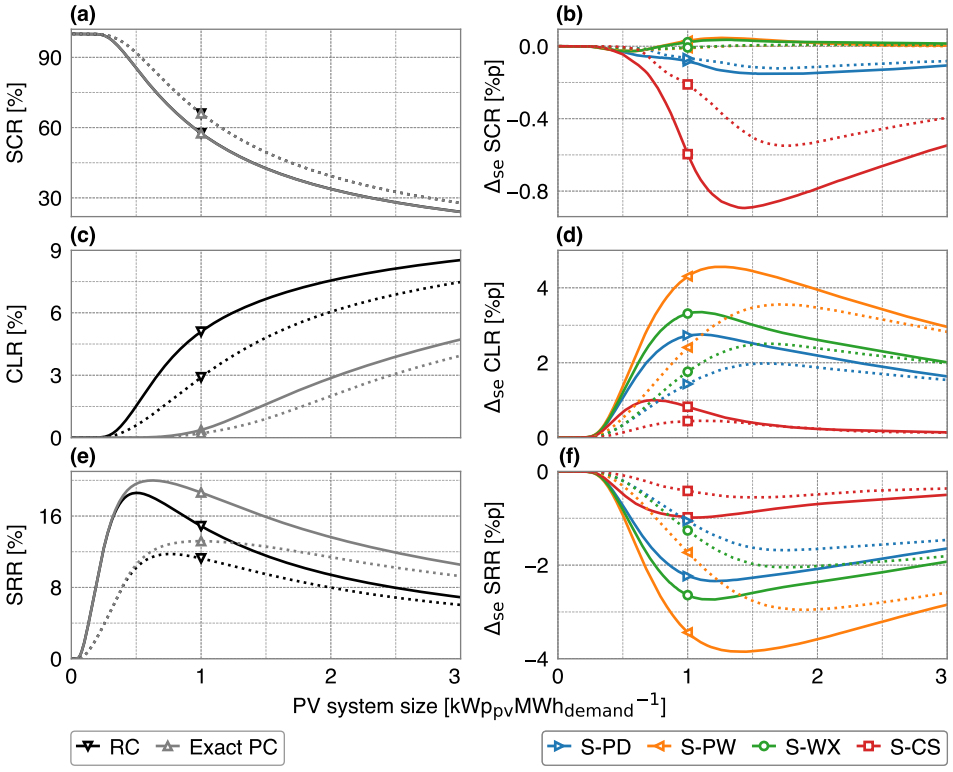

Figure 3.5 · Influence of relative PV system size on SCR (a), CLR (c) and SRR (e) for the real-time control (RC) and the predictive control with exact forecast (Exact PC). Difference between forecast scenario and exact forecast (Δ_{se}) in SCR (b), CLR (d) and SRR (f) are shown for four scenarios in percentage points [%p]. The solid lines show the average value of residential systems and the dotted lines show averages of commercial systems. An overview of the scenarios is given in Table 3.3. Remaining system parameters are given in Table 3.2. The markers indicate the reference PV-battery system values.

as the exact forecast. Larger differences are seen in the S-CS scenario, with SCR of 0.9% point lower for a PV system size of 1.4 kWp. For larger PV systems, a reduction in differences is observed.

A faster increase in CLR is observed for RC strategy compared to exact PC strategy. Differences between residential and commercial CLR are larger for RC than for PC strategy, under all analysed PV system sizes. The S-CS has the largest reduction of curtailment losses, whereas the S-PW scenario has the lowest. All scenarios show a lower CLR for commercial than for residential systems. Storage revenues for PV system sizes increase until 0.4 kWp and are similar for the RC and PC strategy. For larger PV systems, SRR decreases because the battery storage system cannot store all excess PV energy. Consequently, more PV electricity is sold to the grid and electricity is lost due to the feed-in limit. This increases the revenues of a PV system without storage, and thus decreases SRR. Furthermore,

larger differences in revenue between residential and commercial systems are observed. The S-CS scenario shows the best performance, with a SRR difference of ≈ 1% for all analysed PV system sizes.

3.4.2 Battery storage capacity

The impacts of relative battery storage capacities with a 0.01 kWh step size are shown in Fig. 3.6. SCR increases related to larger battery capacities, and is larger for residential than for commercial systems. Residential systems increase from 32.2% to 75.1% and commercial systems from 44.0% to 79.0%. The battery storage capacity has a minor effect on the difference in SCR between the RC and PC strategy. The S-CS scenario overestimates PV yield production, therefore more storage capacity is reserved than is needed to store the excess PV power. So, a large difference is observed between the exact and the S-CS scenario, which peaks at a storage capacity of around 0.5 kWh. The share of reserved battery that

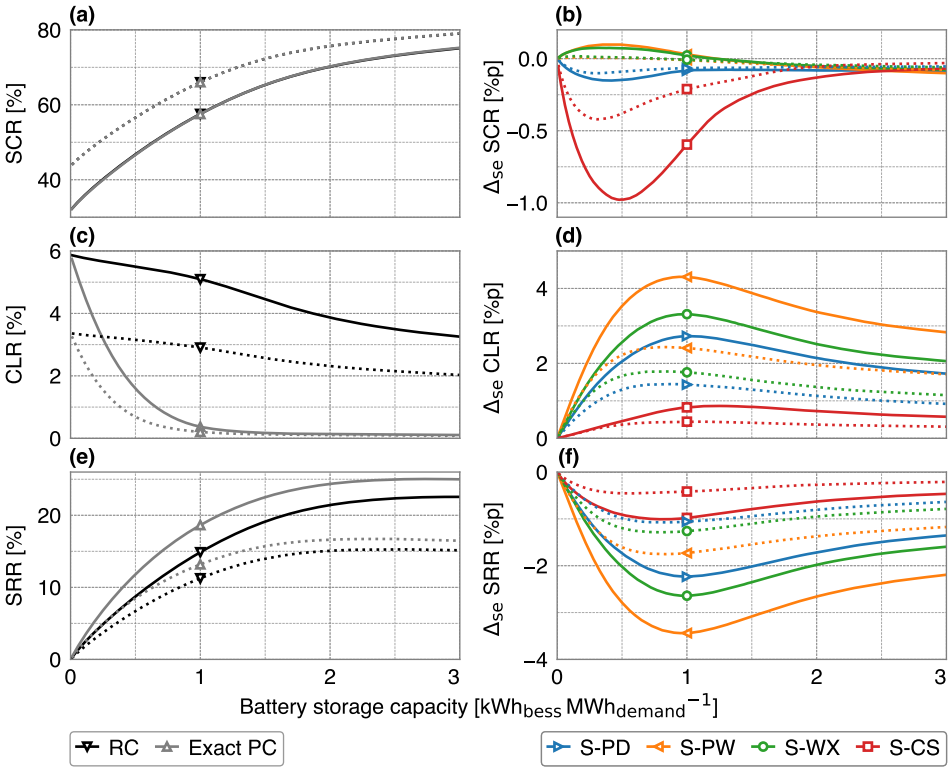

Figure 3.6 · Influence of relative battery system capacity on SCR (a), CLR (c) and SRR (e) for the RC and PC with exact forecast, and difference in SCR (b), CLR (d) and SRR (f) of the scenarios minus the exact forecast. The solid lines show the average value of residential systems and the dotted lines show averages of commercial systems. Reference system values are indicated by the markers.

is overestimated from the total battery capacity reduces with larger battery storage capacities. Consequently, the difference with the exact forecast is reduced and reaches similar values as the other three forecast strategies (at 2.5 kWh).

With an increase in battery size, curtailment losses are faster decreasing for exact PC strategy compared to RC strategy. CLR decreases with the exact PC strategy from ≈5.8% to 0.1% for residential systems and from ≈3.3% to 0.08% for commercial systems. This means that larger battery storage capacities are required to completely eliminate curtailment losses. Large Δ_{se} are shown for the S-PW and small Δ_{se} for the S-CS scenario.

SRRs are higher for residential than for commercial systems, and higher for exact PC strategy than for RC strategy. Storage revenues show an almost linear increase until a storage capacity of ≈ 0.5 kWh. Highest SRRs are reached at capacity of 2.75 kWh, specifically 25.0% for residential systems. Commercial systems reach a maximum SRR of 16.7% at a storage capacity of 2.4 kWh. A small drop in SRR is observed for larger storage capacities, caused by higher share of charging and discharging losses. For this reason, larger battery sizes are not recommended. The S-CS scenario has the largest revenue of all used forecast scenarios, which is similar as observed for the PV system size sensitivity analysis.

3.4.3 Battery inverter rating

The impact of relative battery inverter rating, for steps of 0.0025 kW, is presented in Fig. 3.7. Comparable SCR for the RC strategy as for the exact PC strategy are shown. SCR is rapidly increased until a battery inverter rating of ≈0.1 kW, and converges to a maximum of 57.9% for residential and ≈66.3% for commercial systems. An interesting observation for the RC strategy can be made concerning the relation between battery inverter rating and curtailment loss. CLR decreases until an inverter rating of 0.12 kW, but show an increase for larger capacities. A lower inverter rating limits the charge rate of a battery, i.e. the battery is charged slower. As a result, additional battery capacity becomes available to charge PV peak energy and therefore reduces curtailment loss. This limited battery charging disappears with ratings >0.6 kW because no change in curtailment loss is observed for these capacities.

SRR of residential and commercial systems are increased using the RC strategy until a rating of 0.19 kW. Using the PC strategy, this increase is observed until 0.4 kW for residential and 0.33 kW for commercial systems. Larger inverters have a higher share of energy loss due to the battery and inverter efficiencies, which results in lower revenues. For this reason, battery inverters with ratings >0.4 kW per kWh of storage capacity are not recommended.

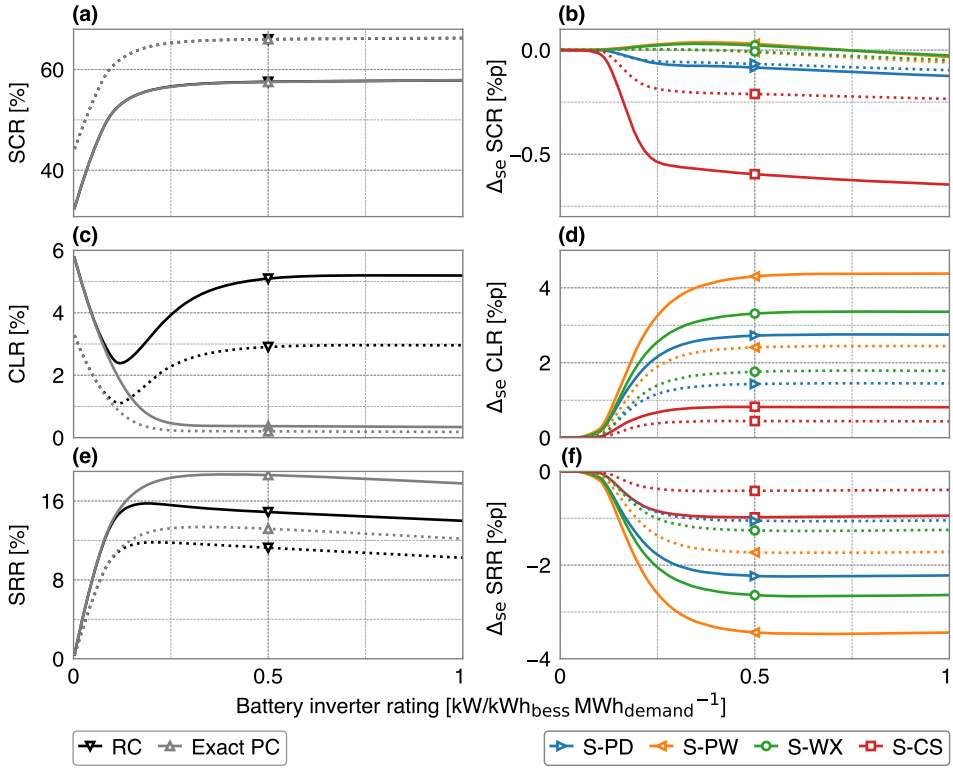

Figure 3.7 · Influence of battery inverter rating on SCR (a), CLR (c) and SRR (e) for the RC and PC with exact forecast, and difference in SCR (b), CLR (d) and SRR (f) of scenarios minus exact forecast. Residential systems are indicated by solid lines and commercial systems are indicated by dotted lines. Reference system values are indicated by the markers.

3.4.4 Feed-in limit

Influence of the relative used feed-in limit with steps of 0.025 kW, are presented in Fig. 3.8. The RC strategy does not affect the timing of battery charging or discharging, thus is not affected by the feed-in limit. With the exact PC strategy, battery capacity is reserved to store PV energy which exceeds the feed-in limit. Consequently, under a restricted feed-in limit, less energy can be stored and discharged on later moments. This results in a small reduction of SCR, especially visible for residential systems.

PC strategies show a decrease of SCR until a certain FIL, thereafter followed with an increase in SCR. This is especially visible for scenarios where there is an overestimation of the PV energy production, namely the S-CS scenario. A more strict limitation (towards 0 kW) requires more reserved battery capacity to store excess PV. Hence, relatively less storage capacity is available to store direct excess PV energy. For more relaxed limitations (towards 1 kW), less PV peak power must

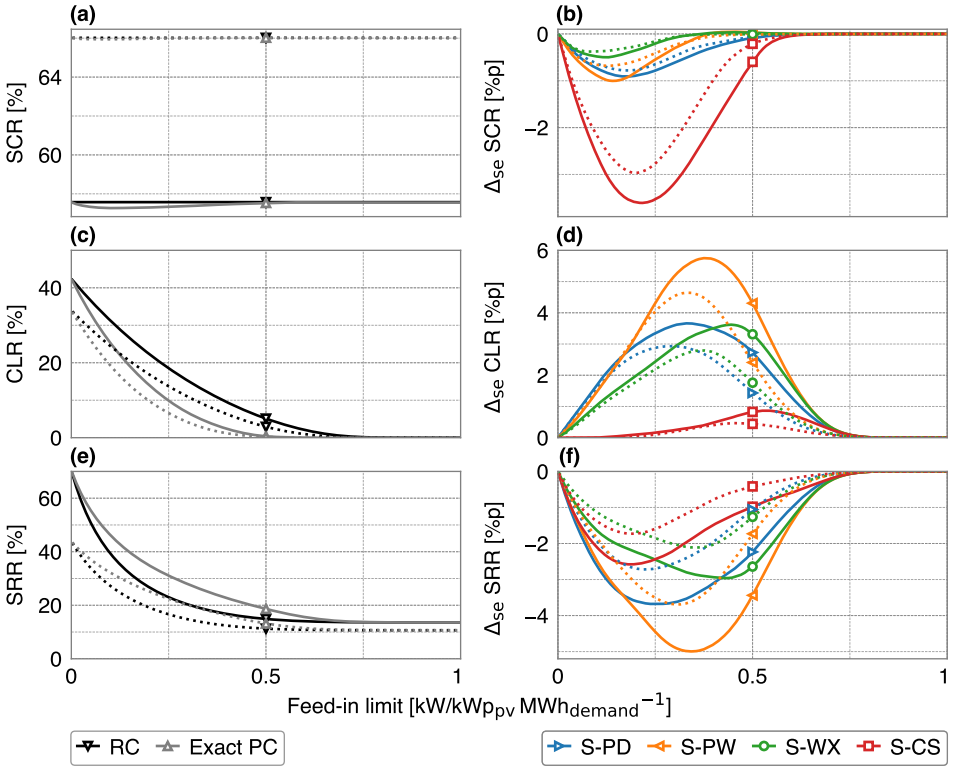

Figure 3.8 · Influence of the relative feed-in limit on SCR (a), CLR (c) and SRR (e) for the RC and PC with exact forecast, and difference in SCR (b), CLR (d) and SRR (f) of scenarios minus exact forecast. Residential systems are indicated by solid lines and commercial systems are indicated by dotted lines. Reference system values are indicated by the markers.

be curtailed. Subsequently, a lower amount of storage capacity is reserved for excess PV peak power, and more storage capacity is available for self-consumption.

Using the RC strategy, curtailment losses are eliminated at a FIL of ≈0.85 kW. The PC strategy completely removes these losses at a FIL of ≈0.7 kW. The FIL shows a large sensitivity of the used forecast scenario. For residential systems, the S-WX scenario has higher CLR reduction compared to the S-PD scenario, with feed in limits <0.4 kW. The opposite is seen for more relaxed FILs. This shows that the weather forecast method underestimate the PV peaks (>0.4 kW) compared to the PV-PD method. This could be caused by the weather forecast time step of 3 h used in the PV-WX forecast method. Therefore, PV peaks are averaged out, which is also shown for the PV-PW method. Subsequently, battery capacity reservations for these higher peaks are lower, and curtailment losses are higher.

When no PV energy can be fed back to the grid, similar SRRs are shown for RC as for PC strategy. Corresponding SRR are 69.2% for residential and 43.4%

for commercial systems. Benefits of PC strategy over RC strategy increase until a FIL of 0.2 kW for both residential and commercial systems. With these feed-in limits, SRR are 8.2% point higher for residential systems and 6.0% point higher for commercial systems, as shown in Fig. 3.8 (e). For more relaxed limitations (towards 1 kW), differences between the RC and PC strategy disappear. Storage revenues with a FIL of 1 kW depend only on the increased PV self-consumption. The S-CS scenario shows the highest SRR, whereas lowest SRR are observed in the S-PW scenario.

3.4.5 Sales to purchase ratio

Sales to purchase ratio solely affects storage revenues, therefore only influences on SRR are presented in Fig. 3.9. SPR was varied with steps of 0.0025 between 0 and 1. Thus, we assumed only electricity feed-in tariffs that are lower than the electricity consumption tariff.

With an SPR of zero, electricity fed back to the grid has no financial value, which means that reducing curtailment loss has no financial benefit. Consequently similar SRRs are seen for RC and PC strategy, with significantly larger values for residential (70.3%) than for commercial system (33.8%). An increase in SPR results in an increased value of sold electricity and thus a decrease in SRR. It is essential to note that the RC strategy drops below zero, at a SPR of 0.86. For this SPR, the value of added self-consumed energy due to energy storage is not sufficient enough to compensate for charge and discharge losses of the BESS. Thus, the battery storage system will have no added revenue for these conditions. Nevertheless, the exact PC strategy has positive SRR for all analysed sales to purchase ratios. In this scenario, PV produced electricity that would be lost due to feed-in limitation is stored and later used which increases the SRR to a positive value.

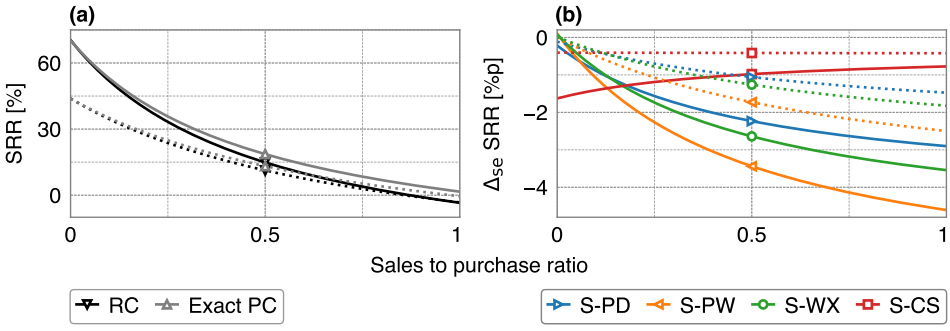

Figure 3.9 · Influence of the sales to purchase ratio on SRR (a) for the RC and PC with exact forecast, and difference in SRR (b) of scenarios minus exact forecast. Residential systems are indicated by solid lines and commercial systems are indicated by dotted lines. Reference system values are indicated by the markers.

A large influence of the PV forecast scenario on SRR of the PV-battery system is seen. A reduction of SPR results in a decrease of the value of sold electricity. Subsequently, the value of self-consumption increases, whereas the value of reducing curtailment loss decreases. The opposite effect occurs for relatively larger SPR. The S-WX scenario shows highest SCR, whereas the S-CS scenario has lowest CLR. Consequently, residential systems with a SPR <0.13 have highest SRR in the S-WX scenario. The S-PD scenario shows the largest SRR for a SPR 0.13 and 0.18, whereas for larger SPR the S-CS scenario has the highest revenue. Commercial systems have a turning point between the S-WX and the S-CS at a SPR of 0.11, which is lower than for residential systems.

3.4.6 Impact of system degradation

A commonly heard concern regarding PV-battery systems is the influence of degradation on the performance of these systems. Therefore, we assessed the influence of PV systems and BESS degradation for a period of 25 years. A relative long lifetime was investigated to assess the possible impact of systems that keep operating even when economic lifetime has passed. We assumed a PV systems degradation value of 0.5% per year[96]. The real-time PV yield pattern and forecasted PV yield patterns were annually reduced with 0.5%. BESS degradation was modelled for a lifetime of 5000 full cycle equivalents and a calendric lifetime of 15 years[97]. 80% of the initial battery capacity is reached after these cycles, or after this lifetime. Rain-flow counting method was used to count the number of battery cycles and depth of discharge for each cycle, for each year of data[98]. These numbers were converted to the number of full equivalent cycles, based on degradation parameters from previous studies[97,99]. Annual PV yield and battery storage capacity degradation were subtracted from the previous year to find the capacity values for the next year.

The impact of PV system and BESS degradation on the performance indicators are presented in Fig. 3.10. PV system degradation reduces PV electricity production over time, which increases PV self-consumption. Battery degradation reduces battery storage capacity and decreases self-consumption. Residential systems show a reduction from 57.6% to 55.6%, with an average reduction of 0.08% point per year. Commercial systems show a slight reduction in SCR until year 18, followed with an increase in SCR. Residential systems utilize the battery more than commercial systems. Therefore the impact of battery degradation is larger than the impact of PV system degradation on self-consumption. This results in a SCR reduction for each year. The battery degradation is less severe for commercial system. After 18 years, a larger effect on the SCR is observed from the PV system degradation than from the battery storage capacity degradation.

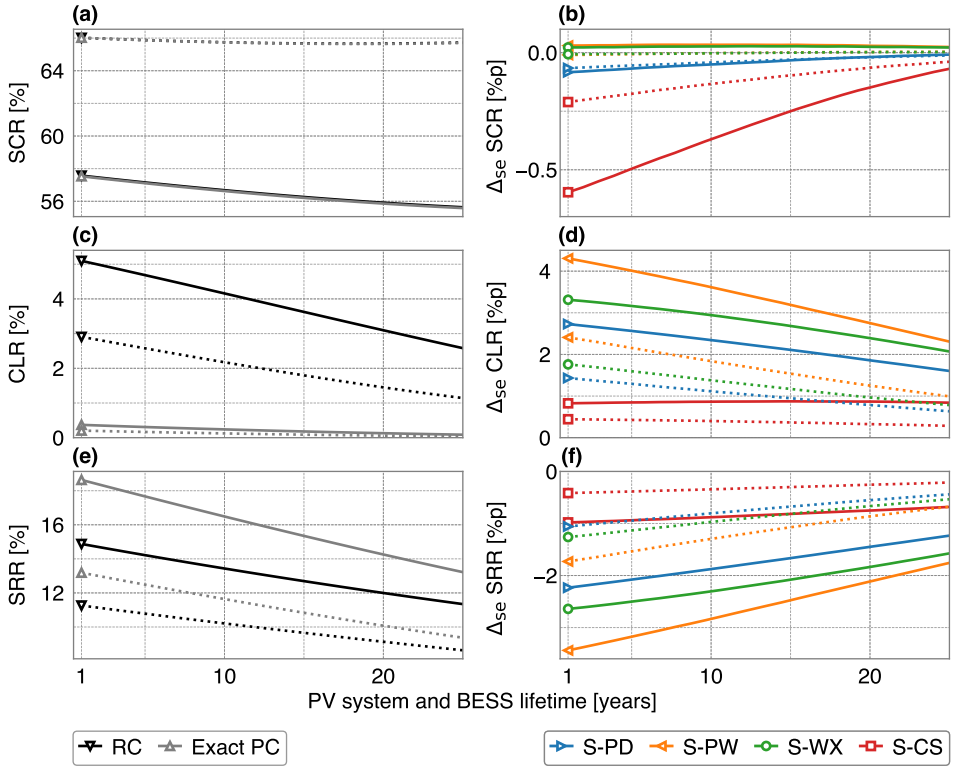

Figure 3.10 · Influence of PV system and BESS degradation on the SCR (a), CLR (c) and SRR (e) for the RC and PC with exact forecast, and difference in SCR (b), CLR (d) and SRR (f) of scenarios minus exact forecast. Residential systems are indicated by solid lines and commercial systems are indicated by dotted lines. Reference system values are indicated by the markers.

The difference between the exact strategy and the forecasting strategies are reduced over the systems lifetime. Larger reduction is shown for the S-CS strategy, caused by a larger reduction in forecasted PV electricity yield. Subsequently, less battery storage capacity is reserved to decrease feed-in losses and more capacity is available to increase self-consumption.

A reduction in PV yield results in lower curtailment losses. CLR show a steeper decrease over time in the RC strategy compared to the exact PC strategy. The forecast scenarios show a reduction over time caused by less PV production, except for the S-CS strategy. This strategy does not show a decrease because the PV yield production is overestimated and therefore the reserved storage capacity was already sufficient to have a low CLR.

A larger reduction of storage revenue over time is seen for residential systems than for commercial systems. Residential systems show a reduction in SRR of 0.21% point per year in the exact PC strategy and of 0.14% point per year in the

RC strategy. This results in a significant loss of storage revenues over the system lifetime of respectively 14.1% and 17.9% in the PC and the RC strategy. Commercial systems have a lower SRR reduction of 10.5% and 12.5% in the PC and the RC strategy. The SRR difference between the exact forecast and the forecast scenarios decreases over time for all scenarios.

3.4.7 Multiple system parameter variation

The influences of simultaneous variation of multiple system parameters on the storage revenue rates have been assessed. The PC strategy with exact forecast was used to examine the potential of this control algorithm on the SRRs. The average SRRs for residential systems are shown for 12 scenarios in Fig. 3.11. Battery storage capacity (horizontal axis, step of 0.01 kWh) and sales to purchase ratio (vertical axis, steps of 0.025) are shown on each of the subplots. Four feed-in limitations (0, 0.25, 0.5, 0.75 kW) and three PV system sizes (0.5, 1 and 1.5 kWp) were assessed. The influence of battery inverter rating which are commonly used (>0.5 kW) on the storage revenue ratio is minor (see Fig. 3.7). Hence, this parameter was kept constant at 0.5 kW per kWh of storage capacity.

Electricity cannot be exported to the grid under a FIL of zero. Consequently, the SPR does not influence SRR and an increase in battery storage capacity results in a non-linear growth of revenues. Similar SRRs are seen for the three PV system sizes with relative small battery storage capacities (<0.5 kW). Larger differences in SRRs are observed with battery capacities of 3 kWh. These are 80.0%, 110.9% and 117.9% for respectively 0.5, 1 and 1.5 kWp PV size. The difference in SRR between a PV system size of 0.5 kWp and 1 kWp is larger than between 1 and 1.5 kWp. Larger PV systems produce more surplus of electricity that could be stored in the battery. Yet, the electricity consumption is similar for all PV system sizes. Therefore, fewer moments occur that the battery will be discharged for these larger PV systems, which results in a lower increase of SRRs.

Electricity is lost in every moment that a battery is charged and discharged. This reduces storage revenue rates, which eventually become negative. For smaller battery capacities, the value added due to reduced curtailment losses is higher than the value lost caused by battery charge and discharge losses. Hence an increase is observed in SRR. A peak in SRR is observed for a certain battery capacity followed by a decrease for larger battery capacities. This peak in the contour lines disappears with a lower SPR, which increase the value of self-consumption.

Only positive SRRs are observed under the FIL of 0.25, whereas under larger other FIL (0.5 & 0.75) negative SRRs are shown. In addition, a FIL of 0.5 shows that the area of negative values decreases for larger PV system sizes. These larger systems produce more PV electricity that exceeds the feed-in limit, which eventually

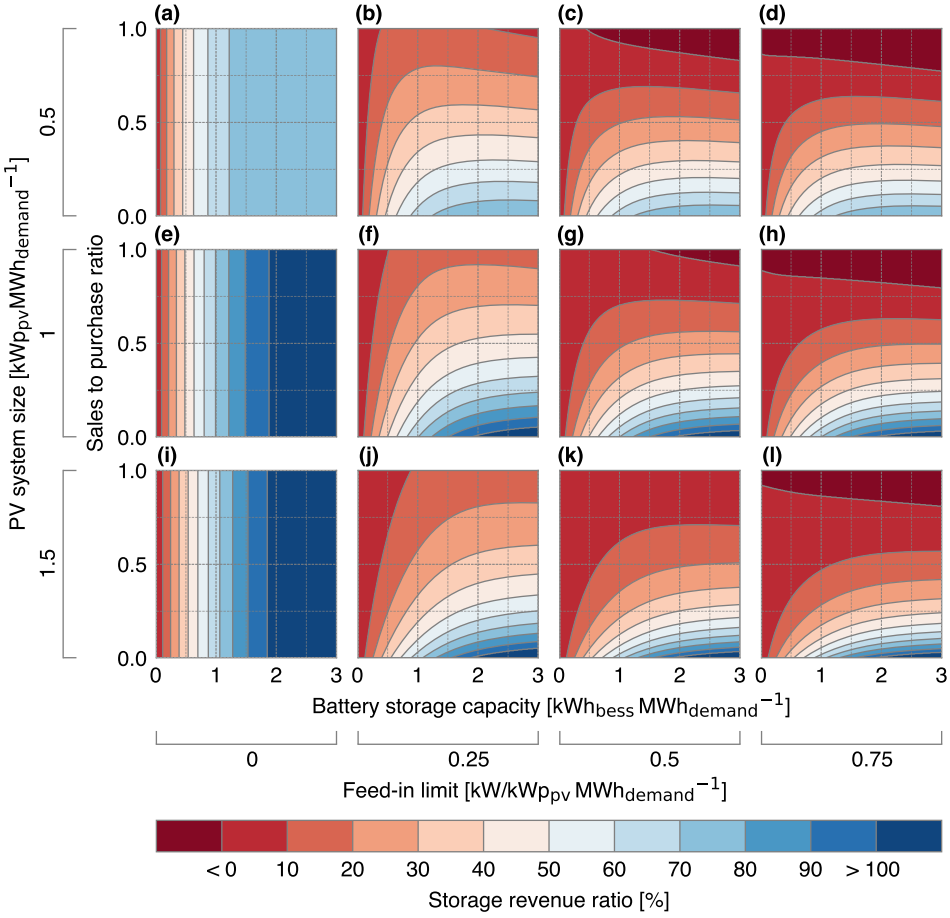

Figure 3.11 · Influence of the battery storage capacity (horizontal axis) and the sales to purchase ratio (vertical axis) on the average storage revenue ratio (colours). The storage revenues were assessed using the PC strategy with the exact forecast for residential systems. Four feed-in limitations (0, 0.25, 0.5, 0.75 kW) and three PV system sizes (0.5, 1 and 1.5 kWp) are shown in the subplots. Similar feed-in limits are shown in columns and PV system sizes in rows. For example, the subplot (a), (e) & (i) show the values for a feed-in limit of 0 kW, and the subplot (a), (b), (c) & (d) show values for a PV system size of 0.5 kWp. The battery inverter ratings were kept constant at 0.5 kW per kWh of battery storage capacity.

increase revenues of a BESS. Less battery capacity is reserved for a FIL of 0.75 kW, therefore more capacity is available to increase self-consumption. However, for high SPRs (>0.85), the added value of self-consumption is negative due to battery charge and discharge losses. Consequently, more electricity is lost by increasing self-consumption than lost by a feed-in limit. This explains why the difference in negative areas of the PV system sizes is much smaller for a FIL of 0.75 than for a FIL of 0.5.

3.5 Discussion

This research developed and assessed four methods for PV forecasting and three methods for demand forecasting. These forecasts were used in a predictive control strategy to increase PV self-consumption and to reduce curtailment losses. We assessed the impact of these forecast methods using a PC strategy on the performance of PV-battery systems.

We found significant impact of the system design parameters on the performance indicators. Increasing the PV system size lowers self-consumption ratios and increases curtailment loss. Larger battery capacities converges the storage revenues towards a maximum, followed by a decrease of revenue. Battery inverter ratings of 0.6 kW for each kWh of storage are sufficient for PV peak power storage, especially with a feed-in limit of 0.5 kW/kWp. A strong decrease in performance indicators is observed for smaller inverter capacities. The ratio between the feed-in tariff and the consumption tariff strongly influence the value of the self-consumed and avoided curtailed energy. Battery degradation substantially reduces the storage revenues over the lifetime of the battery system and should therefore be always included in economic calculations. Overall, these results showed that the system performance heavily depends on the chosen PV-battery design parameters, demand pattern and electricity tariff.

3.5.1 Comparison with previous studies

Forecast errors of predicted PV yield and electricity demand are in line with errors found in previous studies. Artificial neural networks were used to predict hourly PV yield and energy consumption for a German household. PV forecast errors with a nRMSE of 9.5% and electricity consumption errors of nRMSE of 9.3% were found in this study[87]. A nonlinear autoregressive with exogenous input model was tested which used weather and measurements of neighbouring PV systems to create PV yield forecasts, and revealed nRMSE between 9% and 25%[100]. Another research forecast residential load found MAPE errors of ≈1% lower using a multiple linear regression forecast than using the 7 days average, which is a similar method as used in this study[101]. Deep neural network based load forecasting models were used to predict commercial load and found average MAPE of 8.8%[102]. Our study showed lowest annual nRMSE of 11.4% for PV yield forecast and 7.4% as the average for residential demand. Our forecast errors are in line with the more sophisticated models presented in previous studies.

Performance of the PV-battery systems showed similarities with earlier studies. The RC control strategy shows that residential self-consumption ratios are ranging between 51.8% and 65.0%, which is in line with values found in previous studies[76,103]. Similar PV-battery performance is shown for using averaged

energy demand and PV energy production from the previous week[82]. No comparable study was found for commercial systems that were mainly modelled for office buildings. The clear-sky forecast method shows comparable reduction of curtailment loss to a study which used this method with demand patterns from Switzerland[77]. However, this study presents a smaller difference in self-consumption between the RC strategy and PC strategy with exact forecast. This is caused by the used battery capacity reservation algorithm, which uses the demand forecast as input to determine the required battery capacity reservation.

Studies concluded that an overestimation of forecasted PV yield production results in lower self-consumption ratios but also lower curtailment losses[76,80]. No direct comparison could be made on specific storage revenues because this method was not used in previous research. Still, the convergence to a maximum of storage revenue under an increase in battery size was shown before[77,79].

3.5.2 Input data

The energy consumption of residential and commercial buildings was measured using an interval of 15 min. Also, the real-time PV pattern was modelled using radiation data of a 10 min interval. Both patterns were resampled to 5 min interval to match the time step interval. However, actual patterns have a higher fluctuation of power than the used pattern. For example, extreme variation of PV system power output could be expected with passing clouds. Both PV production and demand patterns are more flattened compared to actual patterns. This changes the overlap of the patterns, and therefore affects self-consumption and the operation of battery control strategies. Previous studies examined the effect of time resolution on the performance of PV-battery systems. Relative errors below 6% were found for using 15 min data for self-consumption calculations[67]. Curtailment loss ratio was 2.8% point lower with 15 min data, compared to 5 s data[77]. Consequently, higher storage revenue ratios could be obtained than presented in this study. Therefore, we recommend assessing the proposed forecast methods with data of a higher time resolution.

The obtained weather prediction data has a time resolution of 3 h, but using data with smaller time resolutions could improve this forecast. The PV peak production forecast on clear-sky days will be better predicted. Nevertheless, day-ahead forecasting of moving clouds and thus the right timing of PV peak production is very difficult. Especially, because the Netherlands has a cloudy climate. Further research on the impact of smaller time resolution of weather prediction data on performance of PV-battery systems is recommended.

The average specific yield in the Netherlands is 875 kWh/kWp, which is lower than the specific yield used in our study[104]. The optimal orientation for maximizing PV energy production was chosen to model PV yield, whereas for actual PV systems the orientation of a building influences the PV module orientation. This reduces the PV yield which increases self-consumption and lowers curtailment losses. Both effects cause lower storage revenues. Hence, it is recommended using real PV pattern measurements with different orientations for future studies.

3.5.3 Future trends

Other options to improve PV energy integration in the urban energy systems are currently rapidly developed. These options could compete with local residential and commercial energy storage. Especially, community energy storage could be more economically feasible for reducing low voltage grid impact and increasing locally consumed PV energy[105]. However, a detailed layout of the low-voltage grid is required to accurate include grid-losses. Nevertheless, further research concerning technical and economic comparison of local and community energy storage systems is recommended. Also, the comparison of forecast methods for local and community storage systems could be of interest.

Rescheduling residential and commercial appliances could shift energy consumption to moments with relatively high PV energy generation, for example using dynamic tariffs[106]. However, these options demonstrate relative low improvement in PV self-consumption, therefore having low economic potential[41,42]. Nevertheless, the current increase of electrical vehicle deployment increases the electricity demand within urban areas. This opens new opportunities to increase PV-self-consumption by control strategies for electrical vehicle charging[68]. Also, control strategies that combine thermal and electric storage are investigated to improve residential self-consumption[107].

Battery energy storage systems can provide services for different electricity markets. For example, provision of frequency control to balance and maintain grid frequency. Combining multiple revenue streams for energy storage improves the revenues for battery storage systems[108]. Control strategies that combine revenue streams depend on the associated energy markets and policies. Assessment of these strategies is recommended for future research.

Reducing power flow to the grid lowers grid-investment costs, especially for cables and transformers. A reimbursement to the PV-battery system owner could be provided for this service, resulting in increased storage revenues. Finally, this study used no time-dependent electricity tariffs and feed-in limits. Time-of-use electricity tariffs and dynamic feed-in limits could increase the value of PV-battery

systems. Battery energy storage revenues might differ significantly when time-of-use tariffs will be used for both consumption and feed-in tariffs. These tariffs are commonly used, especially for large commercial buildings. It is expected that the variability in electricity prices will increase with larger share of fluctuating renewable electricity generation capacity. Therefore, trading on electricity markets could increase the economic value of the battery energy storage systems. However, this requires knowledge about the structure and decision models of time-of-use tariffs and dynamic feed-in limits. Forecast methods should be developed and assessed that optimize storage revenue for flexible tariffs and dynamic tariffs. Research in those areas is therefore highly recommended.

3.5.4 Implementation considerations

The implementation of forecast algorithms in battery energy management systems requires some adjustments. First, measurements of historical consumption data are required, which could be obtained from smart energy meters. These electricity meters are currently deployed within the Netherlands and have an option to send measured data to other devices. Historical PV production could be obtained from PV inverters. Predicted weather forecast data requires an internet connection. Clear-sky irradiance data can be calculated internally using the battery energy management system. Also the forecast strategies could be installed on these management systems.

The developed methods could be used in other European countries. These countries have different PV yield and demand patterns compared to the Netherlands. This will influence the accuracy of the forecast methods and the PV-battery performance indicators. For example, more PV peak power is produced in Southern European countries compared to the Netherlands. Therefore, relatively more PV peak power can be stored and therefore the reduction in curtailment losses is larger. Consequently, revenues of battery storage are expected to be higher.

3.6 Conclusion

This study assessed four PV yield pattern forecast methods and three demand patterns forecast methods. These forecasts were used in a predictive control strategy to improve self-consumption, reduce curtailment losses and increase revenues of PV-battery systems. We modelled performance of 48 residential and 42 commercial PV-battery systems, using different combinations of methods.

We found that the PV production patterns with predicted weather data have lowest errors. Energy consumption of residential buildings should be forecasted with using average energy consumption of the previous seven days. Forecast for

commercial systems should use measured historical demand from the previous weekday. Weather forecasts are not required to increase self-consumption ratio, since forecasts using historical PV production data show similar performance. Consequently, external data is not required to optimize PV self-consumption.

Predictive control strategies have higher storage revenues that real-time control. Storage revenues are larger for residential systems than for commercial systems and mainly depend on the value of self-consumed energy and reduced curtailed energy. Higher storage revenues are observed for stricter feed-in limitations. Consequently, a dynamic feed-in limitation could potentially increase storage revenues. The sales to purchase ratio strongly impacts revenues obtained for each used control strategy and forecast method.

To conclude, predictive control strategies are capable to improve self-consumption, as well as reduce curtailment losses. The performance of the battery control strategy depends on PV-battery system design parameters as well as system boundaries conditions, especially feed-in limit and sales to purchase ratio. Hence, it is recommended to customize the battery control strategy based on these conditions.

Acknowledgements

This work is part of the research programme Transitioning to a More Sustainable Energy System (Grant No. 022.004.023), which is financed by the Netherlands Organisation for Scientific Research (NWO). We are grateful to Hubert Spruijt of Senfal, Liander N.V. and the Royal Netherlands Meteorological Institute for providing data.

4

FRR provision by PV-battery systems

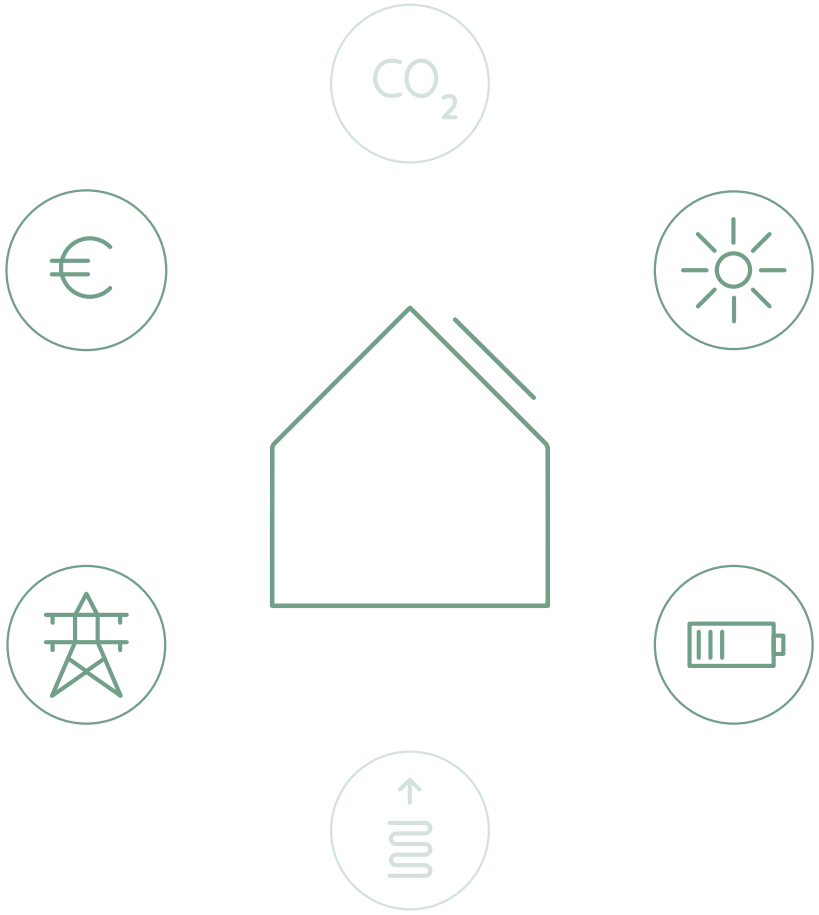

This chapter is based on the publication: G.B.M.A. Litjens, E. Worrell and W.G.J.H.M. van Sark. "Economic benefits of combining self-consumption enhancement with frequency restoration reserves provision by photovoltaic-battery systems". in: *Applied Energy* **223** (2018), pp. 172-187. DOI:10.1016/j.apenergy.2018.04.018

Abstract

Residential and commercial photovoltaic (PV) battery systems are increasingly being deployed for local storage of excess produced PV energy. However, battery systems aimed at increasing self-consumption are not constantly put to use. Additional battery storage capacity is available for a second application to improve the profitability of an energy storage system. One of these options is the provision of frequency restoration reserves (FRR) to the electricity balancing market. This provision can be either negative to compensate for excess power supply, or positive to compensate for excess demand on the power market. This study assesses the benefits for residential and commercial PV-battery systems by combining PV energy storage for higher self-consumption with provision of FRR. Six battery storage dispatch strategies were developed and assessed on the technical and economic performance of 48 residential and 42 commercial PV-battery systems. These systems were modelled over their economic lifetime with a time resolution of 5 min and with historical energy consumption measurements and market prices. FRR provision results in a small drop in the self-consumption rate of 0.5%. However annual revenues are significantly increased. Using battery storage systems only for self-consumption is not profitable with the assumptions used in this study. Provision of negative FRR substantially reduces the electricity bought with the consumption tariff and increases investment attractiveness substantially. Prioritizing the provision of FRR over self-consumption enhancement results in even higher revenues, but significantly reduces self-consumption. We recommend FRR provision to economically investment in residential battery storage systems. Commercial systems need prioritization of both positive and negative FRR provision over self-consumption for a cost-effective investment. In conclusion, combining enhancement of PV self-consumption with the provision of frequency restoration reserves leads to profitable investments.

4.1 Introduction

Photovoltaic (PV) battery systems are increasingly deployed in urban areas to store excess PV energy for later use. In this way, the effect of intermittence of PV generated electricity on a low voltage network is reduced and self-consumption is increased[109]. Furthermore, CO_2 emissions from fossil-based backup power generation are reduced, particularly when curtailment of renewable energy generation is avoided[13].

The cost of stationary battery energy storage systems (BESS) is rapidly decreasing and this is expected to continue due to their current and future potential of deployment[39]. However, the benefits of storing PV electricity are limited, especially in areas with small differences between prices of consumption and feed-in tariffs[110]. The added value that can be generated for each kWh of stored PV energy is restricted. Also, battery systems only use part of their potential storage capacity, especially in locations with large seasonal difference in PV electricity generation. Stationary batteries can be used for a broad range of use cases and are therefore seen as a multi-purpose technology[38]. Combining multiple applications improves the financial attractiveness of these storage systems[111].

A potential additional application of PV-battery systems is offering power and energy to the balancing and ancillary services markets. Two balancing services can be distinguished that are traded on the imbalance markets for the Netherlands, namely frequency containment reserves (FCR) and frequency restoration reserves (FRR). FCR (also known as primary control reserves), are the first tier to balance the grid and are automatically activated. The balancing power capacity is contracted in blocks of one week and the reserved capacity is remunerated[112]. Moreover, the BESS has to be able to deliver the contracted FCR, otherwise the balancing service provider receives financial penalties.

FRR (also known as secondary control reserves) are provided to restore the FCR and to compensate for excess of power supply or an excess of demand. Provision of FRR can be either mandatory or voluntary. Mandatory contributors place bids of energy provision (positive) or energy subtraction (negative) capacities on a bid ladder. These are delivered in blocks of 15 min and can be proposed to the market up to one hour before dispatch. The bid ladder determines the minutely imbalance FRR price. Voluntary contributors observe the current imbalance price and determine if they want to deliver FRR. In case of mandatory contribution, all positive and negative energy delivered is remunerated within a block of 15 min. In case of voluntary contribution, only the energy provision is remunerated if all energy within a 15 min block is positive provision, or all is negative provision[113]. FCR and FRR are contracted and remunerated by the Dutch transmission system operator (TSO) TenneT, in the Netherlands.

4.1.1 Literature review

Few studies were found that assess the combination of self-consumption enhancement with provision of control reserves. The ones found can be distinguished between studies that combine self-consumption with FCR, or with FRR. Revenues of storage systems that combine self-consumption with provision of FCR are about three times higher than if the BESS was solely used for self-consumption enhancement[114]. One study from Germany showed that annual revenue of €185/kW can be obtained from FCR provision by a residential PV-battery system. However, the self-sufficiency was reduced with 18.9%[115]. In addition, larger economic profitability was found for FCR provision than for self-consumption increase for a vanadium flow battery[116]. A significant increase in profitability of battery storage was observed when PV-self-consumption was combined with negative FRR provision to the German market[108]. Also, large scale community storage was found economically feasible for FRR provision[117].

Aggregators can operate these residential and commercial battery systems on this market. Lately, there have been a few commercial parties that are interested in combining self-consumption with FCR provision[118,119]. The request for provision of grid balancing is expected to increase with a large share of renewable generators in the electricity grid[120]. Consequently, grid balancing costs are expected to increase and are a potential barrier for future growth of variable renewable resources[121]. PV-battery storage systems might be useful to provide solutions to overcome this barrier.

4.1.2 Research aim

Literature shows a high potential value that can be added by BESS with providing FCR and FRR. Despite this high potential only a few studies were found concerning this prospective. Besides, these studies use a single demand profile and one year of data. Furthermore, the influence on PV self-consumption, battery degradation or investment attractiveness is not researched in detail. The lack of these results restrains the development of PV-battery systems for balancing services.

In this study, we aim to assess the technical and economic performance of combining self-consumption enhancement with frequency restoration reserves provision. We select FRR since its market conditions are more flexible than the FCR market. Furthermore, a mandatory contribution to the FRR market was selected to obtain both revenues for positive and negative provided FRR. We use historical FRR prices from 2011 to 2016 of the Dutch market and measured energy demand of 48 residential and 42 commercial buildings. We assessed all systems

using six battery storage dispatch strategies, each with a different aim. In addition, we conducted a sensitivity study to identify the most important parameters on economic profitability of a PV-battery system.

The combination of a large range of systems with six different battery dispatch scenarios shows a wide variety of technical and economic results. These novel results provide a first insight in the added value that PV-battery system have when tapping into the frequency restoration reserve market. We identify new directions for future research and help commercial parties to contribute in this field. This will encourage the deployment of multiple purposes battery systems. Subsequently, this will enable a higher share of fluctuating renewable energy sources into the energy systems and help the transition towards a more sustainable energy system.

The remainder of this chapter is arranged as follows. Section 6.2 explains the battery storage dispatch strategies, the used data and the technical and economic performance indicators. Section 6.3 presents the results on the technical assessment of the battery storage dispatch strategies, followed by the economic assessment in Section 6.4. Section 6.5 examines the sensitivity of the reference parameters. Section 6.6 discusses the market assumptions and the implementation considerations of the dispatch strategies. Section 4.7 finalises with the key conclusions.

4.2 Methods

The methodology is explained in the next four subsections. Subsection 4.2.1 describes the battery storage dispatch strategies and the used model equations. Subsection 4.2.2 explains the technical and economic assumptions of the reference PV-battery systems. The used input time series are explained in Subsection 4.2.3. Lastly, Subsection 4.2.4 describes the performance indicators, used to assess the dispatch strategies.

4.2.1 Battery storage dispatch strategies

Six battery storage dispatch strategies were developed to assess the impact on self-consumption, FRR provision and combinations of self-consumption enhancement with FRR provision. Provision of FRR can either be positive or negative: positive FRR delivers electricity to the grid and negative FRR withdraws electricity from the electricity grid. The six developed strategies are:

- PV self-consumption enhancement only (SCO).
- Provision of frequency restoration reserves only (FRRO).
- Prioritizing PV self-consumption over providing FRR (PSC).
- Prioritizing PV self-consumption over providing only negative FRR (PSCN).
- Prioritizing FRR provision over PV self-consumption (PFRR).
- Prioritizing only negative FRR provision over PV self-consumption (PFRRN).

The SCO and FRRO strategies consist of a single application and are examined to distinguish the individual impacts of these applications. The PFRR and PFRRN strategies assess enhancement of self-consumption as a primary application and provision of FRR as a secondary application. The PFRR and PFRRN strategy assessed the provision of FRR as primary storage application and enhancement of self-consumption as secondary application.

The storage dispatch strategies were assessed using a PV-battery model developed in Python (v3.5). The model simulated the battery charging and discharging behaviour with a time step (Δt) of 5 min. A schematic representation of the model is shown in Fig. 4.1. This model consists of three separate blocks: enhancement of PV self-consumption (a), provision of negative FRR (b) and provision of positive FRR (c). The SCO strategy only uses block (a) and the FRRO block (b) and (c). The PSCN and PFRRN use block (a) and (b). The PSC and PFRR strategies use all three blocks.

PV self-consumption enhancement

The SCO strategy operates according to the PV self-consumption enhancement block only (Fig. 4.1 (a)). The difference between PV power production (P_{PV}) and electricity consumption (P_{demand}) is assessed for each time-step (see red rectangle). The battery is charged when excess PV and battery capacity is available. The battery capacity is assessed using the battery state of charge (SOC). Discharging happens if demand exceeds PV production and energy capacity is available in the battery. If no battery capacity is available to charge or discharge, then excess PV electricity is fed into the grid or requested electricity demand is imported from the grid.

A rule based algorithm was used to define the battery inverter power ($P_{B\,inv}$) and the battery state of charge ($E_{B,t}$) for each time moment. First the potential power ($P_{B\,pot}$) for charging or discharging the battery was determined. This power is limited by the battery inverter rating ($P_{B\,inv\,max}$). Then, the potential energy ($\Delta E_{B\,pot}$) was calculated which could be charged to, or discharged from, the

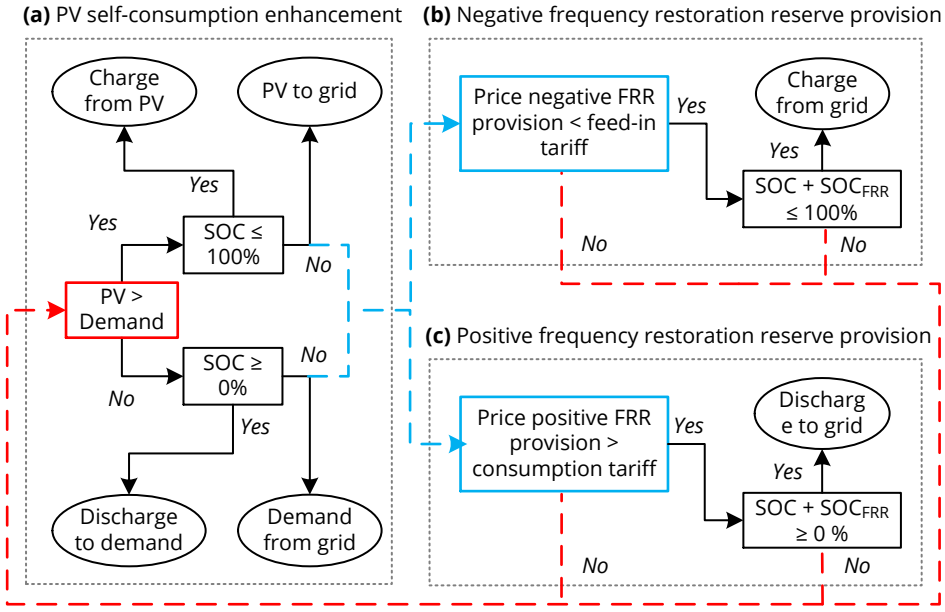

Figure 4.1 · Schematic overview of the model steps used in the battery storage dispatch strategies. The model contains of three blocks: PV self-consumption enhancement (a), negative frequency restoration reserve provision (b) and positive frequency restoration reserve provision (c).

battery. This depends on the charge efficiency (η_{charge}) or discharge efficiency ($\eta_{\text{discharge}}$) of the battery storage system. Next, the actual charged or discharged energy ($E_{\text{B pot}}$) was determined. These are related to the current battery SOC the minimum SOC ($E_{\text{B min}}$) and maximum SOC ($E_{\text{B max}}$). This set of equations are specific for the PV self-consumption enhancement (see block (a)) and are given in Eq. (4.1).

$$P_{\text{B pot}} = \begin{cases} P_{\text{PV}} - P_{\text{demand}} & \text{if } |P_{\text{PV}} - P_{\text{demand}}| < P_{\text{B inv max}} \\ P_{\text{B inv max}} & \text{if } |P_{\text{PV}} - P_{\text{demand}}| \geq P_{\text{B inv max}} \end{cases} \tag{4.1a}$$

$$\Delta E_{\text{B pot}} = \begin{cases} P_{\text{B pot}} \cdot \eta_{\text{charge}} \cdot \Delta t & \text{if } P_{\text{B pot}} > 0 \\ \frac{P_{\text{B pot}}}{\eta_{\text{discharge}}} \cdot \Delta t & \text{if } P_{\text{B pot}} \leq 0 \end{cases} \tag{4.1b}$$

$$\Delta E_{\text{B}} = \begin{cases} \Delta E_{\text{B pot}} & \text{if } E_{\text{B, t}} + \Delta E_{\text{B pot}} \geq E_{\text{B min}} \\ \Delta E_{\text{B pot}} & \text{if } E_{\text{B, t}} + \Delta E_{\text{B pot}} \leq E_{\text{B max}} \\ E_{\text{B, t}} - E_{\text{B min}} & \text{if } E_{\text{B, t}} + \Delta E_{\text{B pot}} < E_{\text{B min}} \\ E_{\text{B max}} - E_{\text{B, t}} & \text{if } E_{\text{B, t}} + \Delta E_{\text{B pot}} > E_{\text{B max}} \end{cases} \tag{4.1c}$$

Lastly, the battery inverter power and battery state of charge ($E_{\mathrm{B\,t+1}}$)) for the next time step were determined according Eq. (4.2).

$$E_{\mathrm{B,\,t+1}} = E_{\mathrm{B,\,t}} + \Delta E_{\mathrm{B}} \tag{4.2a}$$

$$P_{\mathrm{B\,inv}} = \begin{cases} \frac{(\frac{\Delta E_{\mathrm{B}}}{\Delta t})}{\eta_{\mathrm{charge}}} & \text{if } \frac{\Delta E_{\mathrm{B}}}{\Delta t} > 0 \\ \frac{\Delta E_{\mathrm{B}}}{\Delta t} \cdot \eta_{\mathrm{discharge}} & \text{if } \frac{\Delta E_{\mathrm{B}}}{\Delta t} \leq 0 \end{cases} \tag{4.2b}$$

Negative and positive FRR provision

The FRRO strategy uses the negative and positive FRR provision assessment blocks (Fig. 4.1 (a) & (b)). Negative FRR provision is feasible if the price of negative provision (π_{neg}) is smaller than the feed-in tariff ($\pi_{\mathrm{feed\text{-}in}}$). If negative FRR are provided than the price of negative provision is paid to the TSO. Positive FRR provision is feasible if the price of positive provision (π_{pos}) is higher than the consumption tariff (π_{cons}). In this case the price for positive provision is paid by the TSO. We used the consumption and feed-in tariff as the price points for feasible delivery of positive and negative FRR. Therefore it was possible to make a comparison with the other five dispatch strategies. Besides, the state of charge (SOC) of the battery storage must be sufficient to provide FRR. We assume that if power is provided to the FRR market, then it is similar to the maximum inverter rating. As a result, the pooling of battery storage systems from multiple residential or commercial systems will be less complex for an aggregator.

The battery state of charge in the negative and positive frequency restoration reserves provisions blocks were calculated using the following approach. First, the potential battery state of charge was determined by assessing the feasibility of FRR provision. Then, the actual energy that could be charged or discharged was determined, see Eq. (4.3). Lastly, battery inverter power and battery SOC were calculated according to Eq. (4.2).

$$\Delta E_{\mathrm{B\,pot}} = \begin{cases} \frac{P_{\mathrm{B\,inv\,max}}}{-1} \cdot \eta_{\mathrm{charge}} \cdot \Delta t & \text{if } \pi_{\mathrm{neg,t}} < \pi_{\mathrm{feed\text{-}in}} \\ 0 & \text{if } \pi_{\mathrm{neg,t}} \geq \pi_{\mathrm{feed\text{-}in}} \\ \frac{P_{\mathrm{B\,inv\,max}}}{\eta_{\mathrm{discharge}}} \cdot \Delta t & \text{if } \pi_{\mathrm{neg,t}} > \pi_{\mathrm{cons}} \\ 0 & \text{if } \pi_{\mathrm{pos,t}} \leq \pi_{\mathrm{cons}} \end{cases} \tag{4.3a}$$

$$\Delta E_{\mathrm{B}} = \begin{cases} \Delta E_{\mathrm{B\,pot}} & \text{if } E_{\mathrm{B,\,t}} + \Delta E_{\mathrm{B\,pot}} \geq E_{\mathrm{B\,min}} \\ \Delta E_{\mathrm{B\,pot}} & \text{if } E_{\mathrm{B,\,t}} + \Delta E_{\mathrm{B\,pot}} \leq E_{\mathrm{B\,max}} \\ 0 & \text{if } E_{\mathrm{B\,max}} < E_{\mathrm{B,\,t}} + \Delta E_{\mathrm{B\,pot}} < E_{\mathrm{B\,min}} \end{cases} \tag{4.3b}$$

Combining PV enhancement and FRR provision

The PSC strategy combines the PV self-consumption enhancement block with the provision of negative and positive FRR. This strategy starts with similar steps as in the SCO strategy, specifically the assessment of the difference between PV and electricity consumption. If the calculated battery inverter output was zero, then the strategy continued to assess the feasibility of negative FRR provision (see dashed blue lines in Fig. 4.1). This is feasible if the price of negative provision is smaller than the feed-in tariff. Consequently, all negative provided FRR is bought for a lower price than sold excess PV energy and therefore self-consumption is always profitable. Positive FRR provision is feasible when the price of positive provision is higher than the consumption tariff and battery capacity is available. Hence, electricity is always sold with a higher price than it is bought. The PSCN strategy is almost similar as the PSC strategy, yet only provision of negative FRR is possible. Therefore all energy that is charged in the battery is considered as self-consumed energy.

The PFRR strategy starts with the assessment of providing negative and positive FRR. If the battery inverter output is zero, then the dispatch strategy continues to the PV self-consumption block (see dashed red lines in Fig. 4.1). The PFRRN strategy only assesses the provision of negative FRR thus all excess energy stored from a PV system is accounted for as self-consumption. If the battery inverter was not used for self-consumption enhancement, or provision of FRR, then the algorithm continues with the next time step.

4.2.2 Reference PV-battery system

A reference PV-battery system was developed to assess the dispatch strategies for residential and commercial battery storage systems. A similar set of technical parameters were selected for residential and commercial systems, enabling comparison of the demand patterns. An overview of the technical and economic reference parameters used for residential and commercial systems is given in Table 4.1. Some economic parameters were set differently for residential and commercial systems due to the different system capacities and policies in place.

Technical parameters

The layout of an alternating current (AC) coupled lithium-based PV-battery system was selected. This consists of a PV array that is connected to the electricity grid by a PV inverter and a battery storage system that is connected with a battery inverter to the grid. AC coupled systems are most widely used in the literature and are very suitable for retrofit existing PV systems with electricity storage[93].

Table 4.1 · Reference residential and commercial PV-battery system parameters used to model the dispatch scenarios. The technical parameters are given above the dashed line and the economic parameters below the dashed line. Own assumptions are indicated by own.

Parameter	Residential	Commercial	Unit	Sources
PV system size	1		kWp_{PV} MWh_{demand}^{-1}	own
PV system degradation	0.5		%/year	[96]
Storage capacity	1		kWh_{BESS} MWh_{demand}^{-1}	[69,93]
Battery inverter rating	0.5		kW/kWh_{BESS} MWh_{demand}^{-1}	[95]
Total number of FCE	5000		#	[97]
Calendric lifetime	15		years	[97]
Round trip DCη loss	7.8		%	[95]
Storage pack cost	200		€/kWh_{BESS}	[122]
BOS battery system	150	100	€/kW	[123]
EPC battery system	150	100	€/kW	[123]
O&M battery system	1		%/year	[124]
Economic lifetime	25	20	years	own
Discount rate	2	4	%/year	[125]
Consumption tariff	0.178	0.106	€/kWh	[126]
Feed-in tariff	0.11	0.04	€/kWh	[127,128]

The modelled annual average PV electricity production (between 2012 until 2016) is 984 kWh for each kWp of installed PV capacity. Typically in the Netherlands, the PV installed capacity is chosen such that is able to cover the annual electricity consumption. Therefore, the installed PV system size was set to 1 kWp for each MWh of annual electricity consumption. A linear annual degradation of the PV yield reduction of 0.5%/year was assumed[96].

The battery energy storage capacity was set to 1 kWh for each MWh of annual electricity consumption, based on previous studies[69,93]. The battery inverter rating was set to 0.5 kW. This charge rate is commonly used, for example with a Tesla Powerwall[95]. Battery degradation was modelled for a calendric lifetime of 15 years and 5000 full cycle equivalents[97]. A battery round trip direct current (DC) efficiency loss of 7.8% was assumed, almost identical to a commercially available Tesla Powerwall. Normally, a battery system is operated in a limited SOC range in order to limit aging and for safety reasons. However, in this research we want to assess the impact of utilizing the full battery capacity. For this reason, the minimum SOC was set to 0% and the maximum SOC to 100% of the battery storage capacity.

The battery inverter efficiencies were retrieved from the parameters of the inverter efficiency curve of a SMA Sunny Boy Storage inverter, with a step size of 0.01%[94]. The used inverter curve resulted in a California Energy Commission (CEC) efficiency of 96.4%. A battery inverter standby consumption of 0.1% from the rated inverter power was assumed. We assumed a similar maximum AC input

as AC output for the battery inverter. Battery state of charge limits were set to a minimum of 0% and a maximum of 100%, thus the full battery storage capacity was available for electricity storage.

Economic parameters

We assumed a relative low battery storage pack cost of 200 €/kWh for residential and commercial systems[122]. Balance of system (BOS) and Engineering procurement construction (EPC) cost were both set to 150 €/kW for residential systems[123]. Larger system sizes are required for commercial systems, thus we assumed lower BOS and EPC cost for commercial systems of 100 €/kW.

Operation and maintenance costs of the battery storage systems were assumed to be 1% for both residential and commercial systems[124]. We assumed that the battery system is integrated in the energy system of the building. Consequently, a relative long economic lifetime was assumed of 25 years for residential systems and 20 years for commercial systems. Current guarantees for PV modules and micro inverters are in similar ranges. Replacements of broken components before the end of lifetime are included in the operation and maintenance cost. The battery pack will not be replaced after the economic lifetime. Discount rates of 2% for residential and 4% for commercial systems were selected, based on the current low rates for the Netherlands[125]. A higher discount rate for commercial systems was selected due to a shorter lifetime and a lower risk acceptance of commercial investors.

The consumption tariff for residential systems was set to 0.178 €/kWh, based on the average tariff prices for 2014, 2015 and 2016. Commercial systems have a lower consumption tariff of 0.106 €/kWh, mainly due to lower electricity tax for larger energy consumers[126]. Residential systems in the Netherlands profit from a net metering policy for power sold back to the grid, although this policy is currently under debate. Hence, we assumed a feed-in tariff for residential systems 0.11 €/kWh, based on the present feed-in subsidy for stimulation of sustainable energy production[127]. For commercial systems we assumed 0.04 €/kWh based on the average wholesale electricity prices (day-ahead market) in the Netherlands from 2014 until 2016[128].

4.2.3 Input time series

The storage dispatch strategies were modelled for an economic lifetime of 20 or 25 years in the reference scenario. PV yield, demand and FRR prices from 2012 until 2016 were used as input patterns. We repeated the patterns of these five years to create an input pattern of 20 years. Thus, data of the year 2012 were used in the first, sixth, eleventh and sixteenth year.

PV yield patterns were modelled with the python package PVLIB (v0.5.0)[61]. This open source package contains PV system performance models and validated atmospheric functions. Radiation, temperature, dew point temperature, wind speed and pressure were measured on a weather station in De Bilt, the Netherlands. Measurement intervals of radiation (10 min) and remaining weather parameters (one hour) were linearly interpolated to 5 min. These atmospheric parameters were combined with module parameters of the Sanyo HIP-225HDE1 to model a DC PV yield pattern. This pattern was converted to AC power pattern using efficiency parameters from the Enphase Energy M210 inverter which has 95.5% CEC efficiency. Due to a relative low temperature coefficient of the Sanyo module, the influence of temperature in the model is limited.

The PV system was modelled using a PV orientation of 180° module surface azimuth and 35° module tilt. The PV inverter power rating was set to 1 kW/kWp. The PV system yield pattern was linearly scaled to reach a performance ratio of 85%, corresponding with high performing systems for the Netherlands[89]. The annual modelled PV yield ranges between 935 kWh/kWp and 1031 kWh/kWp with an average of 984 kWh/kWp for 5 years.

Electricity consumption of residential buildings was derived from measurements by a Dutch distribution system operator and are publicly available online[64]. From this dataset, 48 demand patterns were selected with different dwelling types for 2013. Measured electricity consumption of 42 commercial buildings, mainly offices, was selected for 2013. Both datasets contains measurement data with a 15 min interval. No data of 2012 and between 2014 and 2016 were available, thus the consumption data of 2013 was used to fill the other four years. Weekdays and weekend days of the missing years were matched with the data of 2013. Heat demand of the buildings was not provided by electricity, therefore reducing the influence of ambient temperature on the electricity consumption. The residential and commercial demand patterns were used in a previous study[90]. All demand patterns were linearly interpolated to a 5 min interval to have a similar time step as the PV yield pattern. Distributions of annual energy consumption of demand patterns are shown in Fig. 4.2. Mean values of the distributions are indicated by the dotted lines. Residential consumption has a significantly lower mean (3.4 MWh) compared to commercial consumption (430 MWh). Median electricity demand of 3.3 MWh and 270 MWh were found for residential and commercial systems respectively.

Prices for providing negative or positive FRR were obtained from the Dutch TSO TenneT. These prices are published online and record the minutely settlement prices for negative or positive FRR provision[129]. The time steps of the price

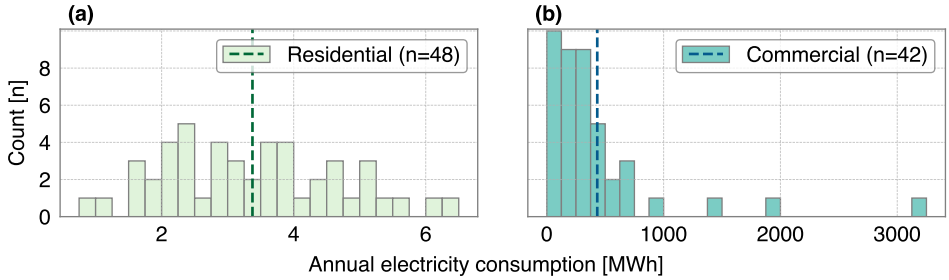

Figure 4.2 · Annual electricity consumption for residential (a) and commercial (b) systems used in this study are shown in a histogram. Mean values of the distributions are indicated by the dashed line. Histogram bins of 250 kWh for residential and 125 MWh for commercial systems were used.

data were reduced to a 5 min interval by taking the average of each 5 min. Distributions of negative and positive frequency restoration reserve prices for 2015 and 2016 are shown in Fig. 4.3. The prices of feasible negative FRR provision are indicated by a blue arrow and positive FRR provision by a green arrow. These areas are feasible for residential systems in the reference scenario.

4.2.4 Performance indicators

We used a set of technical and economic performance indicators to assess and compare the impact of the dispatch strategies. The parameters were calculated over the economic lifetime of the PV-battery systems.

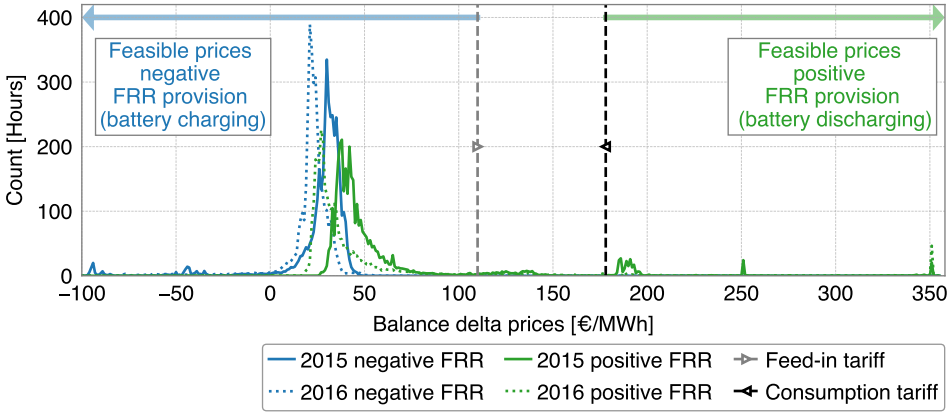

Figure 4.3 · Distribution of balance delta prices for positive and negative secondary reserve provision for 2015 and 2016. A step size of 1 €/MWh was used. Note that there are prices observed which are out of the horizontal axis range. Feasible prices for positive provision are illustrated by the green arrow and for negative provision by the blue arrow. The prices are for the residential systems in the reference scenario.

Technical performance indicators

The contribution of the BESS for PV self-consumption is quantified using the self-consumption contribution ratio (SCCR). This is the share of PV produced power that is used to charge the battery energy storage ($P_{\text{B from PV}}$). The SCCR can be calculated for the SCO, PSCN and PFRRN strategies. No energy from the battery is exported to the grid in these strategies and all energy charged in the battery is accounted as self-consumed energy. The PV power produced and the PV power charged to the battery storage were aggregated for a given time period, from the first time step (t=1) until the last time step (t_{end}), see Eq. (4.4).

$$\text{SCCR} = \frac{\sum_{t=1}^{t_{\text{end}}} P_{\text{B from PV,t}} \cdot \Delta t}{\sum_{t=1}^{t_{\text{end}}} P_{\text{PV,t}} \cdot \Delta t} \tag{4.4}$$

The share of battery storage capacity that was used to provide FRR is defined by the frequency restoration reserve storage ratio (FRRSR), i.e. the share of battery throughput used for FRR provision of the total battery throughput. The electricity provided for FRR consists of the power for positive and negative supply for each time step. The total battery throughput consist of the energy charged and discharged by the battery inverter, see Eq. (4.5).

$$\text{FRRSR} = \frac{\sum_{t=1}^{t_{\text{end}}} (P_{\text{pos}} + P_{\text{neg}}) \cdot \Delta t}{\sum_{t=1}^{t_{\text{end}}} P_{\text{B inv,t}} \cdot \Delta t} \tag{4.5}$$

The storage use ratio (SUR) gives an indication of the share of time that the BESS was used. It is defined as the ratio between the time were the battery inverter load is not zero and the total time (t), see Eq. (4.6).

$$\text{SUR} = \frac{\sum_{t=1}^{t_{\text{end}}} t,\, P_{\text{B inv}} \neq 0}{\sum_{t=1}^{t_{\text{end}}} \cdot \Delta t} \tag{4.6}$$

Battery degradation affects the battery capacity and was therefore determined for each year. Battery degradation consists of calendric degradation (D_{cal}) and cycle degradation (D_{cyc}), see Eq. (4.7). The calendric degradation depends on the lifetime (L_{cal}), which is the time period until 80% of the battery capacity diminishes due to calendric degradation. The cycle degradation depends on the total number of full cycle equivalents (FCE) until 80% of the battery capacity diminishes due to cycle degradation (N_{FCE}). Rain-flow counting method was used to determine the number of cycles and the depth of discharge (DOD)[98]. A curve was used

with the FCE for each DOD, based on parameters given in previous studies[97,99]. This curve was used to convert each cycle to a corresponding FCE. The corresponding FCE was aggregated from the first time step until the last time step of a year. The cycle degradation was found by dividing the number of FCE of a specific year by the number of total FCE used, see Eq. (4.7). The battery capacity reduction caused by calendric and cycle degradation was subtracted from the battery capacity of the previous year to determine the capacity of the following year.

$$D\text{cal} = \cdot \frac{1 - 0.8}{\text{L}_{\text{cal}}} \tag{4.7a}$$

$$D_{\text{cyc}} = (1 - 0.8) \cdot \frac{\sum_{t=1}^{t_{\text{end}}} \text{FCE, DOD}}{\text{N}_{\text{FCE}}} \tag{4.7b}$$

$$D_{\text{BESS}} = D_{\text{cal}} + D_{\text{cyc}} \tag{4.7c}$$

Economic performance indicators

The annual cash flows of a PV-battery storage system consists of two main components. The first component are storage cash flows related to the electricity tariffs (CF_{ET}). The second component are storage cash flows related to provide FRR (CF_{FRR}).

The electricity bought from and sold to the electricity grid reduces with the usage of a PV-battery system compared to a PV system without storage. The storage cash flows related to the electricity tariffs depends on the difference between the electricity cost of a PV system without battery and a PV system with a battery. These depend on the difference in bought electricity (ΔE_{buy}) and sold electricity (ΔE_{sell}) between a PV system and a PV-battery system. The bought electricity difference is the electricity bought by a PV system ($E_{\text{buy PV}}$) minus the electricity bought by a PV-battery system ($E_{\text{sell PV-B}}$). The sold electricity difference is the electricity sold by a PV system ($E_{\text{sell PV}}$) minus the electricity sold by a PV-battery system ($E_{\text{buy PV-B}}$). The value of the bought electricity depends on the consumption tariff and the value of sold electricity on the feed-in tariff. The cash flows related to electricity tariffs is determined by the value of bought electricity minus the value of sold electricity, see Eq. (4.8).

$$\Delta E_{\text{buy}} = E_{\text{buy PV}} - E_{\text{buy PV-B}} \tag{4.8a}$$

$$\Delta E_{\text{sell}} = E_{\text{sell PV}} - E_{\text{sell PV-B}} \tag{4.8b}$$

$$CF_{\text{ET}} = (\Delta E_{\text{buy}} \cdot \pi_{\text{cons}}) - (\Delta E_{\text{sell}} \cdot \pi_{\text{feed-in}}) \tag{4.8c}$$

The storage cash flow related to the provision of frequency restoration reserves is the difference between the cash flow from positive FRR provision and from negative FRR provision. We assume a mandatory provision, hence both the

positive and negative prices are remunerated within 15 min. The cash flow from positive FRR depends on the provided energy and price of positive FRR of each time step. The cash flow from negative FRR depends on the subtracted energy and price of negative FRR of each time step, see Eq. (4.9).

$$CF_{\mathrm{FRR}} = \left(\sum_{t=1}^{t_{\mathrm{end}}} P_{\mathrm{pos,t}} \cdot \pi_{\mathrm{pos,t}} \cdot \Delta t\right) - \left(\sum_{t=1}^{t_{\mathrm{end}}} P_{\mathrm{neg,t}} \cdot \pi_{\mathrm{neg,t}} \cdot \Delta t\right) \tag{4.9}$$

The battery storage investment (I_{BESS}) includes costs of the storage system ($I_{\mathrm{B\,store}}$), BOS cost ($I_{\mathrm{B\,BOS}}$) and EPC cost ($I_{\mathrm{B\,EPC}}$). The battery storage cost are scaled with the size of the battery storage capacity ($S_{\mathrm{B\,store}}$), whereas the other cost are scaled with the battery inverter rating ($S_{\mathrm{B\,inv}}$) , see Eq. (4.10).

$$I_{\mathrm{BESS}} = (I_{\mathrm{B\,store}} \cdot S_{\mathrm{B\,store}}) + ((I_{\mathrm{B\,BOS}} + I_{\mathrm{B\,EPC}}) \cdot S_{\mathrm{B\,inv}}) \tag{4.10}$$

The annual storage revenue (R_{BESS}) are the revenues that can be allocated to the battery storage system. This is the sum of cash flows minus the annual operation and maintenance costs (O&M), see Eq. (4.11). O&M costs of the battery systems were calculated by using a cost factor ($f_{\mathrm{B\,OM}}$) which was multiplied with the battery system investment costs.

$$R_{\mathrm{BESS}} = CF_{\mathrm{ET}} + CF_{\mathrm{FRR}} - (I_{\mathrm{BESS}} \cdot f_{\mathrm{B\,OM}}) \tag{4.11}$$

The simple payback period (PBP) is an indication of the time period required to recover storage investment. The PBP was found by selecting the year (y) where the cumulative cash flow (CCF) is identical to zero. A maximum time period of 50 years was assessed to find the simple PBP, see Eq. (4.12).

$$CCF, y = \sum_{y=0}^{y=50} I_{\mathrm{BESS,y}} - R_{\mathrm{BESS,y}} \tag{4.12a}$$

$$\mathrm{PBP} = \left\{ y \quad \text{where CCF, y} == 0 \right. \tag{4.12b}$$

The profitability index (PI) gives a perspective of the value and risk of the battery storage investment. The profitability index is defined as the present value per € invested. The present value includes the future risk and return in the current value of a project. This value is found by the sum of the annual total revenues for each year minus the investment cost for each year discounted by the rate (r) over the economic lifetime ($\mathrm{L_{econ}}$). Only initial investments are included at the start of a project, see Eq. (4.13).

$$\mathrm{PI} = \frac{\sum_{y=0}^{\mathrm{L_{econ}}} \frac{R_{\mathrm{storage,y}}}{(1+r)^y}}{I_{\mathrm{BESS}}} \tag{4.13}$$

4.3 Technical assessment

The impact of the dispatch strategies on the technical performance indicators is shown using a violin plot in Fig. 4.4. Violin plots combine the box-whisker plot with a density plot and provide a quick indication of the obtained results[65]. Residential PV-battery systems are in all plots shown on the left side of the violin and commercial systems on the right side. Mean values of the distribution are indicated by the solid line and the 25% and 75% percentile by dotted lines. The systems performance indicators are annual values, averaged over the systems lifetime. All results are given for each MWh of annual consumption, enabling a comparison of the systems.

4.3.1 Self-consumption contribution rates

SCCRs were determined for three out of six strategies. No PV energy was used for battery charging in the SCO strategy, thus no increase in PV self-consumption occurred. The SCCRs were not calculated for the PSC and PFRR strategy, because positive FRR was provided in these strategies. Consequently, not all energy stored from the PV system can be counted as self-consumption for these strategies. The SCO strategy shows an average SCCR of 26.5% for residential systems and 23.6% for commercial systems. A small decrease in average SCCR for residential and commercial systems is seen between the SCO and the PSCN strategy of ≈0.5%. The PFRRN strategy shows a small SCCR of 3.4% for residential and 3.8% for commercial systems. In this strategy, it occurs more often that the battery inverter was used to provide negative FRR than it was used to charge excess PV energy. Also, less battery capacity is available to charge PV energy on moments when negative FRR provision was not feasible. Both lead to a reduction in self-consumption of ≈23.1% point for residential and ≈19.8% point for commercial systems.

Residential systems have less overlap of energy consumption and PV production than commercial systems. Therefore, more energy can be shifted by storage with residential than commercial systems. This results in a higher SCCR for residential systems in the SCO and PSCN dispatch strategies. In addition, a higher SCCR in the PFRRN strategy is observed for commercial systems than for residential systems. Commercial systems have a lower feed-in tariff and thus lower prices for negative FRR provision compared to residential systems. Therefore, more negative FRR could be provided by commercial systems. Subsequently, the battery is discharged more often and thus more storage capacity is available to increase PV self-consumption.

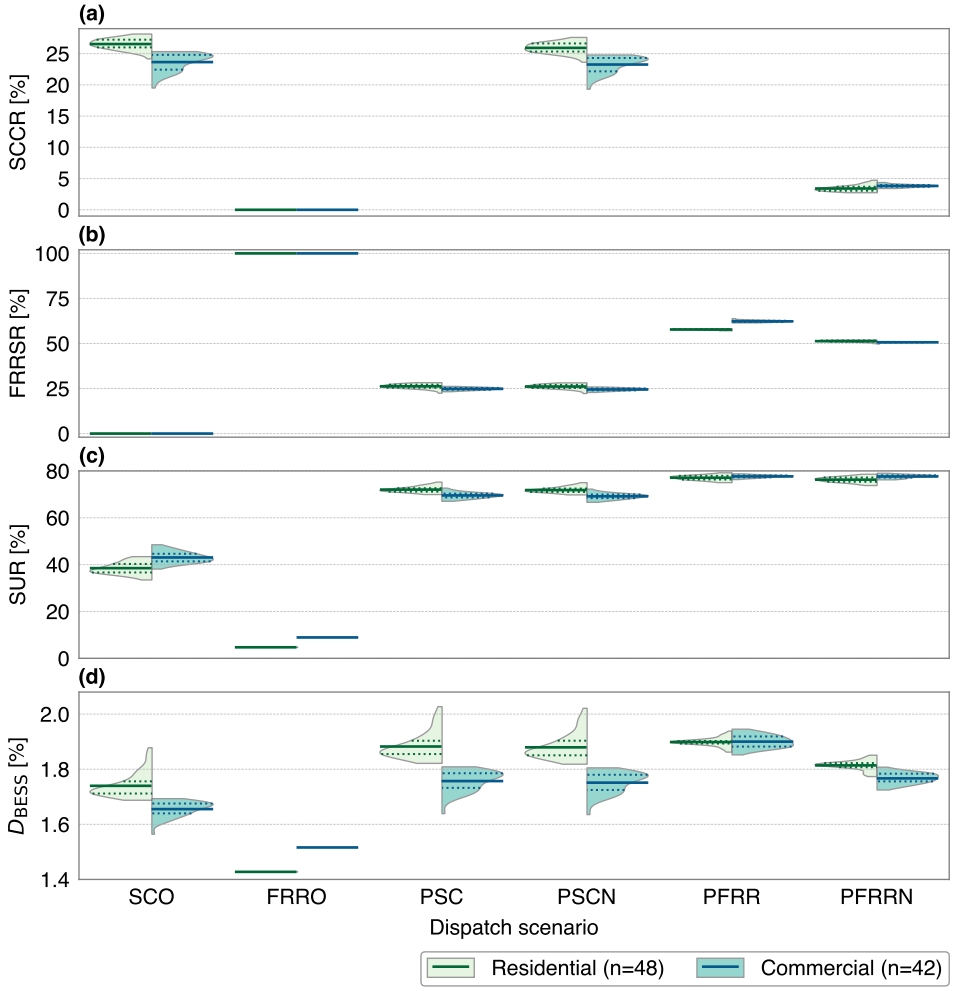

Figure 4.4 · Influence of the dispatch scenarios on the self-consumption contribution rate (a), frequency restoration reserve storage ratio (b), storage use rate (c) and battery degradation (d) for PV-battery systems shown using violin plots. The values are the annual average values over the lifetime of the system. Residential systems are shown on the left side of the distributions and commercial systems on the right. PV-battery system design parameters are given in Table 4.1. Mean values of distributions are indicated by solid lines, and the 25% and 75% percentiles by dotted lines.

4.3.2 Frequency restoration reserve storage ratio

The average FRRSR of the PSC and PSCN strategies are around 26% for residential and 25% for commercial systems. The small FRRSR difference between the PSC and PSCN strategies indicate a minor impact of the positive FRR provision. In these strategies, battery storage is mainly charged by surplus PV energy, which restricts the amount of positive FRR provision.

The occurrence of feasible positive provision is much lower than feasible negative provision (see Fig. 4.3). Therefore the added FRRSR by positive FRR provision is lower than the negative provision. A larger difference between the PFRR and PFRRN strategies is observed for commercial than for residential systems. The consumption tariff of commercial systems is significantly lower than for residential systems, resulting in a larger possibility of positive FRR provision for commercial systems. The PFRR strategy has a higher average FRRSR of ≈6.4% point for residential and ≈13.3% point for commercial systems, compared to the PFRRN strategy. This difference is mainly caused by the additional positive FRR supply. However, FRRSR are in the PFRRN strategy slightly larger for residential systems than for commercial systems, and this is related to the difference in feed-in tariff.

4.3.3 Battery storage use and degradation

The use of the battery storage systems in the SCO strategy is on average 38.5% for residential and 43.1% for commercial systems. Commercial systems have a better overlap of PV production and energy consumption, hence battery storage is charged at a lower capacity during daytime for commercial than for residential systems. This results in a 4.6% point higher SUR for commercial systems. The SUR is greatly increased when FRR provision and self-consumption enhancement are combined. Mean SUR in the PSC and PSCN strategies are 71.9% for residential and 69.4% for commercial systems. The PFRR and PFRRN strategies show a SUR around 77% for residential and commercial systems. The FRRO strategy shows lower SUR values of 4.6% for residential and 10.5% for commercial systems.

The sum of SURs from the SCO with the FRRO strategy is lower than for dispatch strategies that combine both applications. Thus, the battery is used more often when self-consumption enhancement is combined with FRR provision than the sum of each application individually. This is caused by two effects. First, electricity that is originally charged by negative FRR provision is delivered to the building. This increases the SUR for the PSC and PSCN strategies. Second, electricity that is produced by PV energy is used as positive FRR provision. This increases the SUR even more, as shown in the PFRR and PFRRN strategies.

Overall, annual battery degradation is between 1.4% and 2%, but it varies for different dispatch strategies. Low degradation values are observed in the FRRO strategy and high degradation values in the PFRR strategy. Relatively high degradation values of residential system are observed for the PSC and PSCN strategies, which indicate a higher frequency of charge and discharge cycles. Low degradation values in the FRRO strategy are caused by the low utilization of the battery storage. Battery degradation is higher for residential than for commercial systems, except in the PFRR strategy. This strategy has a higher provision of FRR by

commercial systems, leading to higher degradation values.

The electricity time-of-use influences the moment that surplus PV energy is stored or discharged, which varies for each demand pattern. The feasible provision of FRR is less dependent on the demand pattern, but more on the state of charge of the battery. Consequently, all system performance indicators show a larger distribution range for strategies that prioritize PV self-consumption. The distribution range of residential and commercial systems decreases with more FRR provision. Systems in the FRRO strategy are operating solely based on the FRR market prices, which are similar for all systems, so no distribution is seen.

4.3.4 Technical annual variations

Annual mean values for the technical system parameters are presented to provide insights in the yearly variation of the PV-battery systems, see Fig. 4.5. The annual variation of the SCCR and the FRRSR are caused by the variation in PV production, battery storage capacity and FRR prices.

Residential SCCR shows an annual variation of around 8% point for the SCO and PSCN strategies and 1% point for the PFRRN strategy. Commercial SCCR shows a lower variation in the SCO and PSCN strategies of around 5% point, yet a higher variation in the PFRRN strategy of 3% point is observed. PV energy production is reduced over time caused by the PV system degradation. This increases the share of direct consumed PV energy, but reduces the share of PV energy that can be stored. Consequently, less PV energy is stored and SCCR decreases over lifetime. Also, battery storage capacity decreases over lifetime due to degradation. This decreases the PV energy that can be stored and used on later moments, which reduces the SCCR even more. This effect is not visible in the PFRRN strategy, due to the prioritization of FRR provision is the initial SCCR already limited.

Commercial systems provide more negative FRR than residential systems, thus have a higher annual variation in SCCR and FRRSR. The PSC and PSCN strategy have an increase of FRRSR over time caused by the reduction of the battery capacity. As a result of this reduction, a SOC of 0% due to discharge of electricity delivered to a building is achieved more often. Also a SOC of 100% due to the charge of PV energy is realized more frequently. Consequently, the assessment of feasible FRR provision in the PSC and PSCN strategies will occur more often and more FRR is provided. Provision of FRR was already maximized for the PFRR and PFRRN strategies which show a constant FRRSR over time.

The reduction in battery capacity results in more moments that the battery capacity is saturated, in which reduces its moments were a battery can be charged. The fluctuation of request for PV charging is smaller than request of negative FRR provision. Besides, PV energy is charged during daytime, whereas negative

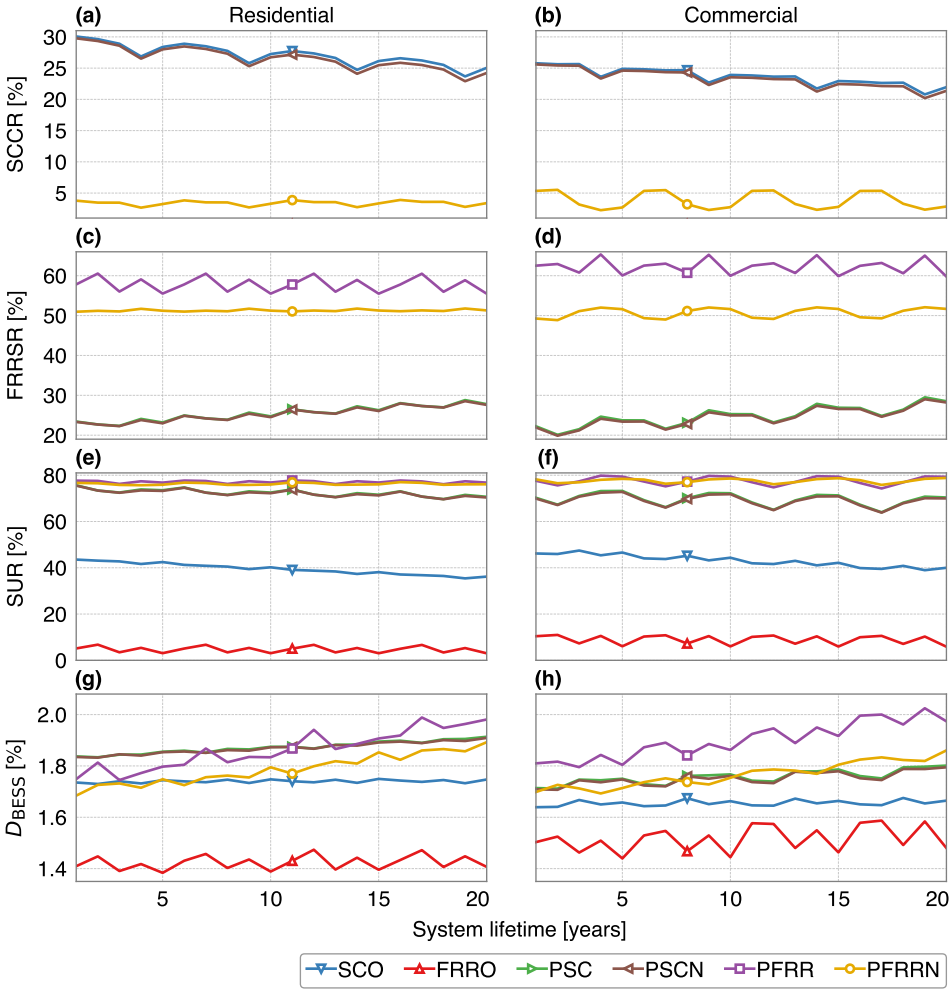

Figure 4.5 · Mean annual distribution values for self-consumption contribution rate (a & b), frequency restoration reserve storage ratio (c & d), storage use rate (e & f) and battery degradation (g & h). The left columns shows residential systems (a, c, e & g) and the right columns commercial systems (b, d, f & h). PV-battery system design parameters are given in Table 4.1.

provision fluctuates over the course of the day. Hence, the SCO strategy shows a strong decrease in SUR, whereas the PSC and PSCN strategies show a weaker decrease. A minor reduction of SUR is seen for dispatch strategies that prioritize self-consumption enhancement. Annual battery degradation increases over time for all dispatch strategies, except the self-consumption only strategy. The power charged and discharged for FRR provision stays constant over time but the storage capacity decreases. Therefore storage cycle depths and consequently battery degradation both increase.

4.4 Economic assessment

The impact of BESS dispatch strategies on the economic performance indicators is presented in Fig. 4.6. The cash flow from the electricity tariffs, cash flow from FRR provision and the storage revenues are annual averaged values over the lifetime of the systems.

4.4.1 Annual cash flows and storage revenue

The cash flow obtained with the electricity tariffs for the SCO strategy are on average ≈ €9 for residential and ≈ €11 for commercial systems. These cash flows increase significantly when negative FRR is provided because less electricity is bought with the consumption tariff. The PSC and PSCN dispatch strategies have cash flows of €42 and €27 for residential and commercial systems respectively. Prioritizing FRR provision before self-consumption increases the cash flow even more. Yet, the cash flow from the electricity tariffs are higher for providing only negative FRR than when both positive and negative FRR are supplied. If positive FRR is provided, than electricity from the battery is used for positive FRR provision instead of using it for the electricity demand of the building. Thus, more electricity is bought which reduces these cash flows related to the electricity tariffs.

The cash flows related to FRR provision are only positive in the FRRO and PFRR strategies. Largest cash flows from FRR are seen for the FRRO strategy, since all negative FRR provision is sold back as positive FRR provision. These are €25 for residential and €33 for commercial systems. The PFRR strategy has a higher cash flow from positive FRR provision than costs from negative FRR provision. This results in a net cash flow for FRR provision of €11 and €21 for residential and commercial systems respectively. The consumption tariff of commercial systems is lower than for residential system. Hence, more moments in time occur for commercial systems for which a positive FRR is feasible. Therefore, the cash flow from commercial systems is ≈ €10 higher than for residential systems in the PFRR strategy. The PFRRN strategy shows the lowest cash flows, yet has the largest reduction of electricity that is bought with the consumption tariff.

Highest storage revenues are observed in the PFRR strategy with €83 for residential and €58 for commercial systems. Lowest revenues are made with self-consumption only, of €6 and €8 for residential and commercial systems respectively. The difference in storage revenues between the SCO strategy and the other five strategies is an indication for the annual profit that can be obtained by operating on the frequency restoration reserve market. The largest differences are observed in the PFRR strategy of ≈ €77 for residential and ≈ €50 for commercial systems. Strategies that prioritize self-consumption (PSC & PSCN) have a lower differences of ≈ €28 for residential and ≈ €12 for commercial systems. The PSC

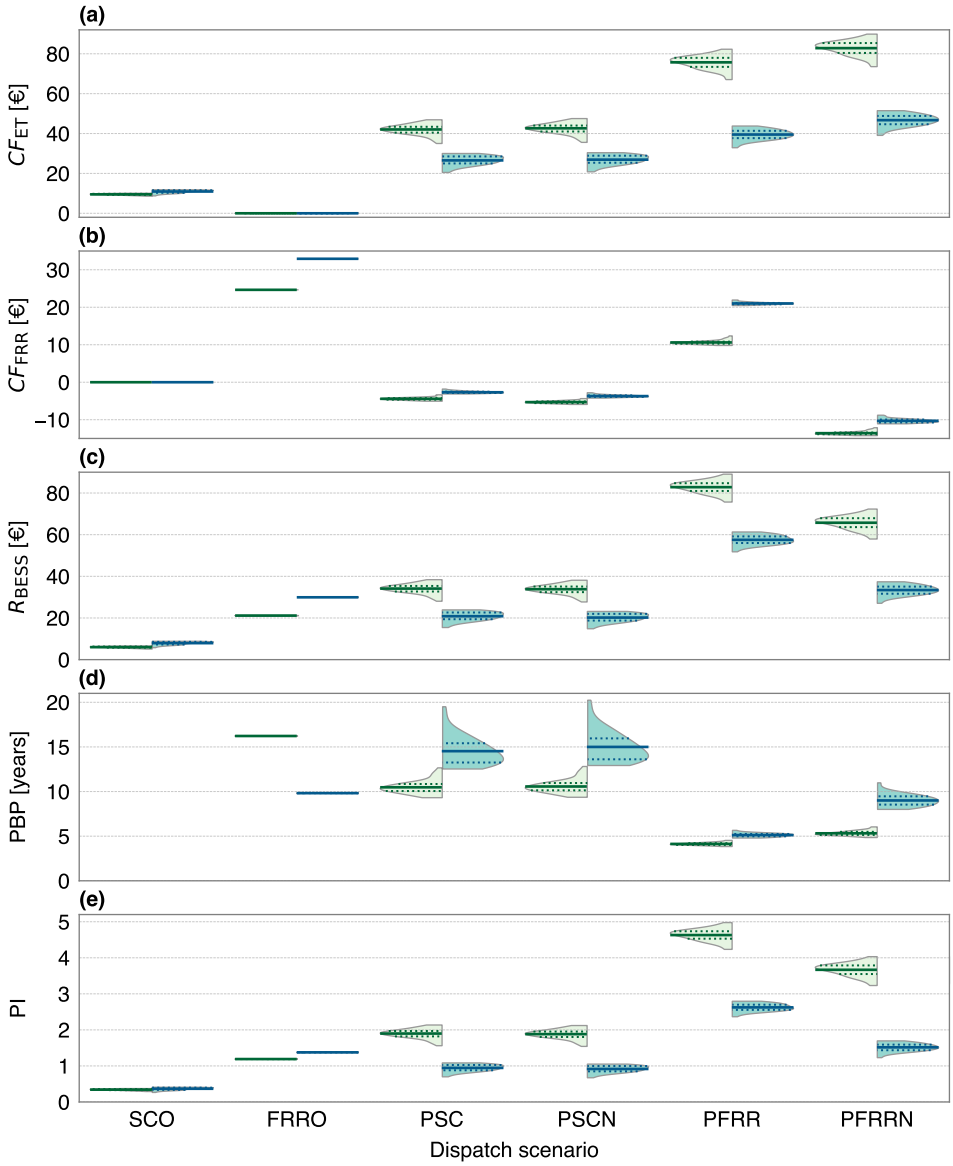

Figure 4.6 · Influence of the dispatch scenarios on the annual average cash flow from electricity tariffs (a), annual average cash flow from frequency restoration reserve provision (b), annual average storage revenue (c) payback period (d) and the profitability index (PI) for PV-battery systems shown using violin plots. PV-battery system design parameters given in Table 4.1. Mean values of distributions are indicated by solid lines, and the 25% and 75% percentiles by dotted lines.

strategy shows slightly higher storage revenue than the PSCN strategy due to the benefits of positive FRR provision.

Residential storage revenues of the FRRO strategy are smaller than the revenues obtained in the PSC and PSCN strategy, yet commercial systems show larger revenues. The lower consumption and feed-in tariffs of commercial systems result in more feasible moments for FRR provision, and higher revenues in the FRRO strategy. The variation of electricity time-of-use during the day for commercial systems is lower than residential systems. Subsequently, the distribution range of commercial systems is smaller than for residential systems.

4.4.2 Investment attractiveness

Simple payback periods of the SCO dispatch strategy are larger than 50 years for residential systems and larger than 43 years for commercial systems so are not shown in Fig. 4.6. Payback periods are significantly lower for strategies that prioritize FRR provision. If self-consumption enhancement is prioritized before FRR provision, then PBP of residential systems is lower than commercial systems. The difference between the feed-in and consumption tariffs is larger for residential than commercial systems, resulting in larger benefits for PV self-consumption.

The profitability index value should be higher than 1 for an economically profitably investment. The PI in the SCO dispatch shows values smaller than 1 for residential and commercial systems, making the investment in battery storage not economically feasible. The FRRO strategy has higher PI for commercial than residential systems, thus the price points used for feasible FRR provision should be closer to commercial tariffs than for residential tariffs. The PI of residential systems is above 1 in the other four strategies, indicating a positive investment. Commercial systems show PI above 1 for all systems in the PFRR and PFRRN dispatch strategy, but for the PSC and PSCN strategies an average PI below 1 is observed.

It is remarkable that the simple PBP for the PFRR and the PFRRN strategies is lower for residential than for commercial systems, whereas the PI shows the opposite. This is caused by differences in economic assumptions made for the systems. Residential systems have an economic lifetime of 25 years and a discount rate of 2%, whereas commercial systems have a shorter economic lifetime of 20 years and a higher discount rate of 4%. The time period needed to recover the investments is shorter for commercial systems. Also the future value of the storage revenues decreases faster due to a higher discount rate. Both these effects results in a lower PI for commercial systems than residential systems.

4.4.3 Economic annual variations

Annual mean values for cash flow from electricity tariffs, cash flow from FRR provision, storage revenue and discounted storage revenues are shown in Fig. 4.7. The SCO strategy shows a reduction of annual cash flow from electricity tariffs for residential and commercial systems over time. A reduction in self-consumption increases electricity costs (see Fig. 4.5). Residential systems can obtain more storage revenues for self-consumption than commercial systems. Hence, the drop in revenue is larger for residential than commercial systems. The PSC and PSCN

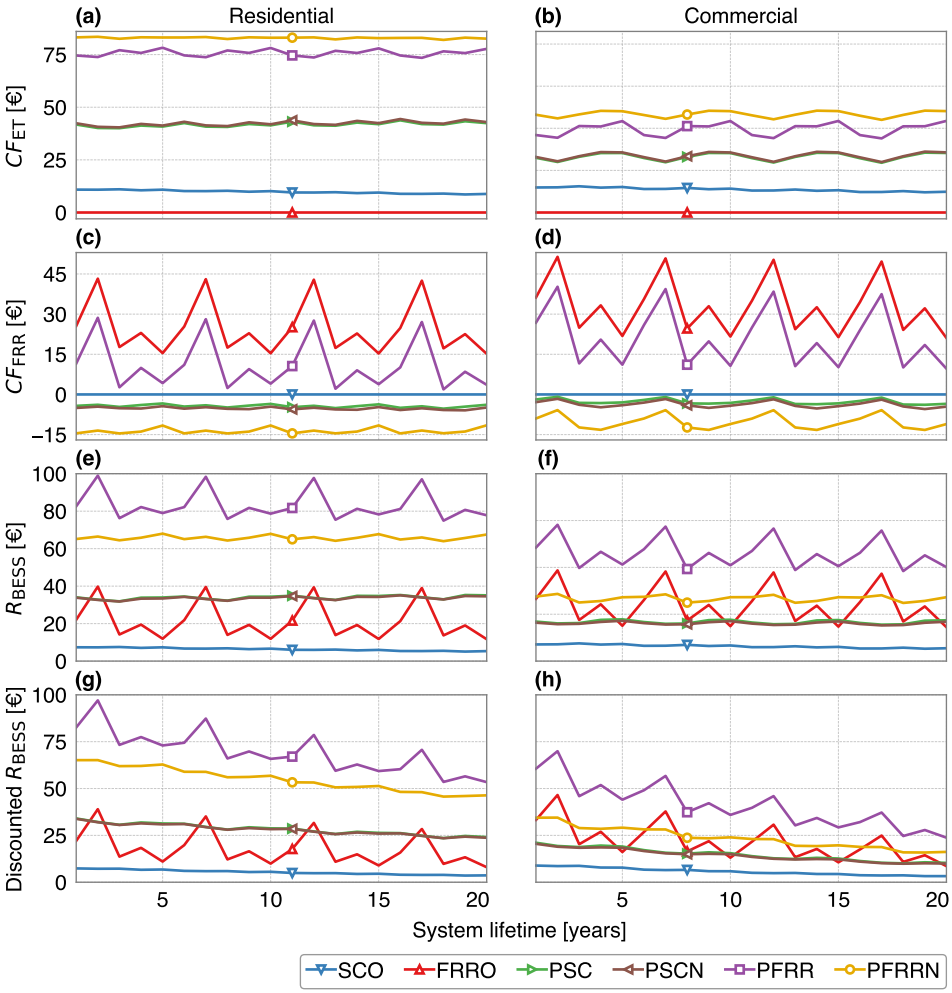

Figure 4.7 · Mean annual distribution values for cash flow from electricity tariffs (a & b), cash flow from frequency restoration reserve provision (c & d), storage revenue (e & f) and discounted storage revenues (g & h). Residential systems (a, c, e, & g) are shown on the left and commercial systems (b, d, f & h) are shown on the right. PV-battery system design parameters are given in Table 4.1.

strategies show that losses due to the reduction of self-consumption are compensated by the additional benefits of negative FRR provision. Hence, a slight increase in cash flow from electricity tariffs is observed. Besides, more revenue in providing negative FRR is obtained by residential than commercial systems. As a result, the increase in cash flow from electricity tariffs is larger for residential than for commercial systems.

The cash flows from FRR provision show large fluctuations for the FRRO and PFRR strategies, caused by price fluctuation of positive FRR provision. A slight decreasing trend is seen over time due to reduced battery capacity. The FRR cash flows over time are constant for the PFRRN strategy while the PFRR revenues show small decreases. Less positive reserves can be provided over time due to the reduced battery capacity. Commercial systems supply more positive FRR and thus show a larger variation than residential systems. The storage revenues decrease in all dispatch strategies with the SCO strategy as being the most severe. The discount rate for commercial systems is twice as high as for residential systems. Consequently, the discounted storage revenues show a steeper decrease for commercial than residential systems. The impact of the battery degradation combined with a discount rate results in $\approx$ 60% decrease of storage revenue in the SCO strategy.

4.5 Sensitivity analysis

4.5.1 Reference parameters sensitivity

A sensitivity study of the system reference parameters was conducted on the PI for the SCO, FRRO, PSC and PFRR dispatch strategies. The PSCN and PFRR dispatch strategies are excluded in the sensitivity study, because these options are less realistic to implement. We varied all reference parameters between +50% and -50% of the initial reference value, see Table 4.1. The sensitivity of the profitability index for the SCO, FRRO, PSC and PFRR dispatch strategies are presented in a tornado diagram in Fig. 4.8. The impact of each PV-battery system parameter varies per dispatch strategy. Therefore, we could not rank the parameters according to sensitivity range.

Residential systems show no feasible investment in the SCO strategy with most system parameters. The SCO strategy only becomes economically profitable when the consumption tariff is increased or the feed-in tariff is reduced. The FRRO strategy requires a reduction of consumption tariff, storage cost or capacity to increase the profitability above 1. An increase in economic lifetime or inverter rating could also be a possibility to improve the PI substantially. If the economic lifetime or the consumption tariff is reduced than the investment attractiveness

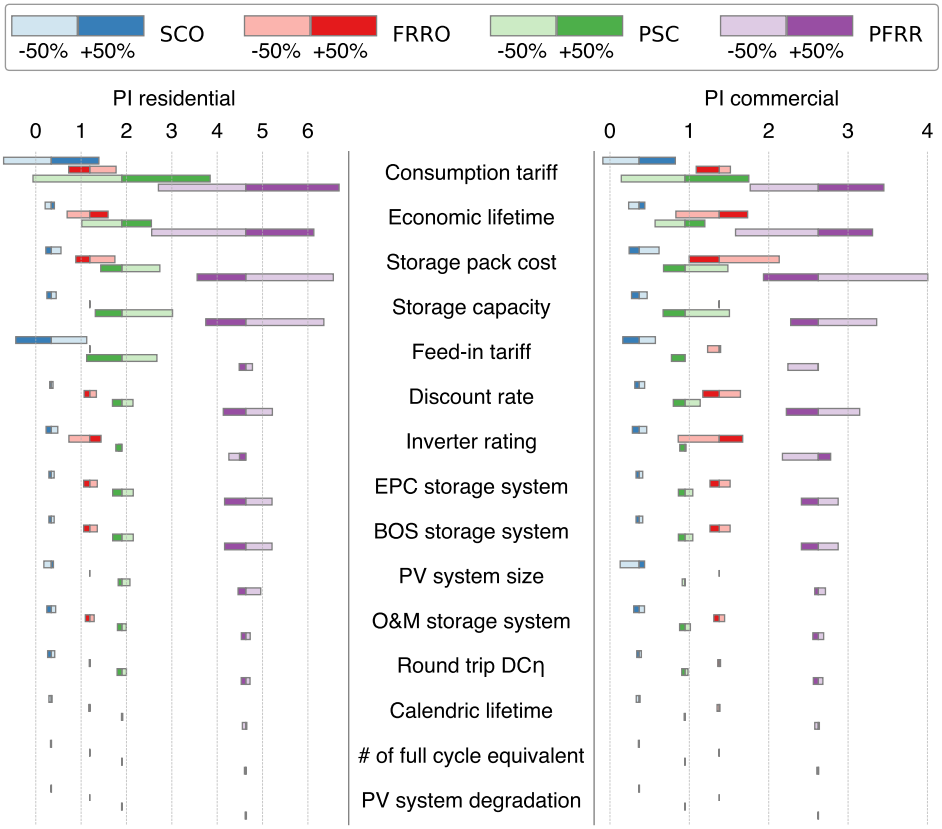

Figure 4.8 · Sensitivity of the PV-battery system parameters on the profitability index of residential and commercial systems. The lighter colours indicate the -50% values whereas the darker colours show the +50% values. Each system indicators shows from top to bottom the SCO, FRRO, PSC & PFRR battery storage dispatch strategies. Note that the PV-battery system parameters are not ranked on range of sensitivity.

is lost for the PSC strategy. The PFRR strategy shows PI of higher than 1 for all investigated parameters. Commercial systems show no PI value above 1 in the SCO strategy. In contrast to residential systems, commercial systems show a higher certainty for the FRRO strategy to obtain a positive investment. The PFRR dispatch strategy only shows PI values larger than 1, similar as for residential systems.

Large influences of consumption tariff are seen on all dispatch strategies, especially for the strategies that include enhancement of self-consumption. The feed-in tariff shows a lower influence on the FRRO and dispatch strategies that prioritize frequency restoration reserve provision for residential systems. For commercial systems, an increase in feed-in tariff in the FRRO and PSC strategies results in higher PI, whereas in the other strategies a reduction on PI is observed. More details and explanations on the sensitivity of electricity tariffs and

FRR prices are given in subsection 4.5.3.

The sensitivity of battery storage capacity and battery inverter rating are parameters that are highly affected by the used dispatch strategy. A reduction of battery storage capacity results in a larger decrease in self-consumption than in FRR provision. The enhancement of self-consumption is the main objective in the PSC strategy. Consequently, a larger impact of storage capacity than storage pack cost is seen for this strategy. The other strategies show a larger impact of storage pack cost. A decrease in inverter rating reduces the cost of an inverter, but also reduces the FRR power that can be provided. In the SCO strategy, the benefit of reduced inverter cost is higher than the loss of power provision. Strategies which provide positive FRR provision show the opposite, especially visible for commercial systems.

An increase in PV system size results in more excess PV production and consequently more moments when the battery can be charged to enhance self-consumption. Therefore the PI in the SCO strategy increases with larger PV systems. However, strategies that provide FRR show a reduction of PI with an increased PV system. In these strategies, more storage capacity will be used to store excess PV energy. Consequently, less storage capacity is available for FRR provision which reduces the PI.

The operation and maintenance cost is the only parameter that has a similar impact on the PI for all strategies. These costs are fixed for the system, therefore not dependent on the strategy used to charge or discharge the battery. The influence of round trip battery efficiency and PV system degradation is found to be minimal on the PI of the systems with all dispatch strategies. The impact of calendric lifetime and the number of full cycle equivalents is also limited. More details and clarifications on the sensitivity of battery degradation parameters are given in subsection 4.5.4.

4.5.2 Storage capacity and inverter rating

The sensitivity of battery storage capacity and relative inverter rating was investigated in detail using the reference scenario. We used contour plots to analyse the combined effect of these influences on four dispatch strategies, presented in Fig. 4.9. Storage capacities were varied with steps of 0.1 kWh and relative inverter values with steps of 0.1 kW. Residential systems are shown in the top graphs and commercial systems in the bottom graphs. The red points indicate the maximum PI within the investigated range of battery storage and inverter ratings.

The SCO strategy shows only profitability indexes below 1 for residential and commercial systems. The PI in the FRRO strategy is mainly depending on the relative inverter rating. A higher inverter rating can deliver more power and thus

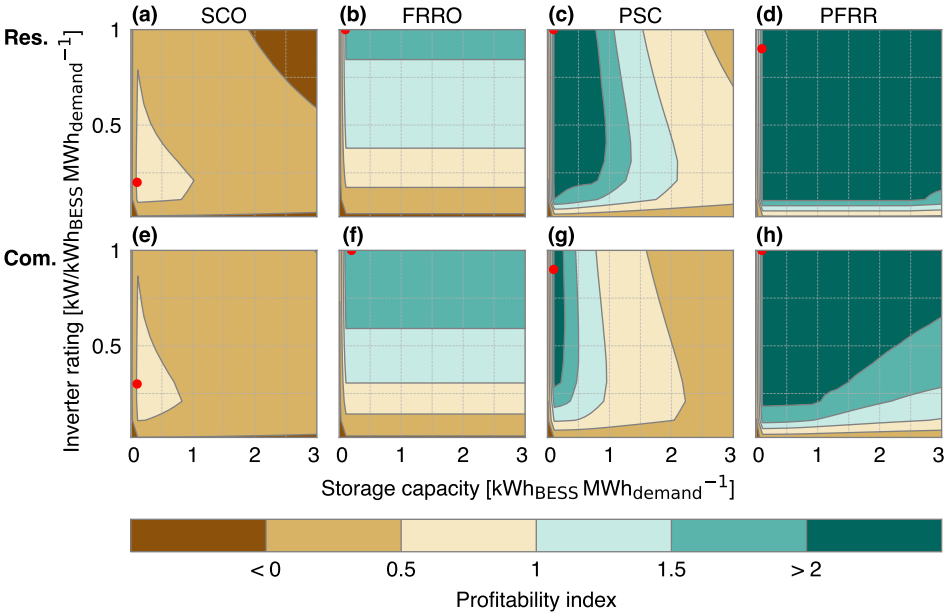

Figure 4.9 · Influence of battery storage and relative inverter ratings of four strategies, indicated above the graphs. Mean values of the residential systems are shown at top graphs (a, b, c & d, indicated with Res.) and mean values of commercial systems are shown at the bottom graphs (e, f, g & h, indicated with Com.). The red points indicate the maximum profitability index within the system values of the sensitivity study. Other parameters are kept constant according to the reference PV-battery system scenario.

increases the PI. The PSC dispatch strategy shows that a larger inverter does not automatically increase the PI. A larger inverter can charge and discharge a battery faster. Consequently, more energy can be delivered for the FRR market with equal battery storage capacity. Yet, a reduction of PI is observed in the PSC strategy. Larger inverter ratings will also increase the charged surplus PV electricity or the discharged electricity to the building. Hence less battery capacity is available to provide FRR and also the PI is reduced. The PFRR strategy shows a significantly increase in PI for residential as well commercial systems. An increase in storage size results only in higher PI if inverter ratings increase as well.

A lower inverter rating was found when no FRR was provided. The SCO shows an optimal inverter size of 0.2 kW for residential systems and 0.3 kW for commercial systems. The strategies that provide FRR have an inverter rating of 0.9 or 1. The optimal battery storage size is for each strategy 0.1 kWh per MWh of electricity consumption, except for the commercial FRRO strategy. Commercial systems can provide more positive reserves than residential systems due to the lower price point used. Hence commercial systems benefit more from a larger storage capacity.

4.5.3 Electricity tariffs and FRR prices

Future electricity tariffs and frequency restoration prices are highly uncertain due to changes in policy or technology. Therefore, the sensitivity of the annual price variation on dispatch strategies was analysed using four price scenarios.

P1 Consumption tariff was varied, feed-in tariff and FRR prices were constant.

P2 Feed-in tariff was varied, consumption tariff and FRR prices were constant.

P3 Consumption and feed-in tariff were constant and FRR prices were varied.

P4 Both tariffs and FRR prices were simultaneously varied.

The sensitivity of dispatch strategies for each price scenario is presented in Fig. 4.10. The annual variation was modelled between -2.5% and +2.5% in steps of 0.1%/year.

Price scenario 1 shows an increase in PI for all strategies, except the FRRO strategy. The value of self-consumed energy and consequently storage increases with higher consumption tariffs. Residential systems have a higher initial consumption tariff, thus a larger increase in absolute values and higher PI. Also the price difference between consumption tariff and feed-in tariffs is larger for residential systems than for commercial systems. Consequently, the impact of electricity price variation is higher for residential systems. A higher consumption tariff results in reduced moments for feasible provision of positive FRR. The FRRO

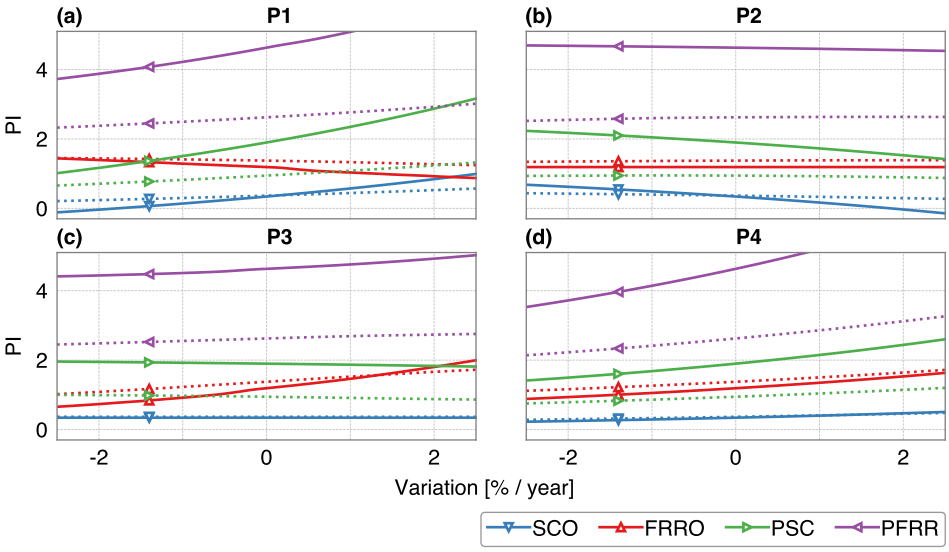

Figure 4.10 · Sensitivity of prices from electricity tariffs and secondary reserve provision for the four price scenarios on the profitability index of four strategies (a, b, c & d,). The solid lines show the average value of residential systems and the dotted line shows averages of commercial systems.

strategy shows a steeper decrease of the PI for residential than for commercial systems. This is a result of the larger absolute difference of price points for residential systems.

The P2 scenario shows a decreasing profitability index with increasing annual variation of the feed-in tariff in all strategies except in the FRRO strategy and in the commercial PFRR dispatch strategy. The increase of feed-in tariffs has two main effects. First the difference between the consumption tariff and the feed-in tariff is reduced. Consequently the value of self-consumed energy and stored energy lowers, resulting in a reduced PI. Second, the increase of feed-in tariffs leads to more moments when negative provision becomes feasible. Therefore, less energy is bought with the consumption tariff, increasing the PI. Residential systems have a larger difference between the consumption tariff and the feed-in tariff than commercial systems. Also the feed-in tariff is larger for residential systems. Hence, the first effect is larger for residential systems, and the second effect is bigger for commercial systems. The commercial PFRR is the only strategy in which the benefits of more negative FRR provision is larger than the loss in self-consumption.

Price scenario 3 shows different trends between the dispatch strategies. The PSC dispatch strategies show a decrease of PI with increasing annual variation. Higher prices reduce the feasibility of negative FRR provision and more energy must be bought from the grid to fulfil the local energy demand. The PSC strategy has a lower battery storage use ratio due to the prioritization of self-consumption, see Fig. 4.4. Hence, the likelihood to provide positive FRR is lower than to provide negative FRR. Thus, the benefits of the higher positives FRR prices are lower than the loss of the negative FRR prices. This results in a decrease of PI in the PSC strategy. The FRRO and the PFRR show an increase in PI because more time moments occur when delivery of power for the FRR market becomes feasible. The influence of the variation of consumption and feed-in tariffs is larger than the influence of the FRR market prices, thus P4 shows an increase in PI for all strategies.

4.5.4 Battery capacity degradation

A commonly heard concern is the influence of the calendric lifetime and the number of full cycle equivalents on battery capacity. Therefore, we assessed the influence of these parameters on the battery storage capacity that is remaining after the economic lifetime of the systems expires, see Fig. 4.11. The number of full cycles was varied with steps of 250 and the calendric lifetime with steps of 1 year. Remaining parameters were kept constant according to the reference scenario.

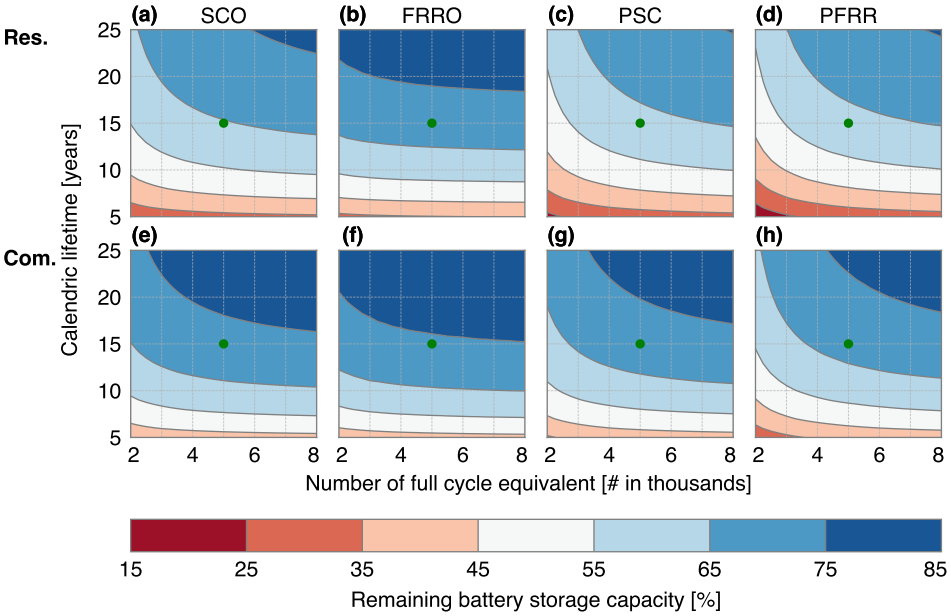

Figure 4.11 · Influence of the number of full cycle equivalent and the calendric lifetime on the remaining battery capacity after the economic lifetime of the systems expires. Mean values of the residential systems are shown at top graphs (a, b, c & d, indicated with Res.). The bottom graphs indicate the mean values of commercial systems (e, f, g & h, indicated with Com.). The green dot indicates the reference scenario.

A larger range in storage capacity degradation is observed for the investigated battery degradation parameters. Between 17.5% to 83.3% of the battery capacity remains after the economic lifetime. The impact of calendric degradation decreases with a higher number of FCE. The economic lifetime of the commercial systems is 5 years shorter than the residential systems. Consequently, the reduction in storage capacity is more severe for residential than for commercial systems.

When the reference battery degradation parameters would be changed to a calendric lifetime of 5 years and 2000 FCE, than a substantial capacity reduction would occur with all dispatch strategies. The remaining storage capacity in the SCO strategy would decrease from 64.5% to 27.6% for residential systems and from 71.6% to 37.2% for commercial systems. The revenue of storage decreases even more due to the discounting of the future revenues. Therefore, the impact of the battery degradation on the PI is less substantial than on capacity reduction. The average PI decreases from 0.34 to 0.22 for residential systems and from 0.37 to 0.28 for commercial systems.

Similar reductions in battery capacity are observed for the FRRO strategy, with

a decrease from 69.8% to 32.6% for residential and from 73.7% to 38.6% for commercial systems. However, a smaller reduction in PI is observed, specifically from 1.19 to 1.14 for residential and 1.38 to 1.31 for commercial systems. Hence, the battery degradation has a significant lower impact on the profitability of the FRRO strategy than on the SCO strategy. Largest capacity reductions are observed for the PFRR strategy, of -44.5% point for residential and -40.3% point for commercial systems. Also a larger reduction is seen in PI of -0.24 for residential and -0.13 for commercial systems. These results are in agreement with results on the SUR presented in Section 6.3. The PSC strategy shows a small increase in PI for residential systems (0.04) due to the increased FRR provision over the lifetime. Commercial systems have a small reduction of -0.02 because of lower benefits of negative FRR provision.

4.6 Discussion

This research assessed PV-battery systems that combine self-consumption enhancement with provision of frequency restoration reserves. We found that provision of FRR significantly increases storage revenues of PV-battery systems. The minimum feasible price for positive FRR provision and maximum feasible price for negative FRR provision show a large impact of the profitability on FRR provision.

4.6.1 Market assumptions

The largest uncertainty in our study is the use of historical negative and positive prices for frequency restoration reserve provision in our model. Perfect price forecasting was assumed which led to optimal PV-battery system benefits. However, FRR prices are difficult to predict since this market is designed to handle the unexpected variation between energy supply and demand[130]. This leads to higher financial risks. Voluntary contribution to the FRR market would significantly reduce these risks, but also reduces the obtained revenues. In our research the consumption and feed-in tariff were selected as price points for FRR provision, yet different price points could increase the revenues from FRR provision. Besides, positive and negative prices should always be selected in respect to each other[113]. We recommend additional research on the impact of these points for the profitability of FRR provision.

Future market prices could significantly change with a higher share of renewable electricity production. The increase in wind and solar electricity generation result in larger power input fluctuation on the grid. As a result, it is expected that demand for frequency restoration reserve will increase and a larger fluctuation of

prices will occur[131]. This market behaviour could invite more actors to operate on the balancing markets, especially with a reduction in battery storage cost[132]. These new actors can cause an increase of FFR provision, which could eventually lead to a decrease in FRR market prices. Modelling of market prices in not yet studied in great detail because of the small number of actors and low revenues on this market. Hence, one of the major challenges is to improve the current models for FRR price and volume prediction.

The Dutch market size for providing positive FRR was 45.8 GWh and for negative FRR 167.7 GWh, for 2014[133]. This market size limits the number of PV-battery storage systems that can provide FRR. We assessed the market potential by determining the number of systems that can be installed before the market saturates, for 2014. We used reference PV-battery system parameters (see Table 4.1) and the median annual electricity consumption from the used demand patterns. These are 3.3 MWh and 270 MWh for residential and commercial buildings, respectively. The number of systems (in thousands) for positive and negative FRR provision is shown in Table 4.2.

The number of systems that could provide positive FRR is an order of magnitude larger than the number that could provide negative FRR. This difference is related to the lower number of feasible moments to provide positive FRR. More residential storage system can enter the market than commercial systems. Around 300.000 residential PV systems were already installed before 2016 in the Netherlands[134]. If a battery storage system of 1 kWh is added for each kWp of installed PV system capacity, then the market for negative provision is already saturated. Therefore, it is important to take these limitations into account, especially so with a growing number of installed PV-battery storage systems.

An increase in electricity market prices, additional taxes or grid fees results in higher consumption tariffs for both residential and commercial systems. On the other hand, the feed-in tariffs for residential systems are currently dependent on

Table 4.2 · Estimated number (in thousands) of reference battery systems participation before secondary reserve market saturation for residential and commercial systems for 2014.

	Residential ($\cdot 10^3$)		Commercial ($\cdot 10^3$)	
	Positive	Negative	Positive	Negative
FRRO	732	168	4.22	0.98
PSC	28011	72	143	1.07
PSCN	-	71	-	1.07
PFRR	787	24	4.11	0.29
PFRRN	-	26	-	0.34

subsidy policies for renewable energy generation. It is expected that these subsidies will be abolished and that the feed-in tariffs will drop. This will increase the value of self-consumed energy and benefits of energy storage. Other applications, such as electrical vehicles or heat pump systems could be used to provide balancing services. These applications could influence balancing costs[133,135]. European grid interconnections are increasing and cross border balancing markets are under development. This results in more connections between the international market and therefore a larger market is created for balancing reserves, which influences prices[136].

4.6.2 Implementation considerations

Normally, residential PV-battery storage systems are connected to a low voltage grid. The total power that can be provided to this grid or subtracted from this grid is limited by the capacity of the transformers connected to this grid. Aging of transformers is enhanced when the substation transports power to higher voltage networks[22]. Therefore, it is recommended to set limitations on the power capacity that can be used for FRR provision within a low voltage grid. Flexible limitations could be used when accurate knowledge about the power consumption within the local grid is available. Furthermore, planning and communication between district system operators and the active actors of storage systems is advised to prevent problems related to grid and transformer capacities. Research on the impact of providing FRR on the low voltage grid is recommended as a possible next step.

This research provides a first estimate on the monetary benefits for individual battery systems. However, the minimum bid size to trade on the frequency restoration reserve market is 4 MW currently. Battery systems must be pooled to obtain the minimum bid size to comply with these market requirements. Therefore, an aggregator is required to combine the individual battery storage systems to comply with electricity balancing market rules. Larger pools provide more flexibility to trade on the electricity balancing market, but the individual revenue of the systems might decrease. Supplementary communication and battery management software can be required to deliver power to the market on the right moment. This information consists of availability of the battery system, the BESS state of charge and maximum inverter power. Aggregators could play an important role in providing this additional hardware and software. These communication requirements will add costs to a PV-battery system to be able to operate on the balancing market. Therefore the presented revenues from FRR provision could be overestimated. Besides, legal matters concerning battery ownership and taxation of revenues should be investigated before entering the market.

It is also possible to add a third application to the storage systems for even higher profitability. For example, BESS could shift the peak demand and therefore reduce the grid connection cost[137]. The benefits of each storage application and there interaction is highly recommended as future research.

4.7 Conclusion

This work is a first indication on possible additional benefits that residential and commercial PV-battery systems could have when they are combined to improve self-consumption and provide frequency restoration reserve to the balancing market. Six battery dispatch strategies were developed and assessed on technical and economic parameters. We used historical market prices data and energy consumption data of 48 residential and 42 commercial systems.

A small loss of 0.5% self-consumption rate is shown for strategies that prioritize self-consumption over provision of FRR, compared to strategies that provide only self-consumption. Larger reductions of around 23% are seen when FRR provision is prioritized. The battery use is significantly increased when both applications are used and even doubled when FRR provision is prioritized. The dispatch strategies have a minor impact on battery degradation. FRR provision as secondary storage applications increases annual revenue with $\approx$ €28 for residential and $\approx$ €12 for commercial systems for each kWh of storage capacity. Strategies that prioritize FRR provision before self-consumption enhancement have largest revenues of $\approx$ €77 for residential and $\approx$ €50 for commercial systems.

Electricity and FRR prices show a high influence on the profitability of the storage systems. Therefore developments in these prices should be estimated to examine an accurate profitability of BESS investments. The battery inverter ratings should be optimized with the battery storage size and the dispatch strategy to improve the profitability of the storage investment. Models to predict FRR prices and volume need increased accuracy. Limitations concerning future market developments and current electricity infrastructure should be analysed as a next research step.

Acknowledgements

This work is part of the research programme Transitioning to a More Sustainable Energy System (Grant No. 022.004.023), which is financed by the Netherlands Organisation for Scientific Research (NWO). We are grateful to Hubert Spruijt of Senfal, Liander N.V. and the Royal Netherlands Meteorological Institute for providing data.

5

Combing GSHP with PV-battery systems

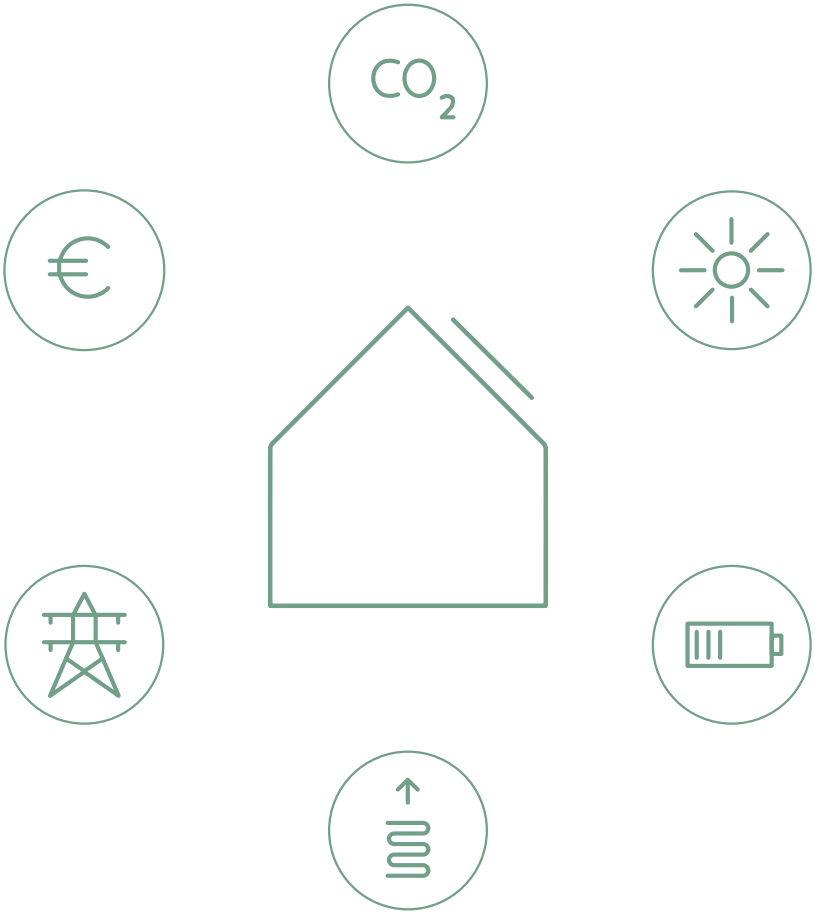

This chapter is based on the publication: G.B.M.A. Litjens, E. Worrell and W.G.J.H.M. van Sark. "Lowering greenhouse gas emissions in the built environment by combining ground source heat pumps, photovoltaics and battery storage". in: *Energy and Buildings* **180** (2018), pp. 51-71. DOI:10.1016/j.enbuild.2018.09.026

Abstract

Ground source heat pumps (GSHPs) have been suggested to replace gas-based heating in urban environments to reduce greenhouse gas emissions and help to comply with the Paris Agreement. The emission reduction from GSHP depends on the carbon intensity of the electricity generation mix. Moreover, grid capacity may be limiting the introduction of these high-electricity demand GSHP systems. Photovoltaics (PV) systems help to provide additional emission reductions for residential GSHP systems. Battery energy storage systems can reduce the peak demand and allow for more GSHPs within the low voltage grid. We developed a techno-economic and environmental assessment model to quantify this impact of PV and batteries combined with residential GSHP systems. Measured demand data of 16 dwellings with GSHP and PV systems from the Netherlands were used. We show that PV can provide around 19% of the GSHP demand, while batteries enhance this by 53% and reduce the peak demand by 45%. Greenhouse gas emission of a GSHP with PV is reduced on average with 73 tCO_2-eq, corresponding to a 80% reduction, over a 30-year lifetime. Dwellings with only a GSHP system have a net present values increase of around €275 per tCO_2-eq of avoided emission. This is reduced to €230 per tCO_2-eq when PV and storage is added to the system. Nevertheless, investment in GSHP systems today is not economically attractive for many dwellings. A sensitivity analysis showed that policies should focus on increasing natural gas tariffs, carbon taxation, investment subsidies or combinations of these routes to encourage sustainable heating.

5.1 Introduction

In the European Union (EU), around half of the buildings are provided with heat by fossil fuel boilers with an efficiency of 60% or lower and were installed before 1992[138]. For example, in the Netherlands, 93.7% of the dwellings is heated using natural gas resulting in 11.1% of the total Dutch CO_2 emissions[134,139]. In line with the Paris Agreement, the Dutch government has set ambitious goals to phase out gas boilers by 2050 and replace them with other technologies to provide heat[140].

Ground source heat pump systems (GSHPs), also known as ground coupled heat pumps, constitute a promising technology to replace fossil based heating systems[141]. GSHPs generate heat from electricity with high efficiencies and are seen as best available technology, especially in combination with renewable sources[138]. Emission reduction is largely dependent on the electricity generation mix in a specific country, GSHPs efficiencies and climate conditions[142–145]. Moreover, GSHPs can deliver flexibility such as demand response services to the electricity system[146]. These advantages led to policies that support investments in GSHPs. For example, in the USA a tax credit of 30% of GSHP investment costs presently exists[147]. In the Netherlands, a variable subsidy based on the installed GSHP capacity can be obtained[148]. In Europe, around 100,000 GSHP units are annually installed[149]. In the USA, over 560,000 units were installed by the end of 2014[150].

Currently, the Dutch electricity generation mix is relatively carbon intensive (490 gCO_2-eq per kWh), which lowers the emission reduction potential of GSHP[151]. Rooftop photovoltaic (PV) systems are a worthwhile option to lower the electricity needs from the grid. Consequently, greenhouse gas (GHG) emissions can be lowered by avoiding electricity generation from fossil based power plants[13]. The direct use of PV electricity (referred to as self-consumption) is limited, due to a mismatch in time between PV production and electricity consumption. This can be increased by using a stationary battery energy storage system (BESS) that charges surplus PV electricity so that it can be used on later moments. The electrification of heating and the use of energy storage are highly recommended technologies to allow for more intermittent renewable energy in the electricity system worldwide.[4,29].

The implementation of GSHPs could be restricted by the capacity of existing low voltage utility grid, due to the larger peak demand of dwellings with GSHP[152]. BESSs are suitable for peak shaving of the power demand and PV electricity production[153]. The latter application reduces potential energy losses due to PV curtailment requirements[154]. Consequently, more PV systems and GSHP systems can be installed on a local grid without expansion requirements. This reduces the societal grid costs and helps the profitability of BESSs[108]. Furthermore,

less power generation capacity is required to meet peak electricity demand, especially for colder winter months. These associated benefits may result in a rapid deployment and cost decline of BESSs[39]. However, BESSs have charging and discharging losses that result in higher system emissions. These systems are only recommended if the share of renewable electricity generation is a large share of the total electricity generation[155].

5.1.1 Literature review

Several studies assessed the technological, economical or environmental advantages of GSHP systems combined with PV and storage. PV self-consumption of dwellings with GSHP systems show a clear seasonal effect, with significantly higher self-consumption in summer months than in winter months[156]. A GSHP control algorithm that used weather forecasts showed a limited increase of 7% in PV self-consumption for a Swedish building[157]. Another study using a residential dwelling from Switzerland found that controlling a heat pump on the availability of surplus PV power increases self-consumption with 1.5%[158]. Also, a few percent lower self-sufficiency by PV electricity was found when a heat pump was included for a residential dwelling in Germany[159].

A German study developed a mixed linear programming model to optimize size the PV system, thermal and battery storage for residential dwellings with a heat pump[160]. It was found that the optimal battery storage size is mainly determined by the electricity demand and hardly influenced by the PV system size. Another study presented a multi objective model to reduce the GSHP consumption peak, using thermal storage and demand response for residential buildings in Belgium[161]. They found that the peak demand can be decreased with 2.5 kW per building, at an estimated capacity cost of 25 €/kW related to a lifetime of 25 years.

Combining a GSHP with a PV system was found to be a preferred option from an energy and economical point, then combining GSHP with a solar thermal collector. This is mainly because for each kWh of PV electricity produced, a multifold of heat can be produced with a GSHP system[162]. A study modelling residential heating options for buildings in Belgium found that GSHP reduce annual emissions with $\approx$ 1.5 tCO_2. With the combination of a PV system, the annual emission reduction was 0.6 to 0.9 ton higher[163]. Also, higher CO_2 abatements cost were found for GSHP than air source heat pumps[145]. When surplus PV electricity is converted to heat using a GSHP and be exported to a district heating grid, then larger PV system capacities are economic suitable[164]. Also conversion of surplus PV electricity to heat was a better environmental option than exporting the electricity to the grid. This is related to the higher carbon intensity of district heating

compared with the electricity generation mix[165]. A study conducted in the South of Spain compared 4 systems for provision of cooling heating and power demand to building. A system including an absorption chiller, an auxiliary heater, PV modules and solar thermal modules showed the best performance from an economic and environmental perspective[166]. Another study conducted in Italy found a 70 - 80% reduction in primary energy when a GSHP system is coupled with a PV system[167].

The literature illustrates that GSHP systems combined with PV and storage show great potential for emissions reduction. Most studies focus on a single or a few research topics, and a broader integrated study combing technological economic and environmental impact was not found. These multidisciplinary studies are essential for a better understanding of the broader impact of PV and storage on GSHP systems. Furthermore, almost all studies use building models to assess the impact of these systems, since measurement data is difficult to obtain. If measured data was used, than only a single or a few buildings were included in the studies. Therefore the influence of real heating demand patterns is not well known.

5.1.2 Research aim

In our study, we present a broader integrated techno-economic and environmental impact for residential dwellings with a GSHP combined with PV and BESS. While most studies solely used a single or modelled consumption timeseries, our research used 16 measured residential electricity consumption and PV production timeseries with duration of 2-years at a 15 min time resolution.

We assessed the impact of 5 systems architectures by comparing the systems with a reference case over the 30-years lifetime. This reference case consists of dwellings with a condensing gas boiler (CGB) and no PV or storage installed. A battery control strategy was developed that aims to increase self-sufficiency and reduction of grid impact simultaneously. The economic impact was assessed and we provide policy options to increase the economic attractiveness of GSHP systems.

Avoided life cycle GHG emissions and payback periods for GHG emissions were determined for each system and compared with each other. The sensitivity of the electricity carbon intensity on the avoided emissions was assessed. Furthermore, we compared the results with surrounding western European countries. Consequently, our results could be used as an indication of emission reduction potential of GSHP combined with PV and batteries for these countries. The obtained knowledge is valuable for a broad range of users, from system owners, installers, distribution system operators and policy makers.

5.2 Method

This research assessed the impact photovoltaic and storage on residential dwellings using a techno-economic and environmental assessment model. First, electricity consumption and PV electricity production of 16 residential dwellings were measured and selected based on data availability and reliability. Also remaining model input parameters required were obtained from literature. Next, a battery storage model was developed which increased PV self-consumption and reduced the peak power on the local electricity grid. Then, technical, environmental and economic performance of each system design was assessed over their lifetime. We selected a 30-years lifetime based on the minimum expected lifetime or a renovation cycle of a residential dwelling[168]. Replacement cost of system components with a lifetime shorter than 30 years were also included. Finally, a sensitivity study on the input parameters was conducted. An overview of the used input data and model steps with corresponding sections and chapters is shown in Fig. 5.1.

5.2.1 Energy production and consumption time series

An overview of the PV electricity production and energy consumption data selection is provided in this section. Also, key parameters containing statistics of PV electricity production and energy consumption from dwellings is provided. Further insights on the time series and patterns are given in appendix 5.A.

Rooftop PV system production and residential electricity consumption timeseries of 38 dwellings were measured in the Netherlands from 2013 until 2015. This was measured during the project called Your Energy Moment which assesses the influence of dynamic tariffs on residential demand. Data of this project has been validated and used in previous studies[106,169]. The electricity consumption of the dwelling, the GSHP system and PV electricity production were measured separately with a 15 min time step. The measured data from 1st of July 2013 until 30th of June 2015 was selected to obtain a period of 2 years. Only timeseries with a data availability of higher than 96% were selected. Furthermore, time series were manually analysed on incorrect measurements which reduced the dataset to 16 dwellings. Remaining missing data points were refilled using data from a similar time moment of the first available previous day or following day. As a result, each used timeseries contains 70,080 data points.

The dwellings are detached and semi-detached family houses, build in 2012, with highly insulated roofs, walls and windows, which are representative for typically newly build houses in the Netherlands. They contain PV systems that are

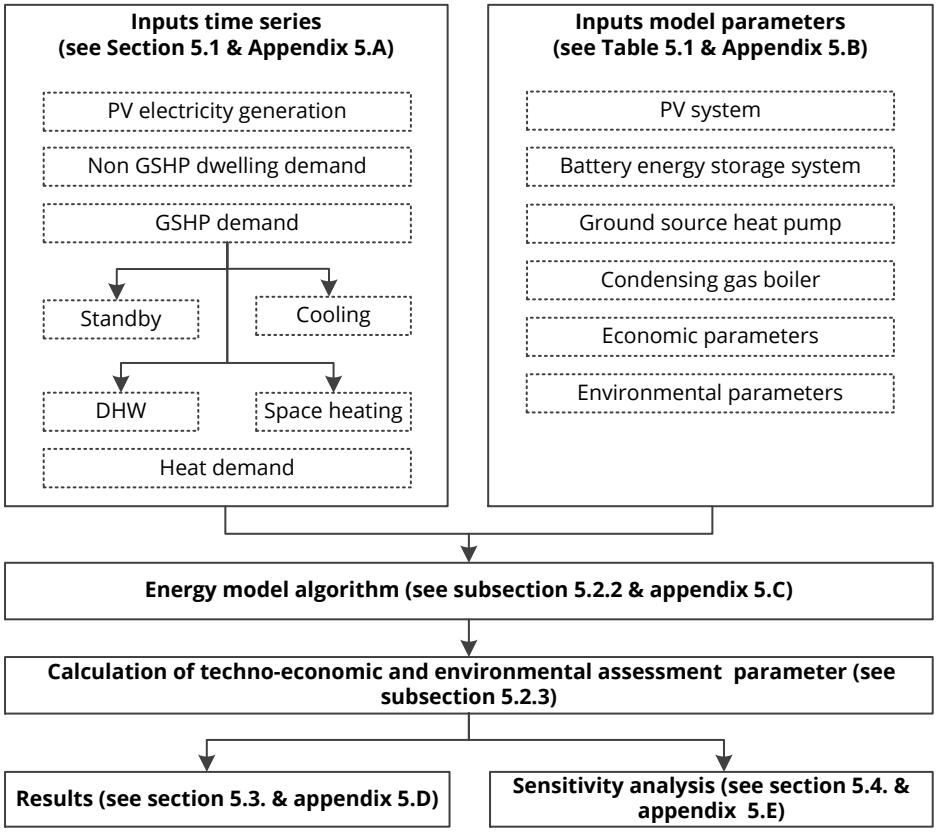

Figure 5.1 · Overview of the techno-economic and environmental assessment model input data and model steps with corresponding sections and chapters.

oriented between 170° and 210° and have a module tilt of 10°. Further technical and environmental performance statistics of the PV systems are provided in appendix Fig. 5.9.

Each dwelling holds a GSHP unit with a nominal output of 4 kW thermal. The GSHP provided the dwellings with three services: space heating, domestic hot water (DHW) provision and cooling. The GSHP system power requirements of the space heating are 1.1 kW and 1.8 kW for DHW production. The heat pumps are connected to a closed loop vertical soil heat exchanger that was designed to achieve a relative high brine temperature of 4°C. Dwellings are heated using low temperature floor heating (28°C). Combined with the high brine temperature, this results in a coefficient of performances (COP) of 5.7 for space heating. DHW production requires a higher temperature (60°C), which results in a lower COP of 1.9[170]. DHW is stored in 190 L storage tanks, which are refilled if reaching a lower water level. The GSHP can also cool the inside temperature with a few degrees

using the floor heating system. Therefore, cool water from the ground source is circulated through the floor heating system. If cooling is applied, the GSHP uses $\approx$ 0.15 kW for the circulation pumps. In addition, the GSHP system uses electricity for standby use.

The minimum and maximum GSHP power consumption for each time step were measured. Consequently, we could separate the GSHP consumption time series into four profiles for each function, based on the maximum energy consumption measured for each time step. Electricity consumption below 0.08 kW was allocated to standby usages. Consumption between 0.08 and 0.2 kW was allocated to cooling use. The consumption between 0.2 and 1.4 kW was allocated to heating and above 1.2 kW allocated to DHW production. The heat demand was derived from the electricity demand required for space heating and DHW production. The natural gas demand was determined from the heat demand using the efficiencies of the condensing gas boiler, which can be found in Table 5.1.

Statistics of the residential electricity consumption and the share of the GSHP functions are presented in appendix Table 5.2. Also the estimated natural gas consumption statistics are shown in appendix Table 5.3. The two years measurement period was scaled to a 30-years period by duplicating the 2 years period. We assumed no future change in electricity consumption from the dwellings. More details on the hourly, daily and seasonal fluctuation of the electricity consumption are presented in the appendix with Fig. 5.10 & Fig. 5.11. The winter months in the used time period (December, January and February) had higher temperatures than the long term average of 3.4°C. The winter of 2013-2014 had an average winter temperature of 6°C and the winter of 2014-2015 had an average temperature of 4.1°C. The overall temperatures for 2014 and 2015 were respectively 11.7°C and 10.9°C compared to a long term-average of 10.1°C[171]. Solar radiation during the used time periods was also a few percent higher[90].

5.2.2 Model input assumptions and explanation

The model assumed input values to determine the technical, environmental and economic performance of the assessed systems. An overview of the model input assumptions for the various system components is shown in Table 5.1. A detailed explanation of theses model assumptions is given in appendix 5.B.

The dwellings had no BESS installed, therefore we modelled the battery energy storage behaviour. An AC (alternating current) coupled lithium-based PV-battery storage system was assumed. AC coupled systems are very suitable to retrofit existing PV systems with storage, and are widely used in literature[93]. The

Table 5.1 · System input assumptions used in this study. The PV system, battery energy storage system, ground source heat pump system, condensing gas boiler, and remaining system input assumptions are separated by dashed lines.

Parameter	Value	Unit	Sources
PV system size	1	kWp_{PV}/MWh_{demand}	[154]
PV system degradation	0.5	%/year	[96]
PV system cost	1200	€/kWp	[172]
Annual O&M PV system	1	% of investement	[124]
PV inverter lifetime	15	year	[93]
Repl. cost PV inverter	100	€/kWp	[172]
PV manufacturing emissions (made in China)	1590	gCO_2-eq/Wp_{PV}	[173]
PV manufacturing emission (made in EU)	824	gCO_2-eq/Wp_{PV}	[173]
Storage capacity	1	kWh_{BESS}/MWh_{demand}	[93]
Battery inverter rating	0.5	kW/kWh_{BESS}	[95]
# of full cycle equivalent	5000		[97]
Calendric lifetime	15	years	[97]
Round trip DCη loss	92.2	%	[95]
Storage pack cost	200	€/kWh	[122]
BOS + EPC BESS	300	€/kW	[123]
Annual O&M BESS system	1	% of investement	[124]
BESS system lifetime	15	year	[93,174]
Replacement cost storage pack	100	€/kWh	[39]
Replacement cost battery inverter	100	€/kW	[123]
Storage pack manufacturing emission	110	gCO_2-eq/Wh_{BESS}	[175]
BOS BESS mfg emis.	124	gCO_2-eq/$W_{BESS\,cap}$	[173]
GSHP COP space heating	5.7		[170]
GSHP COP DHW	1.9		[170]
GSHP system investment	14000	€/unit	[145,176]
GSHP investment subsidy	20	%	[148]
Annual O&M GSHP system	50	€	[177]
Heat pump system lifetime	20	year	[145,177]
Replacement cost heat pump	3600	€/unit	[145,178]
GSHP manufacturing emission	1760	kg CO_2-eq/unit	[143]
CGB eff. space heating	95	%	[163]
CGB eff. DHW	85	%	[163]
CGB investment	1500	€/unit	[140]
Annual O&M CGB	100	€	[179]
CGB system lifetime	15	year	[140]
Replacement cost CGB	1500	€/unit	[140]
CGB manufacturing emission	160	kg CO_2-eq/unit	[180]
Discount rate	2	%/year	[125]
Natural gas tariff	21.84	€/GJ HHV	[181]
Electricity cons. tariff	0.176	€/kWh	[181]
Electricity feed-in. tariff	var.	€/kWh	[182]
Annual change NG tariff	0.5	% /year	[183]
Annual change elec. tariff	0.5	% /year	[183]
Emis. electricity grid (2016)	490	gCO_2-eq/kWh	[151]
Zero grid emissions in year	2050		[184]

behaviour of the BESS was modelled using a novel algorithm aimed for two applications simultaneously: increase in self-consumption and reduction of grid impact. Self-consumption was enhanced by storing surplus PV energy to use this on later moments. Grid impact was reduced by peak shaving of the imported and exported peak. The novelty of this algorithm is to predict the annual peak shaving potential by including the expected self-consumption enhancement. This potential depends on the used battery capacity and battery inverter rating.

This algorithm was written in Python (v3.5) and uses electricity production and demand profiles of the dwellings. The battery charge and discharge flows were simulated for 30 years using a time step of 5 min. This time step was used to obtain a good accuracy of battery storage capacity degradation. Battery degradation consists of cycle degradation and calendric degradation and was determined annually. The diminished storage capacity was subtracted from the original storage capacity for each year. After 15 years the battery storage is replaced and the capacity is set back to the full storage capacity. The used battery degradation model is explained in detail in a previous study[185]. Perfect forecasts of the PV energy production and the electricity consumption patterns were assumed. These were used to predict the moments to charge or discharge the battery storage system and consequently reduce the power impact on the local grid. An overview of the energy model algorithm with the description and explanation of the model steps is presented in appendix 5.C. Furthermore, the model is clarified using two days as example, graphical supported by Fig. 5.12.

5.2.3 Calculation of assessed parameters

Calculation of self-sufficiency and grid impact

The self-sufficiency ratio was used to assess the impact of the PV self-consumption. The self-sufficiency ratio indicates the share of electricity demand (P_{demand}) that is fulfilled by direct or indirect PV self-consumption. The direct self-consumption consists of PV produced power which is directly used in the dwelling ($P_{\text{direct SC}}$). The indirect self-consumption contains power that is discharged from the battery and delivered to the dwelling ($P_{\text{B discharge}}$). The self-consumed power is aggregated over the total lifetime of the system from the first time step of the first year (t=1) until the last time step of the final year (t_{end}), with a 5 min time step see Eq. (6.2).

$$\text{SSR} = \frac{\sum_{t=1}^{t_{\text{end}}} (P_{\text{direct SC,t}} + P_{\text{B discharge,t}}) \cdot \Delta t}{\sum_{t=1}^{t_{\text{end}}} P_{\text{demand,t}} \cdot \Delta t} \tag{5.1}$$

The specific self-sufficiency ratio (SSR_{specific}) indicates the share of electricity consumption of each of the four GSHP functions that could be fulfilled by the direct or indirect self-consumption. The GSHP self-consumed power was divided into four temporal subsets (T_{TF}), based on moments with power demand for each GSHP function. This self-consumed power was aggregated and divided by the electricity consumption of each function ($P_{\text{demand,GSHP,t}}$) see Eq. (5.2).

$$SSR_{\text{specific}} = \frac{\sum\limits_{t \in T_{TF}} (P_{\text{direct SC,t}} + P_{\text{B discharge,t}}) \cdot \Delta t}{\sum\limits_{t \in T_{TF}} P_{\text{demand,GSHP,t}} \cdot \Delta t} \tag{5.2}$$

The impact of the grid was assessed using four parameters. The maximum import power peak and export power peak to the grid (P_G) over the lifetime of the system was determined. This peak is a valuable indicator for distribution system operators to assess the impact of the residential system on their network. The other two parameters are the import peak to average ratio (IPAR) and export peak to average ratio (EPAR). The IPAR is defined as the ratio between the maximum import power peak and the average imported power from the grid. The export peak to average ratio EPAR is defined as the maximum exported power to the grid and the averaged exported power. These parameters are an indicator for the variability and magnitude of the power flows on the network, see Eq. (5.3).

$$\text{Import peak} = Max(P_{\text{G,t}} < 0) \tag{5.3a}$$

$$\text{Export peak} = Max(P_{\text{G,t}} > 0) \tag{5.3b}$$

$$\text{IPAR} = \frac{\text{Import peak}}{\frac{1}{n} \cdot \sum\limits_{t=1}^{n} (P_{\text{G,t}} < 0)} \tag{5.3c}$$

$$\text{EPAR} = \frac{\text{Export peak}}{\frac{1}{n} \cdot \sum\limits_{t=1}^{n} (P_{\text{G,t}} > 0)} \tag{5.3d}$$

Calculation of investment attractiveness

The investment attractiveness of each system depends on the initial investment cost of a system (I_{total}) and the annual cash flows (CFs) over the lifetime of the systems. The investment cost depends on the expenses for the heating system (I_{HS}), the cost of the PV system(I_{PV}) and investment cost of the storage system (I_{BESS}), see Eq. (5.4). The cost of the PV and storage systems depends on the installed system capacities.

$$I_{\text{total}} = I_{\text{HS}} + I_{\text{PV}} + I_{\text{BESS}} \tag{5.4}$$

The total cash flow depends on the annual (y) energy cost from natural gas and electricity. The cash flow from natural gas (CF_{NG}) depends on the imported

natural gas (NG_{import}) and the natural gas tariff (π_{NG}). The cash flow of electricity (CF_{Elec}) depends on the imported electricity ($Elec_{\text{import}}$) and exported electricity ($Elec_{\text{export}}$) and the consumption tariff (π_{cons}) and the feed-in tariff ($\pi_{\text{feed-in}}$). The operation and maintenance (O&M) cost contain the cost of maintaining the installed heating system ($O\&M_{\text{HS}}$), PV system ($O\&M_{\text{PV}}$), and battery storage system ($O\&M_{\text{BESS}}$). We assumed a constant O&M cost factor over the lifetime. The total annual cash flow is the energy cash flows plus the O&M cash flow, see Eq. (5.5).

$$Elec_{\text{import}} = \sum_{t|P_{\text{G,t}}<0}^{t_{\text{end}}} P_{\text{G,t}} \tag{5.5a}$$

$$Elec_{\text{export}} = \sum_{t|P_{\text{G,t}}>0}^{t_{\text{end}}} P_{\text{G,t}} \tag{5.5b}$$

$$CF_{\text{NG}} = \text{NG}_{\text{import}}, y \cdot \pi_{\text{NG}}, y \tag{5.5c}$$

$$CF_{\text{Elec}} = \tag{5.5d}$$
$$(Elec_{\text{import}}, y \cdot \pi_{\text{cons}}, y) - (Elec_{\text{export}}, y \cdot \pi_{\text{feed-in}}, y)$$

$$\text{O\&M} = O\&M_{\text{HS}} + O\&M_{\text{PV}} + O\&M_{\text{BESS}} \tag{5.5e}$$

$$CF, y = CF_{\text{NG}} + CF_{\text{Elec}} + \text{O\&M} \tag{5.5f}$$

The attractiveness of the investment in the system architectures was evaluated using the net present value (NPV), cost reduction, internal rate of return (IRR) and discounted payback period (DPBP), defined according Eq. (5.6). The NPV gives a perspective of the current value by including the future risk and returns of the investment. The NPV provides an absolute number that can help in the decision process for the system selection of dwelling owners. A positive NPV represents a feasible investment, while a negative NPV shows an unwise investment. The future risk and return is included with the discount rate (r) and used to calculate the diminishing value of future returns over the economic lifetime (L_{econ}) of the system. The NPV was calculated by subtracting the reference NPV ($NPV_{\text{reference}}$) minus the actual NPV (NPV_{actual}). The reference NPV included cash flows and investment cost from the reference case, and the actual NPV included the cash flow and investment cost of the analyzed system architecture. The cost reduction ($C_{\text{reduction}}$) is the relative reduction in NPV of the actual system compared cash flow to the reference system. The IRR gives an indication of the discount rate required to obtain a feasible investment. This was obtained by solving the discount rate with an NPV identical to zero. Thus the IRR shows the influence of the discount rate on the investment. The DPBP presents the time period until an economic investment is recovered. This was found by solving the year in which the NPV is identical to zero. System payback periods are frequently

used in the residential PV and GSHP market, therefore DPBP was selected as an economic indicator. A maximum lifetime of 50 years was included in the mathematical solver. We included lifetimes longer than the economic lifetime of the systems to give a clear depiction of the DPBP diversity.

$$NPV_{\text{reference}} \,\&\, NPV_{\text{actual}} = \sum_{y=0}^{\mathrm{L_{econ}}} \frac{CF, y}{(1+r)^{y}} - \mathrm{I_{total}} \tag{5.6a}$$

$$\mathrm{NPV} = NPV_{\text{reference}} - NPV_{\text{actual}} \tag{5.6b}$$

$$C_{\text{reduction}} = \frac{NPV_{\text{reference}} - NPV_{\text{actual}}}{NPV_{\text{reference}}} \tag{5.6c}$$

$$\mathrm{IRR} = \left\{ r \quad \text{where NPV, r} == 0 \right. \tag{5.6d}$$

$$\mathrm{DPBP} = \left\{ y \quad \text{where NPV, y} == 0 \right. \tag{5.6e}$$

Calculation of avoided GHG life cycle emissions

The life cycle emissions of each system mainly depends on two emissions categories. The first category are emissions released during manufacturing and installation of the specific system components (GHG_{mfg}). These emissions are from the heating system ($GHG_{\text{mfg HS}}$), PV system ($GHG_{\text{mfg PV}}$), and battery storage system ($GHG_{\text{mfg BESS}}$). Emissions from PV systems manufactured in China were selected since more than half of PV module globally are currently produced in China[6]. The emissions from the heating system are per unit, emissions from PV per kWp capacity and BESS per kWh storage capacity, see Eq. (5.7).

$$GHG_{\text{mfg}} = GHG_{\text{mfg HS}} + GHG_{\text{mfg PV}} + GHG_{\text{mfg BESS}} \tag{5.7}$$

The second category contains emissions associated with the imported energy ($\mathrm{GHG_{E\,import}}$) and potential avoided emissions due to the exported energy ($\mathrm{GHG_{E\,export}}$). The emissions associated with imported energy consist of the emissions from electricity imported and emissions from natural gas combustion. Emissions from imported and exported electricity are calculated by multiplying the annual electricity import and export with the average annual emission factor of electricity (EFE). An annual linear reduction from the current emission factor towards zero for a certain future year was assumed. The emissions associated with exported electricity depend on the exported electricity multiplied by the annual emission factor, see Eq. (5.8). Emissions from the natural gas consumption were included when a system contained a CGB to provide space heating and DHW. A emission factor of 50.93 kg CO_2/GJ HHV was used to obtain the emissions from natural gas consumption.

$$GHG_{\text{E import}} = \sum_{y=1}^{y_{\text{end}}} Elec_{\text{import}}, y \cdot \text{EFE}, y \tag{5.8a}$$

$$GHG_{\text{E export}} = \sum_{y=1}^{y_{\text{end}}} (Elec_{\text{export}}, y \cdot \text{EFE}, y) + (NG_{\text{import}}, y \cdot 50.93) \tag{5.8b}$$

A larger share of renewable PV production capacity could result in PV feed-in limitations. Moreover, exported PV produced by the dwellings could replace other renewable sources and these future marginal GHG emissions of the electricity systems are difficult to predict. Therefore, we assessed the avoided life cycle GHG emissions using two system boundaries: from an electricity system perspective (GHG_{system}) and from a dwelling perspective (GHG_{dwelling}). In the first perspective, all exported PV electricity is allocated to replace emissions from electricity generated by other sources. From the dwelling perspective, exported PV electricity does not account for additional avoided emissions, see Eq. (5.9).

$$GHG_{\text{system}} = GHG_{\text{mfg}} + GHG_{\text{import}} - GHG_{\text{E export}} \tag{5.9a}$$

$$GHG_{\text{dwelling}} = GHG_{\text{mfg}} + GHG_{\text{E import}} \tag{5.9b}$$

The avoided emissions (GHG_{avoided}) are defined as the difference in emissions of the reference system ($GHG_{\text{reference}}$) and the actual system (GHG_{actual}) architecture. The reference system contains a CGB for heating demand that has similar standby consumption as the GSHP. Also the reference system included the emissions from import electricity and natural gas. The reduction is defined as the ratio between the avoided emissions and the reference emissions, see Eq. (5.11).

$$GHG_{\text{avoided}} = GHG_{\text{reference}} - GHG_{\text{actual}} \tag{5.10a}$$

$$GHG_{\text{reduction}} = \frac{GHG_{\text{avoided}}}{GHG_{\text{reference}}} \tag{5.10b}$$

The GHG payback period (GHGPBP) is an indication of the time period to offset the additional emissions from manufacturing and installation of the actual system ($GHG_{\text{mfg actual}}$) compared to the reference system ($GHG_{\text{mfg ref}}$). The avoided emissions excluding the emissions from manufacturing ($GHG_{\text{avoided ex}}$) from the reference system and the actual system were determined for each year. These were calculating according to Eq. (5.8) and Eq. (5.9), excluding the emissions from manufacturing. The GHG payback period was found by selecting the time step for which the cumulative avoided emissions excluding manufacturing (CAE) are identical to the extra emissions due to manufacturing, according Eq. (5.11).

$$\text{CAE}, y = \sum\nolimits_{y=0}^{y=end} GHG_{\text{avoided ex}} - (GHG_{\text{mfg actual}} - GHG_{\text{mfg ref}}) \tag{5.11a}$$

$$\text{GHGPBP} = \left\{ y \quad \text{where CAE, y} == 0 \right. \tag{5.11b}$$

5.3 Results

This section provided the technical, economic and environmental impact of the GSHP systems combined with PV and storage. The results of each individual system was visualized using violin plots[65]. This type of graphical illustration gives a quick indication of the distribution of results obtained from each dwelling and system. The results are presented for normalized PV system capacities of 1 kWp for each MWh of annual electricity consumption and battery storage capacities of 1 kWh per MWh annual consumption. Technical, economic and environmental impact of smaller and larger PV system sizes and battery storage capacities are presented in in appendix 5.D.

5.3.1 Self-sufficiency ratio and grid impact

SSR distributions of dwellings and their specific GSHP functions are visualized using violin plots in Fig. 5.2 (a & b). PV systems with GSHP show an average SSR of 25%, with a range between 21% and 31%. Adding BESSs increases this SSR on average with 18% point, ranging from 39% until 49%. Dwellings without GSHP show a higher SSR of 31% on average for PV only and 49% with BESS. Clearly, adding a GSHP reduces SSR. This is simply due to the fact that PV production occurs mainly in the summer months, whereas most GSHP demand consumption occurs during colder winter months (see appendix Fig. 5.10 & Fig. 5.11).

Each of the specific heat pump functions shows a different contribution to the SSR (Fig. 5.2 (b)). Cooling demand shows the largest specific SSR of which 53% directly is provided by the PV system. This number can be increased to 94% when a storage system is added. The SSR of space heating is limited to 9% in case of PV only and 14% when a storage system is used, since most space heating occurs during colder winter months. DHW is temporarily stored in a tank and therefore DHW production has a demand side management potential. The average SSR of DHW increased by 12% with storage and by 23% with twice the storage capacity, see appendix Fig. 5.14. Based on these numbers, we estimated that a quarter of DHW production has the potential to be shifted to moments with excess PV electricity. This will increase the direct self-consumption of DHW production and reduce the storage requirements for batteries. In total, 19% of the GSHP consumption can be provided by direct PV electricity and an additional 10% by BESS.

The influences of the systems on the electricity grid are presented in Fig. 5.2 (c to f). Dwellings with GSHP have an average 0.8 kW higher import peak than dwellings without GSHP, however the maximum peak demand of the GSHP system is 1.8 kW. Hence, power peaks from GSHP are not occurring at the same moment as power peaks of remaining dwelling appliances. Deploying BESS systems leads to an average reduction in import peak of 45% for dwellings with GSHP and of

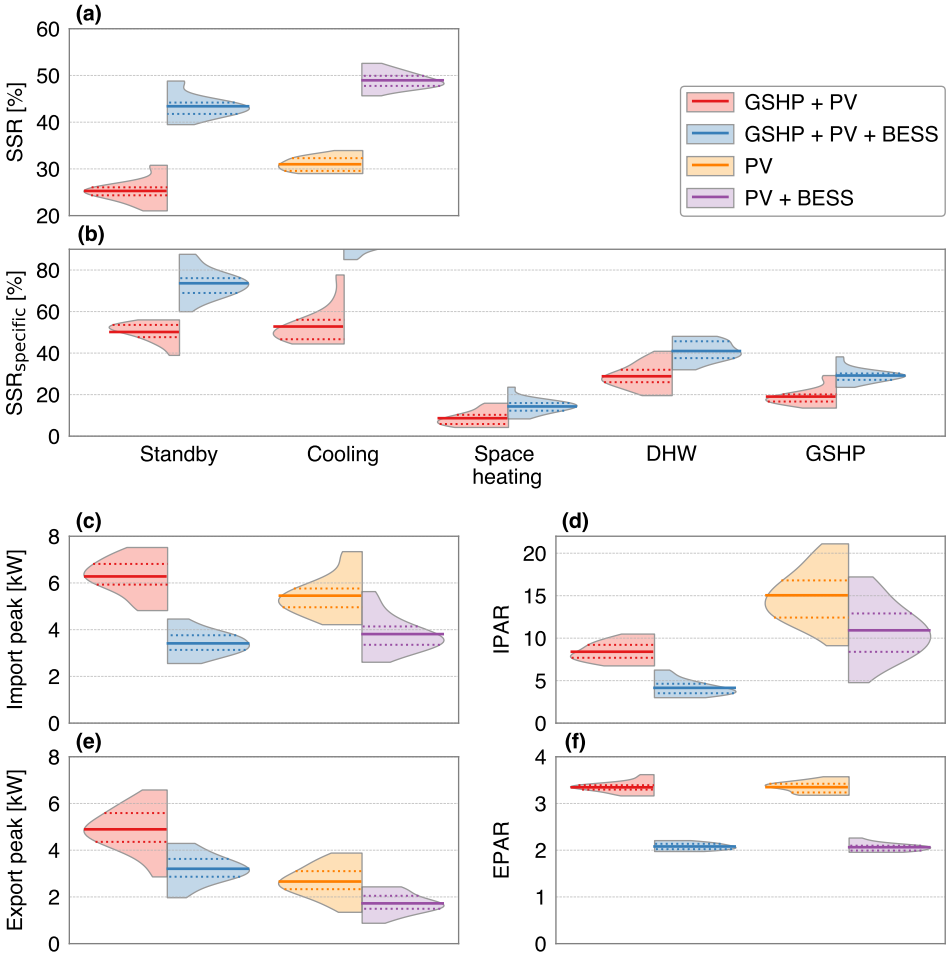

Figure 5.2 · Distribution of the self-sufficiency ratios for the four system configurations (a) and distributions of specific self-sufficiency ratios for each of the heat pump functions (b). The impact of power flows from the electricity grid is shown by the import peak distributions (c) and the import peak to average ration (d). The impact of power flows to the grid is presented by the export peak (e) and the export peak to average ratio (f). The left part of the violin plot shows the distribution of a PV system only and the right part of the distribution with a storage system. Distributions are shown for a 30-year lifetime. Mean values of distributions of the 16 dwellings are indicated by solid lines, and the 25% and 75% percentiles by dotted lines.

30% for dwellings without GSHP. Dwellings with GSHP systems show an average reduction of import peak to average ratio from 15 to 11 when BESS are used. The reduction of exported peak PV power is around 38% for both dwellings with and without GSHP. Export peak to average ratio are reduced from 3.3 to 2.1 when storage was included in the system. Larger storage capacities lead to larger reduction of the import and export peaks, see appendix Fig. 5.15. Also shown here is that on average 0.09 % of the total charged energy was pre-charged to reduce peak

demand and only 0.04% of discharged energy was pre-discharged to store future PV peaks. Furthermore, SSR are 0.07% lower due to the peak shaving application. Moreover this figure shows the impact of three potential PV feed-in limitations. These results show that BESS have a large potential in enabling more GSHP and PV systems on existing low voltage grids.

5.3.2 Investment attractiveness

The investment attractiveness for 16 dwellings and 5 systems architectures is presented in Fig. 5.3. A large distribution range in net present value is shown for dwellings with a GSHP, highly influenced by the dwellings heat consumption. The GSHP system shows a net present value range from $€-1.6 \cdot 10^3$ to $6 \cdot 10^3$, with a mean of $\approx$ €1100. 7 of the 16 dwellings with solely a GSHP system have a negative NPV. A PV system combined with GSHP results in a positive average NPV of $€5.7 \cdot 10^3$. A BESS reduces the average NPV around €1100, showing that investing in storage is not profitable.

The average cost reduction of a PV system with GSHP is larger than for only a PV system. However, highest internal rate of returns are shown for PV systems only, with an average of 7.5%. The investment in a GSHP system is two to three times larger than the investments in a PV system. Consequently, the internal rate of return is higher for solely a PV system than for a PV system with GSHP. The GSHP systems show an average IRR of 2.6% and GSHP systems with PV an average

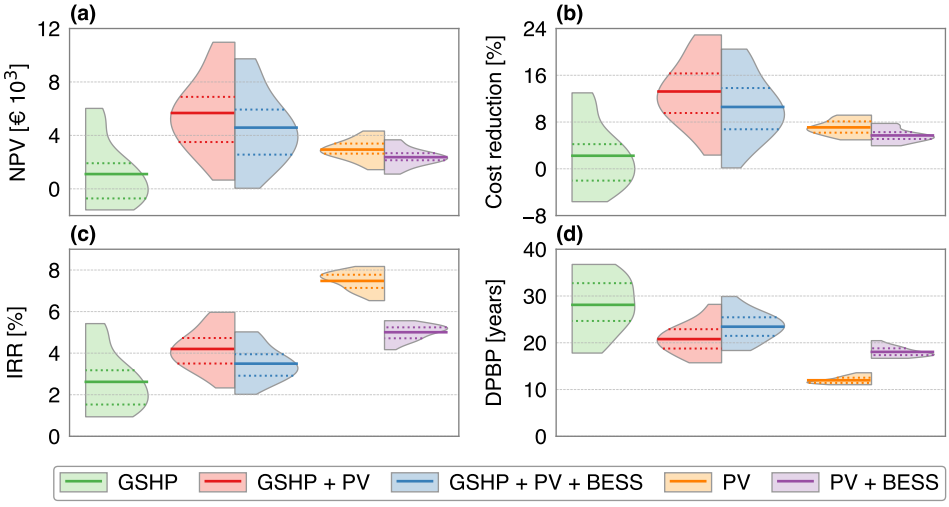

Figure 5.3 · Distribution of net present value (a), cost reduction (b), internal rate of return (c) and discounted payback period (d) for 16 residential systems. Five system configurations are presented, explained in the figure legend. Mean values of distributions are indicated by solid lines and the 25% and 75% percentiles are indicated by dotted lines.

of and 4.2%. Discounted payback period of GSHP systems are between 18 to 37 years, whereas solely PV systems show an average of 12 years. Distribution range for DPBP by only GSHP is substantially larger than the distributions seen from only a PV system. The revenue of GSHP is caused by the avoidance of natural gas consumption and is highly dependent on the occupancy and behaviour of the residents as well as the dwelling properties. The DPBP decreases with larger PV system or BESS capacities (see appendix Fig. 5.16.)

5.3.3 Avoided life cycle GHG emissions

Distributions of avoided life cycle GHG emissions, GHG emission reduction and GHG payback periods are presented in Fig. 5.4. Avoided emissions from an electricity system perspective show a relative large distribution spread, especially for systems with GSHP. Avoided emissions of GSHP systems are between 30.6 and 59.2, with an average of 42.4 tCO_2-eq for the 16 dwellings. Systems with PV have an average of 72.7 tCO_2-eq, demonstrating that PV systems contributes with 30.3

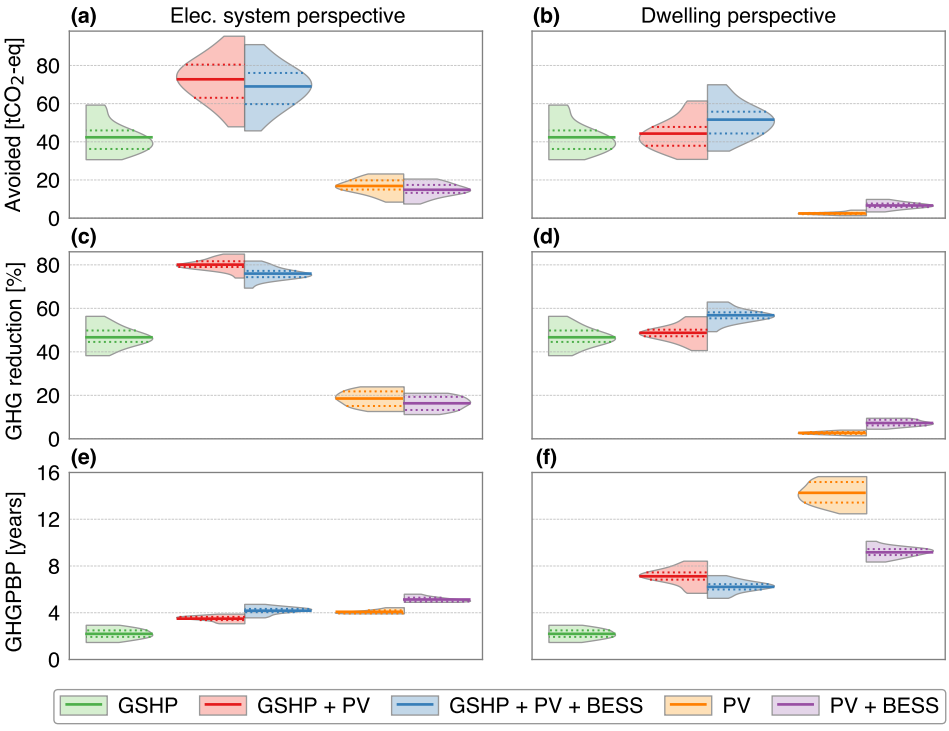

Figure 5.4 · Distribution of avoided life cycle system emissions (a & b), emission reduction (c & d) and GHGPBP (e & f) for 16 residential systems. The left columns shows the distribution from an electricity (Elec.) system perspective and the right columns show the distribution from a dwelling perspective. Mean values of distributions of the 16 systems are indicated by solid lines, and the 25% and 75% percentiles are indicated by dotted lines.

tCO_2-eq on average of avoided emissions. Avoided emissions are larger for dwellings which include a GSHP due to the larger PV capacities. BESS systems lower the avoided emissions from an electricity system perspective, mainly caused by charge and discharge losses. The higher avoided emissions by storage are caused by the higher SSR of 10%. Larger PV system capacities have more avoided emissions from an electricity system perspective, see appendix Fig. 5.17. Emissions are reduced by 47% using a GSHP and 80% with the use of a PV system. GHGPBP are lowest for a GSHP system only with 2.5 years of time required to offset the emissions from manufacturing and installation. All system configurations have an average GHGPBP below 6 years from a system perspective.

Avoided emissions were also determined from a dwelling perspective, which only includes emissions avoided within a dwelling. This perspective is currently not realistic since surplus PV electricity can be exported to the grid without limit, and is shown purely as a theoretical indicator. Avoided emissions show an average of 44.3 tCO_2-eq for GSHP with PV, and an additional 7.3 tonne when storage is included. The higher avoided emissions by storage are caused by the higher SSR of 10%. Larger PV system capacities have more avoided emissions from an electricity system perspective, but less avoided emissions from a dwelling perspective, see appendix Fig. 5.17. Also, the GHG reduction from the dwelling perspectives are lower and the GHGPBP from this perspective higher.

5.3.4 Techno-economic correlations with avoided emissions

Observable correlations between technological or economic parameters with the avoided life cycle GHG emissions parameters are given in Fig. 5.5. The contribution of the PV system to the avoided life cycle GHG emissions from a dwelling perspective is shown using the self-sufficiency ratio. A clear linear trend is observed between the SSR and the avoided GHG emissions by a PV system. A minimal SSR of 22% is required to obtain net positive emissions. For SSR >22%, avoided emissions from a dwelling perspective increase with $\approx$ 80 gCO_2-eq per Wp for each percentage point SSR.

Another clear correlation is shown between the net present value and the total avoided emissions from a system perspective. The NPV increases with $\approx$ €275 for each additional ton of avoided tCO_2-eq. Around 40 tCO_2-eq should be avoided to obtain benefits from emissions reduction. Dwellings with a GSHP system plus PV and storage show an NPV increase of around €230 for each additional ton of avoided tCO_2-eq. Complementing these dwellings with storage shows a comparable slope. Dwellings with PV show a NPV increase of $\approx$ €180 for each ton of avoided emissions. This is decreased to €170 when storage is added. These numbers show that avoiding emissions with PV systems obtain lower

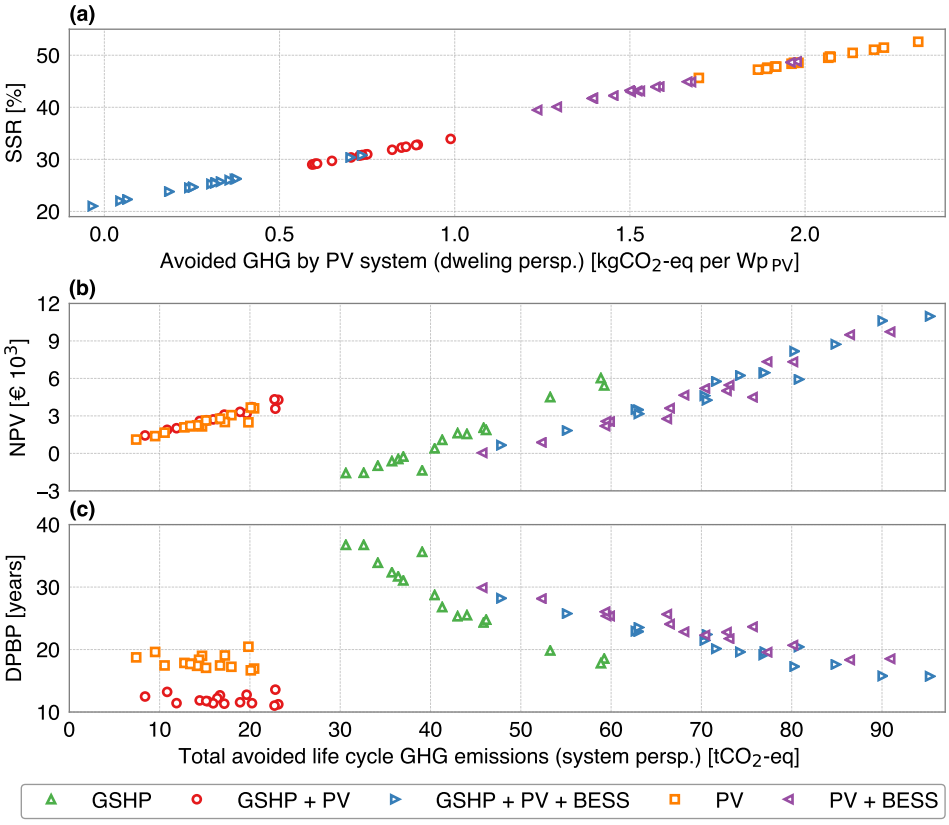

Figure 5.5 · Correlation of self-sufficiency ratio on the avoided life cycle GHG emission by PV systems from a dwelling perspective (a), and correlation of net present value (b) and discounted payback period (c) on the total avoided emissions from a system perspective. Correlations are shown for 16 residential dwellings. Note that a similar horizontal axis is used for subplot (b) and (c).

benefits as avoiding emissions using GSHP systems per tCO_2-eq. However, PV systems show only positive NPV values, whereas GSHP system needs a minimum of avoided emissions to obtain a positive NPV number.

Discounted payback periods are decreasing with avoided emissions. Dwellings with GSHP systems only show a decrease of 0.7 year for each tonne. The dwellings with the largest avoided emissions of 58 tCO_2-eq show the lowest DPBPs of 18 years. GSHP systems with PV and storage have a DPBP reduction of $\approx$ 0.25 year per tCO_2-eq. Dwellings with PV only show a decrease in DPBP of 0.03 year per ton tCO_2-eq, or 12 days.

5.4 Sensitivity analysis

5.4.1 Discounted payback period sensitivity

A sensitivity analysis of five input parameters on the DPBPs of GSHP systems and GSHP with PV and with PV + storage is presented in Fig. 5.6. Dwellings with only a GSHP system need an increase of 1.2% per year in natural gas tariff to obtain DPBP <30 years for all dwellings. Higher electricity tariffs lead to higher DPBP and are even sharply increase when these changes are above 2%. Yet, the impact of higher electricity tariffs is greatly reduced when a PV system is added to the dwelling. The value of self-consumed energy increases with higher electricity tariffs, therefore PV systems obtain more revenue. This is even more reduced when a battery storage system is added due to the increased self-consumption.

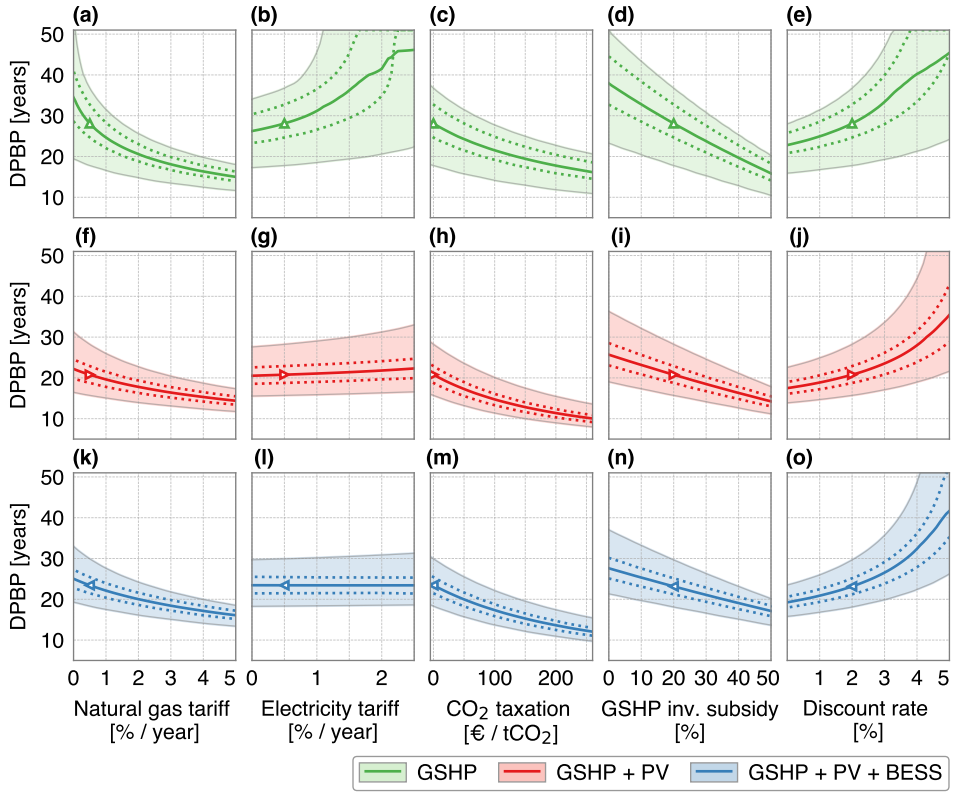

Figure 5.6 · Impact of increase in natural gas tariff (a, f & k), increase in electricity tariff (b, g & i) CO_2 taxation (c, h & m) GSHP investment subsidy (d,i & n) and discount rate (e, j & o) on the discounted payback period of the 16 residential systems. The impact of solely GSHP systems are shown in the top row, GSHP systems with PV system in the middle row and with storage in the bottom row. Mean values of distributions are indicated by solid lines and the 25% and 75% percentiles are indicated by dotted lines. The markers indicate the reference scenario values.

Consequently, the DPBP of GSHP with PV and BESS are only slightly increasing with higher electricity tariffs.

A CO_2 taxation on the used electricity and gas consumption of around €70 per tCO_2 reduces the DPBP <30 year for all dwellings. An additional 11% cost reduction results in similar DPBP. This is a realistic cost reduction for the future GSHP mass market scenario[178]. Yet, an increase in the discount rate, from 2% to 3%, results in an average DPBP to 33 years. In general, the PV and PV battery systems decrease the DPBPs of the overall system.

Two extended sensitivity analyse on the DPBPs are given in appendix 5.E. First, the combined impact of natural gas tariffs and electricity tariffs is presented. For example, it is shown that for dwellings with a GSHP, a 1% increase in both electricity tariff and natural gas tariff will keep the average DPBP between 25 and 30 years. Furthermore, lower electricity tariff are positive for GSHP payback periods but negative for PV and battery storage payback periods. Consequently, GSHP combined with PV and storage level out the influences of higher or lower electricity tariffs. Second, the combined impact of a change in GSHP investment subsidies with a change of natural gas tariff, electricity tariff, CO_2 taxation or discount rate is shown. This shows that a combination of GSHP investment subsidy with a decreasing natural gas tariff, or increasing CO_2 taxation shows a steep reduction in DPBP. For example, an additional 10% additional subsidy and a €65 /tonne CO_2 will reduce the average DPBP for GSHP systems to 20 years.

5.4.2 Avoided life cycle GHG emissions sensitivity

Avoided system emission depends on the carbon intensity of electricity from the grid. This intensity is expected to decrease in the next decades due to a larger share of renewable electricity generation capacity. Yet, the gradient of this decrease depends on policy and technological development. We assessed the impact of this reduction by assuming a linear reduction of 2016 GHG emissions to zero emissions for a given year, presented in Fig. 5.7. A faster decrease in emission intensity results in lower avoided emissions by PV and BESS, but more emissions are avoided using a GSHP. From a dwelling perspective, the emissions due to manufacturing of solely a PV system are not recouped before 2040. A sixth scenario was added which presents the impact of a PV system made in the EU. In this case, the emissions due to PV system manufacturing are already recovered by 2029, caused by the lower emissions during production of PV in the EU compared to China[13].

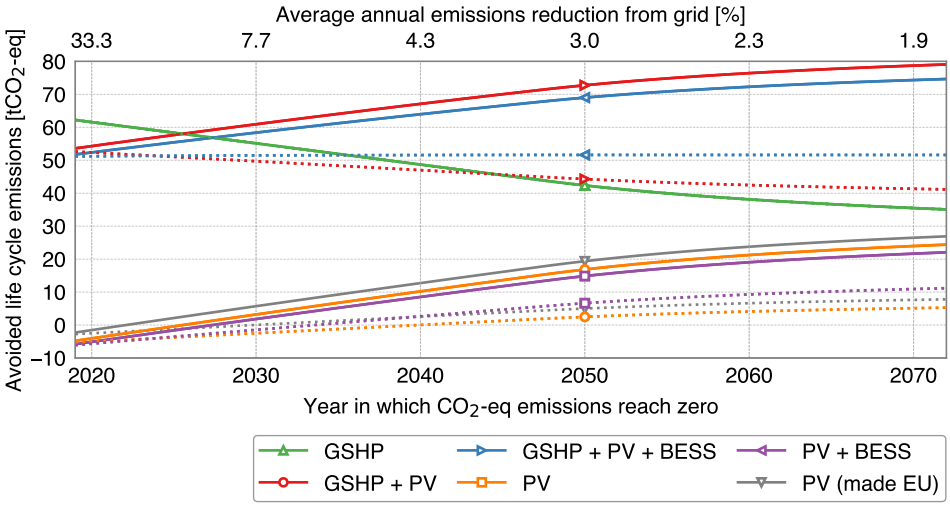

Figure 5.7 · Avoided life cycle GHG emission averaged over the 16 dwellings of an electricity system perspective (solid lines) and dwelling perspective (dotted lines), depended on the year in which the GHG electricity reach zero and assuming a linear reduction from 2016 onwards. The top horizontal axis shows the corresponding average annual emission reductions in percentage. A sixth option (PV made in EU) was added to visualize the impact of PV manufactured in the EU. The markers indicate the reference scenario values.

5.5 Discussion

This research assessed the techno-economic and environmental impact of GSHP systems combined with PV and storage. We showed that PV systems contribute to one fifth of the total GSHP electrify demand. Battery energy storage reduces the GSHP impact on the local grid. Also GSHP systems can greatly reduce the life cycle GHG emissions of dwellings by replacing natural gas-fired boilers.

5.5.1 Comparison with previous studies

PV self-sufficiency ratios are comparable as found in previous studies[39,103,155]. Thus, the models used in these studies are representative for real applications. We found that investment attractiveness of systems is highly dependent on the total avoided life cycle GHG emissions. An NPV increase of €275 per tCO_2-eq was observed for GSHP systems, which are in a similar range as found previously[145]. At least 40 tCO_2-eq of life cycle GHG emission should be avoided to obtain a positive NPV for these systems. With a PV and storage system, the NPV decreases to €230 per tCO_2-eq. No comparable studies were found which assessed this combined influence.

Results on the environmental impact are comparable with previous studies that investigated avoided emissions using GSHP systems from German, Belgium or the UK. These countries have similar climate and dwelling conditions as the

Netherlands. We found that GSHP systems reduce life cycle GHG emissions between 18 and 56% compared to a natural gas boiler. This corresponds to annual avoided emissions ranging between 1 and 2 tCO_2-eq for GSHP systems. These results are comparable with previous studies that investigated savings for Germany, Belgium or UK[142,143,145]. If PV is added to the systems, than an additional 1 ton of avoided CO_2-eq emissions can be achieved, similar as found before for Belgium[163].

We did not find studies that assessed emission reductions from GSHP systems combined with PV and storage. A large share of heat demand in dwellings is provided by fossil fuels in France, Germany and United Kingdom. This heat demand can be fulfilled by GSHP systems[138]. Therefore we provide a first indication of this potential for these countries, shown in Fig. 5.8. This shows that United Kingdom and France would have respectively 22% and 45% more avoided emissions for GSHP systems respectively, compared to the Netherlands.

Yet the impact of solely PV is lower, with even negative emissions for France due to the large share of nuclear electricity generation. However, if we would assume that PV systems were produced in Europe, then the PV system footprint per kWh would be almost similar as the emission factor of France, see appendix Fig. 5.9. Consequently, negative emissions would be reduced to -1.1 tonne of CO_2-eq. Moreover, Germany has a higher electricity tariff of ≈ 0.30 €for each kWh[186]. This results in higher electricity costs for GSHP but also larger revenues from PV and BESS systems. We analysed the impact of this tariff and found that a solely GSHP system would be far from profitable. However, GSHP with PV and storage would have a lower DPBP than presented in our research.

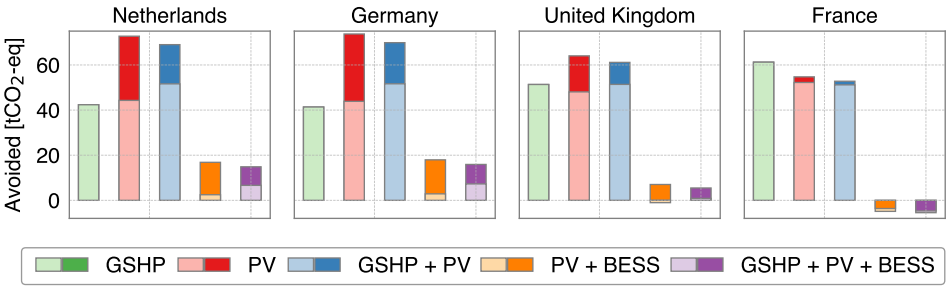

Figure 5.8 · Avoided life cycle emissions using electricity grid emissions factors of four Western European countries. Light colours represent avoided emissions from the dwelling perspective and darker colours from a system perspective. Used emission factors for Germany, United Kingdom and France are 514, 275 and 38 gCO_2-eq for each kWh respectively[187]. Also, we assumed a 10% larger PV production for France and kept remaining model parameters similar[27].

5.5.2 Implementation challenges

Dwellings used in this study use low temperature floor heating, resulting in highly efficient GSHP operation and thus avoid more emissions compared to using a conventional dwelling heating system. Existing dwellings must be renovated and insulated to a certain level to effectively use a GSHP system[188]. Sufficient ground area and proper subsurface characteristics should be available for the ground heat source[189]. As a result, for densely populated urban areas, other heating systems could be more beneficial from an environmental and economic perspective. For example, heating using solar water heating, bio gas combustion or district heating systems are excellent alternatives[190]. Moreover, sufficient roof area should be available to install the PV system. The assumed PV systems sizes for the dwellings with GSHP are between 3.5 and 7.8 kWp. Assuming a 0.2 Wp/m^2 capacity factor, the required roof area are between 17.5 m^2 and 39 m^2. This could be a limitation in densely populated areas. Nevertheless, 2 million dwellings in the Netherlands are detached or semi-detached, that have a high prospective to install GSHP with sufficient roof space for a PV system. The annually avoided emissions for all these dwellings would be 4.8 Mt, reducing the total annual CO_2 emissions with 2.9% in the Netherlands[139].

Other cost reduction options excluded in this research are also available. The decrease of power flows by BESS could potentially reduce grid connection cost, yet a flexible or dynamic capacity tariff structure should be available to obtain monetary benefits[137]. In addition, BESS revenues can be increased by provision of energy arbitrage or frequency control restoration[38]. Also, collaborative planning and investing in PV, storage and GSHP systems is highly recommended to decrease cost.

5.5.3 Limitations and further research

Our research has several limitations that could affect the findings. We used data of 2 years thereby including the relative colder winter period of the beginning of 2015. However, future winters are expected to be warmer due to global warming[191]. This would lower heating demand, and therefore slightly reduce the investment attractiveness of GSHP systems. Moreover, annual electricity prices and emission factors were assumed, but future residential energy tariffs could change every 15 min due to an increased share of variable renewable energy generation.

It is expected that emission factors from power generation will have a higher variability due to the larger share of renewables. Avoided emission of PV systems could be lower when power of these systems will not replace fossil fuels. Consequently, storage is required to keep avoiding emissions, and could even

increase avoided emissions. Especially, when battery storage systems could discharge energy to the dwelling on moments when a large share of fossil fuel fired power plants are in the power generation mix. Therefore new battery control strategies should be developed that include the marginal emissions factors. Future research should focus on the role of marginal emissions factors and dynamic tariffs.

5.6 Conclusion

This study assessed the technical, economical and avoided life cycle GHG emissions of GSHP systems with PV and battery energy storage. We used measured data of 16 dwellings and assessed the performance over a 30-year lifetime.

Dwellings with a PV system show a SSR of around 31%, while the use of a GSHP system reduces this to 25%. PV can supply 19% of the total GSHP demand, while this can be increased to 29% using battery energy storage. Moreover, storage reduces the peak demand with 45% of dwellings with a GSHP, which enables more GSHP systems on the low voltage grid. The investment attractiveness for dwellings with a GSHP shows DPBPs between 19 and 34 years. PV and storage have significant lower DPBPs helping to reduce the overall systems DPBP.

Avoided life cycle GHG emissions from GSHP systems are between 31 and 59 tCO_2-eq for the 16 dwellings. The NPV increases with €275 per tonne of avoided emissions. Adding a PV system to the dwelling increases the average avoided life cycle GHG emissions with 30 tCO_2-eq. Also, this lowers the NPV increase per tonne of avoided emissions to €230. Battery energy storage only avoids emissions from a dwelling perspective. Therefore, storage is currently not recommended to reduce emissions since all PV electricity can be exported.

The sensitivity study provides recommendations to improve the investment attractiveness of GSHP systems. Policies should focus on higher natural gas tariffs or include CO_2 taxation to encourage less natural gas use and switch to GSHP systems. Also, additional GSHP investment subsidies combined with these policies show promising results to obtain economic feasibility investments in GSHP system.

Acknowledgements

This work is part of the research programme Transitioning to a More Sustainable Energy System (Grant No. 022.004.023), which is financed by the Netherlands Organisation for Scientific Research (NWO). We are grateful to Daphne Geelen from Enexis for providing data.

Appendices

5.A Input time series statistics

Technical and environmental performance statistics of the PV systems over the assessed lifetime are shown in Fig. 5.9. Used PV system capacities for dwellings without a GSHP have an average capacity of 3.3 kWp, varying between 1.7 and 4.9 kWp. Dwellings with GSHP have an average capacity of 5.9 kWp. The annual specific yield of the systems ranges between 791 and 886 kWh per kWp, with an average of 853 kWh per kWp. Note that this performance includes a 0.5% annual degradation. The PV systems show a good performance which is comparable with other Dutch PV systems[27]. GHG emissions are on average 67 gCO_2-eq per kWh for PV modules manufactured in China and 37 gCO_2-eq per kWh for PV modules manufactured in Europe.

Statistics of residential electricity consumption and contribution of the GSHP functions are given in Table 5.2. Annual average electricity consumption without GSHP is 3139 kWh, which corresponds to the average consumption of Dutch households[192]. The electricity consumption shows a relative large range, between 1557 kWh and 4727 kWh. This is mainly influenced by the household appliances and composition. Dwellings with GSHP show an average electricity consumption of 5920 kWh. The contribution of a GSHP shows a more narrow distribution, from 1933 kWh to 3760 kWh. GSHPs contribute to an average of 48% of the total electricity demand, ranging between 35% and 60%. The largest share of the GSHP consumption is used for space heating with an average of 27%. Cooling and standby consumption shows smallest shares of respectively 1.7 and 2.6%. The GSHP consumption is mainly influenced by space heating consumption, which has the largest range between a minimum share of 17.1% and a

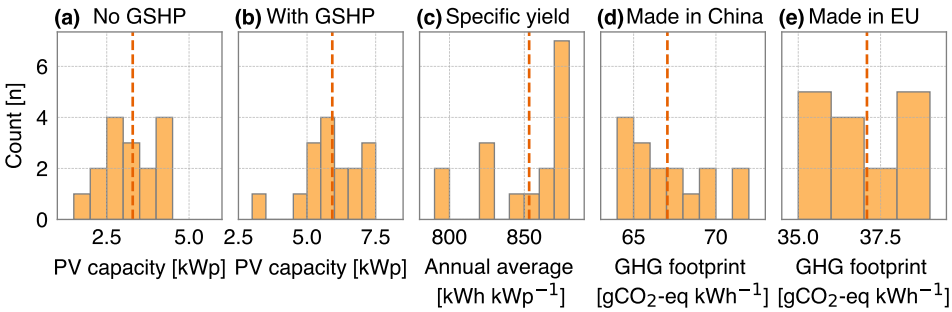

Figure 5.9 · Technical and environmental statistics of the PV systems used in our study. The distributions show the PV system sizes for dwellings without a GSHP (a) and with a GSHP (b) using bins of 0.5 kWp. Distributions of annual average specific yield over a 30-year lifetime of the systems are shown in (c) with bins using bins of 25 kWh per kWp. Distributions of GHG footprint of PV systems are given for systems made in China (d) and PV made in EU (e) using bins of 1 gCO_2-eq per kWh.

Table 5.2 · Annual electricity consumption statistics of the 16 dwellings included in this study. The absolute values are given in the left columns and the shares of the total is given in the right columns

	Average		Min		Max	
	[kWh]	[%]	[kWh]	[%]	[kWh]	[%]
No ground source heat pump	3139	52.4	1557	39.8	4727	65.4
Standby	150	2.6	97	1.2	212	4.1
Cooling	97	1.7	1	0.0	200	3.8
Domestic hot water	910	15.1	434	11.2	1944	24.8
Space heating	1623	28.1	1223	17.1	2270	41.1
Ground source heat pump	2780	47.6	1933	34.6	3760	60.2
Total	5920	100.0	3491	100.0	7824	100.0

maximum share of 41.1%.

The estimated natural gas consumption for DHW production and space heating is shown in Table 5.3. 17% of the natural gas consumption is used for DHW production and 83% for space heating. The total annual natural gas consumption is between 30 and 58 GJ, with an average of 42 GJ. This corresponds to an annual natural gas demand of 1490 m^3, which agrees with the average natural gas consumption of Dutch households[192].

The average stacked daily energy consumption of the 16 residential dwellings is shown in Fig. 5.10. The conventional electricity consumption is relative constant with an average of $\approx$ 9 kWh. The energy consumption for space heating shows a high volatility, related to the outdoor temperature. Cold winter days have the most significant impact on the variation in daily electricity consumption of the dwellings. Besides, the winter months of 2015 required more space heating than the winter months of 2014, due to lower temperatures. This shows the relevance of using multiple year consumption data for this type of research.

Distributions of hour of the day and monthly electricity demand from the 16 dwellings and from the specific GHSP functions are shown using a violin plot in Fig. 5.11. Conventional electricity consumption shows a clear trend with higher consumption during daytime and peaks between 5 until 6 pm. The consumption

Table 5.3 · Annual natural gas consumption statistics for the 16 dwellings used in this study. The absolute values are given in the left columns and the shares of the total is given in the right columns

	Average		Min		Max	
	[GJ]	[%]	[GJ]	[%]	[GJ]	[%]
Domestic hot water	7.3	17.3	3.5	11.5	15.6	35.1
Space heating	35.1	82.7	26.4	64.9	49.0	88.5
Total	42.4	100.0	30.4	100.0	58.1	100.0

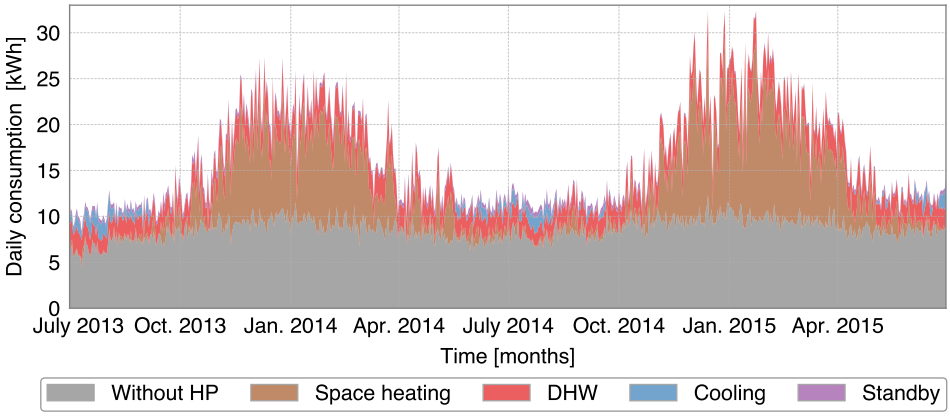

Figure 5.10 · Average stacked daily energy consumption of the 16 dwellings. The daily energy consumption of the 16 dwellings was selected from 1st of July 2013 until 30th of June 2015. The ground source heat pump consumption is separated into space heating, domestic hot water production, cooling and standby consumption.

of the GSHP shows a clear increase of consumption over all hours. The average standby consumption shows a small increase during daytime, indicating that the GSHP is less used for other functions during these moments. The cooling demand shows a decrease during daytime, and increases during night-time when residents are sleeping. Also, the dwellings are highly insulated and therefore the heating of the dwellings by the environments encounters a time lag. DHW and space heating have an order of magnitude higher demand than the standby and cooling consumptions. DHW electricity demand shows a low consumption during the night, and peaks in the morning and evening hours, mainly caused by showering. Space heating shows high demand during the night and decreases and low during daytime. The distribution range of electricity consumption for space heating and DHW is highly dependent on the dwelling and its residents.

The conventional consumption is quite constant over the months, whereas the heat pump consumption shows a seasonal effect. Higher consumption is seen by the cooling demand in the summer months, whereas space heating shows peaks in winter months. Standby consumption shows a small increase in the summer month, caused by the lower utilization of the heat pump system for other functions. The DHW demand shows a small increase of demand during winter months. The majority of electricity demand is caused by space heating which increases the overall demand of GSHP system in winter months.

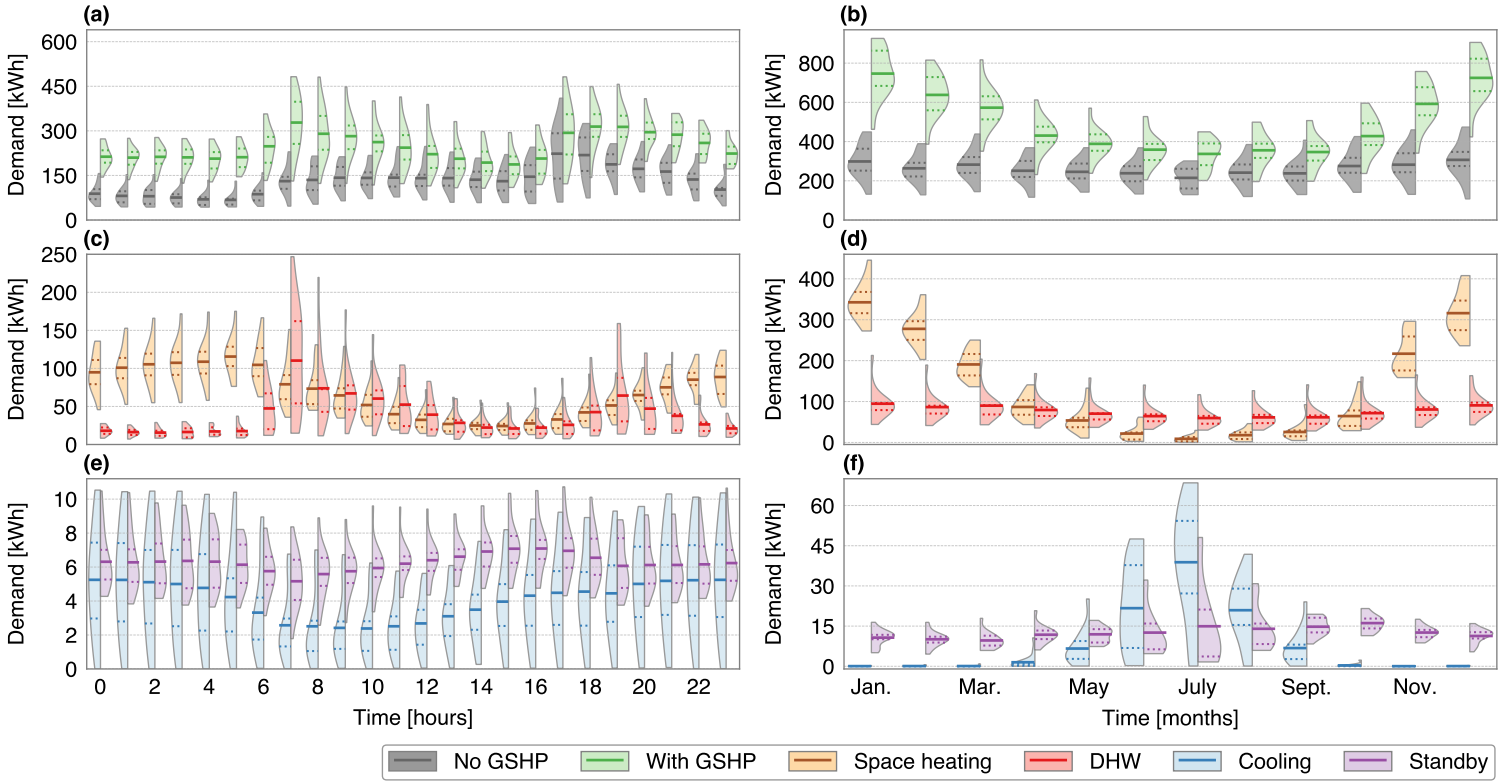

Figure 5.11 · Hour of the day (a, c & e) and monthly (b, d & f) electricity consumption distributions shown using violin plots. The distributions are split up in a left violin and a right violin, for example the top plots (a & b) show the conventional electricity demand at the left part of the violin and heat pump electricity demand patterns at the right part of the violin. The distributions contain the consumption of the 16 dwellings. Mean values of the distributions are marked by solid lines, and the 25% and 75% percentiles are indicated by the dotted lines.

5.B Explanation model input assumptions

This section provided an additional explanation of the input parameters used, also shown in Table 5.1.

PV system assumptions

Currently, net-metering policy is in place for residential PV systems. This policy enables system owners to offset the cost of electricity from the utility with their own generated PV electricity. Consequently, most system owners installed a PV system capacity that is able to cover the annual electricity consumption. Therefore, the installed PV system size was set to 1 kWp for each MWh of annual electricity consumption[154]. The electricity production of the PV system was reduced with 0.5% per year by PV system degradation[96]. PV system costs of 1500 €/kWp were assumed, including all components and installations[172]. In the Netherlands, value added tax (21%) of the PV system investment can be reclaimed, which results in a net investment cost of 1200 €/kWp. Annual maintenance cost (O&M) were set to 1% of the PV system investment costs[124]. The PV inverter is replaced after 15 years[93]. Replacement cost of the PV inverter are 100 €/kWp[172]. Emissions from manufacturing PV systems with multi crystalline silicon modules were expected to be 1590 gCO_2-eq for each Wp when made in China, and 824g CO_2-eq for each Wp when made in Europe[173]. Emissions from PV produced in Europe are significantly lower due to lower emission intensity of the European (ENTSO-E) electricity mix.

Battery energy storage system assumptions

The battery energy storage capacity was set to 1 kWh for each MWh of annual electricity consumption, based on previous research on optimal storage system designs for residential dwellings[93]. A commonly installed battery inverter rating of 0.5 kW per kWh of storage capacity was used[95]. Thus, two hours are required to completely charge the battery capacity from 0% until 100%. The battery state of charge (SOC) range was set between 0% and 100% of the battery storage capacity, so the full capacity potential could be assessed. A constant battery (direct current) DC-DC efficiency of 96% was assumed for battery charging and discharging, almost similar as the commercial available Tesla Powerwall[95]. The battery inverter efficiency curve from SMA Sunny Boy Storage was used to model the AC-DC and DC-AC conversion[94]. A BESS standby consumption of 0.1% of the rated inverter power was assumed. A battery cycle lifetime of 5000 full equivalent cycles and a calendric lifetime of 15 years were used based on a previous study[97]. We expected battery storage pack cost of 300 €/kWh and storage balance of system (BOS) and EPC (Engineering, Procurement, and Construction)

costs of 200 €/kW[122]. Annual maintenance cost (O&M) were set to 1% of the investment cost of battery energy storage system[124]. The battery inverter and battery cells are replaced after 15 years[93]. Replacement cost of the battery inverter is assumed 100 €/kW[172]. Replacement cost for the battery energy storage pack are 100 €/kWh, based on learning curves[39]. For the production of Li-Ion battery energy storage systems 110 gCO_2-eq for each Wh of Li-Ion storage was selected[175]. 124 gCO_2-eq was used for the production for each W of battery inverter, based on production requirements for a PV inverter[173].

Ground source heat pump system assumptions

A constant coefficient of performances was assumed based on the relative constant temperatures of the ground sources. A COP for space heating of 5.7 and a COP of 1.9 were assumed based on the technical specification of the heat pump[170].The largest cost component of a 4 kW GSHP is the drilling and installation of the vertical ground loop, which is estimated at €6000[176]. The EPC cost is expected to be €4000. The cost for the heat pump are estimated €1000 for each kW of nominal thermal output, thus euro 4000 for a 4 kW thermal unit[145].This results in a total of a GSHP of €14000 for the 4 kW unit. Heat pump systems in the Netherlands are subsidized depending on the thermal power and system type[148]. The investment subsidy for this system is €2800, which is similar to an investment subsidy of 20% of the total GSHP investment. Annual maintenance costs for GSHP are estimated 50% lower than the maintenance cost of CGB systems, specifically 50 €[177]. The lifetime of the heat pump is expected 20 years[145,177]. We expect that future heat pump costs will be reduced with 10% and that no subsidies can be used for the replacement of a heat pump. This results in heat pump replacement costs of 3600 €per unit[178]. Emissions for manufacturing, transportation and installation of the 4 kW GSHP are estimated to be 1760 kg of CO_2-eq per unit[143].

Condensing gas boiler assumptions

The efficiency of the condensing gas boiler depends on the required temperature of the heated water. These requirements are set similar as the temperatures delivered by the ground source heat pump system, specifically 28°C for space heating and 60°C for domestic hot water. Corresponding efficiency are 95% for space heating and 85% for domestic hot water[163]. The efficiencies are based on a higher heating value of Dutch natural gas of 35.17 MJ/Nm^3[193]. The cost of the reference residential CGB are €1500[140]. CGB have a lifetime of 15 years and a similar replacement cost of €1500 was selected. The CGB requires annual

services cost of €100 which is estimated based on the average service contract in the Netherlands for 2015[179].

Remaining systems assumptions

Costs of replacing components that are not mentioned above were included in the maintenance costs, as well as the EPC cost of replacing components. We assumed no salvage value for the system components. Also, we expect that emissions from manufacturing are 25% lower for the replaced components, except for the GSHP system. For this component we assumed 440 gCO_2-eq per unit since only the heat pump is replaced.

A discount rate of 2% was selected based on the currently low interest rates[125]. The consumption tariff was set to 0.178 €/kWh, based on the average household retail prices for electricity from 2014 until 2016[181]. The net metering policy in the Netherlands is currently in place and probably will be replaced with a feed-in premium by 2020. This feed-in premium will be gradually reduced from 0.12 €/kWh in 2020 to 0 €/kWh by 2036[182]. Next to the feed-in premium, residential consumers will receive a fee based on the wholesale electricity price. We assumed that this is similar as the expected wholesale electricity price. A linear increase from 0.032 €/kWh in 2020 until 0.044 €/kWh in 2030 was assumed, based on the wholesale market prices projections for 2030 in the Netherlands[194]. From 2030 onwards, we assumed a 0.5% increase for this wholesale electricity price. The natural gas consumption price was set to 21.84 €/GJ based on the average household retail prices for natural gas from 2014 until 2016[181]. An 0.5 % increase in gas and electricity tariffs was selected due to additional energy taxes for supporting investments of renewable energy generation[183]. An average CO_2 emissions intensity factor of 490 gCO_2-eq per kWh for 2016 was used[151]. A linear reduction of CO_2 emissions to zero in the year 2050 was assumed based on the Dutch energy agreement for sustainable growth[184]. The emission factor for natural gas is 56.6 kg CO_2/GJ using a low heating value of 31.65 MJ/Nm^3[195]. In this research we used the high heating value, thus the emission factor was converted to correspond with the HHV. This results in an emission factor of 50.93 kg CO_2/GJ.

5.C Detailed energy model algorithm explanation

The used energy model algorithm is explained with a schematic overview, shown by Fig. 5.12. Before the model algorithm is executed, the power export limit (P_{EL}) and power import limit (P_{IL}) were defined. These are pre-defined limitations for exporting and importing power respectively to and from the grid. These limits depend on the maximum peak shaving capacity of the battery storage systems. This depends on the used battery inverter rating and the battery storage capacity. The

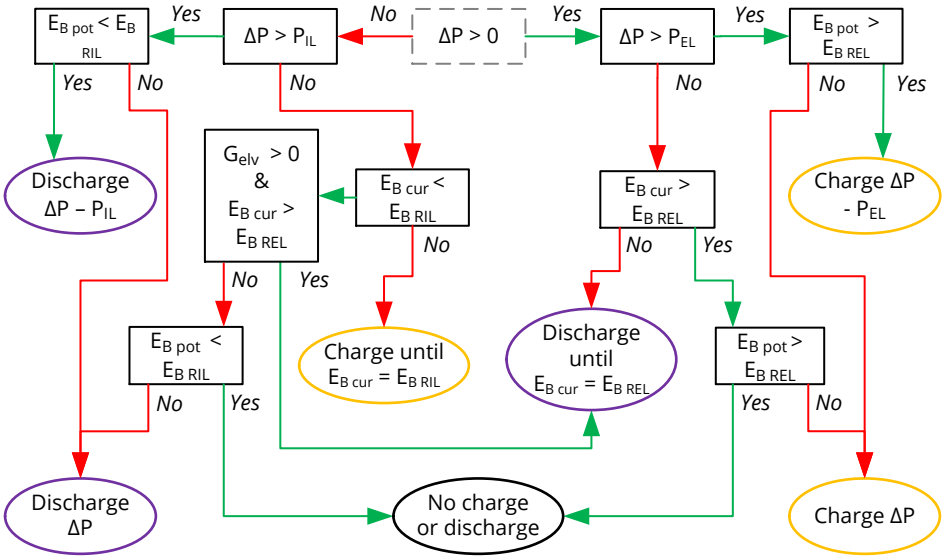

Figure 5.12 · Schematic overview of the energy model algorithm and the battery storage model steps.

5

inverter rating determines the maximum height of the peak that can be shaved. The storage capacity determines the maximum duration of the peak that can be shaved. The PV peak power and peak demand that could be stored by BESS was calculated for each day of a year. This calculation included pre-charging of energy to the battery to shave the demand power peak on a later moment. Also pre-discharging of energy to shave the PV production power peak was included. The power export and import limits were determined from the maximum PV peak and peak demand that could be stored.

Each model time step starts with the assessment or surplus of PV power is available or power demand from the building is requested, see grey rectangle with dashed lines. The difference between PV power and electricity demand is given by (ΔP). If more PV electricity is produced than consumed in the dwelling, then the power difference will be compared with the power export limit. When the power difference is larger than the export limit, then the potential SOC for the next time step ($E_{B\,pot}$) is determined. This depends on the current and expected charge potential for the next time step. The potential battery SOC is compared with the battery SOC reserved to charge the PV peak power that is larger than the export limit ($E_{B\,REL}$). The reserved amount of charged or discharged energy is limited by the maximum battery SOC ($E_{B\,max}$) and minimum SOC ($E_{B\,min}$), as well by the battery inverter rating.

If the potential SOC is higher than the reserved SOC for PV peak charging, then the battery will only charge the PV peak difference. Else, the battery inverter will

charge all surplus PV electricity. If ΔP is smaller than (P_{EL}), then the battery SOC reserved for PV peak charging is compared with the current SOC ($E_{B\,cur}$). When the current SOC is larger, then the battery is discharged until the current SOC is similar as the reserved SOC for PV peak charging.

When more electricity is consumed than produced by the PV system, then ΔP is compared to the power import limit (P_{IL}). When this limit is smaller, then the potential SOC for the next time step is determined, which in this case depends on the current and expected discharge potential. The potential SOC is compared with the battery SOC reserved to discharge the peak demand ($E_{B\,RIL}$). If the potential SOC is lower than the revered SOC, then the battery will only discharge the peak demand. Else, the battery inverter aims to discharge all required electricity. If P_{pot} is smaller than P_{IL}, then the battery SOC reserved for load peak discharging is compared with the current SOC $E_{B\,cur}$. When the current SOC is below the reserved SOC level, then the battery is pre-charged until the reserved SOC is reached. If the current SOC is larger than the reserved SOC level, then the model assesses or pre-discharging is required to charge PV peaks on later moments. This is conducted when the solar elevation (G_{elv}) is >0° and if the current SOC is larger than the revered SOC for PV peak charging $E_{B\,REL}$. The model time step ends with an action to charge, discharge or do nothing. Afterwards the algorithm continues to the next time-step, back to the assessment of P_{pot}.

The model behaviour for a summer and a winter day is graphically explained in Fig. 5.13. The 13th of June has a larger forecasted PV production than a forecasted electricity consumption. Consequently, battery storage capacity is reserved to charge the excess PV power peak, visualized by the reserved capacity to reduce the exported peak power ($E_{B\,REL}$). To obtain this reserved capacity, a small amount of storage is discharged to the grid in the early morning around 6.00. Consequently PV peak production is used for charging and stored in the battery. The battery is fully charged at 15.00, and discharged later in the evening and night. The 14th of June has less PV production forecasted, therefore a lower amount of capacity is reserved for PV peak shaving. No electricity from the grid was used during these two summer days.

The winter days show a different consumption pattern with significantly higher electricity consumption by the GSHP, mainly used for space heating. A demand power peak is forecasted around 12.00 on 14th of December. Consequently, battery energy storage is required to supply this demand peak. The battery storage is pre-charged on 13th of December to provide the peak demand of the next day. The small amounts of PV produced electricity are directly used or stored.

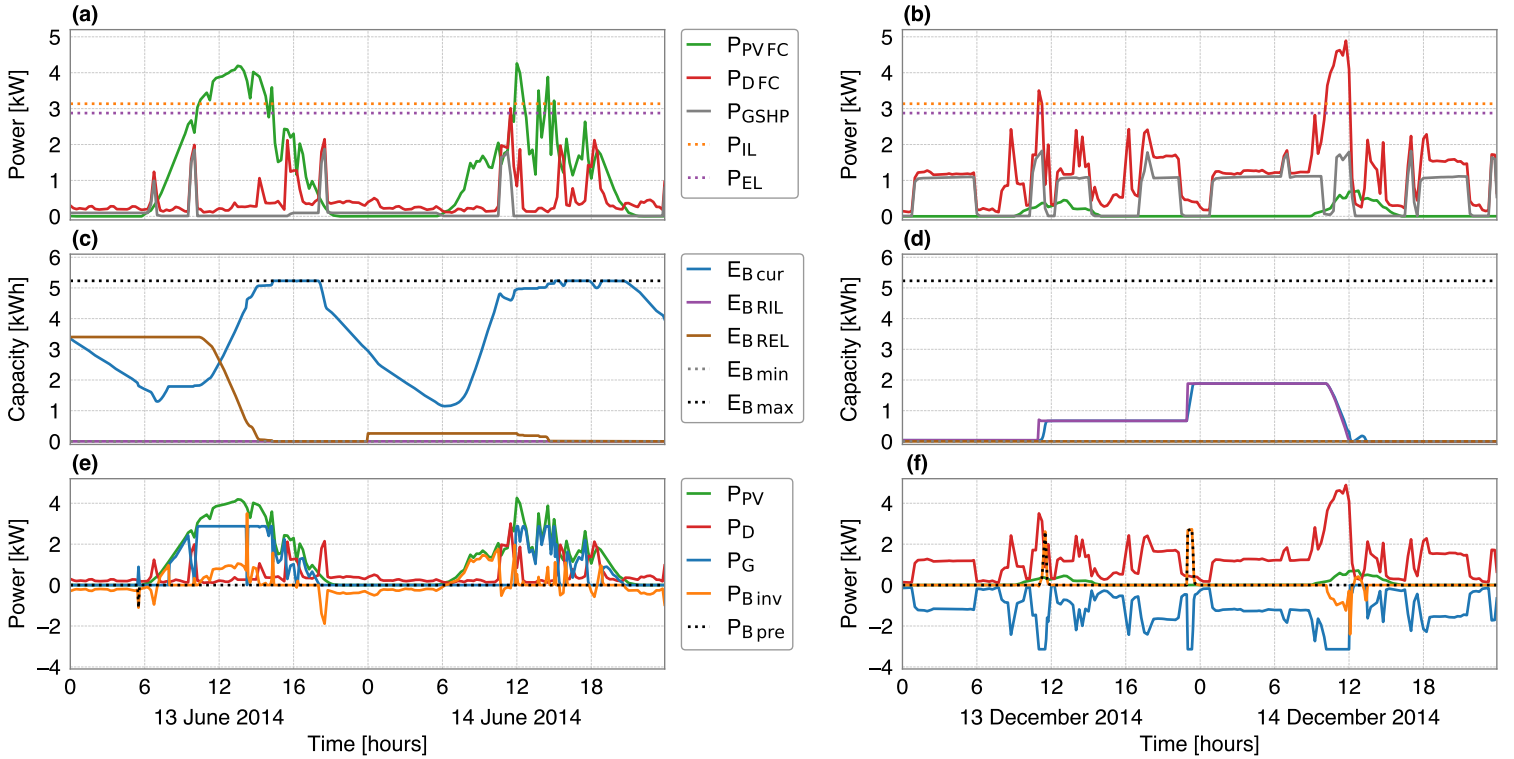

Figure 5.13 · Example of the behaviour of the battery control strategy for two summer and two winter days on a residential dwelling with GSHP, PV and battery storage installed. The left graphs (a, c & e) show the strategy for two days in the summer and the right graphs (b, d & f) for two days in the winter. The top graphs (a & d) show the forecasted PV production ($P_{PV\,FC}$) and electricity consumption ($P_{D\,FC}$) with the predicted import and export power limits. Besides the electricity consumption of the GSHP (P_{GSHP}) is shown. The middle graphs (c & d) displays the actual battery state of charge and the reserved state of charge for the imported and exported electricity. The bottom graphs (e & f) shows the power flows to the grid (positive) and from the grid (negative). In addition, the battery charge (negative) and discharge (positive) power flows and the pre-charged power flows are given. The annual electricity consumption of this dwelling is 5.23 MWh. A PV system size of 5.23 kWp and a battery storage capacity of 5.23 kWh with an inverter capacity of 2.62 kW were used.

5.D Impact of PV and storage capacity

Self-sufficiency impact

Self-sufficiency ratios and specific self-sufficiency ratios for smaller and larger PV systems and storage capacities are shown in Fig. 5.14. Self-sufficiency ratios are increasing with larger PV system capacities. A higher SSR is observed for dwellings without a GSHP than dwellings with a GSHP. The influence of the individual demand pattern on the SSR decreases with larger PV system capacities. Furthermore, the distribution range increases due to the larger influence of the demand patterns on the SSR. Battery energy storage results a larger increase in SSR for bigger PV systems than for smaller PV systems. A 1 kWh storage system increases

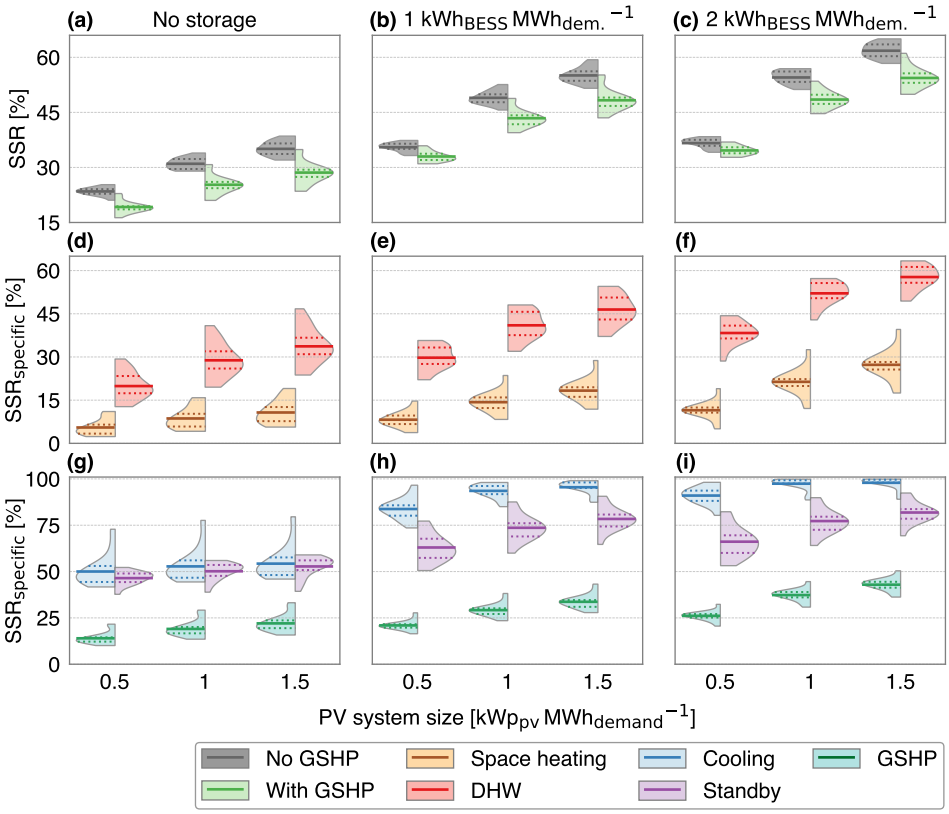

Figure 5.14 · Distribution of the impact of PV and battery energy storage on the self-sufficiency of the dwellings and the specific GSHP functions, shown using a violin plot.The distributions of dwellings without a ground source heat pump and with ground source heat pump are shown in the top row (a, b & c). The distributions are shown for three PV system sizes, and scaled with the annual electricity consumption. Specific self-sufficiency ratios are given for the domestic hot water and space heating (d, e & f) and for standby, cooling and the total GSHP consumption (g, h& i). Mean values of distributions of the 16 systems are indicated by solid lines, and the 25% and 75% percentiles by dotted lines.

the SSR with 14% for a 0.5 kWp PV system with GSHP. This increase is 20% in SSR for a 1.5 kWp PV system with GSHP. Larger storage sizes, of 2 kWh per MWh of annual demand, increase only the SSR of PV systems with a capacity of 1 or 1.5 kWp.

The specific self-sufficiency ratio of space heating is relatively low compared to the other GSHP consumption components. PV production occurs mainly in the summer months, whereas most space heating demand request occurs in the winter months (Fig. 5.11). A 1 kWh storage system does not show a slightly improvement of the SSR. Specific SSRs for domestic hot water are significant larger than space heating and go up to 58% with a 1.5 kWp PV system and a 2 kWh storage system. DHW production occurs largely during evening hours, which makes storage ideal to improve SSR. Cooling demand occurs in the summer months, and thus shows the highest specific SSR. Also, cooling reaches the highest specific SSR when storage is deployed.

Grid impact

The impact of smaller and larger storage capacities on the maximum import peak, maximum export peak, import peak to average ratio and export peak to average ratio are shown Fig. 5.15. Also three other indicators are presented. The pre-charged percentage shows the ratio of energy that is charged in the battery used for demand peak provision to the total charged energy. The pre-discharged percentage shows the ratio of energy used to discharge the battery for PV peak storing to the total discharged energy. The curtailment loss ratio (CLR) is an indicator of the share of PV energy which cannot be exported due to a potential future feed-in limit. This is the PV energy above a certain feed-in limit divided by the total produced PV energy. The PV feed-in limit is given in kW per kWp of installed PV capacity.

With a 2 kWh storage capacity, the import peak for dwellings without GSHP is reduced to an average of 2.8 kW and with a GSHP to 3.1 kW. The reduction using a 1 kWh storage capacity is larger for dwellings with GSHP than dwellings without, yet the opposite is shown for smaller and larger storage sizes. For smaller storage sizes, the absolute storage size for systems with a GSHP are larger, hence more peak demand can be shaved. For larger storage sizes, the peak demand reduction of dwellings with a GSHP is already reaching a limit. This limit is due to the width of the peak, which is increasing significantly when the peak is further reduced. IPAR for dwellings without a GSHP is greatly reduced with storage, from 15.0 with no storage to 8.1 with 2 kWh of storage. Dwellings with a GSHP show a smaller reduction, from 8.1 to 3.8. The pre-charged distribution shows an average value of around 0.3% for a 2 kWh storage capacity.

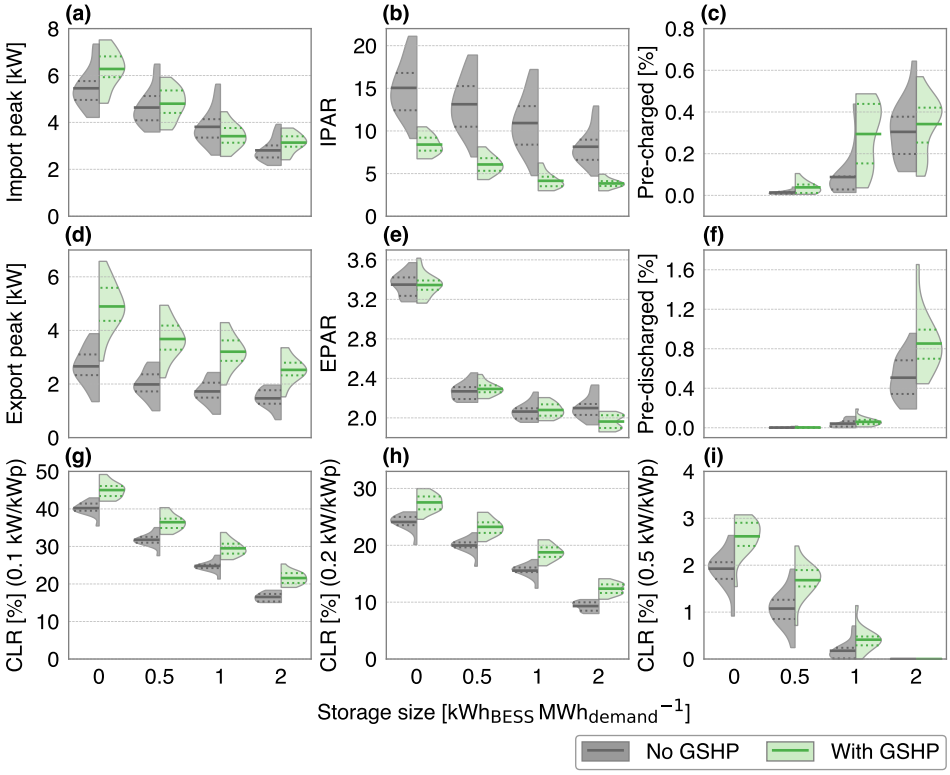

Figure 5.15 · Distribution of the influence of battery storage capacities on lowering demand power peaks from the grid and reducing PV peaks to the grid. The reduction of the demand peak on the grid is given by the import peak (a), import peak to average ratio (b), pre-charged ratio (c). The reduction of the PV system peaks on the grid is shown using the export peak (d), export peak to average ratio (e), pre-discharged ratio (f). The impact of storage on the curtailment loss ratios for potential feed-in limitations are shown for a 0.1 kW/kWp feed-in limit (g), a 0.2 kW/kWp feed-in limit (h) and a 0.5 kW/kWp feed-in limit (i). Distributions are shown for dwellings without and with a heat pump. A normalized PV system size of 1 kWp$_{pv}$ for each MWh$_{demand}$ was selected. Note that the battery storage capacities are not equally dispersed.

The export peaks are reduces in a similar way for both dwellings without and with a GSHP. A remarkable increase in EPAR from a 1 kWh battery to a 2 kWh battery is observed for dwellings without GSHP. Larger storage capacities reduce the peak PV power, but also reduce the average exported power, since more electricity is used for self-consumption. If the average power is reduced more than the peak power, then a higher EPAR occurs. A significantly higher percentage of a 2 kWh battery storage capacity is pre-discharge for dwellings with GSHP than dwellings without GSHP. Dwellings with GSHP have a relative higher storage capacity since their electricity consumption is larger. Consequently, more energy is still stored in the battery before the next morning, especially in the summer months with relative low night consumption from the GSHP. As a result, more electricity

is pre-discharged which is required to obtain empty storage capacity for PV peak charging.

The curtailment loss ratios are shown for three potential PV feed-in limitations. CLR are higher for dwellings with a GSHP then systems without. The most restricted feed-in limit (0.1 kW/kWp) shows an average PV energy loss of 40% without GSHP and 45% with a GSHP. With a 2 kWh storage capacity, this can be reduced to 17% and 22% for respectively dwellings without and with a GSHP. Moreover, with a feed-in limit of 0.5 kW per kWp, a 2 kWh storage capacity can almost completely abolish the potential curtailment losses.

Impact on discounted payback periods

The impact of smaller and larger PV system and battery storage capacities on the discounted payback periods is presented in Fig. 5.16. DPBPs for dwellings without GSHP are in increasing with PV system size when no storage is used. Dwellings with GSHP show a slight reduction in average DPBP with an increase of PV capacity. The results also show that storage systems are not profitable under all scenarios. If a storage system is added, then it should be designed based on the installed PV capacity. If the PV system size is relative small, then an oversized storage capacity will greatly increase the DPBP.

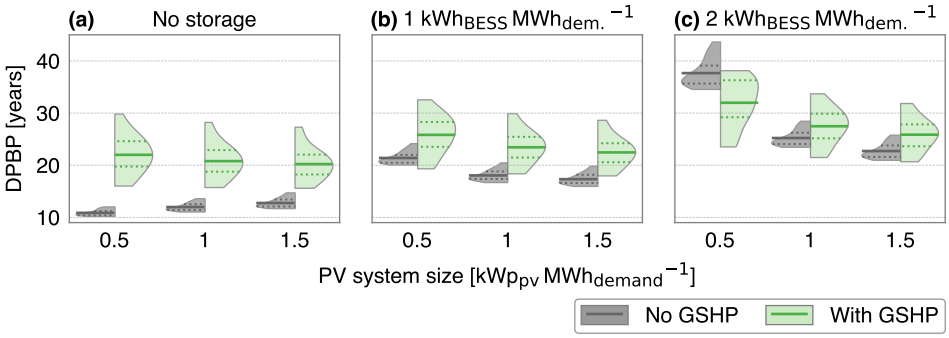

Figure 5.16 · Distribution of the impact of PV system capacity and battery energy storage capacity on the discounted payback periods of 16 dwellings.

Impact on avoided life cycle GHG emissions

The avoided life cycle GHG emissions from an electricity system perspective and dwelling perspective for smaller and larger PV system and storage capacities are presented in Fig. 5.17. Avoided emissions from an electricity system perspective increase linearly with larger PV system capacities, but also show a small decrease with bigger storage capacities. Emissions from a dwelling perspective show a different behaviour. When no storage is included, then larger PV systems lead to a reduction of avoided GHG emissions. With storage, the largest emission reductions are obtained with a 1 kWp PV system. This is especially visible for a 2 kWh storage capacity per MWh demand. Smaller PV systems have a higher direct self-consumption, therefore the avoided emissions with self-consumption by storage are lower. Larger PV systems have much more electricity production resulting in more storage and avoided emissions. However, these larger PV systems (2 kWp) also have higher emissions from manufacturing, which results in lower net avoided emissions compared to a 1 kWp PV system.

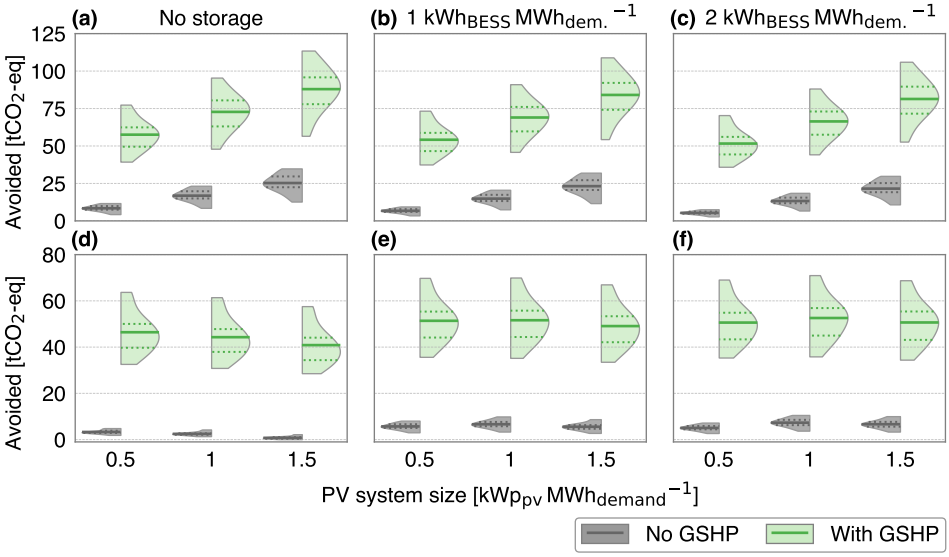

Figure 5.17 · Distribution of the impact of PV and battery energy storage on the avoided life cycle GHG emissions from an electricity system perspective (a, b & c) and from a dwelling perspective (d, e & f) of the 16 dwellings. The distributions include 16 dwellings and are shown for three PV system sizes, and scaled with the annual electricity consumption.

5.E Extended sensitivity analysis on the discounted payback period

The combined impact of a change in natural gas tariff and a change in electricity tariff is presented in Fig. 5.18. A combined increase in electricity tariff and decrease in natural gas tariff results in a rapid increase of DPBP. An annual increase of 1.4% in electricity tariff shows an average DPBP of the GSHP of 35 years. Yet, a 2.2% annual increase in natural gas tariff decreases the average DPBP of the GSHP of 20 years. The change in electricity tariff has a lower influence on dwellings with only a PV system than for dwellings with PV and storage. The average DPBP of the latter system will be lower than 15 years with an electricity tariff increase of 2.9% per year. The value of self-consumption increases with higher electricity tariffs, thus the revenues of storage are higher. Lower electricity tariff are positive for GSHP payback periods, but negative for PV and battery storage payback periods. Consequently, GSHP combined with PV and storage level out the influences of higher or lower electricity tariffs, as can be seen in subplot (c).

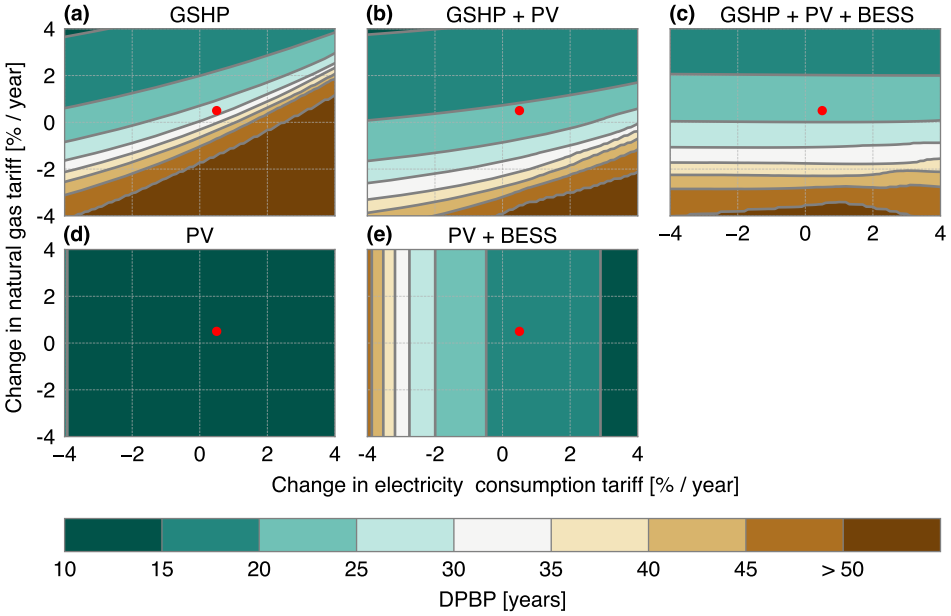

Figure 5.18 · Extended analyses on the impact of electricity consumption tariff and the natural gas tariff on the average discounted payback period of the 16 dwellings for 5 system configurations. The red dot indicates the reference scenario value.

The influences of a higher GSHP investment subsidy combined with four other parameters are shown in Fig. 5.19. The combination of a higher GSHP investment subsidy and a decrease in natural gas tariff show a strong reduction in DPBP. For example, a 10% increase in subsidy combined with a natural gas tariff increase of 1.3% results in average DPBP of 20 years. Also, the combination with CO_2 taxation is promising to obtain lower DPBP. With a significantly increase in investment subsidies, higher discount rates and electricity tariffs become feasible to obtain DPBP below 25 years.

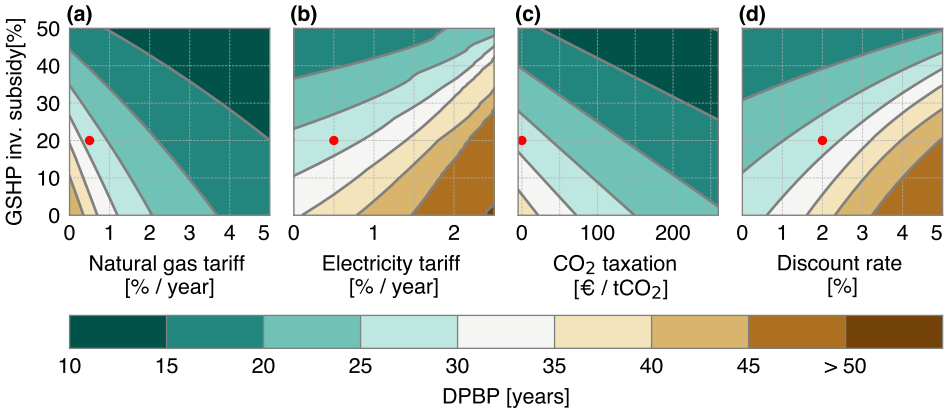

Figure 5.19 · Extended analyses on the impact of the GSHP investment subsidy combined with the impact of the natural gas tariff (a), the electricity gas tariff (b), the CO_2 taxation (c) and the discount rate (d) on the average discounted payback period of the 16 residential dwellings with a GSHP system only. The red dot indicates the reference scenario value.

6

Spatio-temporal model for PV integration

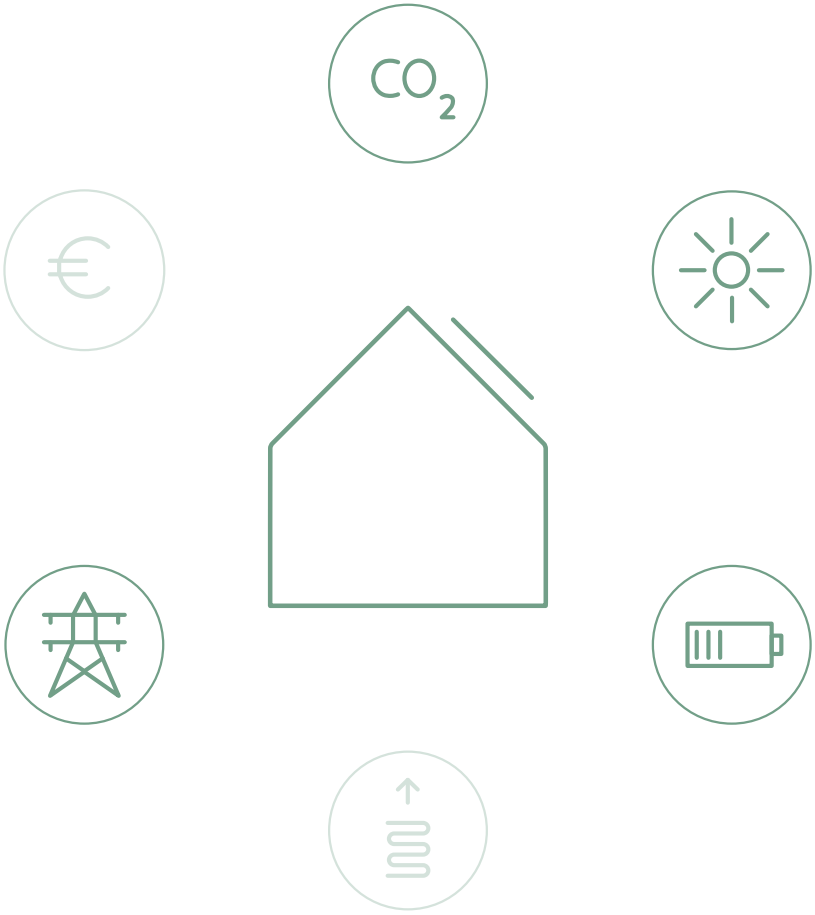

This chapter is based on the publication: G.B.M.A. Litjens, B.B. Kausika, E. Worrell and W.G.J.H.M. van Sark. "A spatio-temporal city-scale assessment of residential photovoltaic power integration scenarios". in: *Solar Energy* **174** (2018), pp. 1185-1197. DOI:10.1016/j.solener.2018.09.055

Abstract

Cities have a significant potential to host residential photovoltaic systems (PV). The direct consumption of PV generated electricity reduces the need for electricity import, while excess PV electricity production can be stored for later usage or can be used directly to charge electric vehicles (EVs). In this way, more energy is locally consumed, greenhouse gas emissions are reduced, and self-sufficiency of cities can be increased. In this paper, we present a spatio-temporal framework to evaluate the electricity demand that can be fulfilled by PV energy. We assess the impact of penetration of EVs and the influence of battery energy storage. We demonstrate the usefulness of this framework for 88 neighbourhoods in the city of Utrecht, the Netherlands. Spatial mapping was used to identify areas with high potential for EVs and storage. Results shows that direct PV self-consumption ratios vary between 34% and 100%. When EVs charging is included in the neighbourhoods, then self-consumption is increased on average by 12%. Battery energy storage increases self-consumption on average by 25%. The self-sufficiencies due to direct PV energy consumption are between 6% and 40% in the neighbourhoods. These are decreased by EVs with an average of -0.6%, and increased by battery energy storage with an average of 14%. Avoided life cycle greenhouse gas emissions over a 30-year period are on average 12 tCO_2-eq per address. The large variation in results between neighbourhoods indicates that area dependent investments and supporting policies could improve the PV power integration in cities. Our developed framework can be easily adapted and used for other cities. Moreover, our results are useful for local governments to guide and design effective policies to accelerate the transition to more sustainable cities.

6.1 Introduction

Currently, cities host more than 50% of the global population and account for 70% of the global greenhouse gas (GHG) emissions[196]. One of the solutions to reduce CO_2 emissions from cities is the deployment of residential solar photovoltaic (PV) systems. Yet, PV system installation may be limited due to lack of suitable space. An added difficulty is the daily power fluctuation of the solar resources. This results in export of surplus PV electricity during daytime from cities and requires import of electricity during night time. Shifting energy demand to daytime results in higher PV self-consumption within cities and reduces CO_2 emissions from fossil-based backup power generation[13].

The use of battery energy storage systems (BESSs) allows storage of surplus PV electricity to be used at later moments. The cost of BESSs is rapidly decreasing due to their increasing deployment[39]. Currently, the number of electric vehicles (EVs) is rapidly increasing in the Netherlands, which increases the electricity demand within cities[133,197]. BESS and EVs are becoming more economically attractive, especially due to cost reduction of Li-ion storage technology[198]. Furthermore, EV costs are decreasing as a result of economic scaling effects. A shift from a gasoline-based car fleet to electric vehicles reduces emissions and air pollutants considerably, thereby contributing to improve air quality and quality of life in cities[30,199].

Due to increased deployment of PV, EVs and domestic electric heating, it is expected that more overloading will occur on the medium voltage grid than on the low voltage grid,[200]. Consuming more PV generated electricity in the city can lower medium voltage distribution grid losses and reduces investments in cables and transformers. Smart EV charging and battery energy storage help to increase urban PV self-consumption[201]. For all these benefits, enhancement of PV self-consumption is seen as an important accelerator to reach a higher share of domestic PV installations and at the same time contribute to a reduction in greenhouse emissions[47].

6.1.1 Literature review

Commonly, spatio-temporal PV potential in urban areas is assessed using geographic information systems (GIS) combined with numerical solar irradiation algo-rithms[202,203]. PV integration studies focus mainly on using the generated PV electricity directly within the buildings or on community scale[103,204]. Some studies combined the PV integration assessment with local or regional energy demand. Most of these studies assessed the provision of the net electricity consumption on an annual basis. A study assessed the potential of PV systems on rooftops and facades of 27 European countries. They found that the produced

PV energy could provide in 22% of the projected 2030 annual electricity demand for these countries[205].

A spatial model concluded that 2/3 of the current electricity demand could be covered by PV production for a small city in eastern Slovakia[206]. Of all the municipalities in Germany, 30% could be net self-sufficient when the full residential roof potential was used[207]. In another study involving 34 German municipalities, it was found that 77% of the net electricity consumption could be provided by PV[208]. Furthermore, rooftop PV systems could provide 25% of the total annual electricity demand in Switzerland[209]. A study including a municipality in Sweden found that 88% of the annual demand can be provided with PV. Yet over 3000 hours a year have more PV production than demand[210]. A study of a city in Chile found that 24% of actual demand could be provided by PV, with the main limitation being the infrastructure of the grid[211].

Few studies included temporal (hourly, daily) factors to assess the spatial potential of PV systems. A real-time platform containing a PV simulator and a distribution network simulator was presented and tested for the city of Turin, Italy. It was found that the actual distribution grid was not adequate to accommodate all PV generated electricity, if the available rooftop surface would be fully used[212]. A PV penetration level of 40% was found for a German rural municipality to achieve a high PV self-consumption level[213]. Another spatio-temporal model analysed the impact of electric vehicles on the urban distribution network. This model provided insights in the critical local grid components that require upgrades for larger shares of electric vehicles[214]. Only 27% of the electrical vehicles that are not in transit, are required to store excess PV produced power produced for the city of Yokohama, Japan[215].

6.1.2 Research aim

A limited number of studies are available that include both spatial and temporal effects of PV system integration. Furthermore, no research was found that assessed the spatial and temporal influence of electrical vehicles and storage on the PV self-consumption and PV self-sufficiency, except for a Dutch study with very coarse spatial resolution[197].

Therefore, this research aims to assess the role of EVs and BESSs for the PV self-consumption potential of a city. We developed a spatio-temporal framework that uses models to estimate the potential of PV yield, battery storage systems and electric vehicles. We demonstrate the framework using the city of Utrecht (the Netherlands) as a case study. The PV yield potential was assessed using the rooftop area of all residential buildings of this city. A time resolution of 5 min was used to assess the self-consumption and self-sufficiency potential at a

neighbourhood level, over a 30-year lifetime. Neighbourhoods were identified that have surplus PV production to store in BESSs or charge EVs, or have limited PV yield production due to roof space limitations. Furthermore, we estimate the avoided life cycle GHG emissions due to PV electricity from two perspectives.

This study also includes socio-economic factors, e.g. household statistics and current number of cars in a neighbourhood. Two EV charging algorithms were incorporated, i.e., normal (uncontrolled) charging and smart solar charging. The latter charging method aims to charge EVs at moments with surplus PV power enhancing PV self-consumption. The results on each neighbourhood give information on the potential usage of the transformers within these neighbourhoods. The area of buildings connected to the transformers usually does not cross the borders of the neighbourhood. As a consequence, obtained results are valuable for distribution system operators (DSOs) to plan grid extensions and EV charging infrastructure. Furthermore, the results help local governments to design realistic and effective policies to develop carbon-neutral cities. The developed methodology can be modified and used for other cities and regions.

This study is arranged as follows. Section 6.2 explains the spatio-temporal framework and the used technical and environmental performance indicators. Section 6.3 presents the spatial results for the 88 neighbourhoods using maps of the city of Utrecht, the Netherlands. Section 6.4 assesses the sensitivity of the rooftop utilization rate, EV smart solar charging shares and battery storage capacities. Limitations concerning assumption, data availability and implementation challengers are discussed in section 6.5 and the paper finalises with key conclusion in section 6.6.

6.2 Methods

6.2.1 Spatio-temporal framework

A spatio-temporal framework was developed to combine spatial and temporal parameters. An algorithm was developed that combines time and location of PV production with time and location of electricity demand in the city. The main inputs of this algorithm are two time series for each neighbourhood: PV yield and total electricity consumption. The latter time series consists of the electricity consumption profile of buildings, with and without the consumption profile of electric vehicles. Both PV production and consumption time series are used in algorithms that determined self-consumption ratios and self-sufficiency ratios over a lifetime of 30 years. An EV charging algorithm and BESS charging algorithm are used to assess the impact of EV and storage. An overview of the spatial level of

the input data and model steps is shown in Fig. 6.1. We used reference parameters to compare the spatial self-consumption and self-sufficiency influence of the neighbourhoods, see Table 6.1. Also, the avoided life cycle GHG emissions from the PV systems are determined.

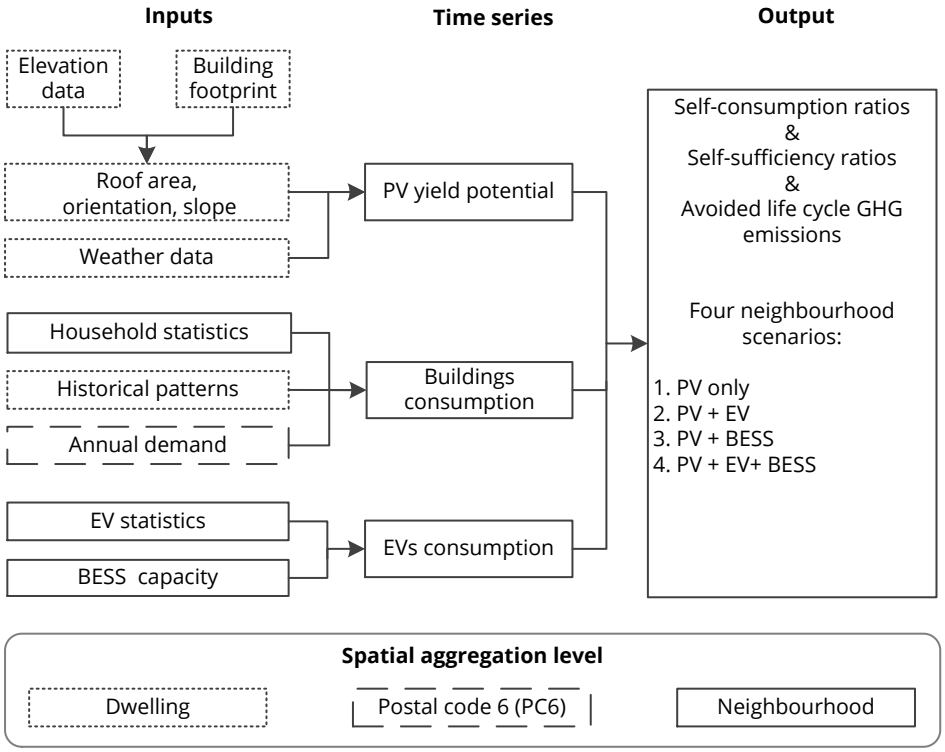

Figure 6.1 · Overview of the input data and model steps with corresponding spatial level to model the self-consumption ratios, self-sufficiency ratios and avoided life cycle greenhouse gas emissions for four scenarios

Table 6.1 · Main reference model input parameters.

Reference parameter	Value	Unit
PV capacity	200	Wp/m^2
Rooftop utilization factor	50	%
EV constant charging share	75	%
EV smart solar charging share	25	%
Relative battery storage size	1	$kWh_{BESS}\ MWh_{demand}^{-1}$
Relative battery inverter rating	0.5	$kW/kWh_{BESS}\ MWh_{demand}^{-1}$

The impact of the PV system potential on these parameters was assessed using four scenarios in the following sections:

- Neighbourhoods with PV systems only
- Neighbourhoods with PV systems and EVs
- Neighbourhoods with PV systems and BESS
- Neighbourhoods with PV systems, EVs and BESS

The framework was implemented using the city of Utrecht in the Netherlands. This city (latitude 52°05'38" North, longitude 5°05'12" East) is the fourth largest city in the Netherlands with 340,000 inhabitants. The city of Utrecht consists of 10 districts which make up 99 neighbourhoods. Neighbourhoods with 250 addresses or less were excluded from the analyses since these are mainly industrial or rural areas. As a result, 9 districts and 88 neighbourhoods were selected for the study. Each neighbourhood is made up of smaller areas that are specified by a postal code 6 (PC6) level. A total of 63,494 buildings containing 132,671 residential addresses were used in the study. The distribution of buildings per PC6 area and within each neighbourhood is shown in Fig. 6.2. The majority of PC6 areas consist of a single building. The number of buildings within each neighbourhood shows a large variation.

6.2.2 PV yield potential

Roof statistics

The first step to assess the PV potential is the calculation of the roof statistics for each of the 63,494 buildings. The rooftop statistics consist of the roof area, orientation (azimuth and tilt) and the incoming plane of array (POA) irradiance. The

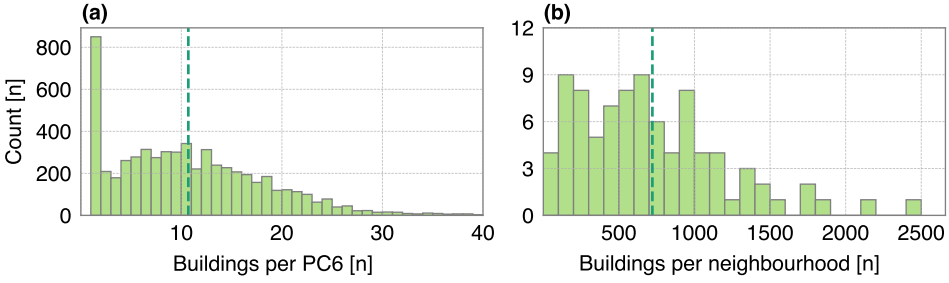

Figure 6.2 · Distribution of buildings containing residential addresses within each postal code 6 areas (a) and distribution of these buildings within each neighbourhood (b), both shown using a histogram. Mean values of the distribution are indicated by the dashed lines. Histogram bins of 1 building per postal code 6 and 100 buildings per neighbourhood were used. Note that 50 postal code 6 areas have more than 40 buildings and are not shown in histogram (a).

incoming POA irradiance was determined using the Area Solar Radiation Tool of the ArcGIS Spatial Analyst[216]. The Area Solar Radiation tools calculated the POA irradiation across areas based on the hemispherical viewshed algorithm. These tools were developed by[217] and further refined by[218].

The Area Solar Radiation tools calculations require a building footprint layer and a digital elevation model (DEM). The building footprint layer for the city of Utrecht was obtained from the Basisregistratie Adressen en Gebouwen (BAG) provided by the Dutch Cadastre, Land Registry and Mapping Agency[219]. The DEM was derived from high resolution elevation data, which was obtained from the Actueel Hoogte Bestand Nederland[220]. The DEM has a spatial resolution of 50 cm and was used as main input in the solar radiation tools. The roof area, slopes and azimuths for each rooftop were calculated in GIS based on the DEM.

The default settings of the Area Solar Radiation Tool model were used containing the following default settings[216]. The latitudes for the buildings were calculated automatically based on the DEM metadata. Skysize was set to 200 and proved to be sufficient for time interval of 14 days. Horizon angles (number of calculation angles) are set to 32 which is adequate for complex topography. Diffusivity was set at 0.3 and transmissivity at 0.5 which is an indication of generally clear sky conditions. Using a fixed atmospheric value does impact the irradiation output on a smaller time scale (days or weeks). We observed that standard factors were sufficient to achieve a good fit with the measured values from the closest meteorological station (Royal Netherlands Meteorological Institute KNMI in De Bilt, The Netherlands).

The calculation took into account the effect of shadow due to nearby buildings, trees, and other roof obstacles like chimneys or gable style roofs. The digital surface model has been used as input for these calculations. The POA irradiation for each roof surfaces was calculated for the year 2015, with a 14 day interval. This time interval is used to calculate the sky sectors for the sun map (the sun's position in the sky across a period of time). These maps are used to calculate the total POA irradiance for a particular roof.

PV yield time series

The second step to determine the PV yield potential was to create a PV yield time serie for each of the assessed rooftops. Buildings with addresses that have a residential function were selected from the building footprint layer. If a building contained only residential users than the full roof area was selected. However, some buildings have addresses with different functions, for example an office,

shop or residence. For these buildings, the share of used surface for each function was obtained from the BAG dataset. The residential rooftop share was multiplied with the total roof area to define the roof area allocated for residential PV systems. We assumed that a maximum of 200 Wp/m^2 could be installed, based on a commercial available 320 Wp module with a dimension of 1.6 m by 1 m.

The PV yield timeseries was created using the open source Python package PVLIB[61]. The roof surface azimuth and tilt angles from the GIS model were binned to obtain 35 different combinations of roof slope and orientations. The roof surface azimuth angles were binned in steps of 45°, and roof slope angles in bins steps of 20°. A maximum tilt angle of 82.5° was selected. Facades were not included in our study. Furthermore, we assume that flat roofs will have a dual-tilt (or east-west) designed PV systems with a slope of 10°.

Radiation, wind speed, pressure and temperature data were obtained for 2015 from the Royal Netherlands Meteorological Institute KNMI in De Bilt, The Netherlands. The measurement intervals of radiation were 10 min and one hour for remaining weather parameters. The weather data is linearly interpolated to 5 min interval and used as input for the PVLIB model. Furthermore, the module parameters of the Sanyo HIP-225HDE1 PV module are used to model the direct current (DC) PV yield time series[62]. This module has a relative low temperature coefficient temperature thus reducing the influence of temperature in the model. The DC time series were converted to alternating current (AC) time series using the efficiency parameters of the Enphase Energy M210 inverter[63]. The AC time series were linearly scaled to obtain a performance ratio of 85%, which is consistent with well performing PV systems in the Netherlands[27].

Also, the PVLIB model calculate the total POA irradiance from the solar radiation data (no shading conditions). This number is used to determine the shade loss factor for each rooftop. This is the POA irradiance with shading (determined by the Area Solar Radiation tools) divided by the POA irradiance on a surface with no shading (determined using PVLIB). An average shade loss factor of 83% was found for all residential buildings. The shade loss factor was multiplied with the AC PV yield time series to determine the PV yield under shaded conditions.

Finally, the PV yield time series were scaled using a rooftop utilization rate. Only a certain part of the roof area can be used for PV modules due to constraints from other roof structures (chimneys, ventilation systems or dormers). We used a 50% roof utilization factor for PV systems, based on a previous study[207]. The PV yield time series for each neighbourhood was created by aggregation of PV yield profiles for all buildings in that neighbourhood. The annual PV yield is reduced with 0.5% per year to account for PV system degradation[96].

6.2.3 Electricity consumption from buildings

Electricity consumption time series were created for each neighbourhood using three main data sources; household statistics, historical residential demand time series and annual electricity consumption from residential grid connections. The household statistics from each neighbourhood in Utrecht are obtained from Statistics Netherlands (CBS) for 2015[221]. This data contains statistics on family compositions: people living alone, people living as a couple and couples with children.

Electricity demand profiles for 30 different households were measured between 2012 and 2014, by Dutch distribution system operator Liander[64]. The time series were measured using a 15 min time step for one year. Three new time series were created for each family composition using the 30 measured demand profiles. These three time series were scaled with share of family composition of each neighbourhood and summed together to create one demand time series per neighbourhood. The annual electricity consumption for each residential grid connection per postal code 6 area is available as open data for 2015[222]. We assumed that each residential address has one grid connection. The electricity consumption of all residential addresses within a neighbourhood was summed to determine the annual electricity consumption of a neighbourhood. This number was used to linearly scale the neighbourhood demand time series. Finally, the neighbourhood demand time series were linearly interpolated to a 5-min time interval. The demand time series of one year were repeated to obtain a 30-year period. The average electricity consumption of households was quite stable for the last 10 years[134]. Therefore, the annual demand is kept constant over the 30-year period.

6.2.4 Electric vehicle consumption

The number of registered cars per household in 2015 were obtained from CBS[221]. The average number of cars within a neighbourhood was 932, with a minimum of 105 and a maximum of 2,690. This corresponds to an average of 0.61 cars per household, with a minimum of 0.10 and a maximum of 1.05 cars per household. This is lower than the average for the Netherlands, which is 0.93 cars per household[223]. Furthermore it is expected that electric vehicles will have a market share of 100% around 2040[197]. Therefore, we assumed that all current light duty gasoline vehicles will be replaced with electric vehicles. The daily power consumption of an EV depends on the average driving consumption multiplied by a seasonal factor. This factor accounts for the seasonal variability of the EV consumption mainly due to the cabin climate control and the battery efficiency. A seasonal factor of 0.8 was used for summer period and 1.2 for the winter period[224]. The summer period consists of the months June until August

and the winter period December until February. Furthermore, we assumed an average driving power consumption of 7.24 kWh per day of which 50% will be charged within the neighbourhood[223]. In addition, a EV charging and discharging efficiency of 90% was assumed[133]. This results in a daily EV demand of 4.01 kWh and an annual demand of 1,463 kWh.

The moments at which cars are connected to the charging stations are highly uncertain and are not well studied. Therefore we developed an algorithm to assess the impact of two different charging strategies on the EV integration potential. In the first strategy, the daily EV charging demand within a neighbourhood is gradually spread over the day. In this case, we assume that the summation of charging demands of each individual EV results in a flattened EV charging profile of a neighbourhood. Hence a constant EV consumption over the day was assumed. In the second option, the EV is directly charged with the produced PV energy. We call this option smart solar charging[68]. In this case, the EV is charged with the excess PV production in the neighbourhood. A maximum charging capacity of 11 kW per EV was assumed, to reduce the impact on the electricity grid. If adequate PV production is not available during the day, then the remaining charging demand is fulfilled when the solar elevation angle is <0. Thus the EV demand is charged using the electricity grid. The charging profiles of both strategies were added to the neighbourhood electricity consumption profile. In the reference case, we assume that 75% of cars are charged using the first strategy and 25% of cars using the second strategy.

The distribution of residential neighbourhood annual electricity consumption including EV charging and the EV share are shown in Fig. 6.3. The total annual electricity consumption per neighbourhood ranges between 1 GWh and 16.3 GWh, with an average of 6.7 GWh. The share of EV consumption varies between 1.8% and 30.1%, with an average of 20.6%. These numbers show that there is

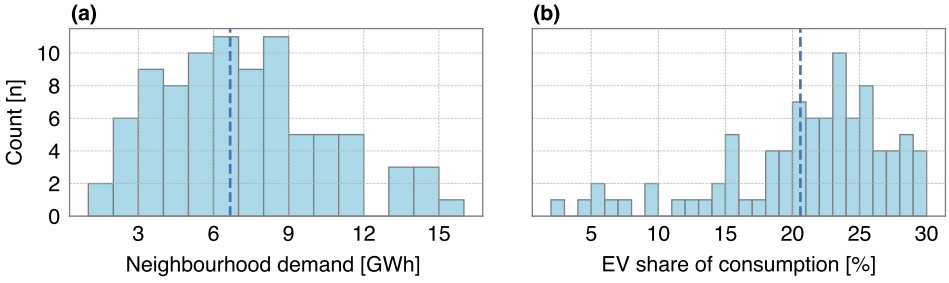

Figure 6.3 · Distribution of residential neighbourhood annual electricity consumption with EVs (a) and share of electricity consumption by EV charging (b) shown using a histogram. Mean values of the distribution are indicated by the dashed lines. Histogram bins of 2.5 GWh for neighbourhood energy demand and 1% for EV share were used.

a larger diversity of electricity consumption within each neighbourhood, mainly related to the number of inhabitants. Also, the EV charging demand within the neighbourhood is assumed to be constant over the 30-year assessment period. The total electricity demand of the 88 neighbourhoods is 466 GWh excluding EV charging and 587 GWh including EV charging.

6.2.5 BESS charging algorithm

Battery charging and discharging was simulated with a simple control strategy, obtained from previous research and written in Python (v3.5)[154]. If more PV electricity is generated than consumed by the neighbourhood, then the battery was charged. If more electricity was consumed than generated, then the battery was discharged. The battery was discharged to fulfil electricity demand of the building. If the battery inverter and battery storage capacity was available, then the battery was also used to charge the electric vehicle.

An AC-coupled PV-battery system was assumed. This means that the PV array is connected via an inverter to the electricity grid and the battery storage pack with a battery inverter to the electricity grid. This is a commonly installed system type and is very suitable for retrofitting or installing community energy storage systems[93]. A battery storage capacity of 1 kWh battery storage capacity per MWh of annual electricity consumption per neighbourhood is used in the reference case[93]. Note that if EVs were included in the modelling, than the annual consumption in neighbourhoods is higher and thus larger battery sizes are used.

The battery inverter capacity is set to a C-rate of 0.5, meaning that it would require 2 hours to fully charge the battery. Battery state of charge (SOC) is set to a minimum of 0% and a maximum of 100%. In this way, we assess the maximum storage potential to enhance self-consumption. Battery inverter efficiencies were obtained from the inverter efficiency curve of a SMA Sunny Boy Storage inverter, using a step size of 0.01%[94]. A constant battery roundtrip efficiency of 92% was used, close to the round trip efficiency of a Tesla Powerwall[95]. Furthermore, a calendric lifetime of 15 years and a battery cycle lifetime of 5000 full equivalent cycles is used to model the battery capacity degradation[97]. The amount of diminished storage capacity is determined annually and subtracted from the previous year. The battery degradation model is explained in detail in a previous study[185]. We assume that the battery storage is replaced after 15 years, thus the storage capacity is set similar to the original storage capacity for year 16.

6.2.6 Calculation of PV integration indicators

Two temporal PV integration indicators were assessed: self-consumption ratio (SCR) and self-sufficiency ratio (SSR). Self-consumption ratio is used to quantify the share of electricity that is self-consumed from the total annual produced PV energy. Self-sufficiency ratio is the share of electricity consumption that is fulfilled by PV electricity. The self-consumed power consists of the total direct consumed power by the neighbourhood ($P_{\text{direct SC}}$) and the total power that is used for charging the battery ($P_{\text{B charge}}$). The direct consumed power is the PV power (P_{PV}) that is directly consumed as a result of the electricity demand of a building. (P_{demand}). The self-consumed energy is aggregated over the year from timestep (t=1) till the last time step (t_{end}), see Eq. (6.1).

$$P_{\text{direct SC}} = \begin{cases} P_{\text{PV}} & \text{if } P_{\text{PV}} < P_{\text{demand}} \\ P_{\text{demand}} & \text{if } P_{\text{PV}} \geq P_{\text{demand}} \end{cases} \tag{6.1a}$$

$$\text{SCR} = \frac{\sum_{t=1}^{t_{\text{end}}} (P_{\text{direct-consumed,t}} + P_{\text{B charge,t}}) \cdot \Delta t}{\sum_{t=1}^{t_{\text{end}}} P_{\text{PV,t}} \cdot \Delta t} \tag{6.1b}$$

Self-sufficiency ratio is an indicator for the share of electricity consumption that is fulfilled by using PV electricity. This is the share of electricity demand that is fulfilled by the direct consumed PV power and the discharged power that is discharged from the battery ($P_{\text{B discharge}}$), see Eq. (6.2).

$$\text{SSR} = \frac{\sum_{t=1}^{t_{\text{end}}} (P_{\text{direct}-\text{consumed,t}} + P_{\text{B discharge,t}}) \cdot \Delta t}{\sum_{t=1}^{t_{\text{end}}} P_{\text{demand,t}} \cdot \Delta t} \tag{6.2}$$

6.2.7 Calculation of avoided life cycle GHG emissions

A rough indication of the avoided life cycle GHG emissions by the PV systems and battery energy storage systems was provided. Emissions due to manufacturing of the PV systems and BESS (GHG_{mfg}), and the avoided emissions by the PV electricity production are determined. The emissions of manufacturing the PV system depends on the production location[13]. We assume that PV systems are made in China as this country produces the majority of the PV cells and PV modules globally[6]. Emissions from producing PV systems in this country are assumed to be 1590 gCO_2-eq for each Wp[173]. The production of Li-Ion battery energy storage systems uses 110 gCO_2-eq for each Wh[175]. We assumed that emissions from manufacturing a battery inverter are comparable to the emissions from manufacturing a PV inverter and assumed 124 gCO_2-eq per W.[173].

The PV and battery inverter, and the battery storage are replaced after 15 years. Emissions from manufacturing are expected to be 25% lower when these components are replaced.

The avoided emissions by PV electricity production depend on the emission factor of electricity (EFE) from the grid. We assume that these emissions will reduce linearly from current emissions (2016) to zero emissions in 2050, based on the Dutch energy agreement for sustainable growth[225]. Thus, the carbon intensity will decrease linearly from 490 gCO_2-eq per kWh in year 1 to 60 gCO_2-eq per kWh in year 30[151].

The avoided emissions are determined for two system perspectives, i.e., from an electricity system perspective (GHG_{system}) and from a neighbourhood perspective ($GHG_{\text{neighb.}}$). In the electricity system perspective, all PV electricity that was used is allocated as replacing electricity from the grid. The PV power that was used from a system perspective ($P_{\text{PV system}}$), is the PV produced power minus the battery energy storage losses. In the neighbourhood perspective, all PV power used within the neighbourhood is allocated as replacing electricity from the grid. Hence, avoided emissions from electricity exported to the grid are not included in this perspective. The PV power used ($P_{\text{PV neighb.}}$), is the sum of the direct consumed PV and the electricity discharged from storage. The used PV electricity of both perspectives was multiplied with the carbon intensity of the electricity grid for each year. Then, the emissions from manufacturing were subtracted from the total emissions over 30 years to determine the avoided life cycle GHG emissions. The avoided emissions are normalized with the number of addresses within a neighbourhood (N_{address}), see Eq. (6.3).

$$P_{\text{PV system}} = P_{\text{PV,t}} - P_{\text{B charge}} - P_{\text{B discharge}} \tag{6.3a}$$

$$P_{\text{PV neighb.}} = P_{\text{direct}-\text{consumed}} + P_{\text{B discharge,t}} \tag{6.3b}$$

$$GHG_{\text{system}} = \frac{\sum_{t=1}^{t_{\text{end}}} (\text{EFE}, t \cdot P_{\text{PV system,t}}) - GHG_{\text{mfg}}}{N_{\text{address}}} \tag{6.3c}$$

$$GHG_{\text{neighb.}} = \frac{\sum_{t=1}^{t_{\text{end}}} (\text{EFE}, t \cdot P_{\text{PV neighb.,t}}) - GHG_{\text{mfg}}}{N_{\text{address}}} \tag{6.3d}$$

6.3 Results

6.3.1 PV yield potential

The PV yield potential for each of the 88 neighbourhoods was analysed over a period of 30 years using the reference parameters given in Table 6.1. The distributions of average annual PV yield for each address and the average annual PV yield for each neighbourhood are shown in Fig. 6.4. Also, the average annual specific yield for each address and each neighbourhood is presented. Average annual PV yield is 3.3 MWh per address and for the neighbourhoods 3.5 GWh. The specific yields show a larger distribution range for the addresses, with an average of 629 kWh per kWp. Specific yield for neighbourhoods is between 513 and 773 kWh/kWp, with an annual average of 628 kWh per kWp. The average specific yield decrease from 677 kWh/kWp in the first year to 579 kWh/kWp in year 30 due to PV system degradation. This specific yield is significantly lower than the current average specific yield for the Netherlands[27]. This is mainly due to the inclusion of all orientations and the reduced incoming irradiance due to shading. The total PV capacity from all neighbourhoods is 488 MWp and the average annual production 306 GWh.

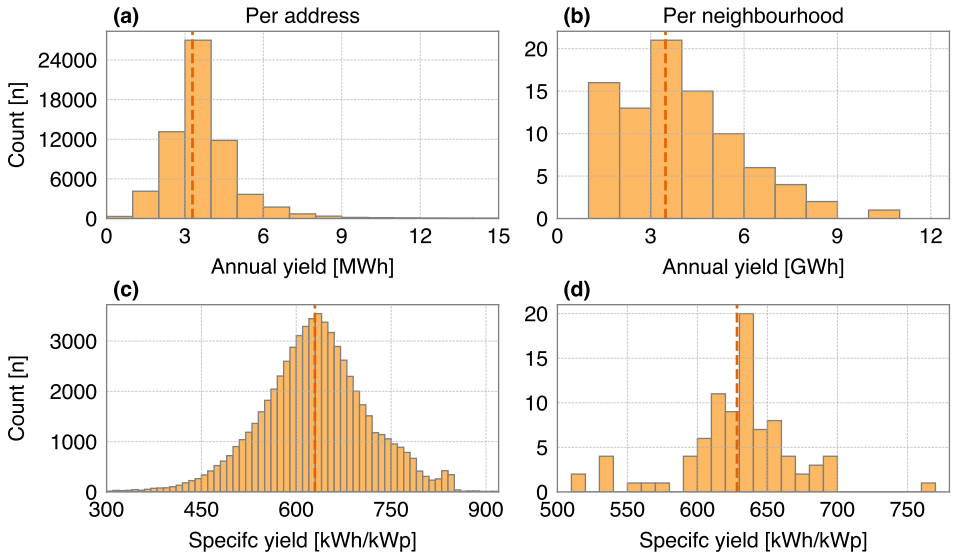

Figure 6.4 · Distribution of average annual PV yield for each address (a), average annual PV yield for each neighbourhood (b), average annual specific yield for each address (c) and average annual specific yield for each neighbourhood (d). Mean values of the distributions are indicated by the dashed lines. Annual yield is shown using bins of 1 MWh for each address and 1 GWh of each neighbourhood. Specific yield is shown using bins of 10 kWh/kWp. Note that 198 addresses have an annual yield higher than 15 MWh and are not shown on the histogram (a). Also 138 addresses with a specific yield of lower than 300 kWh/kWp are not shown on the histogram (c).

The ratio between the total PV production and the total electricity consumption for a period of 30 years provided an indication on the contribution of PV to fulfil the electricity demand. This ratio is shown for each of the 88 neighbourhoods of the city of Utrecht in Fig. 6.5. The ratio is shown for two scenarios, only PV systems and PV systems with EVs. A ratio higher than 100% shows that there is more PV production than electricity consumption. This is the case for 5 neighbourhoods in the PV only scenarios. Neighbourhoods with PV systems only show an average of 68% and neighbourhoods with PV systems and EVs 53%.

6.3.2 Impact of PV systems only

The spatial impact of PV systems on the self-consumption ratio and self-sufficiency ratio for each neighbourhood is visualized using on a color-coded map in Fig. 6.6. Results are shown for 88 neighbourhoods which are separated by grey borders. The 9 districts are separated with solid black lines and the district names are indicated. The white areas are those neighbourhoods of the city of Utrecht that were excluded from the study. For example, the left most neighbourhood in district West is actually a commercial area with a limited amount of residential dwellings.

The average SCR of the neighbourhoods is 53 %, which demonstrates that the PV produced in a neighbourhood can be used most within the same neighbourhood. Moreover, a wide range of SCR between 34 % and 100% demonstrates a large variety in PV integration potential. Low SCR is seen for the suburb of Leidsche Rijn, and in the Noordwest (North-West) district, indicating a large surplus of produced PV energy. These areas contain mainly terraced houses with sufficient roof space available for PV systems.

High SCR was observed in the historical Binnenstad (Inner-city), Oost (East) and Overvecht districts. The inner-city area has a limited PV potential due to high

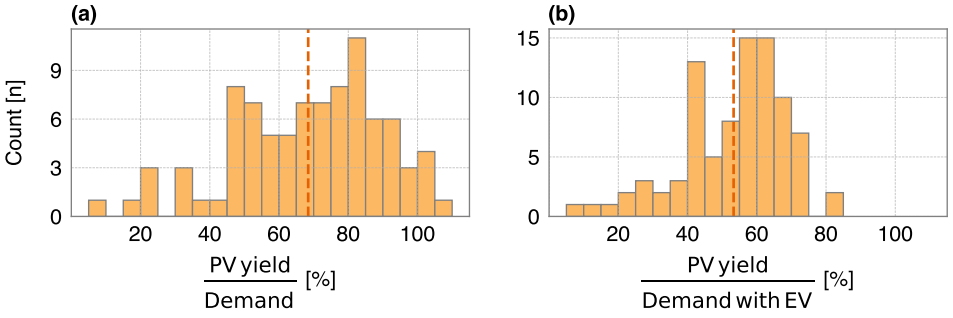

Figure 6.5 · Distribution of ratio between the total PV production and the total consumption of neighbourhoods with PV systems only (a) and neighbourhoods with PV and EVs (b) Mean values of the distribution are indicated by the dashed lines, and bins of 5% were used.

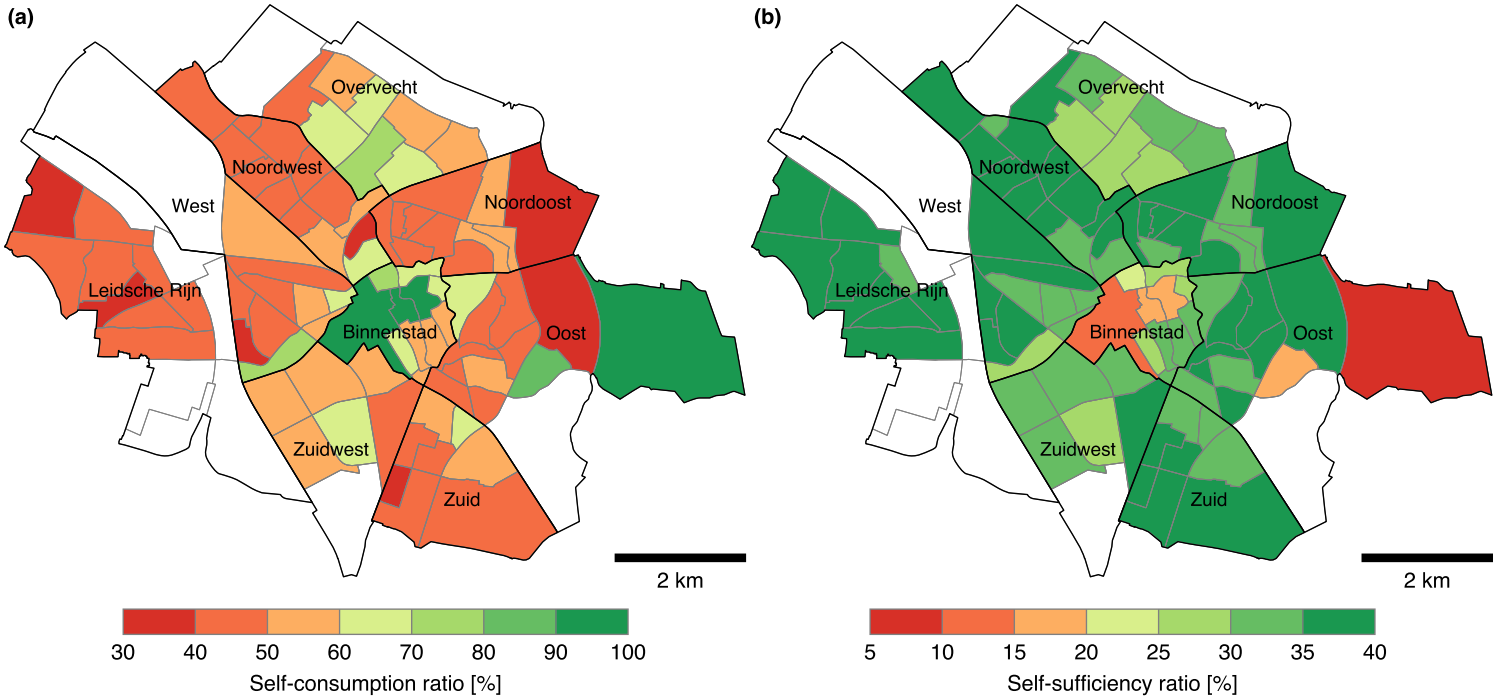

Figure 6.6 · Potential PV self-consumption ratio (a) and self-sufficiency ratio (b) for 88 neighbourhoods with only PV systems, for the city of Utrecht

concentration of historical buildings with relatively small roof areas and a high variation in roof shape and height. These roofs induce shading which reduces the plane-of-array irradiance and as a consequence the PV electricity generation. In addition, population density in the inner city is larger compared to other districts due to the smaller dwellings and apartments. This results in relatively high electricity consumption per unit area and thus a higher SCR. The district of Overvecht contains tall (mostly 10-storey) residential apartment buildings that limit the PV production potential per resident. Also, the district to the extreme East, in which the university campus is located, shows a high SCR. In this area, tall apartment buildings, which serve as student housing are located. Therefore, the roof area available per address is small.

An average SSR of 33% was determined for the neighbourhoods, ranging from 6% to 40%. Low SSRs are observed for the inner-city area, indicating that PV potential is not sufficient to fulfil the electricity demand. Higher self-sufficiency is observed for the suburb Leidsche Rijn, and in the Zuid (South) district. Areas with high SCR and low SSR have limited area to install PV systems and therefore limited PV yield. Areas with relatively lower SCR and higher SSR have more moments in which surplus of PV energy production occurs. The limited SSR indicates that the PV yield potential is not sufficient and electricity import to the city is a requirement.

6.3.3 Impact of EVs or BESSs

The influence of two scenarios, PV systems with EVs and PV systems with BESSs, on the self-consumption enhancement is presented in Fig. 6.7. Deployment of BESSs shows a larger impact on the SCR than the deployment of EVs. The replacement of gasoline-based cars by EVs results in an average increase in SCR of 12% points in the neighbourhoods. The SCR increase varies between 0% and 17% points, showing a broad impact of electric vehicles. Neighbourhoods with already high self-consumption due to the electricity consumption of the residential buildings show limited SCR enhancement by electric vehicles. The average self-sufficiency of neighbourhoods with introduction of EVs has barely changed. Observed differences in SSR are between -2.0% and 0.1% points with an average of -0.7% points. Only for two neighbourhoods EVs have a positive impact on SSR, namely Rijnsweerd and Hoge Weide. These neighbourhoods are in the Oost (East) and the Leidsche Rijn districts, respectively. The Rijnsweerd neighbourhood also has the lowest SCR without EVs. This shows that for almost all neighbourhoods the additional EV demand increases the need for imported electricity.

An average SCR increase of 25% points can be achieved with a battery capacity of 1 kWh for each MWh of electricity consumption. The SCR enhancement varies

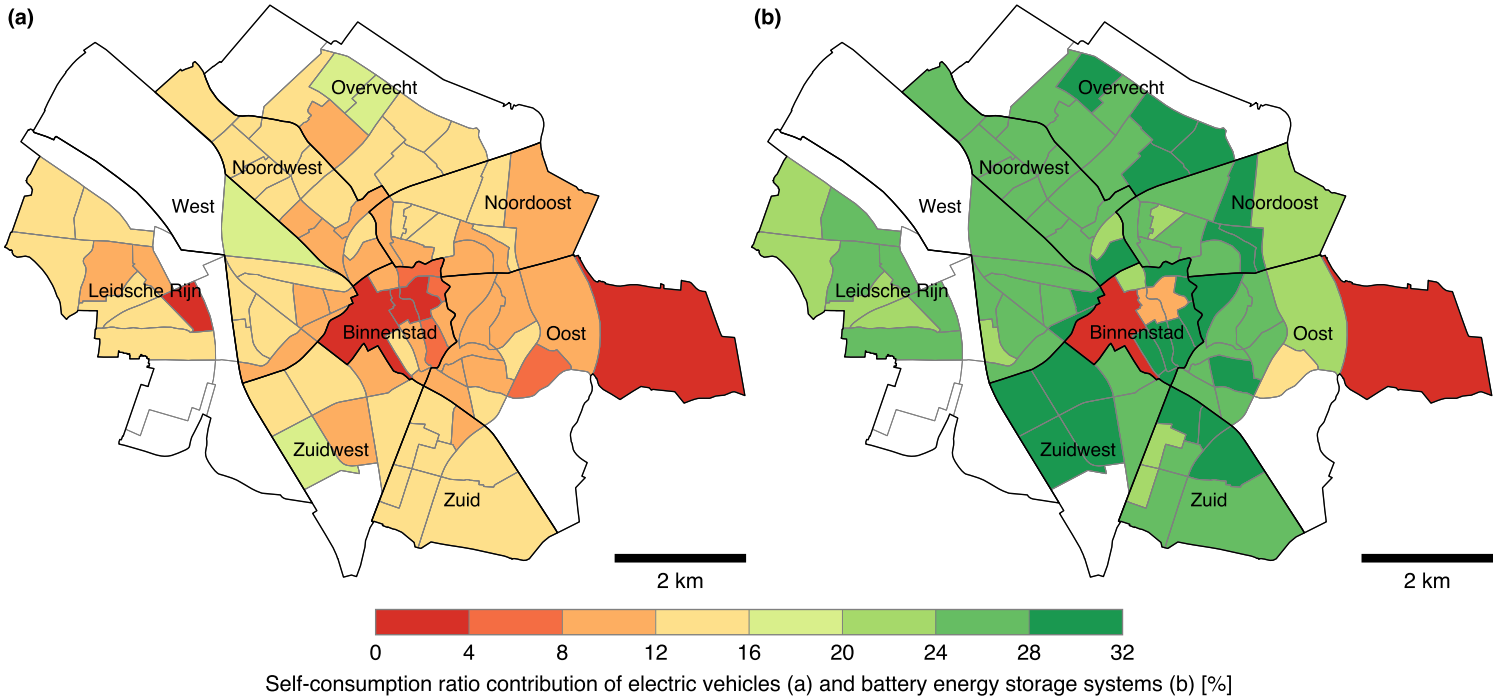

Figure 6.7 · Potential contribution of electric vehicles to the PV self-consumption ratio (a) and potential contribution of battery energy storage systems to the PV self-consumption ratio (b) for 88 neighbourhoods.

between 0% and 30% points. Neighbourhoods with a low self-consumption of PV systems only (Leidsche Rijn) have a SCR impact of ≈ 20% points from battery storage. In this case, the influence is limited by the battery storage capacity. The neighbourhoods with a high initial SCR (Binnenstad) have a limited BESS impact since most of the electricity is directly consumed anyway and the storage capacity is not utilized. Neighbourhoods with an initial self-consumption of around 60% (Overvecht) show the largest self-consumption impact. These neighbourhoods can store most surplus PV production and utilize the storage capacity. In addition, the SSR impact by storage varies between 0% and 18% points with an average of 14% points. As a result, 42 neighbourhoods obtain a self-sufficiency ratio >50%

For a dwelling owner with a PV system, it could be advantageous to use storage under certain economic conditions[153]. However, if this dwelling is located within a neighbourhood with low impact of storage on self-consumption, then this electricity could better be used by dwellings with insufficient roof space for a PV system. As a result, more electricity is directly used, and less electricity is lost by energy storage conversions. Moreover, some neighbourhoods are surrounded by neighbourhoods with a high initial SCR. For, example the North-West district has a relatively low SCR, but is surrounded by districts with higher SCR. Hence, it could be more beneficial to export surplus PV to these areas, instead of increasing storage capacities. On the other hand the historical inner-city is enclosed by neighbourhoods with lower SCR. These neighbourhoods could provide the inner-city with electricity instead of storing surplus PV electricity in batteries.

6.3.4 Combined impact of EVs and BESS

The impact of the PV systems with electric vehicles and battery storage on SCR and SSR are presented in Fig. 6.8. A total of 10 neighbourhoods have a self-consumption ratio of almost 100%, indicated by the blue dots. For the majority of these neighbourhoods a SCR impact of around <15% is seen. Overall, an average SCR enhancement of 35% can be achieved when EV and storage are added to the neighbourhoods. This results in a high average SCR of 88% within the neighbourhoods, with a range from 67% till 100%.

The self-sufficiency ratios show an average increase of 10% due to EVs and storage, ranging between -0.6% and 16%. The SSR impacts show negative values in two neighbourhoods. These neighbourhoods have a larger additional electricity demand by EVs, than the demand that can be shifted by battery energy storage. Overall, the average SSR increases to 43%, ranging between 6 % and 54%. Also, 17 neighbourhoods have a SSR >50% with EV and storage.

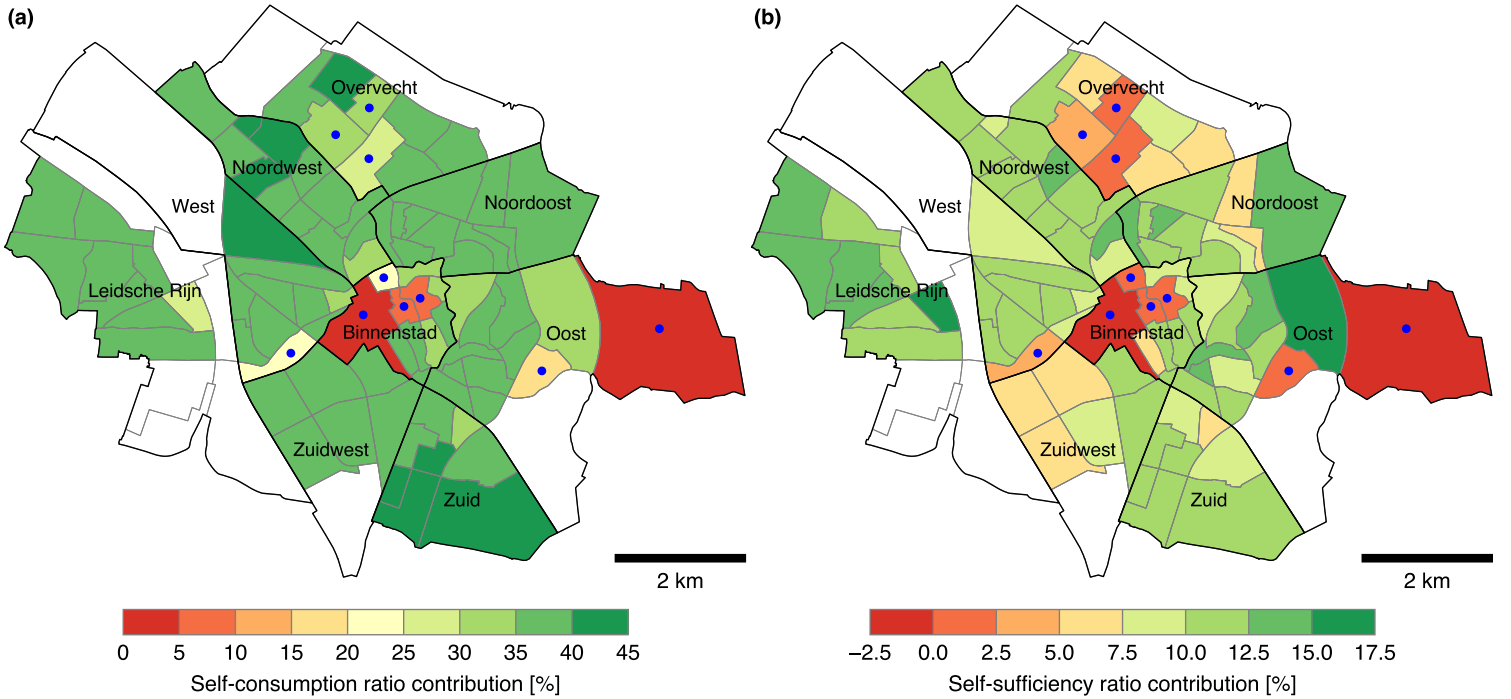

Figure 6.8 · Potential contribution of electric vehicles with battery energy storage system to the PV self-consumption ratio (a) and contribution to the self-sufficiency ratio (b) for 88 neighbourhoods. Areas with a self-consumption ratio of >99% are indicated by the blue dot.

6.3.5 Avoided life cycle GHG emissions

The avoided life cycle GHG emissions from an electricity system and neighbourhood perspective were assessed with the reference parameters including electric vehicles and battery energy storage system, see Fig. 6.9. The avoided GHG emissions are given for the 30-year period per residential address. The emissions show large differences between the neighbourhoods. Avoided GHG emissions from an electricity system perspective are on average 11.5 tCO_2-eq, ranging between 0.3 to 28.1 tCO_2-eq per address. Average avoided GHG emissions from a neighbourhood perspective are 8.6 tCO_2-eq per address, which is around 0.3 tCO_2-eq for each year.

Neighbourhoods with 100% SCRs have almost similar emissions from an electricity system perspective as from a neighbourhood perspective, since all PV electricity is directly used. These neighbourhoods are located in the centre of the city. The suburb Leidsche Rijn shows high avoided emissions from a neighbourhood perspective, due to high PV potential and large SCR impact by storage and electric vehicles. The North-West district has similar SCR as the Leidsche Rijn suburb, yet lower avoided emissions are seen here. This is due to the lower electricity demand and the lower PV yield potential for each address in North-West district. The neighbourhood with the lowest self-consumption ratio (Rijnsweerd in the East district) shows the largest emission reductions from system perspective.

PV modules made in Europe are produced with lower greenhouse gas emissions compared to PV made in China, due to the lower carbon intensity of the electricity generation mix in Europe. We compared the impact of PV made in China with PV made in the EU on the avoided emissions. 824 gCO_2-e for each Wp were assumed as emissions from PV manufactured in Europe[173]. The avoided GHG emissions of China and Europe, and the relative change between these areas are shown for both perspectives in Fig. 6.10. No change in emissions from manufacturing battery storage was assumed.

When using PV modules manufactured in the EU, the avoided emissions are increasing to averages of 14.4 tCO_2-eq from an electricity perspective and to 11.5 tCO_2-eq from a neighbourhood perspective. The relative change in avoided emissions between China and Europe are significantly higher from a neighbourhood perspective than from an electricity system perspective. An average of 28% is shown for the system perspective and 36% from a neighbourhood perspective. Neighbourhoods with high PV system potential have larger emissions from manufacturing and therefore relatively lower avoided emissions from a neighbourhood perspective. Consequently, the distribution in relative change of avoided emissions from a neighbourhood perspective is larger compared to the avoided emissions from a system perspective.

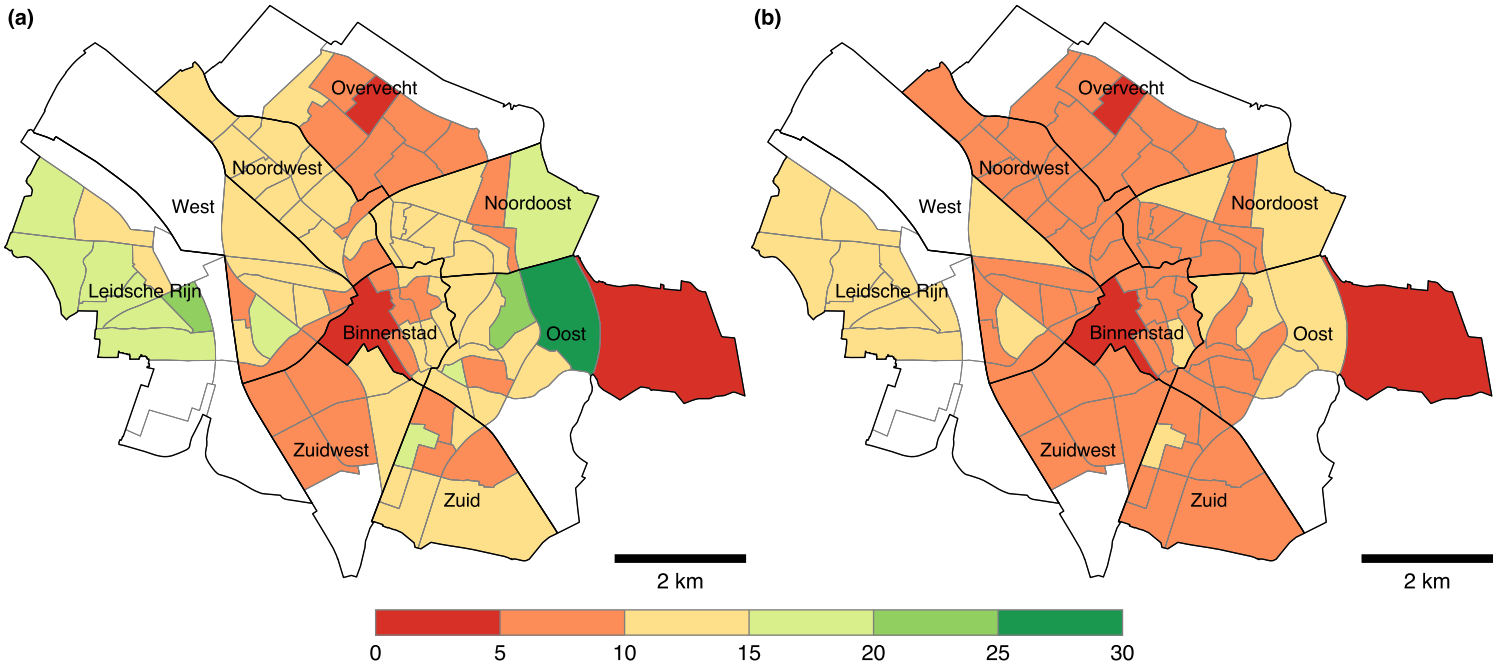

Figure 6.9 · Potential of avoided life cycle GHG emissions per address from a electricity system perspective (a) and from a neighbourhood perspective (b). The avoided emissions are presented for the reference scenario including electric vehicles and battery storage. Note that the avoided emissions are normalized with the number of addresses within each neighbourhood.

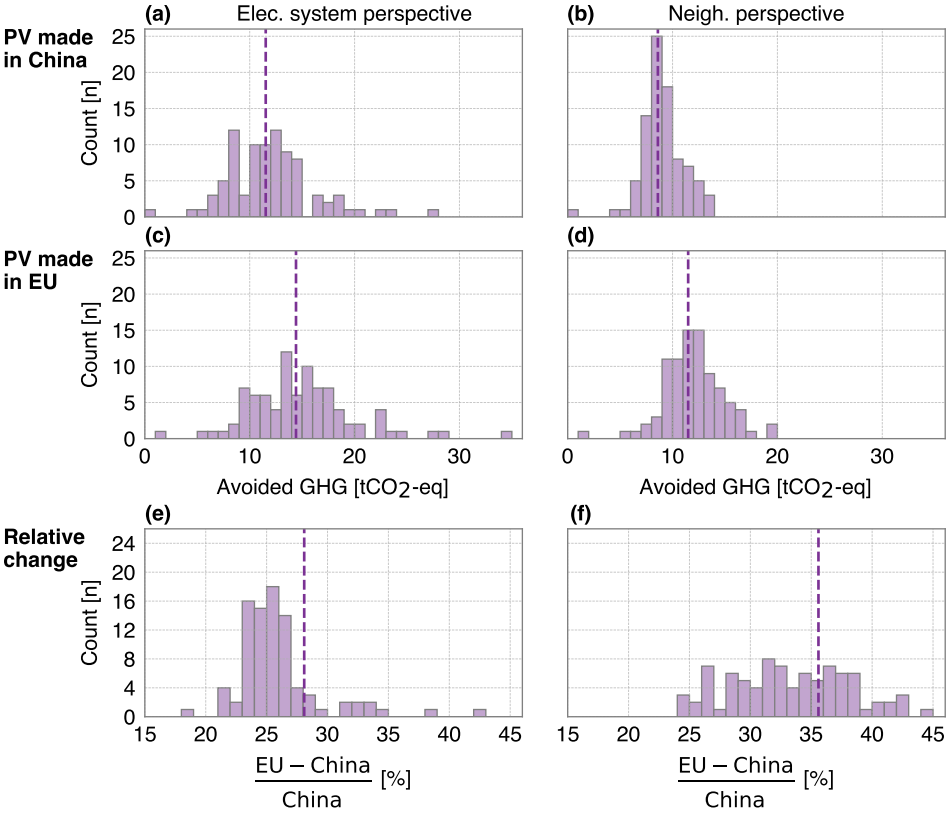

Figure 6.10 · Distribution of avoided life cycle GHG emissions per address of the neighbourhoods with PV made in China (a & b), PV made in Europe (c & d) and the relative change in avoided emissions between these areas (e & f), The left column shows the avoided emissions from an electricity system perspective and the right columns shows the avoided emissions from a neighbourhood perspective. Mean values of the distribution are indicated by the dashed lines. Histogram bins of 1 tCO_2-eq were used for the avoided emissions and bins of 1% for the relative change. Note that a relative change larger than 45% is observed for one neighbourhoods from a electricity system perspective, and two neighbourhoods from a neighbourhood perspective. These are not shown in histogram (e) and (f).

6.4 Sensitivity analysis

A sensitivity analysis was conducted for four different rooftop utilization rates. These utilization rates were combined with a larger share of EV solar charging or with smaller or larger battery storage capacities. Other input parameters, see Table 6.1, were kept constant. Three parameters were assessed; SCR, SSR and avoided life cycle GHG emissions per address from a neighbourhood perspective. The avoided emissions from a system perspective were not shown, since these are less dependent on the PV self-consumption. Some of the scenarios assessed here are not realistic but purely theoretical. A 100% rooftop utilization rate is currently not practical to implement. Moreover, a high smart solar charging share, of

75% or even 100%, requires major investments in charging infrastructures. Furthermore, EVs should be available for charging within the neighbourhood.

6.4.1 EV smart solar charging share

The influence of five smart solar charging shares of four rooftop utilization rates is presented in Fig. 6.11. The 25% rooftop utilization scenario shows an average SCR of 85% when no EV is smart charged. This is increased by 11%, if all EVs would apply smart solar charging. In this rooftop utilization scenario, a >99% SCR is reached for 20 neighbourhoods. This limits the average increase of the SCR. Battery energy storage shows an average SCR close to 100%, for all EV smart charging shares. Thus, energy storage reduces the impact of smart solar charging

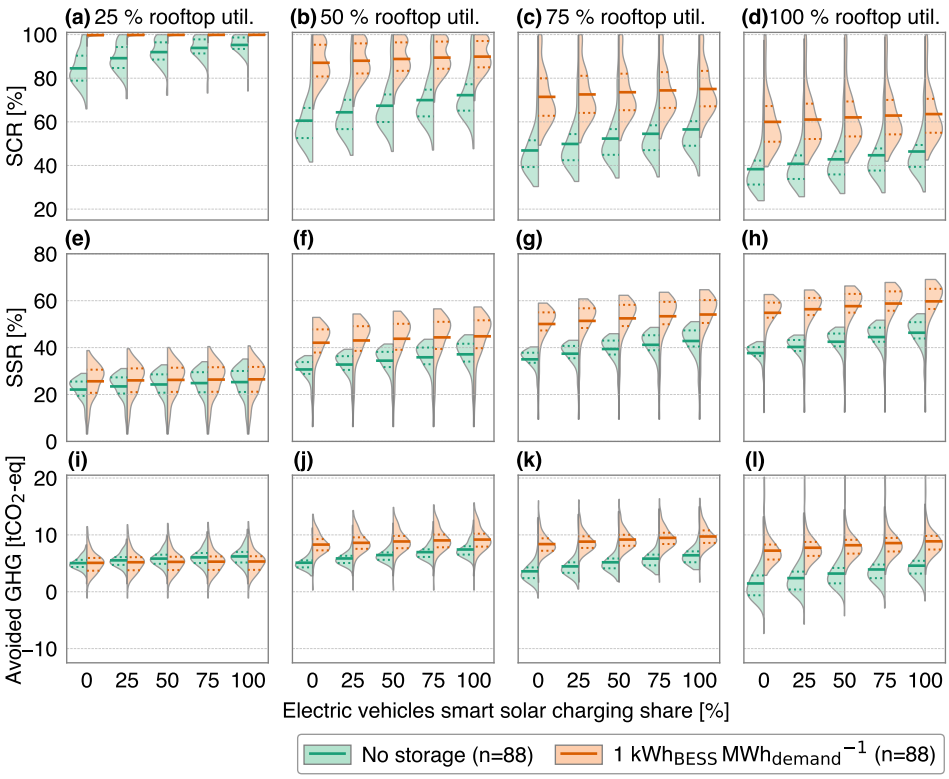

Figure 6.11 · Influence of the rooftop utilization (util.) factor on the self-consumption ratio (a to d), self-sufficiency ratio (e to h) and avoided life cycle emissions per address from a neighbourhood perspective (i to l). The distributions are shown for the 88 neighbourhoods and five electric vehicle charging scenarios using violin plots. The left side of the violin plot shows the distributions without battery storage and the right side of the violin plot shows the distributions with a 1 kWh storage capacity for each MWh of annual electricity consumption. Mean values are indicated by the solid lines and 25% and 75% percentiles are indicated by dotted lines.

to almost nothing. Therefore, it is not recommended to invest in smart charging infrastructure with storage under the 25% rooftop utilization rates.

Under the 50% rooftop utilization, a shift from 0% solar charging share to a 100% solar charging share increases the average SCR by 12% points. This is a slightly larger increase than shown for the 25% rooftop utilization rate. Fewer neighbourhoods reach the maximum SCR, thus the average increase in SCR is larger. However, under the 75% rooftop utilization, the increase in SCR due to higher smart charging shares is reduced to 10%, which is 2% lower than under the 50% rooftop utilization rate. Higher rooftop utilization rates have significantly more surplus PV available. Therefore, the impact of smart charging share on the SCR is reduced.

Neighbourhoods with storage have a larger PV self-consumption. Consequently, the SCR increase due to an increase of solar charging share from 0% to 100% is only 2.8% points under the 50% rooftop utilization scenario. This number is increased to 3.6% under the 100% rooftop utilization rate, since more surplus PV energy is available for storage. Also, the widest distribution between neighbourhoods is seen with a 100% rooftop utilization rate. A larger smart solar charging share reduces the surplus PV that can be stored in batteries. Subsequently, the SCR impact of storage is reduced with higher EV smart solar charging shares. Still, these high smart solar charging shares are not realistic, thus investing in battery energy storage could be worthwhile.

Self-sufficiencies increase slightly for the 25% rooftop utilization rate, with averages from 22% with no smart solar charging to 25% for a 100% solar charging share. SSR are limited when storage is added, with an average of around 26%. Yet, the impact of storage is significantly higher with a 50% utilization rate, and largest for a 100% rooftop utilization rate. Furthermore, the increase in EV smart solar charges share shows a significantly larger impact on the SSR. For a 50% utilization rate and no storage, a shift from 0% to 100% solar charging share results in a SSR increase of 6.5% points. This difference is increased by 8.7% points under a 100% rooftop utilization rate. When storage is added to the neighbourhoods, then this increase is 4.8% points. An increase in rooftop utilization rates causes an expansion of the first 25% percentile for both neighbourhoods with and without storage. Neighbourhoods with a low SSR have a far higher electricity demand. Hence, the absolute increase in SSR due to higher PV capacity is smaller for neighbourhoods that already show high SSR.

Avoided life cycle GHG emissions, from a neighbourhood perspective and per addresses, were found to be increasing from a 25% to a 75% rooftop utilization rate. However, the avoided emissions have decreased for a 100% rooftop utilization compared to a 75% rooftop utilization. Some neighbourhoods even showed

negative values. This means that the emissions due to manufacturing of PV and storage systems are larger than the avoided emissions due to the direct consumption at the neighbourhood level. Furthermore, under the 25% rooftop utilization rate, avoided emissions are lower for neighbourhoods with storage than without storage.

Yet, from an electricity system perspective, the average avoided emissions increased by rooftop utilization rates. Neighbourhoods without storage and a 25% solar smart share showed averages of 7, 14, 21 and 27 tCO_2-eq of avoided emissions for 25, 50, 75 and 100% rooftop utilization rates respectively. Neighbourhoods with storage and a 25% solar smart share showed lower avoided emissions of 5, 12, 18 and 25 tCO_2-eq of for 25, 50, 75 and 100% rooftop utilization rates respectively.

6.4.2 Battery storage capacity

The influence of increasing battery storage capacities under four rooftop utilization rates is presented in Fig. 6.12. SCR increased under all scenarios with larger storage capacities and when EVs are included. With 25% of rooftop utilization, the SCR is maximized with the use of energy storage and electric vehicles. With 50% rooftop utilization, we found that a 2 kWh storage system per MWh demand does not impact the upper 25% percentile of the neighbourhoods. Hence, a quarter of the neighbourhoods can consume all locally produced PV electricity under these conditions. A 75% and 100% rooftop utilization rate results in a higher impact of larger battery storage capacities. The addition of electric vehicles to the neighbourhoods results in higher SCR values. For these high rooftop utilization rates, the average SCR impact from energy storage is quite similar for neighbourhoods with and without EVs. Also in this case, surplus PV electricity is not fully utilized by EVs charging and therefore storage can have a similar impact. Furthermore, additional demand is added with EVs, which results in relatively larger storage capacities and thus higher SCR.

Self-sufficiency ratios gradually increase with higher rooftop utilization rates. With 25% rooftop utilization, the highest SSR were observed for a battery size of 1 kWh per MWh demand. Larger storage capacities resulted in more electricity losses caused by charging and discharging of the batteries. Consequently, self-sufficiency is reduced within the neighbourhood.

Neighbourhoods with EVs have a higher direct PV self-consumption, thus less surplus PV electricity can be shifted by storage. As a result, the influence of storage is smaller for neighbourhoods with EVs than for neighbourhoods without EVs. Under the no storage scenarios, almost similar SSR distributions were observed for neighbourhoods with EVs and without EVs. This indicates that power

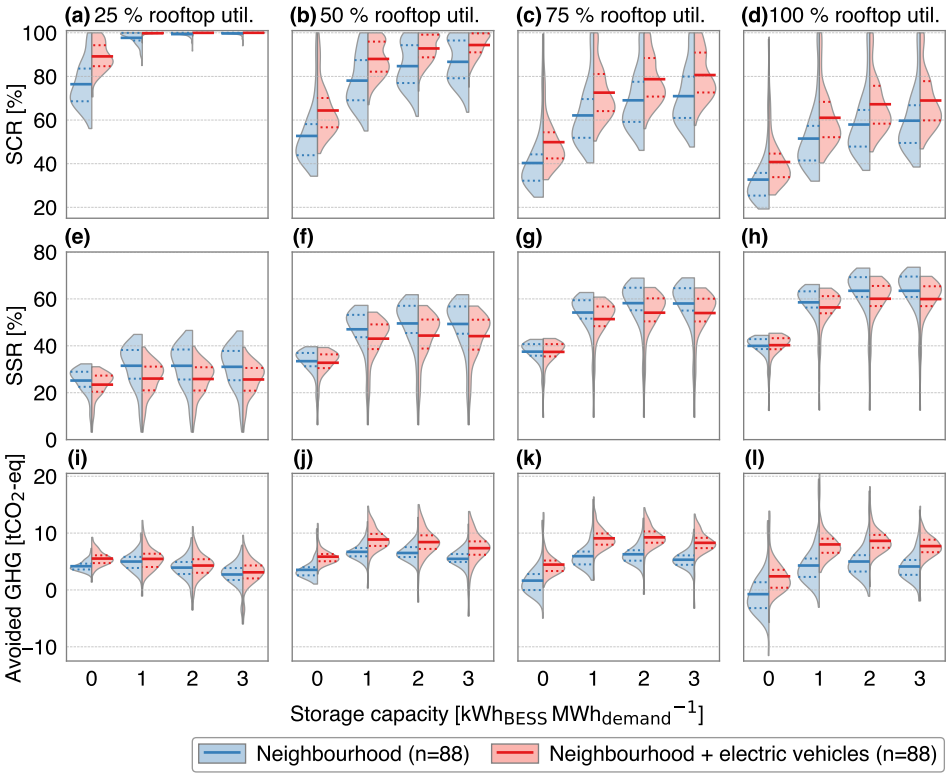

Figure 6.12 · Influence of the rooftop utilization (util.) factor on the self-consumption ratio (a to d), self-sufficiency ratio (e to h) and avoided life cycle emissions per address from a neighbourhood perspective (i to l). The distributions are shown for the 88 neighbourhoods and four battery storage capacities using violin plots. The left side of the violin plot shows the distributions with electricity consumption of the neighbourhood only and the right side of the violin plot shows the distributions of the neighbourhood with electric vehicles. The electric vehicles have a 25% solar charging share. Mean values are indicated by the solid lines and 25% and 75% percentiles are indicated by dotted lines

consumption time series of the EVs is comparable to the electricity consumption time series of the neighbourhoods.

Avoided emissions per address are largely dependent on rooftop utilization rate and installed storage capacities. Under the 25% rooftop utilization scenario, the increase in storage capacity shows a significant reduction in avoided emissions. For higher rooftop utilization rates, an increase in avoided emissions can be seen when shifting from no storage to 1 kWh per MWh capacity. However, larger storage capacities show a reduction of avoided emissions. For these larger capacities, the emissions due to manufacturing are higher than the avoided emissions due to the self-consumption. Moreover, EVs add demand to the neighbourhood and therefore avoided life-cycle emissions increase.

6.5 Discussion

This research showed that PV self-consumption and self-sufficiency potential varies significantly between neighbourhoods. These variations are primarily related to limited residential roof area for PV siting, higher electricity demand, or higher expected electric vehicle penetration rates. A number of limitations concerning assumptions and data availability were made in this research that could impact the outcome substantially.

6.5.1 Data limitations

The PV potential of facades from residential buildings was not included in the study. Especially, facades from tall residential buildings can significantly increase the PV potential in neighbourhoods[204]. For example, the district of Overvecht contains numerous tall residential buildings, consequently limiting the self-sufficiency ratio. Also, including facades would substantially increase the self-sufficiency ratio of these types of buildings. Furthermore, by using east and west oriented facades, the PV yield over the day is extended beyond the noon peak to early morning and late afternoon. This will provide a higher direct PV self-consumption and decrease the need for storage[90]. However, assessment of PV potential of facades is computation-intensive, since another dimension is added to the radiation model[226]. Furthermore, information about the share of windows and other building facade components makes the model complex. In addition, this information is not easily available.

The annual incoming POA irradiance on each rooftop was assessed using the ARCGIS tools. This number was used to linearly scale down PV yield time series obtained from the PVLIB model. Consequently, we assumed that the shade was homogeneously spread over the PV yield time series. However, the impact of shade on the PV yield depends on the position of the sun in the sky and the location of the obstructions which block the direct sunlight. We aggregated the individual PV time series of each roof to a time series for a neighbourhood. Also, we assumed the shades on each PV system in the neighbourhood do not occur simultaneously. Subsequently, the influence shade on the individual PV system decreases. Determining incoming POA irradiance for each roof for a smaller time step is recommended for further research. However, this requires significant more computation time or different calculation tools. Furthermore, we assumed that all incoming irradiance on the PV module would be converted to electricity. This conversion could be decreased due to partial shading of the module. The impact of partial shading on the PV yield depends on the installed system architecture and the module design[227].

We used one year of data (2015) to assess the rooftop PV potential and corresponding PV integration parameters, due to data availability and computation time. The year 2015 had a relative high annual irradiance compared to pre 2015 years[90]. Consequently, the PV yield production is overestimated with a few percent. Subsequently a higher self-consumption is expected but also a lower self-sufficiency. Furthermore, we assumed that excess PV power is distributed to other residential buildings within the neighbourhood using the low voltage grid. Power and voltage constraints within the low voltage grid were not considered. A detailed map of the low voltage grid should be included for future research for assessment of these potential limitations.

We assumed a constant emission factor for electricity over the year. Consequently, results showed that storage does not contribute to emission reductions from an electricity system perspective. However, with a larger share of renewables, a higher variability of emission factors from power generation can be expected. Consequently, the avoided emissions from storage could increase. If batteries would discharge at moments with a large share of fossil fuel fired power plants in the power generation mix, then this would avoid more emissions. Battery control strategies that include the marginal emissions factor should be developed.

6.5.2 Implementation considerations

Currently, over 90% of residential buildings are heated using natural gas-based systems[134]. The Dutch government has set goals to replace these with other technologies, e.g. heat pumps. This could increase the electricity demand of cities in the Netherlands. But the expected electricity demand of heat pumps in cities is hard to predict. Firstly, the residential buildings should be selected in which heat pumps are the most economically viable option to replace natural gas boilers. For example, district heating systems can also be used to replace natural gas heating systems, especially in densely populated cities[190]. Secondly, the electricity demand of heat pumps mainly depends on the heat source (air or ground) and the characteristics of the buildings. Especially old buildings should be insulated before installation of any heat pump system. The assessment of future electricity demand from residential buildings due to electric heating is highly recommended in future research.

The electricity demand for electric vehicles could be underestimated if more people will charge their EV within the city than was assumed. This could potentially occur when fast charging stations are introduced within the city, yet this would also require additional grid expansion measures. On the other hand, this

demand could be overestimated due to reduced policy support for charging stations within cities. Furthermore, car sharing could result in less need for privately owned cars, and therefore reduce the demand. Moreover, a lack of parking spots or improved public transport can reduce the number of electric vehicles.

The technical PV potential in our study was assessed using 50% of the roof area. However, the estimated economic potential is lower due to the following reasons. First, the net-metering policy is established in the Netherlands. Consequently, dwelling owners with a relative large roof area will probably only install a PV capacity sufficient to provide in their annual electricity consumption. Second, PV systems with a relative low specific PV yield will not be installed due to a significantly larger payback period.

PV power density of 200 Wp/m^2 are assumed, but are expected to increase in the future due to higher module efficiencies. This would increase the PV yield potential and decrease the self-consumption, but increase the self-sufficiency. Also, we expect that future cost of PV systems will decrease based on the historical learning rates of around 20%[13]. Consequently, the economic profitability of PV systems for orientations with lower incoming irradiance will increase.

6.6 Conclusion

This study developed a spatio-temporal model that aimed to assess residential PV electricity integration options. The impact of electricity consumptions from buildings, electric vehicles and battery energy storage system was investigated for each neighbourhood in the city of Utrecht, the Netherlands. A large variety in PV yield potential, self-consumption ratio and self-sufficiency ratio was found between the neighbourhoods. Self-consumption ratios are between 34% and 100% for the neighbourhoods. This could be increased on average by 12% by electric vehicles and 25% with battery storage. Avoided life cycle emissions are between 0 and 28 tCO_2-eq, with an average of 12 tCO_2-eq per address.

The spatial analysis identified neighbourhoods with potential surplus PV electricity that could be used to provide electricity to surrounding neighbourhoods with lower PV potential. We recommend using battery storage capacities only in areas in which storage has a high impact on self-consumption enhancement. Also, supporting policies for smart solar charging of electric vehicles should focus on neighbourhoods with large PV potential and relatively low electricity consumption. Especially for neighbourhoods were the low voltage grids require considerable expansion to host the potential PV capacity. Moreover, PV supporting policies should focus on neighbourhoods with a higher potential of avoided life

cycle GHG emissions. The dissimilarity of results between the neighbourhoods indicates that area dependent investments and supporting policies could improve the PV power integration in cities. Therefore, we recommend the use of our spatio-temporal model for other cities to assist local governments and district system operators in the transition towards sustainable cities.

Acknowledgment

This work is funded by three projects. First, the research programme Transitioning to a More Sustainable Energy System (Grant No. 022.004.023), funded by the Netherlands Organisation for Scientific Research (NWO). Second, the Advanced Solar Monitoring project, funded by the Netherlands Enterprise Agency RVO (Grant No. TKIZ01015). Third, the Advanced Scenario Management - Phase 2, funded by the Netherlands Enterprise Agency RVO (Grant No. TEUE116903). We are grateful to the Royal Netherlands Meteorological Institute for providing data.

7

Synthesis of the main findings

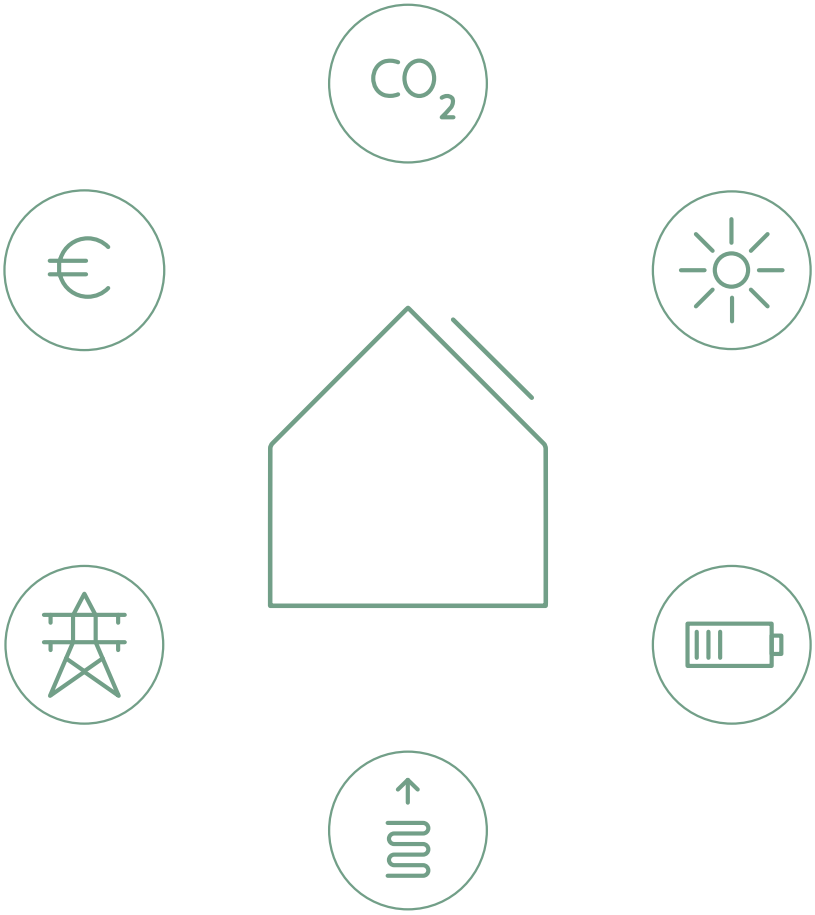

7.1 Synthesis framework

This chapter combines methods and results obtained from previous chapters to provide new insights regarding the four sub research questions, described in section 1.4. Three datasets were used for residential buildings and one dataset for commercial buildings. An overview of the characteristics, assumptions and research questions associated with these four datasets are presented in Table 7.1. Annual electricity consumption was kept constant over the simulated time periods. The datasets were combined with battery energy storage control algorithms and electric vehicle charging algorithms. The results from these datasets and algorithms provide answers to the research questions from multiple perspectives. Questions Q 1., Q 2. and Q 3. are answered for residential and commercial buildings, while Q 4. is answered solely for residential buildings. The synthesis results are used to provide final key conclusions and recommendations in chapter 8.

7.2 On improving PV self-consumption and self-sufficiency

This section aims to provide insights regarding the following research question:

Q 1. How can PV self-consumption and self-sufficiency be improved?

PV self-consumption was quantified using the self-consumption ratio (SCR). This is the share of self-consumed PV energy from the total produced PV energy. Self-sufficiency was quantified using the self-sufficiency ratio (SSR), which is the

Table 7.1 · Main characteristics, assumptions and research questions associated with the different datasets used in this synthesis. Residential neighbourhoods is denoted by res. neigh. and assumptions as asm. Performance ratios are given for the first and last year of the simulated time PV periods. The used datasets for each research questions and associated sections are indicated with bullets.

Dataset		Res-1	Res-2	Res-3	Com-1
Used in chapter		2, 3 & 4	5	6	2, 3 & 4
Demand unit & count		48 dwellings	16 dwellings	88 res. neigh.	42 offices
PV pattern category		modelled	measured	modelled	modelled
PV data used timeseries		2012 to 2016	07-2013 to 06-2015	2015	2012 to 2016
Performance ratio		85% to 74%	Variable	85% to 72%	85% to 77%
Simulation period		25 year	30 year	30 year	20 year
		4.2.3	5.A	5.A	4.2.3
Used for research questions in sections	Q 1. section 7.2	●	●	●	●
	Q 2. section 7.3	●	●	●	●
	Q 3. section 7.4		●	●	●
	Q 4. section 7.5		●	●	

share of total self-consumed energy from the total consumed energy.

PV self-consumption can be separated into direct and indirect self-consumption. Direct self-consumption depends on the total electricity consumption, the demand pattern, PV system orientation and PV system capacity. These were mainly assessed in chapter 2, 5 and 6. Indirect self-consumption is the increase in self-consumption due to battery energy storage. This depends mainly on the battery storage capacity, battery inverter rating and the battery control strategy. These parameters were mainly evaluated in chapter 3 and in 4.

7.2.1 For residential buildings

Chapter 2 analysed the impact of the PV orientation on the energy yield and the PV self-consumption. The influence of the PV orientation on the average SCR and average SSR is presented in Fig. 7.1. The largest self-consumed can be achieved with an average orientation of 212° azimuth and a tilt of 25°. This is the orientation with the largest self-sufficiency rate. A large variety in optimal orientations for self-consumption was found, between 172° and 247° module azimuth and between 11° and 38° module tilt. The influence of PV orientation was assessed by the difference between optimal orientation for self-consumption and optimal orientation for maximizing energy yield. It was found that PV self-consumption can be increased with a maximum of 4.6% for certain PV systems. However, the

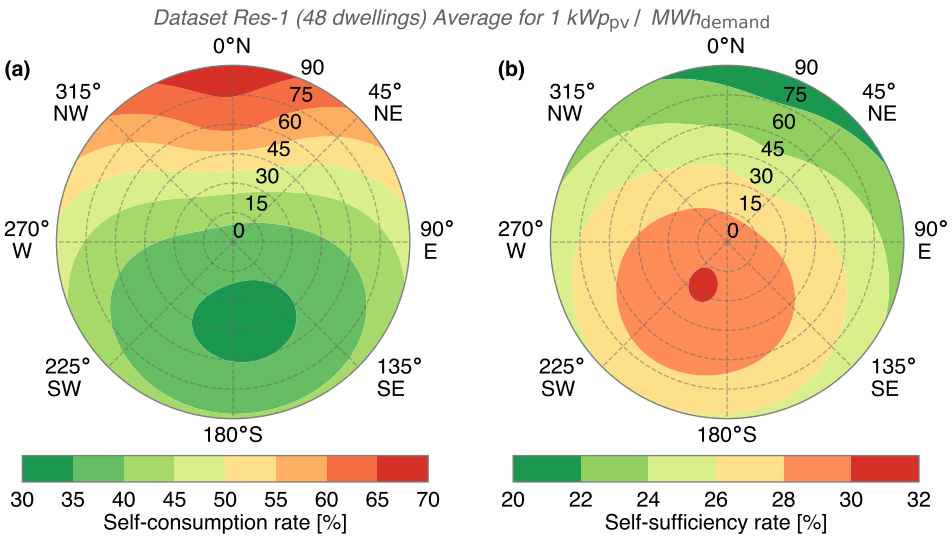

Figure 7.1 · Average self-consumption rate (a) and self-sufficiency rate (b) of dataset Res-1, depending on PV module orientation shown using a polar plot. Module azimuth angles are indicated by the directions on the outer axis and module tilt angles are indicated by the inner circles. Both angles were varied with 1° using the algorithm presented in chapter 2.

average increase is 1.5% using one year of data. This number decreases to 0.9% over the lifetime of a system due to PV system degradation.

The results from other chapters related to the SCR and SSR of residential buildings are presented in Fig. 7.2. Distributions are shown for three fixed PV system capacities and one for variable PV capacities. The PV capacities were normalized to annual electricity demand and are shown for 48 residential buildings. PV system sizes of 1 kWp per MWh annual demand can provide almost all annual electricity demand. The most left violin plots show the distributions of PV systems

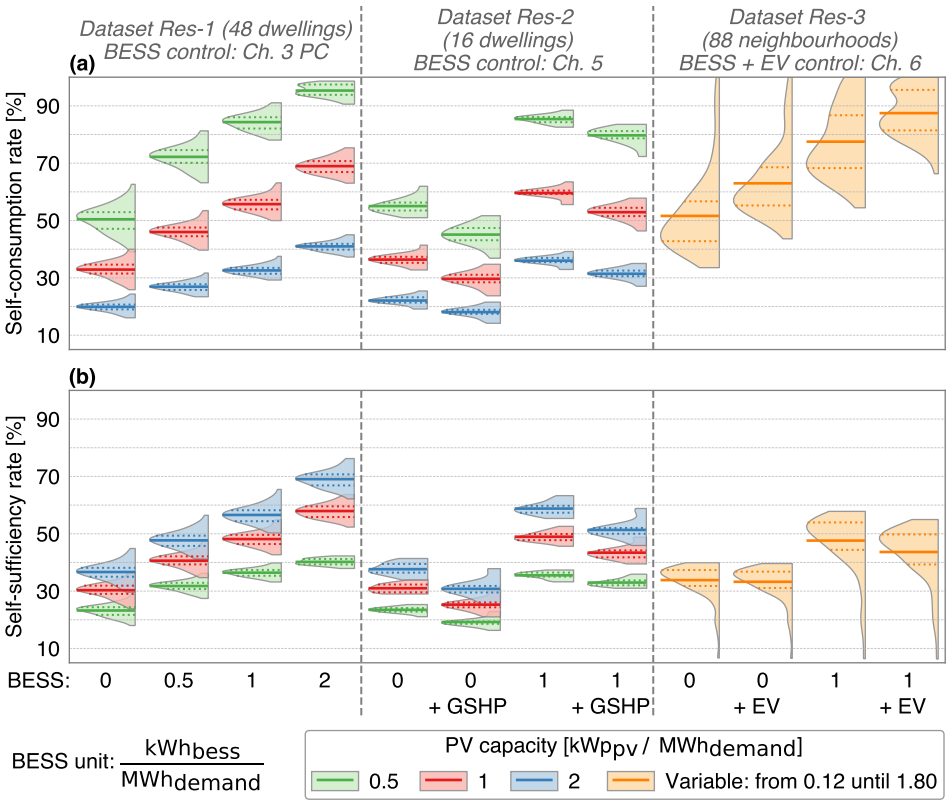

Figure 7.2 · Distributions of self-consumption (a) and self-sufficiency (b) for residential buildings using three datasets. The colour coded violin plots are shown for three fixed PV system capacities and one variable PV capacity, all normalized to the annual electricity consumption. Battery energy storage system (BESS) capacities are indicated by the number at the horizontal axis. The 1st to the 4th violin plots show the results for dataset 1, using the predictive control algorithm and no feed-in limit, obtained from 3. The 5th to 8th violins show the impact of a ground source heat pump system combined with battery storage for 16 residential dwellings obtained from chapter 5. The 9th until 12th violin plots show the impact of battery storage and electric vehicles for 88 neighbourhoods residential dwellings. These results are obtained with the spatio-temporal model framework presented in chapter 6. Mean values of the distributions are marked by solid lines, and 25% and 75% percentiles are indicated by dotted lines.

oriented to the south (180°) and a module tilt of 35°. SCRs decrease with PV system size and are on average 50%, 33% and 20% for PV capacities of respectively 0.5, 1 and 2 kWp per MWh annual demand. SSRs show a reversed trend, with averages of 23%, 30% and 37% for respectively 0.5, 1 and 2 kWp of PV capacity.

Battery energy storage significantly increased the SCR, which was studied in chapter 3. For a relative PV system size of 1 kWp, SCR increased to 46%, 56% and 69% with storage capacities of respectively 0.5, 1 and 2 kWh per MWh of annual demand. Also, the self-sufficiency is increased with larger storage capacities. A 1 kWp PV system with a 2 kWh storage capacity per MWh of annual electricity consumption could provide more than 50% of the yearly electricity demand. This could also be obtained with a 2 kWp PV system and a storage capacity of 1 kWh.

Also, chapter 3 described the influence of battery control strategies and forecasting algorithms on the self-consumption rates. A novel battery control strategy was developed that aimed to reduce the PV peak power to improve the PV self-consumption. The scenario that used the clear-sky forecast method (S-CS) showed the best performance to reduce PV peak power, with a loss of 0.6% in SCR rate. Likewise in chapter 4, self-consumption enhancement was combined with a different storage application. Here, the possibility to provide frequency restoration reserves (FRR) while improving self-consumption was investigated. It was found that self-consumption could be maintained when self-consumption was prioritized. If FRR provision was prioritized than the lost SCR would be 23% and storage would only contribute to 3.4% self-consumption.

Chapter 5 investigated the impact of PV and storage on the self-consumption of dwellings with a ground source heat pump (GSHP). An average SCR of 36% was found for this second dataset, compared to 33% for the first dataset. Furthermore, a smaller range was observed for the second dataset compared to the first dataset, mainly because fewer dwellings were included. If the electricity consumption of a GSHP was included in the residential demand, then SCR decreased. A relative PV system size of 1 kWp showed a SCR decrease of 6.7% points to 29.6%, while a relative small PV system of 0.5 kWp showed a SCR decrease of 10% points to 45%. A GSHP system added more electricity demand in winter months, therefore reducing the total self-consumption and self-sufficiency. Also, the contribution of storage to the SCR was slightly lower compared to dwellings without GSHP systems. For a 1 kWp PV system, increases of 14% points, 23% points and 30% points are seen for respectively 0.5, 1 and 2 kWh storage capacity.

Chapter 6 analysed the potential self-consumption and self-sufficiency for the city of Utrecht, for 88 different neighbourhoods. PV system size and PV yield were determined based on availability of residential rooftops space and incoming irradiance. Electricity demand patterns of households were combined with battery

energy storage and future electric vehicles demand. Variable relative PV system capacities per neighbourhood were used, with an average capacity of 1.09 kWp for each MWh of demand, and a range between 0.11 and 1.80 kWp per MWh demand. It was found that most neighbourhoods could not provide sufficient PV energy to fulfil the annual demand, even with an average installed capacity above 1 kWp per MWh demand. The research of this chapter included all rooftop orientations and reduced irradiance due to shade of surrounding buildings. Consequently, the average specific yield of the neighbourhoods was 629 kWh per kWp installed PV capacity. As a result, SCR varied between 34% and 100%. 1 kWh of storage capacity per MWh of annual demand contributed to an increase in SCRs between 0% and 30% with an average of 25%. Electric vehicles showed a lower increase to the SCR with an average of 12%.

7.2.2 For commercial buildings

The influence of the PV orientation on the average SCR and average SSR of 42 commercial buildings is presented in Fig. 7.3. Chapter 2 found that the optimal orientation for commercial systems to maximize self-consumption is on average 188° azimuth with a relative low module tilt of 17.2°. The average self-consumption benefits decreases from 1.2% in the first year to 0.9% in year 25.

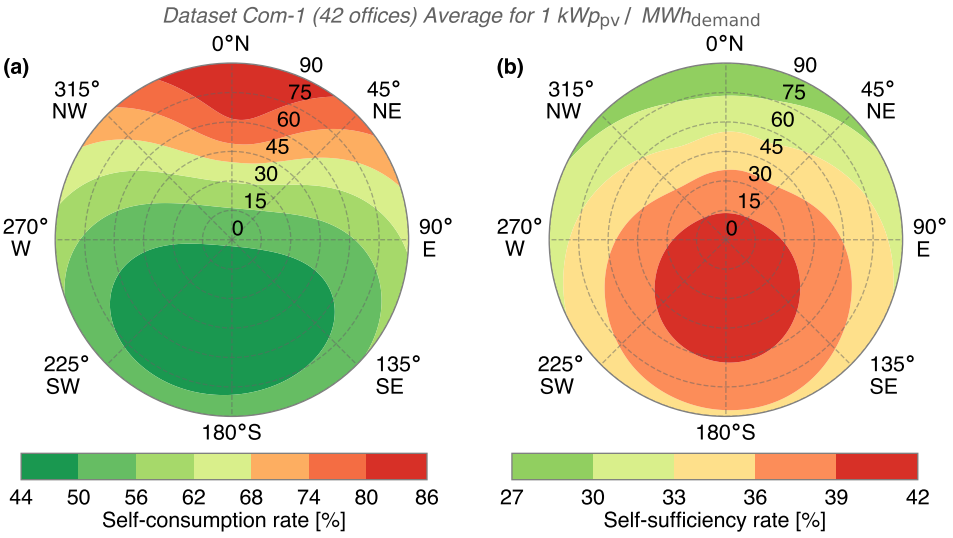

Figure 7.3 · Average self-consumption rate (a) and self-sufficiency rate (b) depending on the PV module orientation of dataset Com-1. Module azimuth angles are indicated by the directions on the outer axis and module tilt angles are indicated by the inner circles. Both angles were varied with 1° using the algorithm presented in chapter 2.

These self-consumption benefits are mainly caused by a lower module tilt than the tilt for maximal energy production (35°).

The findings using methods and data from chapter 3 related to the SCR and SSR is presented in Fig. 7.4. The most left violin plots shows the distributions of SCR and SSR for 42 commercial buildings with an orientation of 180° azimuth and 35° tilt. Average SCR rates are 68%, 44% and 26% for respectively 0.5, 1 and 2 kWp of installed PV capacity per MWh of annual demand. These SCR are larger compared to the SCR for residential buildings, because more energy consumption occurred during daytime on moments of relative large PV production. Also SSR are larger, with averages of 32%, 41% and 49% for respectively 0.5, 1 and 2 kWp PV. The distribution range of residential buildings is larger than commercial buildings. This is due to the large variation in time of energy use for residential buildings compared to commercial buildings.

The SCR of a 1 kWp PV system is increased due to battery energy storage, with 13% points, 22% points and 32% points for respectively 0.5, 1 and 2 kWh per MWh of annual demand. Commercial systems have a larger SCR compared to residential systems. Consequently, the self-consumption gain by storage is lower for PV systems placed on commercial buildings. Two third of the yearly electricity demand from commercial buildings can be provided by a 1 kWp PV system and a 2 kWh storage system per MWh of annual electricity consumption. Also, a maximum average self-sufficiency of 80% can be obtained if a 2 kWp PV

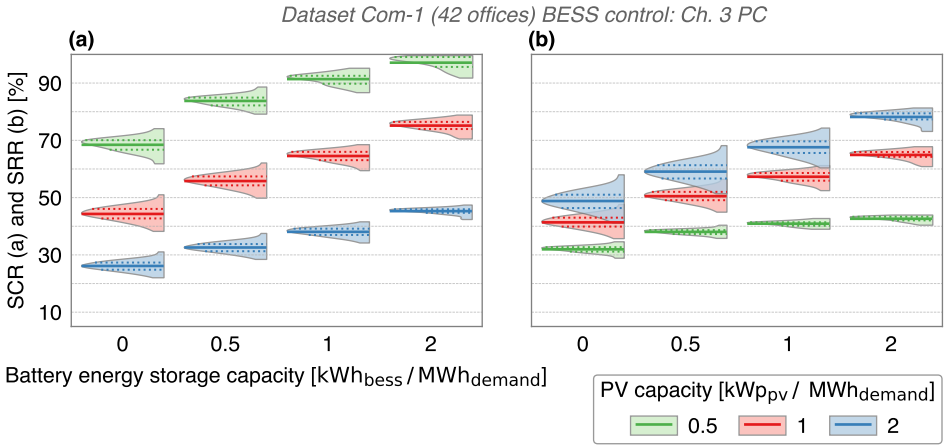

Figure 7.4 · Distributions of self-consumption (a) and self-sufficiency (b) for 42 commercial buildings from dataset Com-1. The colour coded violin plots are shown for three fixed PV system capacities and one variable PV capacity, all normalized by the annual electricity consumption. Battery storage capacities are indicated by the number at the horizontal axis. The impact of energy storage was assessed using the exact PC battery control algorithm from chapter 3. Mean values of the distributions are marked by solid lines, and 25% and 75% percentiles are indicated by dotted lines.

system with a 2 kWh storage capacity is combined.

It was found in chapter 3 that the SCR loss due to peak shaving is only around 0.2% for the best performing forecast algorithm. Thus, the self-consumption can be maintained while reducing PV peak power. Chapter 4 showed that comparable SCR were obtained when FRR was provided as a secondary application. Yet, when FRR provision was prioritized than the lost SCR would be 19.8% and storage would only contribute to 3.8% self-consumption. This contribution is larger than for residential systems and is initially a result of lower retail prices for commercial systems. As a result, more moments occurred to provide FRR with storage to the balancing market. This increased the availability of storage capacity for self-consumption enhancement.

7.3 On reducing feed-in peak power

This section aims to provide insights regarding the following research question:

Q 2. How can PV feed-in peak power be reduced?

The PV feed-in power can be reduced by increasing consumption of PV peak power and by storage of the production peak. The reduction of PV feed-in peak power was quantified using the curtailment loss ratio (CLR). If feed-in limits (FILs) are present, then a maximum amount of PV power can be fed back in to the grid. The power which cannot be fed-back, nor be used, cannot not be generated by the PV system. The CLR is the share of PV energy that is lost from the total share of PV energy that is produced. Thus, the CLR can be seen as a measure to quantify the energy which is not used above a certain feed-in limit.

Two PV FILs were used to present the main findings on reducing PV feed-in peak power; a FIL of 0.5 kW per kWp and a FIL of 0.2 kW per kWp. The peak power produced by the PV system depends on orientation and performance ratio (PR). For a perfect performing system (PR 91 %) and a FIL of 0.5 kW/kWp, around 14% of annual PV energy cannot be exported to the grid. However, the average PR in the Netherlands is around 85%, which results in a CLR of 11.4%. This number decreases over time due to PV system degradation, and is expected to be 6.7% after 30 years. These CLR can be reduced by optimizing the PV module orientation, which was assessed in chapter 2. The performance of forecasting algorithms and a two battery control strategies on the CLR were assessed in chapter 3. The impact of ground source heat pumps and another battery control strategy on the maximum PV and load peak reduction for residential dwellings was assessed in chapter 5.

7.3.1 For residential buildings

The influence of the PV orientation on the curtailment loss ratio for a FIL of 0.5 kW/kWp and a FIL of 0.2 kW/kWp are shown in Fig. 7.5. Chapter 2 found that the optimal orientation for systems to minimize curtailment losses, while maximizing energy production, for a FIL of 0.5 kW/kWp was on average 183° azimuth and ° tilt. Optimal orientation for a FIL of 0.2 kW/kWp was on average 188° azimuth with a relative low module tilt of 24°. Reductions in CLR for a 1 kWp system were 0.5% points and 2% points for FILs of respectively 0.5 and 0.2 kW/kWp. Also, CLR of larger systems could be reduced more when shifting the orientation.

Methods and results from chapter 3 and chapter 5 related to the CLR for residential buildings are presented in Fig. 7.6. The distributions are shown for three PV system capacities, normalized to annual electricity demand. The first row of violin plots show the CLRs for a PV system with an orientation of 180° azimuth and with a module tilt of 35°. Curtailment losses decrease over time due to reduced PV produced power and battery storage capacity, see Fig. 3.10. For a FIL of 0.5 kW, CLR are on average 2%, 4% and 6% for PV system sizes of respectively 0.5, 1 and 2 kWp per MWh of annual demand. Larger PV systems have a higher CLR, whereas smaller PV systems have a lower CLR. A very restricted FIL of 0.2kW shows larger curtailment losses, with averages of 20%, 29% and 35% for PV capacities of respectively 0.5, 1 and 2 kWp.

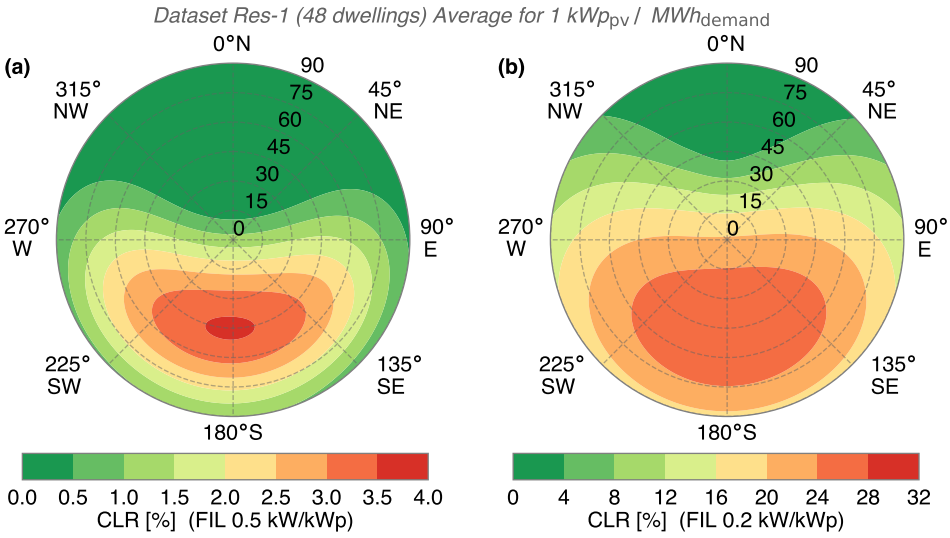

Figure 7.5 · Average curtailment loss ratio for a feed-in limit of 0.5 kW/kWp (a) and for a feed-in limit of 0.2 kW/kwp (b) depending on the PV module orientation using dataset Res-1. Module azimuth angles are indicated by the directions on the outer axis and module tilt angles are indicated by the inner circles. Both angles were varied with 1° using the algorithm presented in chapter 2.

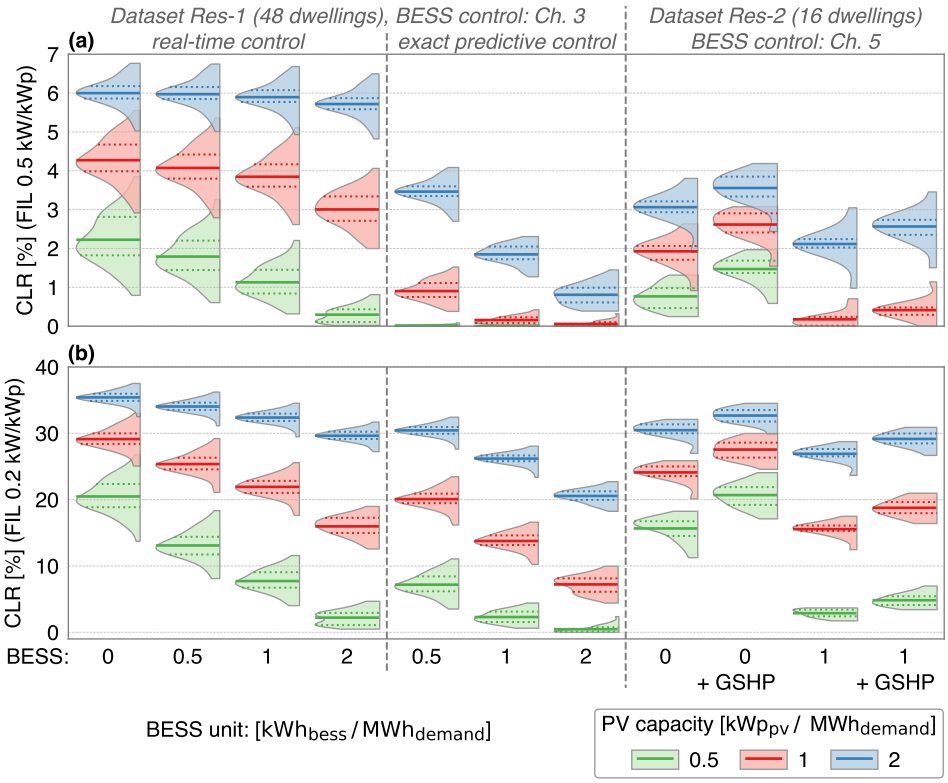

Figure 7.6 · Distributions of curtailment loss ratio for a feed-in limit of 0.5 kW/kWp (a) and for a feed-in limit of 0.2 kW/kWp (b) for residential buildings from two datasets. Battery energy storage system (BESS) capacities are indicated by the number of the horizontal axis. The 1st to 4th violin plots shows the impact of energy storage using the real-time control strategy from chapter 3. The 5th to 7th violin plots show the impact of energy storage using the exact predictive control strategy from chapter 3. The 8th to 11th violin plots show the impact of a ground source heat pump system combined with battery storage for 16 residential dwellings for a 30-year lifetime. These results are obtained using the battery control algorithm presented in chapter 5. Mean values of the distributions are marked by solid lines, and 25% and 75% percentiles are indicated by dotted lines.

Chapter 3 aimed to reduce the CLRs using a novel predictive control (PC) algorithm. A real-time control (RC) algorithm was used as comparison. It was found that battery storage combined with the PC strategy has significantly larger reduction of CLR compared to using the RC strategy. With a FIL of 0.5 kW/kW, a 1 kWh storage system and a 1 kWp PV system, the CLR was reduced with 0.4% points if using the real-time control. The CLR was reduced to 0.1% with the predictive control using the exact forecasted PV and consumption patterns. Forecasting methods to predict PV and demand were developed and used as input for the PC control. Forecasting electricity consumption of residential buildings should use the average electricity consumption of the previous seven days. Clear-sky forecast scenarios showed the best performance to reduce curtailment losses, with a

CLR of 1% larger than obtained with the exact PC algorithm.

Chapter 5 assessed the impact of dwellings with a ground source heat pump and battery energy storage on the curtailment loss ratio. With a FIL of 0.5 kW/kWp, CLRs of the second dataset are significantly lower than compared to the first dataset. The Res-2 dataset contains PV patterns which were measured from real PV systems. These PV systems have a module tilt of 10°, and therefore generate a lower PV peak. Moreover, a battery control algorithm was used which discharged the battery storage during night time. Therefore additional storage capacity is available during the day which slightly recued the curtailment losses. The difference between the Res-1 and Res-2 dataset is smaller for a FIL of 0.2kW/kWp. With this FIL, the storage is already fully charged during the day and the impact of active discharging is lower. Also the influence of the module tilt is lower for this feed-in limit. Dwellings with GSHP systems have a larger relative installed PV system than dwellings without a GSHP system. Therefore the dwellings with GSHP show a larger CLR than dwellings without GSHP

7.3.2 For commercial buildings

The influence of the PV system orientation on the CLR of commercial buildings is shown in Fig. 7.7. It was found in chapter 2 that the orientation for minimizing curtailment losses for a FIL of 0.2 kW/kWp is 182° azimuth and 24° tilt. This is

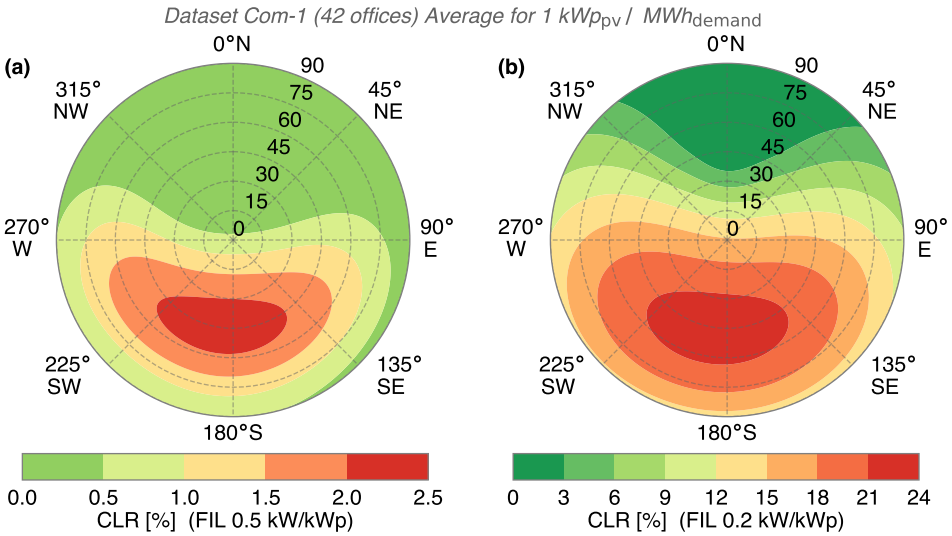

Figure 7.7 · Average curtailment loss ratio for a feed-in limit of 0.5 kW/kWp (a) and for a feed-in limit of 0.2 kW/kwp (b) depending on the PV module orientation using dataset Com-1. Module azimuth angles are indicated by the directions on the outer axis and module tilt angles are indicated by the inner circles. Both angles were varied with 1° using the algorithm presented in chapter 2.

close to the optimal orientation for energy production. As a result, the CLR reduction due to changing PV system orientation is below 1% for both a FIL of 0.5 and 0.2 kW.

The impact of commercial buildings on the CLR from chapter 3 is shown in Fig. 7.8. An orientation of 180° azimuth and 35° tilt was used. For a FIL of 0.5 kW/kWP, CLR are on average 0.8%, 2.5% and 5% for PV sizes of respectively 0.5, 1 and 2 kWp per MWh annual demand. These CLR are considerably lower than observed for residential buildings. Thus electricity demand peaks have a better overlap with PV production peaks for commercial than residential buildings. Also, with a FIL of 0.2 kW/kWP, the CLRs are lower for commercial buildings, especially for PV systems with a relative size of 0.5 kWp per MWh of annual demand.

Also, chapter 3 showed that CLRs for commercial systems are reduced with the predictive control (PC) algorithm. Best performing forecast methods are the clear sky method to forecast PV production and using the electricity consumption of the previous weekday to forecast demand. These forecast methods show a CLR of 0.5% larger than obtained with the PC algorithm which used the exact PV yield and demand forecasts. A 5-year shorter lifetime was assumed for commercial systems compared to residential systems, thus the impact of PV degradation on CLR is smaller for commercial systems. Moreover, electricity consumption forecasts should use measured historical demand time series from the previous weekday.

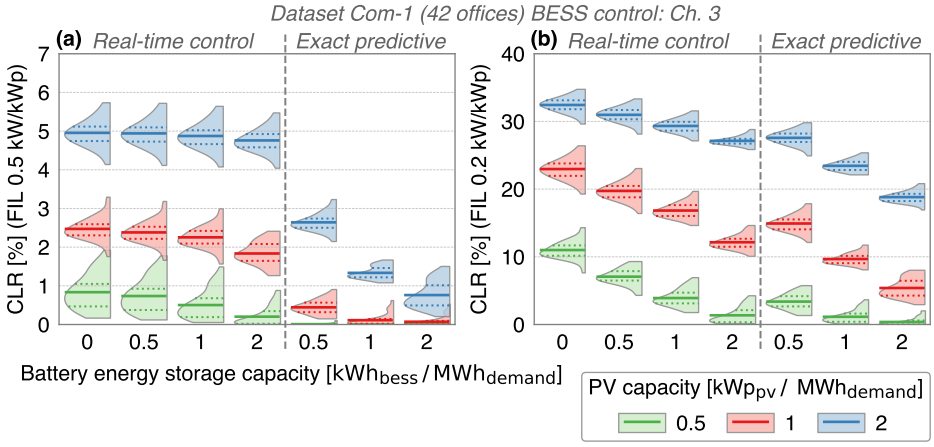

Figure 7.8 · Distributions of curtailment loss ratio for a feed-in limit of 0.5 kW/kWp (a) and for a feed-in limit of 0.2 kW/kWp (b) for 42 commercial buildings from dataset Com-1. Battery energy storage system (BESS) capacities are indicated by the number of the horizontal axis. The 1st to 4th violin plots show results of the impact of real-time control strategy and the 5th to 7th violin plots show results of the impact using the exact predictive control strategy, both presented in chapter 3. The curtailment losses are shown for a PV and storage system with a 20-year lifetime. Mean values of the distributions are marked by solid lines, and 25% and 75% percentiles are indicated by dotted lines.

7.4 On realizing economic benefits

This section aims to provide insights regarding the following research question:

Q 3. What economic benefits can be realized?

Economic benefits can be obtained from PV self-consumption and from reduction of PV feed-in power. The benefits from self-consumption and reduced feed-in power depend on the price of the sold and bought electricity. Additional economic benefits from battery storage can be realized when storage is used for other applications, for example providing balancing services to the electricity grid. Economic benefits due to changing PV orientation were assessed in chapter 2. Benefits from PV self-consumption and from reduction of PV feed-in power using battery storage were assessed in chapter 3.The benefits of combining self-consumption enhancement with frequency restoration reserves provision as a secondary application was presented in chapter 4. Economic benefits of electrification of heating using ground source heat pumps combined with PV and storage was presented in chapter 5.

In this thesis, multiple economic performance indicators were used to assess the economic feasibility. To compare the results of each chapter, the discounted payback period (DPBP) was used. PV system payback periods are commonly used in the residential market, therefore DPBP was selected. Only chapter 5 provided DPBP periods. Consequently, results of other chapters were translated to DPBP, with the equation and assumptions shown in Box.7.1. In addition, a scenario in which PV and storage are installed in 2023 was assessed. In this case, a 25% lower investment cost is assumed. Also, a lower feed-in tariff of 25% for 15 years was assumed.

Box 7.1 · Calculation and assumptions used for discounted payback period

Discounted payback period was calculated by the following steps. First, the annual (y) cash flows obtained from self-consumption (CF_{SC}) were determined by multiplying the annual electricity demand (E_{demand}) with the self-sufficiency rate and the electricity consumption tariff (π_{cons}). Secondly, the annual cash flow obtained from exporting PV electricity was calculated by multiplying the annual PV energy production (E_{PV}) with the share of PV that is exported (1 - self-consumption rate - curtailment loss ratio). This number was then multiplied with the feed-in tariff ($\pi_{feed-in}$). The total annual cash flow is the summation of the cash flows from self-consumption and exporting electricity minus the annual O &M cost. Next the net present value (NPV) was determined. Finally, the discounted payback period was found by selecting the year for which the NPV is identical to zero, see Eq. (7.1).

$$CF_{SC}, y = E_{demand}, y \cdot SSR \cdot \pi_{cons}, y \tag{7.1a}$$

$$CF_{PV.\,export}, y = E_{PV}, y \cdot (1 - SCR - CLR) \cdot \pi_{feed\text{-}in}, y \tag{7.1b}$$

$$CF, y = \mathrm{CF}_{SC}, y + \mathrm{CF}_{PV.\,export}, y - \mathrm{O\&M}_{PV\,BESS}, y \tag{7.1c}$$

$$NPV = \sum_{y=0}^{L_{econ}} \frac{CF, y}{(1+r)^y} - I_{PV} - I_{BESS} \tag{7.1d}$$

$$DPBP = \left\{ y \quad \text{where NPV, y} == 0 \right. \tag{7.1e}$$

The economic assumptions for residential systems are similar to the ones described in section 5.C and Table 5.1, but replacement costs were included in O &M cost. Main economic assumptions for commercial systems are obtained from Table 4.1. The consumption tariff is assumed to be 0.106 €/kWh with a 0.5% annually increase[128]. The feed-in tariff is presumed to be 0.106 €/kWh, assuming the present feed-in subsidy for stimulation of sustainable energy production[228]. After 15 years an feed-in tariff as explained in section 5.C was used. PV systems >100 kWp were assumed based on the annual electricity demand , (see Fig. 4.2) and investements cost are assumed 900 €/kWp[228]. Similar O&M cost were used for PV as for BESS systems.

7.4.1 For residential buildings

The influence of the PV system orientation on the discounted payback periods using dataset Res-1 is shown in Fig. 7.9. The left polar plot shows the DPBP in which a current investment is made and the right polar plot shows the DPBP for a PV system that would be installed in 2023. For the next 30 years, the average ratio between the electricity consumption tariff and the electricity feed-in tariff is around 0.5. Chapter 2 found that the optimal orientation to maximize revenue is 188° azimuth and 34° tilt. PV systems that will be installed in 2023 are expected to receive lower feed-in tariff during their lifetime, but with higher consumption tariffs. Consequently, the optimal orientation for revenues shifts towards 190° and an average tilt of 34° tilt.

Chapter 3 investigated the benefits of self-consumption enhancement and reduction of curtailment losses. These benefits were translated to DPBP for 48 residential PV and storage systems, are presented in Fig. 7.10. The distributions show three feed-in limits: no FIL, a 0.5 kW/kWp FIL and a 0.2 kW/kWp FIL. Currently, PV and storage systems are installed without feed-in limit and have an increase in DPBP with larger PV system or battery storage capacities. Average DPBP of PV systems without storage are 9.1, 9.9 and 10.5 years for PV capacities of respectively 0.5, 1 and 2 kWp per MWh annual demand. The value of self-consumption is not sufficient to recuperate the investments from storage.

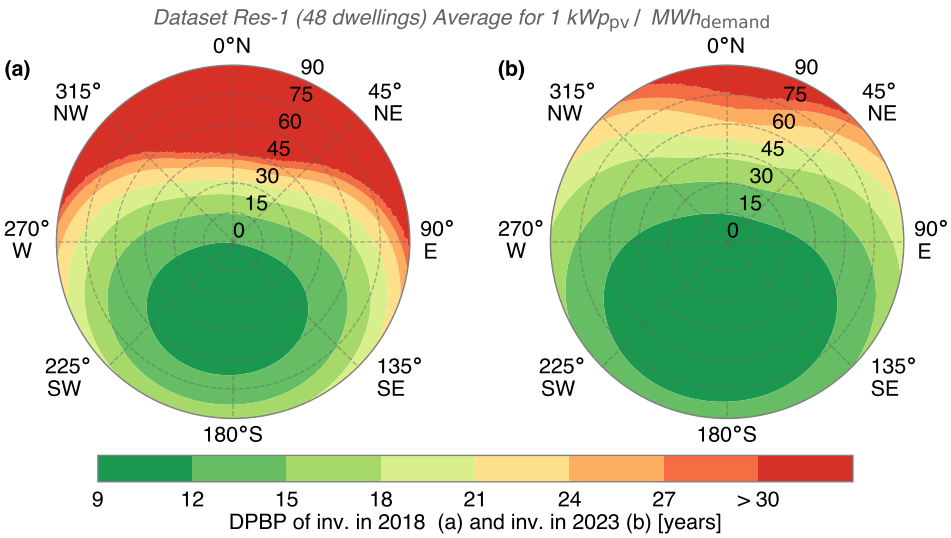

Figure 7.9 · Average discounted payback periods for investing in 2018 (a) for investing in 2023 (b) depending on the PV module orientation using dataset Res-1. Module azimuth angles are indicated by the directions on the outer axis and module tilt angles are indicated by the inner circles. Both angles were varied with 1° using the algorithm presented in chapter 2.

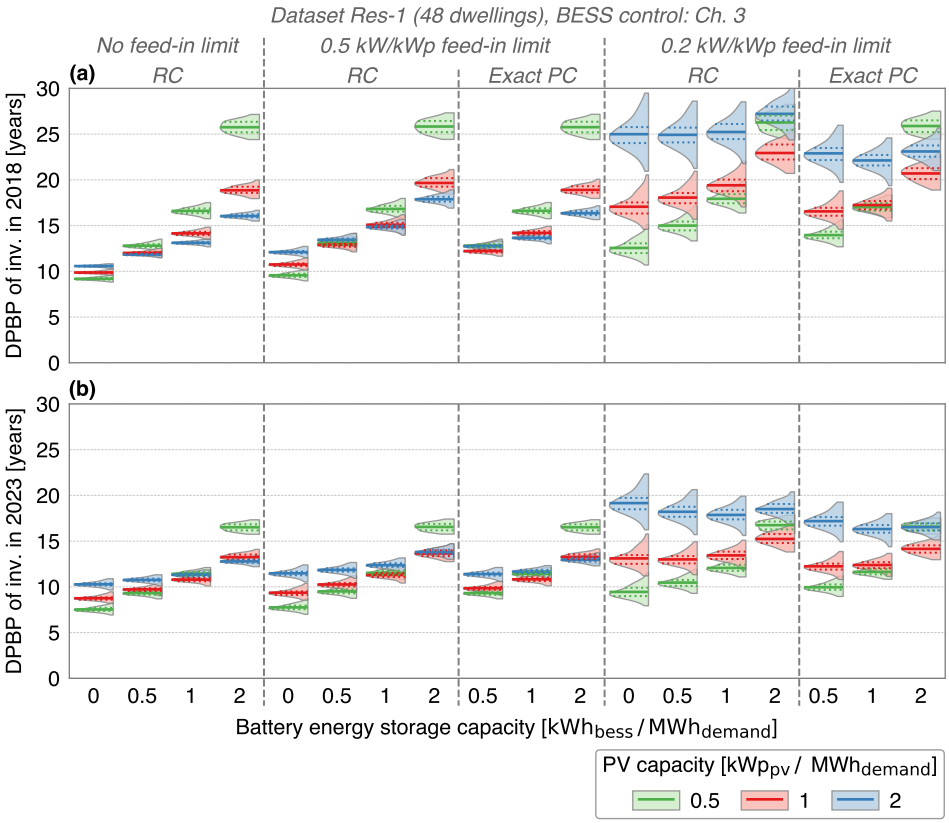

Figure 7.10 · Distributions of discounted payback periods of 48 residential PV battery systems for three relative PV system sizes and two investment scenarios: investing in 2018 (a) and investing in 2023 (b). DPBP larger than 30 years are not shown on the graph. The DPBP are shown for three feed-in limits and obtained using the methods from chapter 3. The 1st to 4th violin plots show the distribution of no feed-in limit present and with the real-time control strategy. The 5th to 11th violin plots show the DPBP of including a feed-in limit of 0.5 kW/kWp. The 5th to 8th violin plots show the results with the real-time control strategy and the 9th to 11th violin plots with the predictive control strategy. The 12th to 18th violin plots show the DPBP of including a feed-in limit of 0.2 kW/kWp. Results from the real-time control strategy are shown in the 12th to 15th violin plots and from the predictive control strategy in the 16th to 18th violin plots. Mean values of the distributions are marked by solid lines, and 25% and 75% percentiles are indicated by dotted lines.

Systems with storage show lower DPBP for 2 kWp/MWh demand installed PV capacity compared to 0.5 kWp. Larger PV systems obtained more absolute revenue which reduced the overall system cost.

A FIL of 0.5 kW/kWp increases the DPBP between 0.4 and 1.5 year depending on the PV system size. Moreover, a small reduction in DPBP is observed for the PC strategy compared to the RC strategy. In case of a FIL of 0.2 kW/kWp, a 0.5 kWh storage capacity per MWh reduces the DPBP with 4 months. Larger storage capacities increase the DPBP, but the benefit of storage increases with larger PV

capacities. As a result, smaller PV systems with storage have higher DPBP than larger PV systems with storage. A FIL of 0.2 kW/kWp significantly increases the DPBP. Also, the difference in DPBP between the RC strategy and PC strategy is larger.

DPBP are slightly reduced when PV and storage systems are installed in 5 years from now. Expected DPBP for PV systems only are 7.5, 8.8 and 10.3 years for PV capacities of respectively 0.5, 1 and 2 kWp per MWh annual demand. The DPBP for a 2 kWp PV system shows a lower reduction compared to the 2018 scenario, since future feed-in tariffs are reduced. A small benefit by storage can be observed for a very restricted feed-in limit of 0.2 kW/kWp, due to a higher value of self-consumption. The value of reducing curtailment loss is lower because of a future feed-in tariff. Consequently, the economic benefit of the PC strategy compared to the RC strategy decreases. Still, a 1 kWp PV system without storage and a feed-in limit of 0.2 kW/kWp shows an average of DPBP of <13 years.

Distributions of DPBP obtained from other chapters are presented in Fig. 7.11. Chapter 4 investigated the additional benefits when frequency restoration reserves were provided by PV-battery systems. The DPBP using the SCO, PSC and PSR battery control strategies were assessed for PV-battery systems and for storage systems only. The battery control strategies that provide FRR provision have a large decrease in DPBP for storage. Consequently, the DPBP of the total PV-battery systems decreases. The control strategy that prioritizes the FRR provision (PSR) has DPBP below 10 years for all assessed PV system sizes.

Installing a PV-battery system in 2023 shows lower DPBP in all scenarios due to larger self-consumption benefits and lower investment cost from PV -battery storage systems. The DPBP from storage of the PSR control strategy shows a relatively small decrease when the system is installed in 2023, despite the 75% reduction in storage cost. The future feed-in tariffs for residential systems are lower while the consumption tariffs increase. This reduces the operating window for FRR provision and therefore the revenues from this service, see Fig. 4.3. As a result, revenues from the FRR market decreases. Yet, revenues of these markets were based on price data from 2012 till 2016, while future balancing market prices are highly uncertain.

Chapter 5 assessed the impact of dwellings with GSHP, PV and battery storage on the DPBP using dataset Res-2. Slightly larger DPBP are observed for dataset Res-2 compared to dataset Res-1. dataset Res-2. This difference is mainly caused by the lower PV production and the addition of replacement cost in dataset Res-2. Dwellings with GSHP systems showed higher DPBP than dwellings without GSHP systems. Moreover, the correlation between net present value and avoided emissions was investigated. Dwellings with GSHP systems increased their NPV with ≈

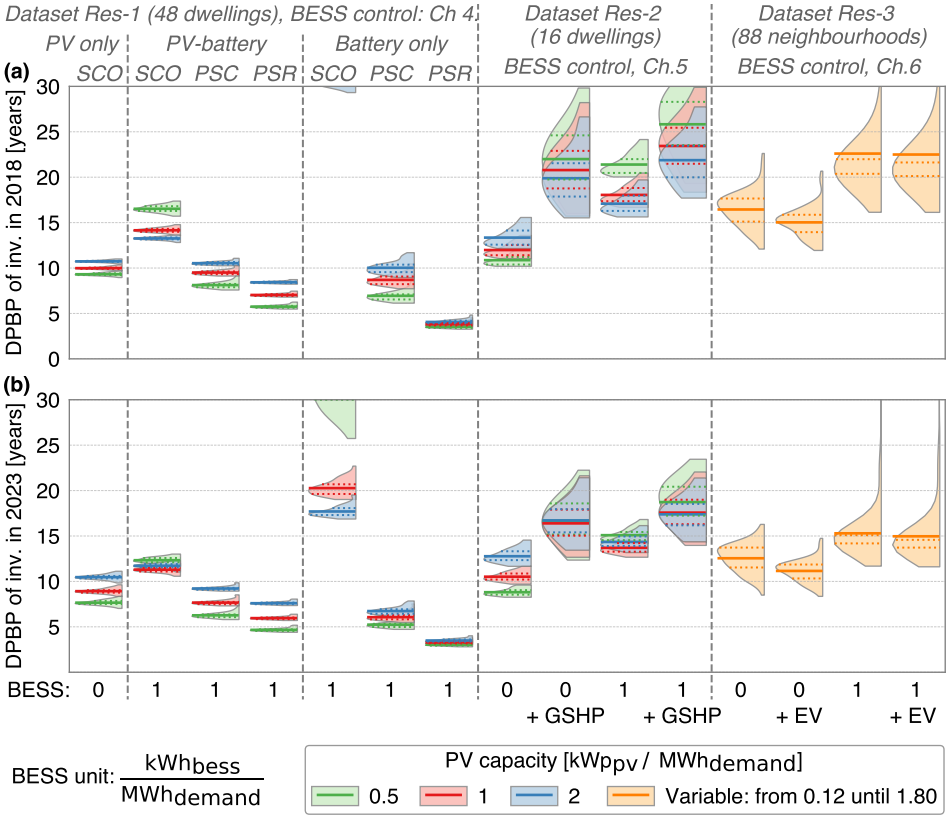

Figure 7.11 · Distributions of discounted payback time from three chapters for investing in 2018 (a) and investing in 2023 (b). DPBP larger than 30 years are not shown on the graph. The 1st to 7th violin plots show the impact of combining self-consumption enhancement with frequency restoration reserves provision, obtained from chapter 4. The 1st and 4th violin plots show the DPBP for the PV and storage system. The 5th and 7th violin plots show the DPBP of only the storage systems, as presented chapter 4. The 1st, 2nd and 5th violin plots are results from the SCO strategy. The 3rd and 6th violin plots show DPBP from the PSC strategy and the 4th and 7th violin plots show distributions from the PSR strategy. The 8th to 11th violins plot show the DPBP of ground source heat pump system combined with battery storage for 16 residential dwellings, from chapter 5. The 12th until 15th violin plot show the impact of a battery storage and electric vehicles for the DPBP for 88 neighbourhoods from chapter 6. Mean values of the distributions are marked by solid lines, and 25% and 75% percentiles are indicated by dotted lines.

€275 for each additional ton of avoided tCO_2-eq emissions. Dwellings with solely a PV system increased the NPV with €180 per tonne. This indicates that emission reduction by GSHP systems would be more profitable than for PV systems. However, dwellings with a GSHP system will need to avoid at least 46 tonne to have a positive NPV, while PV systems will always have a positive NPV. Another important aspect found in this study is the load peak shaving of residential dwellings by storage. The import peak can be reduced with 30% for dwellings with a GSHP.

Consequently, more GSHP systems can be installed without expansion requirements of the low voltage grid. These avoided costs were not included as financial benefits for storage.

Chapter 6 assessed the impact of the PV potential combined with EVs and battery storage on 88 neighbourhoods. Results from the chapter were used to calculate economic benefits. DPBP are 16 years on average for PV systems only, which is significantly larger than found in the other chapters. The DPBP distribution consists of PV systems that were placed under all orientations and were affected by surrounding obstacles. This decreased the PV yield (see Fig. 6.4) and consequently results in higher DPBP. Lower DPBP are observed when electric vehicle charging was included due to the increasing electricity consumption and self-consumption. Moreover, storage does not decrease DPBP for both investing in 2018 and 2023.

7.4.2 For commercial buildings

The influence of the PV system orientation on the DPBP for commercial buildings is shown in Fig. 7.12. The ratio between the electricity consumption and the feed-in tariff for commercial systems is close to 1. Consequently the economic value of self-consumption is low. Chapter 2 found that the optimal orientation to

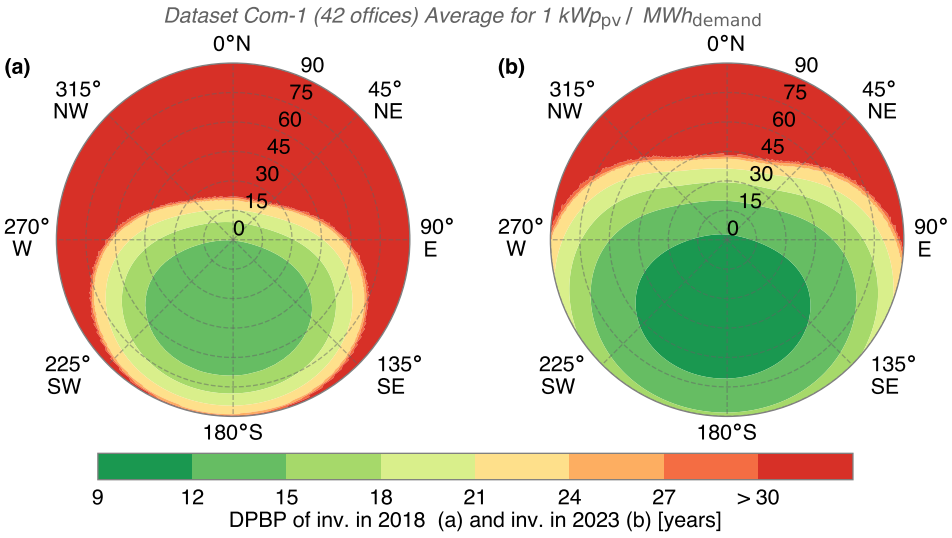

Figure 7.12 · Average discounted payback periods for investing in 2018 (a) for investing in 2023 (b) depending on the PV module orientation using dataset Com-1. Module azimuth angles are indicated by the directions on the outer axis and module tilt angles are indicated by the inner circles. Both angles were varied with 1° using the algorithm presented in chapter 2.

maximize revenue for this ratio is 185° azimuth and 35° tilt, which is similar to the optimal orientation to maximize revenues.

The economic benefits of self-consumption and curtailment loss reduction for 42 commercial systems are presented in Fig. 7.13. Commercial systems show higher DPBP than residential systems under the no feed-in limit scenario. DPBP for only PV systems are around 12.4 years, almost independent of PV system capacity. Investing in commercial PV systems in 5 years from now will reduce the DPBP for PV and PV-battery systems. Also, a difference in PV system size can be observed, due to the increased economic value of self-consumption. However, this value is too small for a profitable use of storage to enhance self-consumption

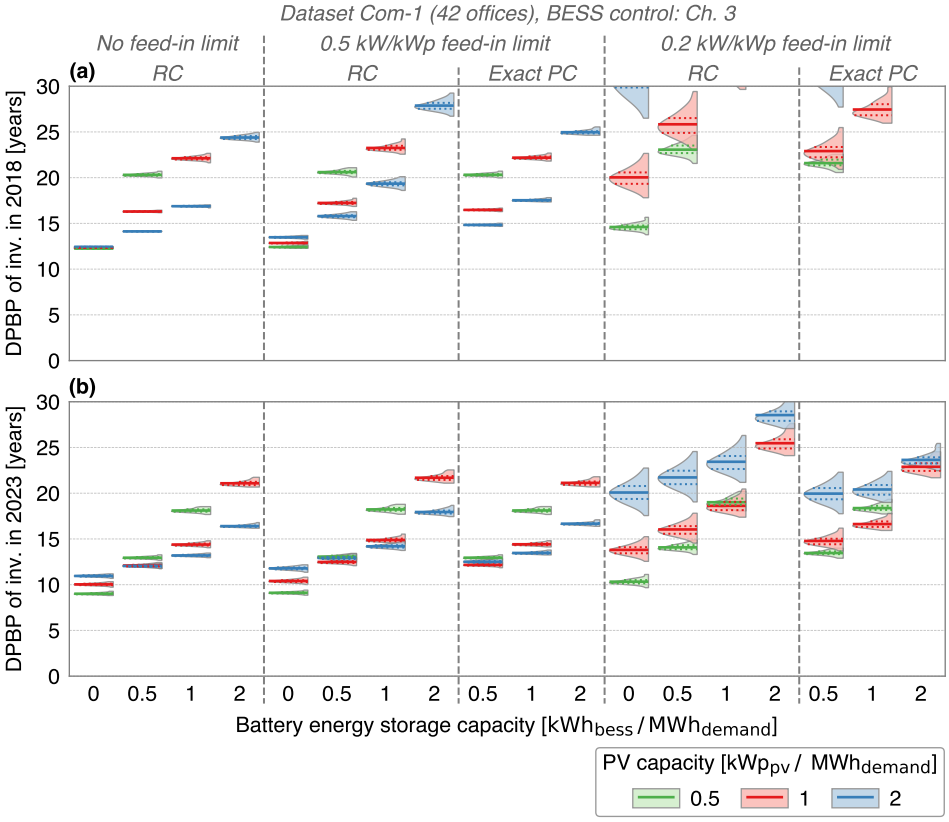

Figure 7.13 · Distributions of discounted payback periods of 42 commercial PV battery systems for three relative PV system sizes two investment scenarios: investing in 2018 (a) and investing in 2023 (b). The DPBP are shown for three feed-in limits and obtained from chapter 3. DPBP larger than 30 years are not shown on the graph. The 1st to 4th violin plots show the distribution of no feed-in limit present and with the real-time control strategy. The 5th to 11th violin plots show the DPBP with a feed-in limit of 0.5 kW/kWp, and the 12th to 18th violin plots show the DPBP of including a feed-in limit of 0.2 kW/kWp. Used battery control strategies are given above the violin plots. Mean values of the distributions are marked by solid lines, and 25% and 75% percentiles are indicated by dotted lines.

and to reduce curtailment loss. Moreover, the economic impact of predictive control strategy on the DPBP is lower for commercial than for residential systems.

The DPBP of residential systems are smaller than for commercial systems. More revenues are obtained from the export of electricity for residential systems than for commercial systems. Also, electricity tariffs for commercial systems are lower than for residential systems, which decrease the value from the direct or indirect consumption of PV electricity. Moreover, a 4% annual discount rate for commercial systems was assumed, which is twice the discount rate as residential systems. Storage has no benefit for commercial systems in all scenarios due to the low self-consumption value.

Chapter 4 analysed additional benefits of combining self-consumption with FRR provision. Results of 42 commercial systems are presented in Fig. 7.14. Prioritizing FRR provision before self-consumption (PSR control strategy) reduces the DPBP. Battery storage cost for commercial systems are lower than for residential systems. However, higher DPBP for systems with batteries are seen for commercial systems than residential systems. This is mainly due to the lower economic value of self-consumption for commercial systems compared to residential systems.

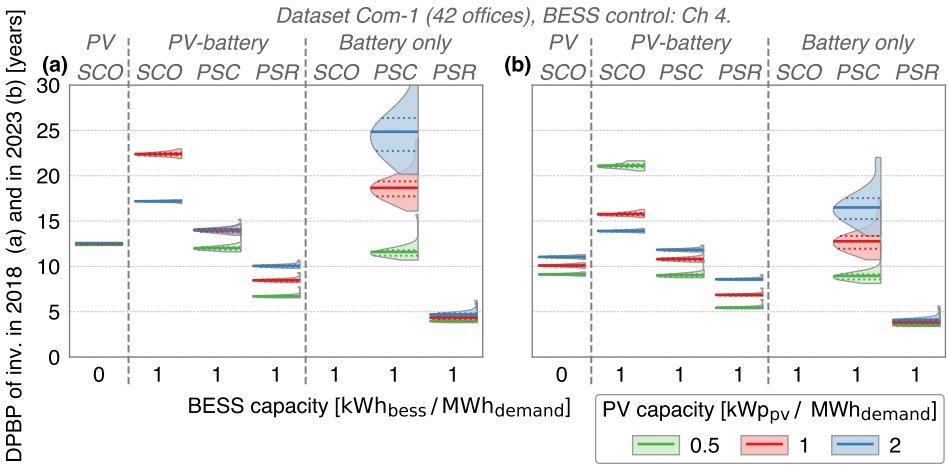

Figure 7.14 · Distributions of discounted payback time for 42 commercial systems, for investing in 2018 (a) and investing in 2023 (b). DPBP larger than 30 years are not shown on the graph. The distributions show the impact of combining self-consumption enhancement with frequency restoration reserves provision, with three battery control strategies obtained from chapter 4. The 1st and 4th violin plots show the DPBP for the PV and storage system, and the 5th and 7th violin plots from storage system only. The used battery control strategies are show above the violin plots. Mean values of the distributions are marked by solid lines, and 25% and 75% percentiles are indicated by dotted lines.

7.5 On realizing GHG emission reductions

This last section of the synthesis chapter aims to provide insights regarding the research question:

Q 4. What GHG emission reductions can be realized?

Direct energy consumption of PV produced electricity lowers the need to import electricity from the grid. Therefore carbon intensive electricity production by fossil fuel fired power plants is substituted. The impact of this substitution to the avoided life cycle greenhouse gas emission was assessed in both chapter 5 and in chapter 6. Emissions were assessed from two perspectives; an electricity system perspective and a dwelling or neighbourhood perspective. In the first perspective, PV electricity exported to the grid is accounted as avoided emissions. In the second perspective, only locally used PV electricity is accounted as avoided emissions. This perspective assumes that PV electricity cannot be used elsewhere in the system.

Distributions of avoided emissions for residential dwellings and neighbourhoods are shown in Fig. 7.15. Chapter 5 analysed the impact on avoided life cycle greenhouse gas emission for 16 dwellings with a ground source heat pump, combined with PV and storage, for a lifetime of 30 year. Avoided life cycle emissions from an electricity system perspective and for a relative PV system size of 1 kWp per MWh of annual demand are between 8 and 23 tonne CO_2-eq, with an average of 17 tonne of CO_2-eq. This is around 560 kg of CO_2-eq for each year. The annual electricity consumption of these dwellings is between 1577 and 4727 kWh with an average of 3139 kWh. Avoided emissions increase with larger PV system capacity, but decrease with larger storage capacities. Avoided emissions from a dwelling perspective are lower. The use of storage increases the avoided emissions significantly, caused by the larger self-consumption. The impact of GSHP on the avoided emissions for residential dwellings was on average 42 tCO_2-eq, see chapter 5. The combined impact of GSHP and PV resulted in avoided emissions of 73 tCO_2-eq, or a 80% reduction in GHG emissions. Furthermore an average emission factor of 67 gCO_2-eq per kWh was found.

Chapter 6 analysed the avoided life cycle emissions for neighbourhoods with PV, storage and electric vehicles. Avoided emissions are given per address for a period of 30 years. Avoided emissions from an electricity system perspective are around 12 tCO_2-eq per address from a neighbourhood perspective and 9 tCO_2-eq. These avoided emissions are lower than presented chapter 5 due to smaller PV system sizes.

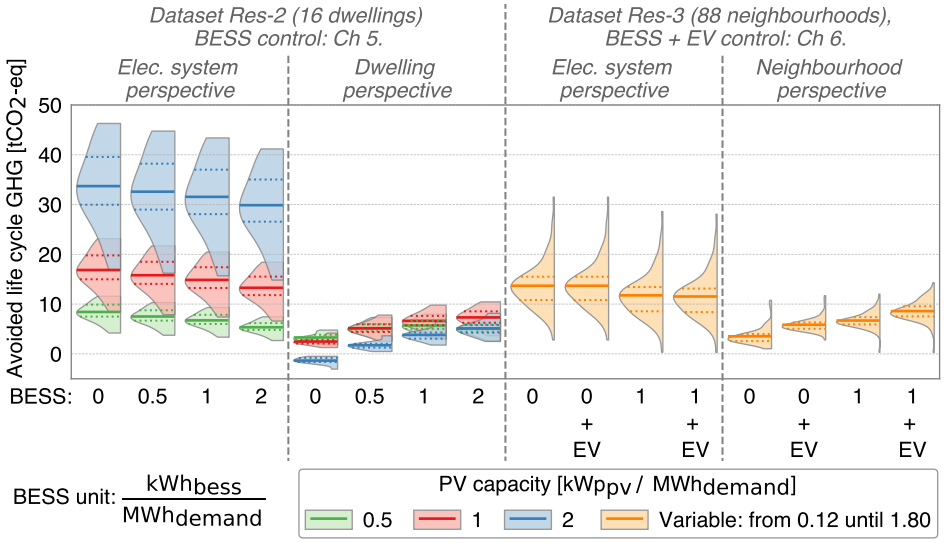

Figure 7.15 · Distributions of avoided life cycle greenhouse gas emissions for two datasets obtained from 2 chapters. The 1st to 8th violin plots show the results from chapter 5 and the 9th to 16th violin plots show results from chapter 6. Three fixed PV systems capacities and one variable PV capacity are presented, all normalized to the annual electricity consumption. Battery storage capacities are indicated by the number at the horizontal axis. The 1st to 4th violin plots and the 9th to 12th violin plots show the avoided emissions from a electricity system perspective. The 5th to 8th violin plots show results from a dwelling perspective and the four right violin plots from a neighbourhood perspective. All distributions assume that PV modules were made in China. Mean values of the distributions are marked by solid lines, and 25% and 75% percentiles are indicated by dotted lines.

8

Conclusions and recommendations

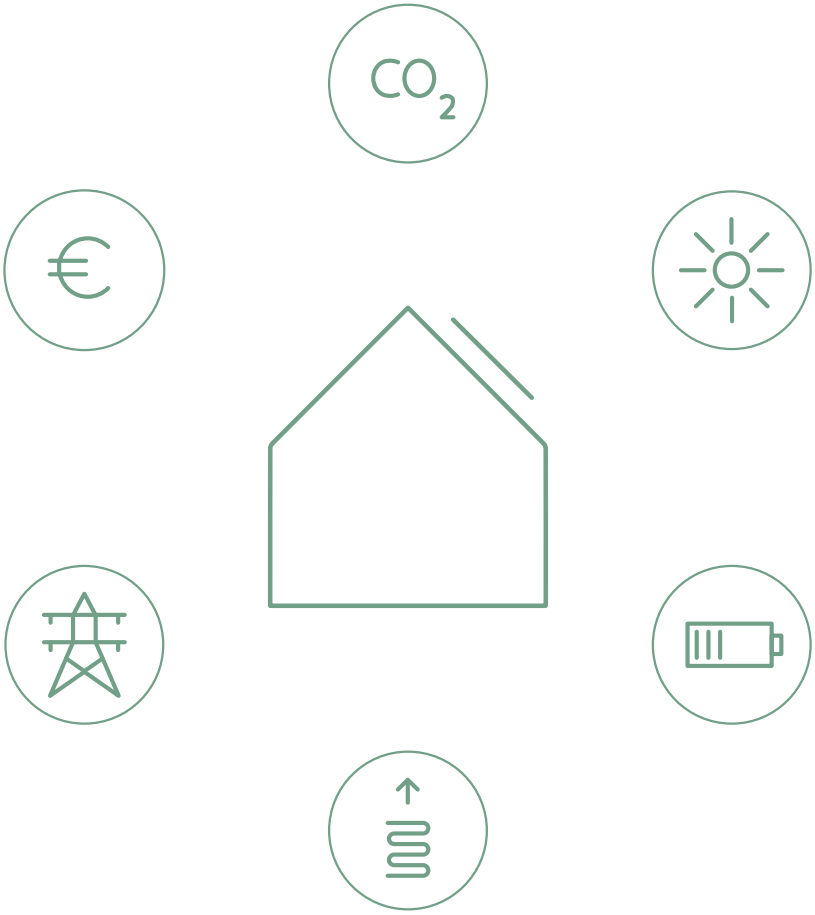

8.1 Research context

Over the last decade, global installed photovoltaic capacity showed an exponential growth while PV system costs were reduced by 20% for each doubling of globally installed PV capacity. Projections estimate that PV systems will provide a major share of electricity in a future zero carbon energy system. In the Netherlands, PV systems are increasingly deployed on rooftops and facades of buildings, with an expected capacity of 25 GWp by 2030. These systems will be mainly connected to the low voltage grid, which results in PV power integration challenges. These are mainly related to reverse power flows in the grid and grid capacity limits. This can be tackled by grid infrastructure expansion or by reducing the feed-in power to the grid.

Another important aspect is how the PV electricity is used in the energy system. Electrification of heating and transport (light-duty vehicles) increases the electricity demand and changes the electricity demand profile. Providing this demand by PV power will help to decarbonize these energy sectors. Also, surplus PV power can be stored and used when power from renewable resources is not sufficient. Both options result in increased use of PV (peak) power, and therefore more PV can be installed and connected to our electricity system.

The main aim of this thesis was to quantify and to research options to improve this PV self-consumption for both residential and commercial buildings in the Netherlands. Also, the potential reduction of PV feed-in power to the electricity grid by self-consumption or by energy storage was assessed. The economic and environmental benefits which can be obtained from self-consumption and storage were analysed to provide a broader context of the locally PV energy use.

8.2 Key conclusions

The main question of this thesis is:

What technical, economic and environmental benefits can be obtained from the local use of electricity generated by rooftop PV systems?

This research question is answered by the following four key conclusions:

- **Self-consumption** mainly depends on the installed PV capacity, energy storage capacity and building type. For a residential building, about one third (33% $\pm$ 7%) of the electricity can be directly provided by a PV system with a capacity of 1 kWp for each MWh of annual electricity demand. A ground source heat pump system reduces this self-consumption by 5%. Commercial buildings have a higher self-consumption, of 44% $\pm$ 7%. PV self-consumption can be increased

with battery energy storage. A 1 kWh storage capacity for each MWh of annual electricity demand increases self-consumption of residential buildings to 56% (± 6%). Storage systems have a lower impact on commercial buildings than residential buildings. High self-sufficiencies (>70%) can be obtained with PV systems >2kWp combined with battery storage capacity of >2kWp per MWh annual demand. The effect of changing PV orientation (compared to a south orientated system) on self-consumption is limited to a few percent. The highest self-consumption for residential buildings can be obtained with a PV orientation of 212° azimuth and 26 ° tilt. Commercial buildings can obtain this with 188° azimuth with 17° tilt.

- **PV peak power** fed back into the electricity grid can significantly be reduced, especially with battery storage systems that use forecasting algorithms to peak shave PV production. For a residential PV system, imposing a feed-in limit of 0.5 kW/kWp only results in 4% (± 1.4%) of energy loss over the lifetime of the system. This can be reduced to 0.2% with a 1 kWh storage capacity per MWh of annual electricity demand. Forecast of PV power with the clear-sky method showed the best performance to store PV peak power in batteries and reduce potential curtailment losses. Implementing a very restricted feed-in limit of 0.2 kW/kWp results in 29% of energy lost for a commercial system. This can be reduced to 17% with storage. Curtailment losses due to feed-in limitations are lower for commercial than for residential PV systems.

- **Economic benefits** from PV self-consumption and battery energy storage depend on the electricity tariff structure and the applications of the storage system. Current discounted payback periods for PV with a size of 1 kWp for each MWh annual electricity demand are around 10 years for residential systems and 12 years for commercial systems. Restricting PV feed-in power to a limit of 0.5 kW/kWp increases the discounted payback periods by 1 year. Using battery energy storage for self-consumption or curtailment loss reduction is currently not profitable. In 5 years from now, some scenarios show that reduction of curtailment loss by storage could be profitable. Using battery storage for multiple applications is highly recommended to improve the economic feasibility of storage.

- **Life cycle greenhouse gas emissions** are highly dependent on the installed PV system size. Dwellings with a PV system size of 1 kWp for each MWh annual electricity demand have on average 17 tCO_2-eq of avoided life cycle emissions. Replacement of natural gas heating by ground source heat pumps has a significantly higher impact on avoided life cycle emission. Specifically, 42 tCO_2-eq

without PV and 73 tCO_2-eq with PV per residential dwelling on average. Storage of PV energy only reduces life cycle greenhouse gas emissions if PV energy would not be used elsewhere in the energy system.

8.3 Recommendations for policy makers

Recommendations for policy makers are given for the short term (next 5 years), and for the medium term (5-years from now). The recommendations for the next 5 years offer solutions to provide growth of PV capacity and solve local PV integration problems. PV growth scenarios showed that 11 GWp of cumulative PV will be installed by 2023 in the Netherlands, of which 6 GWp on buildings[18]. The recommendations for the medium term provide solutions to increase the PV capacity installed on buildings to 25 GWp by 2030. For these recommendations, a cost reduction of PV and battery energy storage of 25% was assumed.

8.3.1 Recommendations for the next 5 years

- **Provide policies that support PV systems larger than a 1 kWp per MWh electricity demand.** Self-consumption policies reduce the financial attractiveness of larger PV systems, thereby preventing full utilization of the rooftop potential. A higher feed-in tariff is recommended for systems that produce more than the electricity consumption of a building on annual basis. For example a feed-in tariff similar to the subsidy scheme for stimulation of sustainable energy production can be used to support large residential PV systems.

- **Implement feed-in limitation of 0.5 kW per kWp of PV to avoid grid congestion.** Current low voltage networks are designed on the assumption that residential users have a maximum simultaneous power demand of 1 kW per dwelling. PV system capacities are normally larger than 1 kWp for residential users. Therefore, PV hosting capacity of the grid is constrained by the limited grid capacity. By implementing a feed-in limit of 0.5 kW/kWp, the PV capacity connected to the grid can be doubled. With this feed-in limit, the majority of residential PV systems have curtailment losses <5%. These losses were calculated over the lifetime of the systems. Thus, when doubling the PV capacity, 90% more electricity could be produced during this period. Implementing this feed-in limit results in an increase of discounted payback time from 10 to 11 years. This feed-in limit can be realized by connecting smart meters with PV inverters to limit the PV power production when necessary.

8.3.2 Recommendations for >5 years

- **Develop policies that remunerate grid services provided by third parties**. Ground and air source heat pumps will significantly increase consumption peaks from the low voltage grid, while PV systems will impact the feed-in peaks. Peak shaving by storage reduces the impact of heat pumps and PV on the distribution network, and potentially also on the transmission network. Remunerating storage capacity available for peak and demand shaving will reduce social grid cost and enable more innovative technologies which in turn can lower greenhouse gas emissions. Also, voltage control by PV inverters helps to support the local voltage on the grid. One solution could be the use of a dynamic feed-in tariff to reduce high PV feed-in power. Lower feed-in tariffs at moments when power feed-in is >0.5 kW/kWp of installed PV capacity, will trigger to use this PV peak power for self-consumption or as storage. Consequently, a dynamic feed-in tariff can be used to support the distribution and transmission grids. Currently, the DSOs are not allowed to financially compensate other parties for grid support due to legal regulations. New policies should be developed that provide rules and guidelines on how other parties could be compensated for delivering grid supporting services.

- **Implement a dynamic tax tariff for energy storage based on the marginal emission factor.** With a constant growth of variable renewable energy generation capacity, the volatility of the wholesale prices on the power market will increase. Also, the carbon price is expected to rise, which impacts the power prices of electricity generated with fossil fuels. Energy storage systems can play an important role by trading electricity for certain moments on the power markets and therefore avoiding emissions from fossil fuel fired power plants. For example by charging (surplus) wind energy and later discharging this energy to replace electricity from coal fired power plants. However, a large share of electricity price for consists of electricity tax, especially for consumers which use less than 10,000 kWh annually. Yet, this tax provides an opportunity to support the integration of a higher share of renewable electricity capacity. A dynamic tax structure for providing electricity based on the marginal emission factor of the electricity system is proposed. A lower tax on moments with excess renewable energy production, and a higher tax on moments with limited renewable production, will store more renewable energy. This will increase the profitability of storage and lowers the average electricity emission intensity. The transmission system operator could provide these marginal emissions for each quarter and therefore determine this dynamic tax. Such a tax structure would increase the environmental benefits realized with local storage.

8.4 Recommendations for further research

- **Assess the demand flexibility from electrification of heating and transport.** The potential of local use of PV electricity by electrification of heating and transport was presented in chapter 5 and chapter 6. These applications have a relatively high electricity demand, and potential to shift the electricity demand to moments with high generation of renewable electricity production. However, the demand side management potential of electric vehicles and heat pumps is not well known. For example electric vehicle smart charging potential is dependent on charging location and behaviour of consumers. Also, batteries within electric vehicle could be used to discharge electricity to the grid. However, the electricity in the electric vehicle battery should be available. Combining heat pumps with seasonal thermal storage can also increase the local use of PV and results in higher avoided greenhouse gas emissions. The demand side management potential from these options needs further research.
- **Investigate the use of energy storage for multiple applications.** Another important recommendation is the use of energy storage for multiple applications. Chapter 4 showed the high economic potential of batteries when frequency restoration reserves are provided next to self-consumption enhancement. Moreover, chapter 5 showed that energy storage systems can provide load shaving services and thus could avoid grid expansion cost. However, the potential of these avoided cost are very case specific, depend on regulation, and therefore not well known. Also, larger price fluctuations on power markets are expected with higher shares of variable renewable power generation. This increases the economic potential to trade on power markets by the use of battery storage. Furthermore, it can enable an even higher share of variable renewable energy within the system. Aggregators could provide services that require energy storage capacity. The potential roles and business cases for these aggregators should be further assessed.
- **Develop methods to define feasible dynamic electricity tariff structures.** Dynamic tariff structures could have a large impact on PV self-consumption and energy storage revenues. Yet, the impact will be dependent on the volatility and magnitude of these electricity prices. Also, these dynamic prices are dependent on market regulations and taxes. Methods and models that can estimate this impact of dynamic tariffs must be developed.
- **Develop methods to assess the environmental impact of energy storage.** The environmental impact of battery storage mainly depends on the invested emissions during the battery manufacturing compared to the avoided emissions due to energy storage. These latter emissions depend on the location and

markets in which storage is utilized. Currently, the share of variable renewable electricity production of the total production is low in the Netherlands. Therefore, curtailment of renewable energy rarely occurs. Energy storage can also be used to replace electricity generated from fossil fuel fired power plants. These avoided emissions could be allocated to the energy storage systems. Methods and standards to define the environmental impact should be established.

9

Conclusies en aanbevelingen

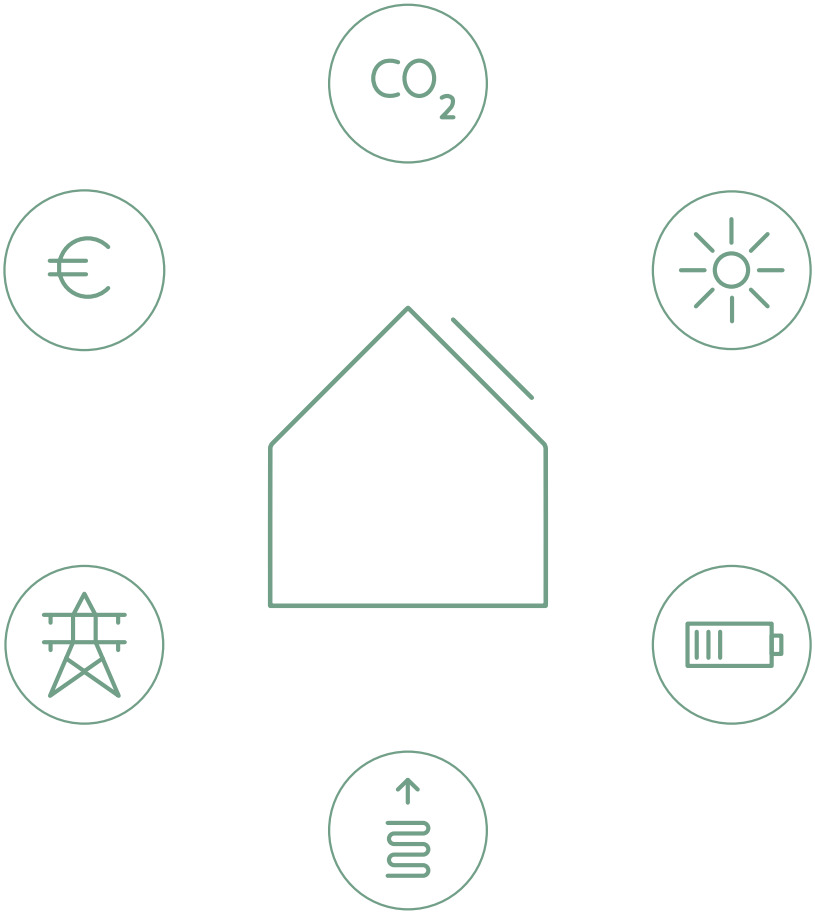

9.1 Onderzoek context

In de afgelopen decennia is er wereldwijd een exponentiële groei ontstaan in het geïnstalleerde vermogen van fotovoltaïsche (PV) systemen. De kosten van PV-systemen zijn daarnaast gedaald met 20% per verdubbeling van wereldwijd geïnstalleerd PV-capaciteit. Voorspellingen laten zien dat PV-systemen een groot deel van de elektriciteit zullen leveren in het toekomstige CO_2-vrij energiesysteem. In Nederland worden PV-systemen steeds vaker geplaatst op daken en gevels van gebouwen. In 2030 is de verwachte capaciteit van deze systemen in totaal 25 GWp. Deze systemen zullen voornamelijk worden aangesloten op het laagspanningsnet, wat zou kunnen leiden tot problemen. Deze problemen ontstaan voornamelijk door teruglevering van elektriciteit in het elektriciteitsnetwerk met name door capaciteitslimieten van dit netwerk. Mogelijke oplossingen hiervoor zijn uitbreiding van de netwerkinfrastructuur of het verminderen van PV-piekvermogen dat wordt ingevoed op het net.

Een ander belangrijk aspect is het gebruik van de opgewekte elektriciteit uit PV-systemen in het energiesysteem. Door middel van elektrificatie van verwarming en transport wordt de vraag naar elektriciteit verhoogd en verandert het verbruikspatroon. Als deze energie wordt geleverd door zonne-energie zullen deze energiesectoren op den duur CO_2-vrij worden. Daarnaast kan overtollige PV-energie worden opgeslagen en later worden ingezet als er onvoldoende duurzame energieproductie beschikbaar is. Deze opties zorgen voor meer bruikbaar PV-piekvermogen, waardoor er meer PV-capaciteit kan worden geïnstalleerd en kan worden aangesloten op het elektriciteitsnet.

Het belangrijkste doel van dit proefschrift is het kwantificeren en het onderzoeken van mogelijkheden om het eigenverbruik van elektriciteit uit PV-systemen te verhogen. Dit is gedaan voor residentiële en commerciële gebouwen in Nederland. Bovendien is de vermindering in PV-piekvermogen bepaald als gevolg van eigenverbruik of energieopslag. De economische en milieuvoordelen van het eigenverbruik van elektriciteit uit PV-systemen zijn ook geanalyseerd, wat een breder beeld geeft van de impact van de verhoging van het eigenverbruik.

9.2 Belangrijkste conclusies

De hoofdvraag van dit proefschrift is:

Welke technische, economische en milieuvoordelen kunnen worden behaald met het lokale verbruik van elektriciteit, gegenereerd door dakgebonden PV-systemen?

Deze onderzoeksvraag wordt beantwoord met de volgende vier belangrijkste conclusies:

- **Eigenverbruik** is voornamelijk afhankelijk van de geïnstalleerde PV-systeemcapaciteit, energieopslagcapaciteit en gebouwtype. Een residentiëel gebouw met een PV-systeem capaciteit van 1 kWp voor elke MWh jaarlijkse elektriciteitsvraag kan ongeveer een derde (33% $\pm$ 7%) van de opgewekte PV-energie direct gebruiken. Een grondgebonden warmtepompsysteem vermindert dit aandeel eigenverbruik met 5%. Commerciële gebouwen hebben een hoger eigenverbruik van 44% $\pm$ 7%. Het eigenverbruik kan worden verhoogd door middel van energieopslag in batterijen. Een batterijopslagcapaciteit van 1 kWh per elke MWh jaarlijkse elektriciteitsvraag verhoogt de bijdrage van eigenverbruik voor woningen naar 56 % ($\pm$ 6 %). Batterijopslagsystemen hebben een lagere impact voor commerciële gebouwen in vergelijking met woningen. Een groot deel in zelfvoorziening (textgreater 70 %) van elektriciteitsverbruik kan worden behaald met een PV-systeemgrote van textgreater 2kWp met een batterijopslagcapaciteit van textgreater 2 kWh per MWh jaarlijks energieverbruik. De verhoging van eigenverbruik door het veranderen van de PV-module oriëntatie (ten opzichte van een zuid georiënteerd systeem) is beperkt tot een paar procent. Voor residentiële gebouwen kan de hoogste bijdrage eigenverbruik behaald worden met een oriëntatie van 212° azimut en een hellingshoek van 26°. Voor commerciële gebouwen is dit 188° azimut en een hellingshoek van 17°.
- **PV-piekvermogen** dat wordt ingevoed op het elektriciteitsnetwerk kan aanzienlijk worden verminderd, vooral met batterijopslagsystemen die voorspellingen van elektriciteitsvraag en PV-productie gebruiken om de PV-energie tijdens piekproductie op te slaan. Voor een residentiëel PV-systeem met een beperking van 0,5 kW per kWp PV-capaciteit op het terugleververmogen resulteert dit in 4% ($\pm$ 1,4%) energieverlies over de gehele levensduur van het systeem. Dit kan verlaagd worden tot 0,2% energieverlies door middel van een batterijopslagcapaciteit van 1 kWh voor elke MWh jaarlijkse elektriciteitsvraag. Voorspellingen van PV-opbrengst die gebruik maken van gemodelleerde zonne-instraling bij een onbewolkte lucht laten de beste prestaties zien om piekvermogen op te slaan in batterijen. Het toepassen van een zeer grote beperking van 0,2 kW per kWp PV-capaciteit op het terugleververmogen leidt tot 29% verloren energie voor een woning met PV. Dit kan worden verlaagd met batterijopslagsysteem tot 17%. Afregelverliezen door beperkingen op het terugleververmogen zijn lager voor commerciële dan voor residentiële PV-systemen.

- **Economische voordelen** door het eigenverbruik van PV-energie en door middel van opslag in batterijen zijn afhankelijk van elektriciteitstarieven en van de toepassingen waarvoor de batterijen gebruikt worden. De verdisconteerde terugverdientijd voor een residentiëel PV-systeem met een capaciteit van 1 kWp voor elke MWh jaarlijkse elektriciteitsvraag is ongeveer 10 jaar. Voor commerciële PV-systemen is dit 12 jaar. Als het terugleververmogen van PV-systemen wordt beperkt tot 0,5 kW per kWp PV-capaciteit, zal de verdisconteerde terugverdientijd toenemen met ëën jaar. Het gebruik van batterijopslagsystemen om het eigenverbruik te verhogen of potentiele afregelverliezen te verlagen is momenteel niet rendabel. Sommige scenario's voor over 5 jaar laten zien dat het verlagen van deze potentiele afregelverliezen door batterijopslagsystemen winstgevend kan zijn. Het gebruik van batterijopslagsystemen voor meerdere toepassingen wordt sterk aanbevolen om de winstgevendheid te verbeteren.
- **Broeikasgasemissies gedurende de levenscyclus** zijn sterk afhankelijk van de geïnstalleerde PV-systeemcapaciteit. Woningen met een PV-systeemcapaciteit van 1 kWp per MWh jaarlijkse elektriciteitsvraag leiden tot vermeden levenscyclusemissies van gemiddeld 17 tCO_2-eq. Het vervangen van aardgasverwarming door grondgebonden warmtepompen zorgt voor meer vermeden levenscyclusemissies. Per woning zijn deze 42 tCO_2-eq zonder PV- geïnstalleerd en 73 tCO_2-eq met PV-geïnstalleerd. Het opslaan van PV-energie in batterijopslagsystemen vermindert de broeikasgasemissies alleen als deze energie niet elders in het energiesysteem gebruikt wordt.

9.3 Aanbevelingen voor beleidsmakers

De aanbevelingen voor beleidsmarkers worden gegeven voor de korte termijn (komende 5 jaar), en voor de middellange termijn (5 jaar vanaf nu). De aanbevelingen voor de komende 5 jaar zijn gericht op het bieden van oplossingen om de groei in PV-capaciteit voort te zetten en eventuele lokale PV-integratieproblemen te voorkomen. Scenario's voor PV-systemen verwachten dat er 11 GWp aan capaciteit is geïnstalleerd in 2023, waarvan 6 GWp op gebouwen[18]. De aanbevelingen voor de middellange termijn bieden mogelijkheden om de PV- capaciteit op gebouwen te verhogen naar 25 GWp in 2030. Voor deze middellange termijn aanbevelingen werd een kostenreductie voor PV-systemen en batterijopslagsystemen aangenomen van 25%.

9.3.1 Aanbevelingen voor de komende 5 jaar

- **Beleid moet PV-systemen groter dan 1 kWp per MWh aan jaarlijks elektriciteitsverbruik ondersteunen.** Beleid gericht op het verhogen van eigenverbruik zorgt ervoor dat grotere PV-systeem minder financieel aantrekkelijk worden. Hierdoor wordt het dakpotentieel van gebouwen niet volledig benut. Een hogere terugleververgoeding is aanbevolen voor PV-systemen die op jaarbasis meer elektriciteit produceren dan in een gebouw wordt verbruikt, bijvoorbeeld door een terugleververgoeding vergelijkbaar met de huidige subsidieregeling voor stimulering van duurzame energieproductie te gebruiken, om zodoende grotere PV-systemen op woningen te stimuleren.

- **Introduceer een beperking van 0,5 kW per kWp PV-capaciteit op het terugleververmogen om netcongestie te voorkomen.** De huidige laagspanningsnetwerken zijn ontworpen met de aanname dat gebruikers een maximale gelijktijdige vraag aan elektriciteit hebben van 1 kW per woning. PV-systemen op daken van woningen zijn meestal groter dan 1 kWp. Dit kan zorgen dat de PV-capaciteit die kan worden aangesloten op het laagspanningsnet gelimiteerd word door de netwerkcapaciteit. Een beperking van 0,5 kW per kWp PV-capaciteit op het terugleververmogen zal zorgen dat de aangesloten PV-capaciteit op het net kan worden verdubbeld. Bij deze beperking heeft een merendeel van de residentiële PV-systemen afregelverliezen van <5%. Deze verliezen zijn bepaald over de gehele levensduur van de PV-systemen. Bij een verdubbeling van PV-capaciteit binnen een netwerk kan dus 90% meer geproduceerd worden voor deze periode. Het invoeren van deze beperking verhoogt de verdisconteerde terugverdientijd van 10 tot 11 jaar. Praktisch gezien kan deze beperking worden uitgevoerd door slimme meters te verbinden met PV-omvormers. Deze omvormers kunnen vervolgens het vermogen uit het PV-systeem reduceren wanneer dit nodig is.

9.3.2 Aanbevelingen voor >5 jaar

- **Maak vergoedingen mogelijk voor het leveren van netdiensten.** Als er meer warmtepompen worden geplaatst, dan zal dit de piekvraag van het laagspanningsnet verhogen. Daarnaast zal de groei van PV-capaciteit het piekvermogen, dat wordt ingevoed in het net, vergroten. Batterijopslagsystemen kunnen deze vraagpieken en terugleveringspieken verlagen. Daardoor zorgen batterijopslagsystemen voor een vermindering van de impact van warmtepompen en PV-systemen op het distributienetwerk en mogelijk ook op het transmissienetwerk. Het vergoeden van batterijopslag om deze pieken te verlagen kan de maatschappelijke kosten van het elektriciteitsnetwerk verminderen. Dit zorgt

weer voor meer toepassingen van innovatieve technologieën die de uitstoot van broeikasgassen verlagen. Spanningsregeling via PV-omvormers kan ook helpen om de spanning op het laagspanningsnet te ondersteunen. Een van de oplossingen is het gebruik van een variabele terugleververgoeding om het PV-piekvermogen te verlagen. Het verlagen van de terugleververgoeding bij een terugleververmogen van >0.5 kW per kWp zal het eigenverbruik of opslag van het PV- piekvermogen stimuleren. Een variabele terugleververgoeding kan worden ingezet om de balans in de distributie- en transmissienetwerken te ondersteunen. Op dit moment is het wettelijk niet toegestaan dat netwerkbedrijven andere partijen financieel compenseren voor het leveren van netwerkondersteuning. Daarom zal nieuw beleid moeten worden ontwikkeld die regels en richtlijnen bevatten betreffende de vergoeding voor het leveren van deze diensten.

- **Implementeer een variabel belastingtarief voor energieopslag gebaseerd op de marginale emissiefactor.** Met een groei van elektriciteitsaanbod opgewekt uit variabele hernieuwbare energiebronnen zal de volatiliteit van de groothandelsprijzen op de elektriciteitsmarkten toenemen. Daarnaast is de verwachting dat de kosten voor het uitstoten van CO_2 zullen stijgen. Dit zal weer invloed hebben op de stroomprijzen van elektriciteit opgewekt uit fossiele brandstoffen. Energieopslagsystemen kunnen een belangrijke rol spelen door energie te verhandelen op bepaalde momenten op de energiemarkten en daardoor emissies van elektriciteit opgewekt uit fossiele brandstoffen voorkomen, bijvoorbeeld door (overtollige) windenergie op te slaan en deze energie later te gebruiken om elektriciteit uit kolencentrales te vervangen. Een groot deel van de elektriciteitsprijs bestaat uit elektriciteitsbelasting, voornamelijk voor gebruikers die minder dan 10.000 kWh per jaar gebruiken. Deze belasting biedt de mogelijkheid om de integratie van meer hernieuwbare elektriciteitscapaciteit te bevorderen. Dit kan door middel van een variabel belastingtarief voor energielevering gebaseerd op de marginale emissiefactor van het elektriciteitssysteem. Een lagere belasting op de momenten met een overschot aan duurzame energieproductie en een hogere belasting op de momenten met een beperkt aanbod van hernieuwbare productie zal een extra financiële prikkel geven om duurzame energie op te slaan. Dit zorgt voor hogere opbrengsten uit energieopslag en verlaagt de emissie-intensiteit voor elektriciteit. De transmissiesysteembeheerder zou de marginale emissies per kwartier kunnen bepalen en daarmee ook deze dynamische belasting. Een dergelijke belastingstructuur kan daarmee de milieuvoordelen verhogen uit lokale energieopslag.

9.4 Aanbevelingen voor verder onderzoek

- **Beoordeel de flexibiliteit van de energievraag door elektrificatie van verwarming en transport.** Het potentieel van eigenverbruik door middel van elektrificatie van verwarming en transport is gepresenteerd in hoofdstuk 5 en hoofdstuk 6. Deze toepassingen hebben een relatief hoge elektriciteitsvraag en daarom ook een groot potentieel om de energievraag te sturen naar momenten met veel aanbod van duurzame elektriciteit. Het potentieel aan vraagsturing via elektrische voertuigen en warmtepompen is echter niet goed bekend. Het potentieel voor slim laden is bijvoorbeeld afhankelijk van de laadlocatie en het rijgedrag van consumenten. Daarnaast kunnen batterijen van elektrische voertuigen gebruikt worden om elektriciteit te exporteren naar het elektriciteitsnet. Echter de batterij van het elektrische voertuig moet dan wel beschikbaar zijn om elektriciteit te leveren. Daarnaast kunnen warmtepompen, gecombineerd met seizoensgebonden thermische opslag, het eigenverbruik van PV-energie verhogen, wat weer leidt tot meer vermeden broeikasgasemissies. De mogelijkheden van deze opties betreffende het potentieel aan vraagsturing vereist meer onderzoek.

- **Onderzoek het gebruik van batterijopslag voor meerdere applicaties.** Een andere belangrijke aanbeveling is het gebruik van energieopslag voor meerdere toepassingen. Uit hoofdstuk 4 blijkt dat het economische potentieel voor batterijen, naast het verhogen van eigenverbruik, kan worden vergroot als regelvermogen aan het elektriciteitsnetwerk wordt verleend. Bovendien laten de resultaten van hoofdstuk 5 zien dat batterijopslagsystemen vraagpieken kunnen reduceren en daarmee kunnen kosten voorkomen worden van eventuele uitbreiding van het elektriciteitsnetwerk. De kosten die voorkomen kunnen worden zijn echter zeer specifiek per geval, afhankelijk van regelgeving en daarom ook niet goed bekend. Ook worden grotere prijsschommelingen op de elektriciteitsmarkten verwacht wanneer er meer opwekkingscapaciteit beschikbaar komt aan variabele hernieuwbare elektriciteit. Dit verhoogt het economisch potentieel om met batterijen op de elektriciteitsmarkten te handelen. Daarnaast draagt het bij tot meer variabel hernieuwbare energie gebruik in het systeem. Aggregators kunnen deze diensten aanbieden door middel van het beschikbaar stellen van batterijopslagcapaciteit. Verder onderzoek is nodig om de mogelijke rollen en business cases voor deze aggregators in kaart te brengen.

- **Ontwikkel methoden om haalbare variabele tariefstructuren te definiëren.** Het toepassen van variabele tariefstructuren kan het aandeel eigenverbruik en de inkomsten uit batterijopslag beïnvloeden. Deze invloed is erg afhankelijk van de volatiliteit en de hoogte van de elektriciteitsprijzen. Daarnaast zijn deze prijzen afhankelijk van marktregelgeving en belastingen. Het is daarom van belang om methoden en modellen te ontwikkelen die de impact van variabele tariefstructuren beter inschatten.
- **Ontwikkel methoden om de milieu-impact van energieopslag te analyseren.** De milieu-impact van batterijopslagsystemen is vooral afhankelijk van de vergelijking tussen de geïnvesteerde emissies tijdens de productie van batterijen en de vermeden emissies als gevolg van energieopslag. Deze vermeden emissies zijn afhankelijk van de opslaglocatie en de markten waar de energieopslagcapaciteit wordt gebruikt. In Nederland is momenteel het aandeel variabele hernieuwbare elektriciteitsproductie laag. Daarom komt het afregelen van hernieuwbare elektriciteit productie zelden voor. Energieopslag kan ook worden gebruikt om elektriciteitsproductie uit fossiele brandstoffen te verlagen. Deze vermeden emissies kunnen worden toegekend aan energieopslag. Er moeten methoden en normen ontwikkeld worden die de milieu-impact van energieopslag bepalen.

Bibliography

1. R. K. Pachauri, M. R. Allen, V. R. Barros, J. Broome, W. Cramer, R. Christ, J. A. Church, L. Clarke, Q. Dahe, P. Dasgupta, N. K. Dubash, O. Edenhofer, I. Elgizouli, C. B. Field, P. Forster, P. Friedlingstein, J. Fuglestvedt, L. Gomez-Echeverri, S. Hallegatte, G. Hegerl, M. Howden, K. Jiang, B. J. Cisneroz, V. Kattsov, H. Lee, K. J. Mach, J. Marotzke, M. D. Mastrandrea, L. Meyer, J. Minx, Y. Mulugetta, K. O'Brien, M. Oppenheimer, J. J. Pereira, R. Pichs-Madruga, G.-K. Plattner, H.-O. Pörtner, S. B. Power, B. Preston, N. H. Ravindranath, A. Reisinger, K. Riahi, M. Rusticucci, R. Scholes, K. Seyboth, Y. Sokona, R. Stavins, T. F. Stocker, P. Tschakert, D. van Vuuren and J.-P. van Ypserle. *Climate Change 2014: Synthesis Report. Contribution of Working Groups I, II and III to the Fifth Assessment Report of the Intergovernmental Panel on Climate Change*. Ed. by R. Pachauri and L. Meyer. Geneva, Switzerland: IPCC, 2014, p. 151. <http://www.ipcc.ch/pdf/assessment-report/ar5/syr/SYR_AR5_FINAL_full_wcover.pdf>.
2. UNFCCC. *Paris Agreement*. 2015. <https://unfccc.int/resource/docs/2015/cop21/eng/l09r01.pdf>.
3. M. Diesendorf and B. Elliston. "The feasibility of 100% renewable electricity systems: A response to critics". In: *Renewable and Sustainable Energy Reviews* **93** (2018), pp. 318–330. DOI: 10.1016/j.rser.2018.05.042.
4. F. Creutzig, P. Agoston, J. C. Goldschmidt, G. Luderer, G. Nemet and R. C. Pietzcker. "The underestimated potential of solar energy to mitigate climate change". In: *Nature Energy* **2**.9 (2017), p. 17140. DOI: 10.1038/nenergy.2017.140.
5. A. Polman, M. Knight, E. C. Garnett, B. Ehrler and W. C. Sinke. "Photovoltaic materials: Present efficiencies and future challenges". In: *Science* **352**.6283 (2016), aad4424–1–aad4424–10. DOI: 10.1126/science.aad4424.
6. G. Masson and I. Kaizuka. *Trends 2017 in Photovoltaic Applications*. Tech. rep. International Energy Agency; Photovoltaic Power Systems Programme, 2017. <http://www.iea-pvps.org/fileadmin/dam/public/report/statistics/IEA-PVPS_Trends_2017_in_Photovoltaic_Applications.pdf>.
7. G. Masson and I. Kaizuka. *Trends in PV Applications, Tables and Figures*. 2017. <http://www.iea-pvps.org/fileadmin/dam/public/report/statistics/IEA-PVPS_Trends_2017-Annex_and_Tables.pptx>.
8. D. Hart and K. Birson. *Deployment of Solar Photovoltaic Generation Capacity in the United States*. Tech. rep. Schar School of Policy and Government George Mason University, 2016, p. 48. <https://www.energy.gov/sites/prod/files/2017/01/f34/Deployment%20of%20Solar%20Photovoltaic%20Generation%20Capacity%20in%20the%20United%20States.pdf>.
9. A. Whiteman, H. Sohn, J. Esparrago, I. Arkhipova and S. Elsayed. *Renewable capacity statistics 2018*. Tech. rep. International Renewable Energy Agency(IRENA), 2018, p. 60. <http://www.irena.org/-/media/Files/IRENA/Agency/Publication/2018/Mar/IRENA_RE_Capacity_Statistics_2018.pdf>.
10. International Energy Agency. *World Energy Statistics and Balances (database)*. 2018. DOI: 10.1787/enestats-data-en.
11. C. Kost, S. Shammugam, V. Jülch, H. tran Nguyen and T. Schlegl. *Stromgestehungskosten erneuerbare Energien märz 2018*. Tech. rep. Fraunhofer-Institut für Solare Energiesysteme ISE, 2018, p. 44. <https://www.ise.fraunhofer.de/content/dam/ise/de/documents/publications/studies/DE2018_ISE_Studie_Stromgestehungskosten_Erneuerbare_Energien.pdf>.

12. A. Beauvais, N. Chevillard, M. G. Paredes, M. Heisz, R. Rossi and M. Schmela. *Global Market Outlook For Solar Power / 2018 - 2022*. Tech. rep. SolarPower Europe, 2018, p. 81. <http://www.solarpowereurope.org/fileadmin/user_upload/SolarPower_Europe_Global_Market_Outlook_2018.pdf>.

13. A. Louwen, W. G. J. H. M. van Sark, A. P. C. Faaij and R. E. I. Schropp. "Re-assessment of net energy production and greenhouse gas emissions avoidance after 40 years of photovoltaics development". In: *Nature Communications* **7** (2016), p. 13728. DOI: 10.1038/ncomms13728.

14. A. Grubler. "The costs of the French nuclear scale-up: A case of negative learning by doing". In: *Energy Policy* **38**.9 (2010), pp. 5174–5188. DOI: 10.1016/j.enpol.2010.05.003.

15. C. Breyer, D. Bogdanov, A. Gulagi, A. Aghahosseini, L. S. Barbosa, O. Koskinen, M. Barasa, U. Caldera, S. Afanasyeva, M. Child, J. Farfan and P. Vainikka. "On the role of solar photovoltaics in global energy transition scenarios". In: *Progress in Photovoltaics: Research and Applications* **25**.8 (2017), pp. 727–745. DOI: 10.1002/pip.2885.

16. R. Heynen, P. Groot, H. Vrisekoop, P. Gijsbers and K. Kolenbrander. *Het Nationaal Solar Trendrapport*. Tech. rep. Solar Solutions Int, 2018. <http://www.solarsolutions.nl/files/NST_2018_[DEF]_LR.pdf>.

17. I. Zanetti, P. Bonomo, F. Frontini, E. Saretta, G. Verberne, M. van den Donker, F. Vossen, K. Sinapis and W. Folkerts. *Building Integrated Photovoltaics: Product overview for solar building skins, Status Report 2017*. Tech. rep. 2018, p. 75. <https://www.seac.cc/wp-content/uploads/2017/11/171102_SUPSI_BIPV.pdf>.

18. W. Folkerts, W. van Sark, C. de Keizer, W. van Hooff and M. van den Donker. *ROADMAP NL - PV Systemen en Toepassingen*. Tech. rep. 2017, p. 50. <https://www.uu.nl/sites/default/files/roadmap-pv-systemen-en-toepassingen-final.pdf>.

19. B. Bayer, P. Matschoss, H. Thomas and A. Marian. "The German experience with integrating photovoltaic systems into the low-voltage grids". In: *Renewable Energy* **119** (2018), pp. 129–141. DOI: 10.1016/j.renene.2017.11.045.

20. J. Lemmens, J. van der Burgt, T. Bosma, R. van den Wijngaart, B. van Bemmel and R. Koelemeijer. *Het potentieel van zonnestroom in de gebouwde omgeving van Nederland*. Tech. rep. 2014. <http://www.pbl.nl/sites/default/files/cms/publicaties/pbl-2014-dnv-gl-het-potentieel-van-zonnestroom-in-de-gebouwde-omgeving-van-nederland_01400.pdf>.

21. J. von Appen, M. Braun, T. Stetz, K. Diwold and D. Geibel. "Time in the Sun: The Challenge of High PV Penetration in the German Electric Grid". In: *IEEE Power and Energy Magazine* **11**.2 (2013), pp. 55–64. DOI: 10.1109/mpe.2012.2234407.

22. N. Leemput, F. Geth, B. Claessens, J. V. Roy, R. Ponnette and J. Driesen. "A case study of coordinated electric vehicle charging for peak shaving on a low voltage grid". In: *2012 3rd IEEE PES Innovative Smart Grid Technologies Europe (ISGT Europe)*. IEEE, 2012. DOI: 10.1109/isgteurope.2012.6465656.

23. European Network of Transmission System Operators for Electricity ENTSO-E. *Dispersed Generation Impact on Continental Europe Region Security*. Tech. rep. European Network of Transmission System Operators for Electricity, 2014, p. 11. <https://docstore.entsoe.eu/Documents/Publications/Position%20papers%20and%20reports/150113_ENTSO-E_Position_Paper_Dispersed_Generation_Impact_on_CE_Security.pdf>.

24. H. Ruf. "Limitations for the feed-in power of residential photovoltaic systems in Germany – An overview of the regulatory framework". In: *Solar Energy* **159** (2018), pp. 588–600. DOI: 10.1016/j.solener.2017.10.072.

25. B. Bletterie, S. Kadam, R. Bolgaryn and A. Zegers. "Voltage Control with PV Inverters in Low Voltage Networks—In Depth Analysis of Different Concepts and Parameterization Criteria". In: *IEEE Transactions on Power Systems* **32**.1 (2017), pp. 177–185. DOI: 10.1109/tpwrs.2016.2554099.

26. F. M. for Economic Affairs and E. Germany. *Renewable Energy Sources Act (EEG 2017)*. Tech. rep. Federal Ministry for Economic Affairs and Energy Germany, 2017, p. 171. <https://www.bmwi.de/Redaktion/EN/Downloads/renewable-energy-sources-act-2017.pdf?__blob=publicationFile&v=3>.

27. B. Kausika, P. Moraitis and W. van Sark. "Visualization of Operational Performance of Grid-Connected PV Systems in Selected European Countries". In: *Energies* **11**.6 (2018), p. 1330. DOI: 10.3390/en11061330.

28. European Network of Transmission System Operators for Electricity ENTSO-E. *hourly load values*. 2018. <https://www.entsoe.eu/data/power-stats/hourly_load/>.

29. N. M. Haegel, R. Margolis, T. Buonassisi, D. Feldman, A. Froitzheim, R. Garabedian, M. Green, S. Glunz, H.-M. Henning, B. Holder, I. Kaizuka, B. Kroposki, K. Matsubara, S. Niki, K. Sakurai, R. A. Schindler, W. Tumas, E. R. Weber, G. Wilson, M. Woodhouse and S. Kurtz. "Terawatt-scale photovoltaics: Trajectories and challenges". In: *Science* **356**.6334 (2017), pp. 141–143. DOI: 10.1126/science.aal1288.

30. T. R. Hawkins, B. Singh, G. Majeau-Bettez and A. H. Strømman. "Comparative Environmental Life Cycle Assessment of Conventional and Electric Vehicles". In: *Journal of Industrial Ecology* **17**.1 (2012), pp. 53–64. DOI: 10.1111/j.1530-9290.2012.00532.x.

31. International Energy Agency. *Global EV Outlook 2018*. Tech. rep. 2018, p. 146. <https://webstore.iea.org/download/direct/1045?fileName=Global_EV_Outlook_2018.pdf>.

32. Rijksdienst voor Ondernemend Nederland. *Statistics Electric Vehicles in the Netherlands*. 2018. <https://www.rvo.nl/sites/default/files/2018/04/Statistics-Electric-Vehicles-and-Charging-in-The-Netherlands-March2018.pdf>.

33. F. Teng, M. Aunedi and G. Strbac. "Benefits of flexibility from smart electrified transportation and heating in the future UK electricity system". In: *Applied Energy* **167** (2016), pp. 420–431. DOI: 10.1016/j.apenergy.2015.10.028.

34. J. H. Williams, A. DeBenedictis, R. Ghanadan, A. Mahone, J. Moore, W. R. Morrow, S. Price and M. S. Torn. "The Technology Path to Deep Greenhouse Gas Emissions Cuts by 2050: The Pivotal Role of Electricity". In: *Science* **335**.6064 (2011), pp. 53–59. DOI: 10.1126/science.1208365.

35. M. Z. Jacobson, M. A. Delucchi, M. A. Cameron and B. A. Frew. "Low-cost solution to the grid reliability problem with 100% penetration of intermittent wind, water, and solar for all purposes". In: *Proceedings of the National Academy of Sciences* **112**.49 (2015), pp. 15060–15065. DOI: 10.1073/pnas.1510028112.

36. B. Dunn, H. Kamath and J. Tarascon. "Electrical Energy Storage for the Grid: A Battery of Choices". In: *Science* **334**.6058 (2011), pp. 928–935. DOI: 10.1126/science.1212741.

37. P. Ralon, M. Taylor, A. Ilas, H. Diaz-Bone and K.-P. Kairies. *Electricity storage and renewables: Costs and markets to 2030*. Tech. rep. International Renewable Energy Agency(IRENA), 2017, p. 130. <http://www.irena.org/-/media/Files/IRENA/Agency/Publication/2018/Mar/IRENA_RE_Capacity_Statistics_2018.pdf>.

38. A. Malhotra, B. Battke, M. Beuse, A. Stephan and T. Schmidt. "Use cases for stationary battery technologies: A review of the literature and existing projects". In: *Renewable and Sustainable Energy Reviews* **56** (2016), pp. 705–721. DOI: 10.1016/j.rser.2015.11.085.

39. O. Schmidt, A. Hawkes, A. Gambhir and I. Staffell. "The future cost of electrical energy storage based on experience rates". In: *Nature Energy* **2**.8 (2017), p. 17110. DOI: 10.1038/nenergy.2017.110.

40. R. Verzijlbergh and a. P. H. Laurens de Vries. *Routekaart Energieopslag 2030 Systeemintegratie en de rol van energieopslag*. Tech. rep. DNV-GL, 2015, pp. 1–116.

41. J. Widén. "Improved photovoltaic self-consumption with appliance scheduling in 200 single-family buildings". In: *Applied Energy* **126** (2014), pp. 199–212. DOI: 10.1016/j.apenergy.2014.04.008.

42. M. R. Staats, P. D. M. de Boer-Meulman and W. G. J. H. M. van Sark. "Experimental determination of demand side management potential of wet appliances in the Netherlands". In: *Sustainable Energy, Grids and Networks* **9** (2017), pp. 80 –94. ISSN: 2352-4677. DOI: 10.1016/j.segan.2016.12.004.

43. E. D. Mehleri, P. L. Zervas, H. Sarimveis, J. A. Palyvos and N. C. Markatos. "Determination of the optimal tilt angle and orientation for solar photovoltaic arrays". In: *Renewable Energy* **35**.11 (2010), pp. 2468–2475. DOI: 10.1016/j.renene.2010.03.006.

44. A. K. Yadav and S. Chandel. "Tilt angle optimization to maximize incident solar radiation: A review". In: *Renewable and Sustainable Energy Reviews* **23** (2013), pp. 503–513. DOI: 10.1016/j.rser.2013.02.027.

45. Í. P. dos Santos and R. Rüther. "Limitations in solar module azimuth and tilt angles in building integrated photovoltaics at low latitude tropical sites in Brazil". In: *Renewable Energy* **63** (2014), pp. 116–124. DOI: 10.1016/j.renene.2013.09.008.

46. M. Lave and J. Kleissl. "Optimum fixed orientations and benefits of tracking for capturing solar radiation in the continental United States". In: *Renewable Energy* **36**.3 (2011), pp. 1145–1152. DOI: 10.1016/j.renene.2010.07.032.

47. European Commission. *Best practices on Renewable Energy Self-consumption*. Tech. rep. Brussels: European Commission, 2015, p. 14.

48. KfW. *KfW-Programm Erneuerbare Energien "Speicher"*. 2017. <https://www.kfw.de/Download-Center/F%C3%B6rderprogramme-(Inlandsf%C3%B6rderung)/PDF-Dokumente/6000002700_M_275_Speicher.pdf>.

49. M. Hummon, P. Denholm and R. Margolis. "Impact of photovoltaic orientation on its relative economic value in wholesale energy markets". In: *Progress in Photovoltaics: Research and Applications* **21**.7 (2012), pp. 1531–1540. DOI: 10.1002/pip.2198.

50. J. D. Rhodes, C. R. Upshaw, W. J. Cole, C. L. Holcomb and M. E. Webber. "A multi-objective assessment of the effect of solar PV array orientation and tilt on energy production and system economics". In: *Solar Energy* **108** (2014), pp. 28–40. DOI: 10.1016/j.solener.2014.06.032.

51. I. H. Rowlands, B. P. Kemery and I. Beausoleil-Morrison. "Optimal solar-PV tilt angle and azimuth: An Ontario (Canada) case-study". In: *Energy Policy* **39**.3 (2011), pp. 1397–1409. DOI: 10.1016/j.enpol.2010.12.012.

52. J. E. Haysom, K. Hinzer and D. Wright. "Impact of electricity tariffs on optimal orientation of photovoltaic modules". In: *Progress in Photovoltaics: Research and Applications* **24**.2 (2015), pp. 253–260. DOI: 10.1002/pip.2651.

53. M. Hartner, A. Ortner, A. Hiesl and R. Haas. "East to west – The optimal tilt angle and orientation of photovoltaic panels from an electricity system perspective". In: *Applied Energy* **160** (2015), pp. 94–107. DOI: 10.1016/j.apenergy.2015.08.097.

54. T. Tjaden, J. Weniger, J. Bergner, F. Schnorr and V. Quaschning. "Impact of the PV generator's orientation on the energetic assessment of PV self-consumption systems considering individual residential load profiles". In: *29th European Photovoltaic Solar Energy Conference and Exhibition*. WIP-Renewable Energies, Munich, Germany, 2014, p. 12459.

55. N. R. Darghouth, G. Barbose and R. Wiser. "The impact of rate design and net metering on the bill savings from distributed PV for residential customers in California". In: *Energy Policy* **39**.9 (2011), pp. 5243–5253. DOI: 10.1016/j.enpol.2011.05.040.

56. J. Widén, E. Wäckelgård and P. D. Lund. "Options for improving the load matching capability of distributed photovoltaics: Methodology and application to high-latitude data". In: *Solar Energy* **83**.11 (2009), pp. 1953–1966. DOI: 10.1016/j.solener.2009.07.007.

57. A. Lahnaoui, P. Stenzel and J. Linssen. "Tilt Angle and Orientation Impact on the Techno-economic Performance of Photovoltaic Battery Systems". In: *Energy Procedia* **105** (2017), pp. 4312–4320. DOI: 10.1016/j.egypro.2017.03.903.

58. S. B. Sadineni, F. Atallah and R. F. Boehm. "Impact of roof integrated PV orientation on the residential electricity peak demand". In: *Applied Energy* **92** (2012), pp. 204–210. DOI: 10.1016/j.apenergy.2011.10.026.

59. M. Hartner, D. Mayr, A. Kollmann and R. Haas. "Optimal sizing of residential PV-systems from a household and social cost perspective". In: *Solar Energy* **141** (2017), pp. 49–58. DOI: 10.1016/j.solener.2016.11.022.

60. J. D. Mondol, Y. G. Yohanis and B. Norton. "Optimising the economic viability of grid-connected photovoltaic systems". In: *Applied Energy* **86**.7-8 (2009), pp. 985–999. DOI: 10.1016/j.apenergy.2008.10.001.

61. R. W. Andrews, J. S. Stein, C. Hansen and D. Riley. "Introduction to the open source PV LIB for python Photovoltaic system modelling package". In: *2014 IEEE 40th Photovoltaic Specialist Conference (PVSC)*. IEEE, 2014, pp. 170–174. DOI: 10.1109/pvsc.2014.6925501.

62. Panasonic. *Panasonic HIP-225HDE1*. 2015. <http://www.technosun.com/eu/products/solar-module-SANYO-HIP-225HDE1.php>.

63. Enphase Energy. *Enphase M215*. 2015. <https://www.enphase.com/sites/default/files/M215_DS_EN_60Hz.pdf>.

64. Liander N.V. *Liander Open data*. 2016. <https://www.liander.nl/over-liander/innovatie/open-data/data>.

65. J. L. Hintze and R. D. Nelson. "Violin Plots: A Box Plot-Density Trace Synergism". In: *The American Statistician* **52**.2 (1998), p. 181. DOI: 10.2307/2685478.

66. M. Hekkenberg, R. M. J. Benders, H. C. Moll and A. J. M. S. Uiterkamp. "Indications for a changing electricity demand pattern: The temperature dependence of electricity demand in the Netherlands". In: *Energy Policy* **37**.4 (2009), pp. 1542–1551. DOI: 10.1016/j.enpol.2008.12.030.

67. T. Beck, H. Kondziella, G. Huard and T. Bruckner. "Assessing the influence of the temporal resolution of electrical load and PV generation profiles on self-consumption and sizing of PV-battery systems". In: *Applied Energy* **173** (2016), pp. 331–342. DOI: 10.1016/j.apenergy.2016.04.050.

68. M. van der Kam and W. van Sark. "Smart charging of electric vehicles with photovoltaic power and vehicle-to-grid technology in a microgrid; a case study". In: *Applied Energy* **152** (2015), pp. 20–30. DOI: 10.1016/j.apenergy.2015.04.092.

69. J. Weniger, T. Tjaden and V. Quaschning. “Sizing of Residential PV Battery Systems”. In: *Energy Procedia* **46** (2014), pp. 78–87. DOI: 10.1016/j.egypro.2014.01.160.

70. International Energy Agency Photovoltaic Power Systems Programme (IEA PVPS). *2015 Snapshot of Global Photovoltaic markets*. Tech. rep. 2016, pp. 1–19.

71. J. Antonanzas, N. Osorio, R. Escobar, R. Urraca, F. J. M. de Pison and F. Antonanzas-Torres. “Review of photovoltaic power forecasting”. In: *Solar Energy* **136** (2016), pp. 78–111. DOI: 10.1016/j.solener.2016.06.069.

72. B. Elsinga and W. G. J. H. M. van Sark. “Short-term peer-to-peer solar forecasting in a network of photovoltaic systems”. In: *Applied Energy* **206** (2017), pp. 1464–1483. DOI: 10.1016/j.apenergy.2017.09.115.

73. A. R. Khan, A. Mahmood, A. Safdar, Z. A. Khan and N. A. Khan. “Load forecasting, dynamic pricing and DSM in smart grid: A review”. In: *Renewable and Sustainable Energy Reviews* **54** (2016), pp. 1311–1322. DOI: 10.1016/j.rser.2015.10.117.

74. J. Torriti. “A review of time use models of residential electricity demand”. In: *Renewable and Sustainable Energy Reviews* **37** (2014), pp. 265–272. DOI: 10.1016/j.rser.2014.05.034.

75. M. Resch, J. Bühler, M. Klausen and A. Sumper. “Impact of operation strategies of large scale battery systems on distribution grid planning in Germany”. In: *Renewable and Sustainable Energy Reviews* **74** (2017), pp. 1042–1063. DOI: 10.1016/j.rser.2017.02.075.

76. J. Moshövel, K.-P. Kairies, D. Magnor, M. Leuthold, M. Bost, S. Gährs, E. Szczechowicz, M. Cramer and D. U. Sauer. “Analysis of the maximal possible grid relief from PV-peak-power impacts by using storage systems for increased self-consumption”. In: *Applied Energy* **137** (2015), pp. 567–575. DOI: 10.1016/j.apenergy.2014.07.021.

77. Y. Riesen, C. Ballif and N. Wyrsch. “Control algorithm for a residential photovoltaic system with storage”. In: *Applied Energy* **202** (2017), pp. 78–87. DOI: 10.1016/j.apenergy.2017.05.016.

78. Y Riffonneau, S Bacha, F Barruel and S Ploix. “Optimal Power Flow Management for Grid Connected PV Systems With Batteries”. In: *IEEE Transactions on Sustainable Energy* **2**.3 (2011), pp. 309–320. DOI: 10.1109/tste.2011.2114901.

79. C. Williams, J. Binder, M. Danzer, F. Sehnke and M. Felder. “Battery Charge Control Schemes for Increased Grid Compatibility of Decentralized PV Systems”. In: *28st European Photovoltaic Solar Energy Conference and Exhibition*. WIP-Renewable Energies, Munich, Germany, 2013, pp. 3751 –3756. DOI: 10.4229/28thEUPVSEC2013-5CO.7.6.

80. J. Bergner, J. Weniger, T. Tjaden and V. Quaschning. “Feed-in Power Limitation of Grid-Connected PV Battery Systems with Autonomous Forecast-Based Operation Strategies”. In: *29st European Photovoltaic Solar Energy Conference and Exhibition*. WIP-Renewable Energies, Munich, Germany, 2014, pp. 2363 –2370. DOI: 10.4229/EUPVSEC20142014-5CO.15.1.

81. A. Zeh and R. Witzmann. “Operational Strategies for Battery Storage Systems in Low-voltage Distribution Grids to Limit the Feed-in Power of Roof-mounted Solar Power Systems”. In: *Energy Procedia* **46** (2014), pp. 114–123. DOI: 10.1016/j.egypro.2014.01.164.

82. E. Waffenschmidt. “Dimensioning of Decentralized Photovoltaic Storages with Limited Feed-in Power and their Impact on the Distribution Grid”. In: *Energy Procedia* **46** (2014), pp. 88–97. DOI: 10.1016/j.egypro.2014.01.161.

83. T. AlSkaif, W. Schram, G. Litjens and W. van Sark. “Smart charging of community storage units using Markov chains”. In: *2017 IEEE PES Innovative Smart Grid Technologies Conference Europe (ISGT-Europe)*. 2017, pp. 1–6. DOI: 10.1109/ISGTEurope.2017.8260177.

84. I. Ranaweera and O.-M. Midtgård. "Optimization of operational cost for a grid-supporting PV system with battery storage". In: *Renewable Energy* **88** (2016), pp. 262–272. DOI: 10.1016/j.renene.2015.11.044.

85. J. Li and M. A. Danzer. "Optimal charge control strategies for stationary photovoltaic battery systems". In: *Journal of Power Sources* **258** (2014), pp. 365–373. DOI: 10.1016/j.jpowsour.2014.02.066.

86. G. Angenendt, S. Zurmühlen, R. Mir-Montazeri, D. Magnor and D. U. Sauer. "Enhancing Battery Lifetime in PV Battery Home Storage System Using Forecast Based Operating Strategies". In: *Energy Procedia* **99** (2016), pp. 80–88. DOI: 10.1016/j.egypro.2016.10.100.

87. A.-L. Klingler and L. Teichtmann. "Impacts of a forecast-based operation strategy for grid-connected PV storage systems on profitability and the energy system". In: *Solar Energy* **158** (2017), pp. 861–868. DOI: 10.1016/j.solener.2017.10.052.

88. A. Louwen, A. C. de Waal, R. E. I. Schropp, A. P. C. Faaij and W. G. J. H. M. van Sark. "Comprehensive characterisation and analysis of PV module performance under real operating conditions". In: *Progress in Photovoltaics: Research and Applications* **25**.3 (2016), pp. 218–232. DOI: 10.1002/pip.2848.

89. P. Moraitis and W. G. J. H. M. van Sark. "Operational performance of grid-connected PV systems". In: *2014 IEEE 40th Photovoltaic Specialist Conference (PVSC)*. IEEE, 2014. DOI: 10.1109/pvsc.2014.6925308.

90. G. B. M. A. Litjens, E. Worrell and W. G. J. H. M. van Sark. "Influence of demand patterns on the optimal orientation of photovoltaic systems". In: *Solar Energy* **155** (2017), pp. 1002–1014. DOI: 10.1016/j.solener.2017.07.006.

91. D. P. Dee, S. M. Uppala, A. J. Simmons, P. Berrisford, P. Poli, S. Kobayashi, U. Andrae, M. A. Balmaseda, G. Balsamo, P. Bauer, P. Bechtold, A. C. M. Beljaars, L. van de Berg, J. Bidlot, N. Bormann, C. Delsol, R. Dragani, M. Fuentes, A. J. Geer, L. Haimberger, S. B. Healy, H. Hersbach, E. V. Hólm, L. Isaksen, P. Kållberg, M. Köhler, M. Matricardi, A. P. McNally, B. M. Monge-Sanz, J.-J. Morcrette, B.-K. Park, C. Peubey, P. de Rosnay, C. Tavolato, J.-N. Thépaut and F. Vitart. "The ERA-Interim reanalysis: configuration and performance of the data assimilation system". In: *Quarterly Journal of the Royal Meteorological Society* **137**.656 (2011), pp. 553–597. DOI: 10.1002/qj.828.

92. P. Ineichen and R. Perez. "A new airmass independent formulation for the Linke turbidity coefficient". In: *Solar Energy* **73**.3 (2002), pp. 151 –157. DOI: 10.1016/S0038-092X(02)00045-2.

93. J. Hoppmann, J. Volland, T. S. Schmidt and V. H. Hoffmann. "The economic viability of battery storage for residential solar photovoltaic systems – A review and a simulation model". In: *Renewable and Sustainable Energy Reviews* **39** (2014), pp. 1101–1118. DOI: 10.1016/j.rser.2014.07.068.

94. SMA Solar Technology AG. *Sunny Boy Storage 2.5*. 2017. <https://www.sma.de/en/products/battery-inverters/sunny-boy-storage-25.html#Downloads-236248>.

95. Tesla Motors, Inc. *Tesla Motors, Inc. Powerwall Product Homepage*. 2016. <http://www.teslamotors.com/nl_NL/powerwall>.

96. D. C. Jordan, S. R. Kurtz, K. VanSant and J. Newmiller. "Compendium of photovoltaic degradation rates". In: *Progress in Photovoltaics: Research and Applications* **24**.7 (2016), pp. 978–989. <https://doi.org/10.1002/pip.2744>.

97. C. Truong, M. Naumann, R. Karl, M. Müller, A. Jossen and H. Hesse. "Economics of Residential Photovoltaic Battery Systems in Germany: The Case of Tesla's Powerwall". In: *Batteries* **2**.4 (2016), p. 14. DOI: 10.3390/batteries2020014.

98. S. Downing and D. Socie. "Simple rainflow counting algorithms". In: *International Journal of Fatigue* **4**.1 (1982), pp. 31–40. DOI: 10.1016/0142-1123(82)90018-4.

99. C. A. Rosenkranz, U. Köhler and J.-L. Liska. "Modern Battery Systems for Plug In Hybrid Vehicles". In: *23rd International Battery,Hybrid and Fuel Cell Electric Vehicle Symposium and Exhibition*. 2007, pp. 650–661.

100. A. G. R. Vaz, B. Elsinga, W. G. J. H. M. van Sark and M. C. Brito. "An artificial neural network to assess the impact of neighbouring photovoltaic systems in power forecasting in Utrecht, the Netherlands". In: *Renewable Energy* **85** (2016), pp. 631–641. DOI: 10.1016/j.renene.2015.06.061.

101. Y. Iwafune, Y. Yagita, T. Ikegami and K. Ogimoto. "Short-term forecasting of residential building load for distributed energy management". In: *2014 IEEE International Energy Conference (ENERGYCON)*. IEEE, 2014. DOI: 10.1109/energycon.2014.6850575.

102. S. Ryu, J. Noh and H. Kim. "Deep neural network based demand side short term load forecasting". In: *2016 IEEE International Conference on Smart Grid Communications (SmartGridComm)*. IEEE, 2016. DOI: 10.1109/smartgridcomm.2016.7778779.

103. R. Luthander, J. Widén, D. Nilsson and J. Palm. "Photovoltaic self-consumption in buildings: A review". In: *Applied Energy* **142** (2015), pp. 80–94. DOI: 10.1016/j.apenergy.2014.12.028.

104. W. G. J. H. M. van Sark, L. Bosselaar, P. Gerrissen, K. Esmeijer, P. Moraitis, M. V. D. Donker and G. Emsbroek. "Update of the Dutch PV Specific Yield for Determination of PV Contribution to Renewable Energy Production: 25% More Energy!" eng. In: WIP, 2014, pp. 4095 –4097. DOI: 10.4229/eupvsec20142014-7av.6.43.

105. D. Parra, M. Gillott, S. A. Norman and G. S. Walker. "Optimum community energy storage system for PV energy time-shift". In: *Applied Energy* **137** (2015), pp. 576–587. DOI: 10.1016/j.apenergy.2014.08.060.

106. E. A. M. Klaassen, C. B. A. Kobus, J. Frunt and J. G. Slootweg. "Responsiveness of residential electricity demand to dynamic tariffs: Experiences from a large field test in the Netherlands". In: *Applied Energy* **183**.Supplement C (2016), pp. 1065 –1074. ISSN: 0306-2619. DOI: 10.1016/j.apenergy.2016.09.051.

107. J. Salpakari and P. Lund. "Optimal and rule-based control strategies for energy flexibility in buildings with PV". in: *Applied Energy* **161** (2016), pp. 425–436. DOI: 10.1016/j.apenergy.2015.10.036.

108. A. Stephan, B. Battke, M. D. Beuse, J. H. Clausdeinken and T. S. Schmidt. "Limiting the public cost of stationary battery deployment by combining applications". In: *Nature Energy* **1**.7 (2016), p. 16079. DOI: 10.1038/nenergy.2016.79.

109. X. Wu, X. Hu, S. Moura, X. Yin and V. Pickert. "Stochastic control of smart home energy management with plug-in electric vehicle battery energy storage and photovoltaic array". In: *Journal of Power Sources* **333** (2016), pp. 203–212. DOI: 10.1016/j.jpowsour.2016.09.157.

110. S. van der Stelt, T. AlSkaif and W. van Sark. "Techno-economic analysis of household and community energy storage for residential prosumers with smart appliances". In: *Applied Energy* **209** (2018), pp. 266–276. DOI: 10.1016/j.apenergy.2017.10.096.

111. G. Fitzgerald, J. Mandel, J. Morri and T. Hervé. *The Economics of Battery Energy Storage: How multi-use, customer-sited batteries deliver the most services and value to customers and the grid.* Tech. rep. Rocky Mountain Institute, 2015.

112. I. Lampropoulos, M. van den Broek, E. van der Hoofd, K. Hommes and W. van Sark. "A system perspective to the deployment of flexibility through aggregator companies in the Netherlands". In: *Energy Policy* **118** (2018), pp. 534–551. DOI: 10.1016/j.enpol.2018.03.073.

113. A. Strassheim, J. E. S. de Haan, M. Gibescu and W. L. Kling. "Provision of frequency restoration reserves by possible energy storage systems in Germany and the Netherlands". In: *11th International Conference on the European Energy Market (EEM14)*. IEEE, 2014. DOI: 10.1109/eem.2014.6861256.

114. J. Engels, B. Claessens and G. Deconinck. "Combined Stochastic Optimization of Frequency Control and Self-Consumption with a Battery". In: *IEEE Transactions on Smart Grid* (2017), pp. 1–11. DOI: 10.1109/tsg.2017.2785040.

115. R. Hollinger, F. Braam, L. M. Diazgranados, B. Engel, G. Bopp and T. Erge. "Distributed solar battery systems providing primary control reserve". In: *IET Renewable Power Generation* **10**.1 (2016), pp. 63–70. DOI: 10.1049/iet-rpg.2015.0147.

116. B. Battke and T. S. Schmidt. "Cost-efficient demand-pull policies for multi-purpose technologies – The case of stationary electricity storage". In: *Applied Energy* **155** (2015), pp. 334–348. DOI: 10.1016/j.apenergy.2015.06.010.

117. A. Zeh, M. Mueller, H. C. Hesse, A. Jossen and R. Witzmann. "Operating a Multitasking Stationary Battery Storage System for Providing Secondary Control Reserve on Low-Voltage Level". In: *International ETG Congress 2015; Die Energiewende - Blueprints for the new energy age*. 2015, pp. 1–8.

118. Senfal B.V. *Energy Storage: using Batteries to Balance the Grid*. 2017. <https://senfal.com/en/2017/08/10/using-batteries-to-balance-the-grid/>.

119. Sonnen GmbH. *Netzdienstleistungen mit Batteriespeichern*. 2017. <https://sonnenbatterie.de/de/netzdienstleistungen-mit-batteriespeichern>.

120. D. A. Halamay, T. K. A. Brekken, A. Simmons and S. McArthur. "Reserve requirement impacts of large-scale integration of wind, solar, and ocean wave power generation". In: *IEEE PES General Meeting*. IEEE, 2010. DOI: 10.1109/pes.2010.5590203.

121. J. Hu, R. Harmsen, W. Crijns-Graus, E. Worrell and M. van den Broek. "Identifying barriers to large-scale integration of variable renewable electricity into the electricity market: A literature review of market design". In: *Renewable and Sustainable Energy Reviews* **81** (2018), pp. 2181–2195. DOI: 10.1016/j.rser.2017.06.028.

122. N. Kittner, F. Lill and D. M. Kammen. "Energy storage deployment and innovation for the clean energy transition". In: *Nature Energy* **2**.9 (2017), p. 17125. DOI: 10.1038/nenergy.2017.125.

123. V. Jülch. "Comparison of electricity storage options using levelized cost of storage (LCOS) method". In: *Applied Energy* **183** (2016), pp. 1594–1606. DOI: 10.1016/j.apenergy.2016.08.165.

124. Y. Zhang, P. E. Campana, A. Lundblad and J. Yan. "Comparative study of hydrogen storage and battery storage in grid connected photovoltaic system: Storage sizing and rule-based operation". In: *Applied Energy* **201** (2017), pp. 397–411. DOI: 10.1016/j.apenergy.2017.03.123.

125. Deposit Markets Pty Ltd. *Netherlands Interest Rates*. 2018. <http://netherlands.deposits.org/>.

126. Centraal Bureau voor de Statistiek. *Electricity price statistics*. 2017. <http://statline.cbs.nl/StatWeb/publication/?VW=T&DM=SLNL&PA=81309NED&D1=0-1,3,5,7-8,11,15&D2=0&D3=a&D4=a&HD=121114-1344&HDR=G1,G2,T&STB=G3>.

127. Rijksdienst voor Ondernemend Nederland. *Zon SDE+ 2017*. 2017. <https://www.rvo.nl/sites/default/files/2016/02/Tabel%20Zon%20SDE%202017.pdf>.

128. The European Power Exchange (EPEX SPOT). *Yearly average base price*. 2017. <http://www.epexspot.com/dib/detail.html>.

129. Tennet. *Tennet, System & transmission data*. 2017. <http://www.tennet.org/english/operational_management/index.aspx>.

130. G. Klæboe, A. L. Eriksrud and S.-E. Fleten. "Benchmarking time series based forecasting models for electricity balancing market prices". In: *Energy Systems* **6**.1 (2013), pp. 43–61. DOI: 10.1007/s12667-013-0103-3.

131. A. S. Brouwer, M. van den Broek, A. Seebregts and A. Faaij. "Impacts of large-scale Intermittent Renewable Energy Sources on electricity systems, and how these can be modeled". In: *Renewable and Sustainable Energy Reviews* **33** (2014), pp. 443–466. DOI: 10.1016/j.rser.2014.01.076.

132. J. Fleer, S. Zurmühlen, J. Meyer, J. Badeda, P. Stenzel, J.-F. Hake and D. U. Sauer. "Price development and bidding strategies for battery energy storage systems on the primary control reserve market". In: *Energy Procedia* **135** (2017), pp. 143–157. DOI: 10.1016/j.egypro.2017.09.497.

133. T. W. Hoogvliet, G. B. M. A. Litjens and W. G. J. H. M. van Sark. "Provision of regulating- and reserve power by electric vehicle owners in the Dutch market". In: *Applied Energy* **190** (2017), pp. 1008–1019. DOI: 10.1016/j.apenergy.2017.01.006.

134. Joost Gerdes and Sjoerd Marbus and Martijn Boelhouwer. *Energietrends 2016*. Tech. rep. 2016, pp. 1–91. <https://www.ecn.nl/publicaties/PdfFetch.aspx?nr=ECN-O--16-031>.

135. M. Brennenstuhl, D. Pietruschka, U. Eicker and M. Yadack. "Towards understanding the value of decentralized heat pumps for network services in Germany: Insights concerning self-consumption and secondary reserve power". In: *2016 IEEE International Smart Cities Conference (ISC2)*. 2016, pp. 1–4. DOI: 10.1109/ISC2.2016.7580827.

136. H. Auer and B. Burgholzer. *D2.1 Opportunities, Challenges and Risks for RES-E Deployment in a fully Integrated European Electricity Market*. Tech. rep. Market4RES, 2015.

137. M. Katsanevakis, R. A. Stewart and J. Lu. "Aggregated applications and benefits of energy storage systems with application-specific control methods: A review". In: *Renewable and Sustainable Energy Reviews* **75** (2017), pp. 719–741. DOI: 10.1016/j.rser.2016.11.050.

138. European Commission. *Communication from the commission to the European parliament, the council, the European economic and social committee and the committee of the regions on an EU Strategy on Heating and Cooling*. Tech. rep. 2016, pp. 1–13.

139. Centraal Bureau voor de Statistiek. *Emissies van broeikasgassen berekend volgens IPCC-voorschriften*. 2018. <{http://statline.cbs.nl/Statweb/publication/?VW=T\&DM=SLNL\&PA=70946ned\&D1=a\&D2=0-1,5,15,18&D3=a\&HD=160823-1750\&HDR=G1\&STB=T,G2}>.

140. S. Hers, F. Rooijers and M. Meyer. *Vereffenen kosten warmtetransitie*. Tech. rep. CE Delft, 2018. <{https://www.ce.nl/publicaties/download/2515}>.

141. I. Sarbu and C. Sebarchievici. "General review of ground-source heat pump systems for heating and cooling of buildings". In: *Energy and Buildings* **70** (2014), pp. 441–454. DOI: 10.1016/j.enbuild.2013.11.068.

142. P. Blum, G. Campillo, W. Münch and T. Kölbel. "CO_2 savings of ground source heat pump systems – A regional analysis". In: *Renewable Energy* **35**.1 (2010), pp. 122–127. DOI: 10.1016/j.renene.2009.03.034.

143. B. Greening and A. Azapagic. "Domestic heat pumps: Life cycle environmental impacts and potential implications for the UK". in: *Energy* **39**.1 (2012), pp. 205–217. DOI: 10.1016/j.energy.2012.01.028.

144. P. Bayer, D. Saner, S. Bolay, L. Rybach and P. Blum. "Greenhouse gas emission savings of ground source heat pump systems in Europe: A review". In: *Renewable and Sustainable Energy Reviews* **16**.2 (2012), pp. 1256–1267. DOI: 10.1016/j.rser.2011.09.027.

145. D. Patteeuw, G. Reynders, K. Bruninx, C. Protopapadaki, E. Delarue, W. D'haeseleer, D. Saelens and L. Helsen. "CO_2-abatement cost of residential heat pumps with active demand response: demand- and supply-side effects". In: *Applied Energy* **156** (2015), pp. 490–501. DOI: 10.1016/j.apenergy.2015.07.038.

146. D. Fischer and H. Madani. "On heat pumps in smart grids: A review". In: *Renewable and Sustainable Energy Reviews* **70** (2017), pp. 342–357. DOI: 10.1016/j.rser.2016.11.182.

147. X. Liu, S. Lu, P. Hughes and Z. Cai. "A comparative study of the status of GSHP applications in the United States and China". In: *Renewable and Sustainable Energy Reviews* **48** (2015), pp. 558–570. DOI: 10.1016/j.rser.2015.04.035.

148. Rijksdienst voor Ondernemend Nederland. *Subsidie voor warmtepompen ISDE*. 2018. <{https://www.rvo.nl/subsidies-regelingen/investeringssubsidie-duurzame-energie-isde/voor-welke-apparaten-geldt-de-isde-1/warmtepompen}>.

149. T. Nowak and P. Westring. *European Heat Pump Market and Statistics Report 2015*. Tech. rep. European Heat Pump Association, 2015.

150. T. H. Lim, R. D. D. Kleine and G. A. Keoleian. "Energy use and carbon reduction potentials from residential ground source heat pumps considering spatial and economic barriers". In: *Energy and Buildings* **128** (2016), pp. 287–304. DOI: 10.1016/j.enbuild.2016.06.060.

151. Centraal Bureau voor de Statistiek. *Rendementen en CO2-emissie elektriciteitsproductie 2016*. 2018. <{https://www.cbs.nl/nl-nl/maatwerk/2018/04/rendementen-en-co2-emissie-elektriciteitsproductie-2016}>.

152. S. Nykamp, A. Molderink, V. Bakker, H. A. Toersche, J. L. Hurink and G. J. M. Smit. "Integration of heat pumps in distribution grids: Economic motivation for grid control". In: *2012 3rd IEEE PES Innovative Smart Grid Technologies Europe (ISGT Europe)*. IEEE, 2012. DOI: 10.1109/isgteurope.2012.6465605.

153. W. L. Schram, I. Lampropoulos and W. G. J. H. M. van Sark. "Photovoltaic systems coupled with batteries that are optimally sized for household self-consumption: Assessment of peak shaving potential". In: *Applied Energy* **223** (2018), pp. 69–81. DOI: 10.1016/j.apenergy.2018.04.023.

154. G. B. M. A. Litjens, E. Worrell and W. G. J. H. M. van Sark. "Assessment of forecasting methods on performance of photovoltaic-battery systems". In: *Applied Energy* **221** (2018), pp. 358–373. DOI: 10.1016/j.apenergy.2018.03.154.

155. R. L. Fares and M. E. Webber. "The impacts of storing solar energy in the home to reduce reliance on the utility". In: *Nature Energy* **2**.2 (2017), p. 17001. DOI: 10.1038/nenergy.2017.1.

156. A. Franco and F. Fantozzi. "Experimental analysis of a self consumption strategy for residential building: The integration of PV system and geothermal heat pump". In: *Renewable Energy* **86** (2016), pp. 1075–1085. DOI: 10.1016/j.renene.2015.09.030.

157. R. Thygesen and B. Karlsson. "Simulation of a proposed novel weather forecast control for ground source heat pumps as a mean to evaluate the feasibility of forecast controls' influence on the photovoltaic electricity self-consumption". In: *Applied Energy* **164** (2016), pp. 579–589. DOI: 10.1016/j.apenergy.2015.12.013.

158. E. Vrettos, A. Witzig, R. Kurmann, S. Koch and G. Andersson. "Maximizing Local PV Utilization Using Small-Scale Batteries and Flexible Thermal Loads". In: *28th European Photovoltaic Solar Energy Conference and Exhibition; 4515-4526* (2013). DOI: 10.4229/28theupvsec2013-6co.14.5.

159. C. J. C. Williams, J. O. Binder and T. Kelm. "Demand side management through heat pumps, thermal storage and battery storage to increase local self-consumption and grid compatibility

of PV systems". In: *2012 3rd IEEE PES Innovative Smart Grid Technologies Europe (ISGT Europe)*. IEEE, 2012. DOI: 10.1109/isgteurope.2012.6465874.

160. T. Beck, H. Kondziella, G. Huard and T. Bruckner. "Optimal operation, configuration and sizing of generation and storage technologies for residential heat pump systems in the spotlight of self-consumption of photovoltaic electricity". In: *Applied Energy* **188** (2017), pp. 604–619. DOI: 10.1016/j.apenergy.2016.12.041.

161. B. Baeten, F. Rogiers and L. Helsen. "Reduction of heat pump induced peak electricity use and required generation capacity through thermal energy storage and demand response". In: *Applied Energy* **195** (2017), pp. 184–195. DOI: 10.1016/j.apenergy.2017.03.055.

162. R. Thygesen and B. Karlsson. "Economic and energy analysis of three solar assisted heat pump systems in near zero energy buildings". In: *Energy and Buildings* **66** (2013), pp. 77–87. DOI: 10.1016/j.enbuild.2013.07.042.

163. D. Patteeuw and L. Helsen. "Combined design and control optimization of residential heating systems in a smart-grid context". In: *Energy and Buildings* **133** (2016), pp. 640–657. DOI: 10.1016/j.enbuild.2016.09.030.

164. B. M. Delgado, R. Kotireddy, S. Cao, A. Hasan, P.-J. Hoes, J. L. Hensen and K. Sirén. "Life-cycle cost and CO 2 emissions of residential heat and electricity prosumers in Finland and the Netherlands". In: *Energy Conversion and Management* **160** (2018), pp. 495–508. DOI: 10.1016/j.enconman.2018.01.069.

165. B. M. Delgado, S. Cao, A. Hasan and K. Sirén. "Multiobjective optimization for lifecycle cost, carbon dioxide emissions and exergy of residential heat and electricity prosumers". In: *Energy Conversion and Management* **154** (2017), pp. 455–469. DOI: 10.1016/j.enconman.2017.11.037.

166. S. Rosiek and F. J. Batlles. "Renewable energy solutions for building cooling, heating and power system installed in an institutional building: Case study in southern Spain". In: *Renewable and Sustainable Energy Reviews* **26** (2013), pp. 147–168. DOI: 10.1016/j.rser.2013.05.068.

167. M. D. Carli, A. Galgaro, M. Pasqualetto and A. Zarrella. "Energetic and economic aspects of a heating and cooling district in a mild climate based on closed loop ground source heat pump". In: *Applied Thermal Engineering* **71**.2 (2014), pp. 895–904. DOI: 10.1016/j.applthermaleng.2014.01.064.

168. N. H. Sandberg, I. Sartori and H. Brattebø. "Sensitivity analysis in long-term dynamic building stock modeling—Exploring the importance of uncertainty of input parameters in Norwegian segmented dwelling stock model". In: *Energy and Buildings* **85** (2014), pp. 136–144. DOI: 10.1016/j.enbuild.2014.09.028.

169. S. van der Stelt, T. AlSkaif and W. van Sark. "Techno-economic analysis of household and community energy storage for residential prosumers with smart appliances". In: *Applied Energy* **209** (2018), pp. 266–276. DOI: 10.1016/j.apenergy.2017.10.096.

170. Alpha-InnoTec GmbH. *Brine/Water Heat Pumps Brine Heat Station, Operating Manual PWZS(V) H1, H3 series*. 2016. <http://old.alpha-innotec.com/secureFolders/sd_ait/669c3afa-8a6e-e611-b2d1-005056990ce0/83056500jUK_BA_PWZSV.pdf>.

171. Royal Netherlands Meteorological Institute (KNMI). *Archief maand/seizoen/jaaroverzichten*. 2018. <{https://www.knmi.nl/nederland-nu/klimatologie/maand-en-seizoensoverzichten/}>.

172. W. G. J. H. M. van Sark and T. Schoen. "Photovoltaic System and Components Price Development in the Netherlands". In: *33rd European Photovoltaic Solar Energy Conference and Exhibition* (2017), pp. 2866–2869. DOI: 10.4229/eupvsec20172017-7dv.1.17.

173. M. J. M. de Wild-Scholten. "Energy payback time and carbon footprint of commercial photovoltaic systems". In: *Solar Energy Materials and Solar Cells* **119** (2013), pp. 296–305. DOI: 10.1016/j.solmat.2013.08.037.

174. A. Jaiswal. "Lithium-ion battery based renewable energy solution for off-grid electricity: A techno-economic analysis". In: *Renewable and Sustainable Energy Reviews* **72** (2017), pp. 922–934. DOI: 10.1016/j.rser.2017.01.049.

175. J. F. Peters, M. Baumann, B. Zimmermann, J. Braun and M. Weil. "The environmental impact of Li-Ion batteries and the role of key parameters – A review". In: *Renewable and Sustainable Energy Reviews* **67** (2017), pp. 491–506. DOI: 10.1016/j.rser.2016.08.039.

176. P. Blum, G. Campillo and T. Kölbel. "Techno-economic and spatial analysis of vertical ground source heat pump systems in Germany". In: *Energy* **36**.5 (2011), pp. 3002–3011. DOI: 10.1016/j.energy.2011.02.044.

177. Q. Lu, G. A. Narsilio, G. R. Aditya and I. W. Johnston. "Economic analysis of vertical ground source heat pump systems in Melbourne". In: *Energy* **125** (2017), pp. 107–117. DOI: 10.1016/j.energy.2017.02.082.

178. P. Hardy, L. Sugden and C. Dale. *Potential Cost Reductions for Ground Source Heat Pumps*. Tech. rep. Department of Energy & Climate Change, 2016.

179. Consumentenbond. *CV-ketel-onderhoud-prijspeiling*. 2015. <{https://www.consumentenbond.nl/cv-ketel/cv-onderhoudscontracten-prijspeiling}>.

180. G. Vignali. "Environmental assessment of domestic boilers: A comparison of condensing and traditional technology using life cycle assessment methodology". In: *Journal of Cleaner Production* **142** (2017), pp. 2493–2508. DOI: 10.1016/j.jclepro.2016.11.025.

181. Centraal Bureau voor de Statistiek. *Aardgas en elektriciteit, gemiddelde prijzen van eindverbruikers*. 2017. <{http://statline.cbs.nl/StatWeb/publication/?VW=T\&DM=SLNL\&PA=81309NED\&D1=0-1,3,5,7-8,11,15\&D2=0\&D3=a\&D4=a\&HD=121114-1344\&HDR=G1,G2,T\&STB=G3}>.

182. M. Londo, R. Matton, O. Usmani, M. van Klaveren and C. Tigchelaar. *De salderingsregeling: Effecten van een aantal hervormingsopties*. Tech. rep. Energieonderzoek Centrum Nederland (ECN), 2017. <{https://www.ecn.nl/publications/PdfFetch.aspx?nr=ECN-E--17-023}>.

183. Ministerie van Economische Zaken. *Wet opslag duurzame energie*. <http://wetten.overheid.nl/BWBR0032660/2018-01-01>.

184. Sociaal-Economische Raad. *The Agreement on Energy for Sustainable Growth*. Tech. rep. Sociaal-Economische Raad (Social and Economic Council), 2013. <https://www.ser.nl/~/media/files/internet/publicaties/overige/2010_2019/2013/energieakkoord-duurzame-groei/energieakkoord-duurzame-groei.ashx>.

185. G. B. M. A. Litjens, E. Worrell and W. G. J. H. M. van Sark. "Economic benefits of combining self-consumption enhancement with frequency restoration reserves provision by photovoltaic-battery systems". In: *Applied Energy* **223** (2018), pp. 172–187. DOI: 10.1016/j.apenergy.2018.04.018.

186. Eurostat. *Electricity price statistics*. 2018. <{http://ec.europa.eu/eurostat/statistics-explained/index.php/Electricity_price_statistics}>.

187. I. A. G. Wilson and I. Staffell. "Rapid fuel switching from coal to natural gas through effective carbon pricing". In: *Nature Energy* **3**.5 (2018), pp. 365–372. DOI: 10.1038/s41560-018-0109-0.

188. R. McMahon, H. Santos and Z. S. Mourão. "Practical considerations in the deployment of ground source heat pumps in older properties—A case study". In: *Energy and Buildings* **159** (2018), pp. 54–65. DOI: 10.1016/j.enbuild.2017.08.067.

189. J. Luo, J. Rohn, W. Xiang, D. Bertermann and P. Blum. "A review of ground investigations for ground source heat pump (GSHP) systems". In: *Energy and Buildings* **117** (2016), pp. 160–175. DOI: 10.1016/j.enbuild.2016.02.038.

190. A. Lake, B. Rezaie and S. Beyerlein. "Review of district heating and cooling systems for a sustainable future". In: *Renewable and Sustainable Energy Reviews* **67** (2017), pp. 417–425. DOI: 10.1016/j.rser.2016.09.061.

191. W. Ligtvoet, B. Bregman, R. van Dorland, W. ten Brinke, R. de Vos, A. Petersen and H. Visser. *Klimaatverandering - Samenvatting van het vijfde IPCC-assessment en een vertaling naar Nederland*. Tech. rep. 2015, pp. 1–134.

192. Centraal Bureau voor de Statistiek. *Energy consumption private dwellings; type of dwelling and regions*. 2016. <{http://statline.cbs.nl/StatWeb/publication/?DM=SLEN\&PA=81528eng}>.

193. Energie Beheer Nederland. *Annual Report 2017*. 2017. <{https://www.ebn.nl/wp-content/uploads/2018/04/Annual-Report-2017.pdf}>.

194. K. Schoots, M. Hekkenberg and en Pieter Hammingh. *Nationale Energieverkenning 2017*. Tech. rep. Energieonderzoek Centrum Nederland, 2017, pp. 1–238. <https://www.ecn.nl/publicaties/PdfFetch.aspx?nr=ECN-O--17-018>.

195. Netherlands Enterprise Agency. *The Netherlands: list of fuels and standard CO2 emission factors version of January 2018*. 2018. <{https://english.rvo.nl/sites/default/files/2017/04/The_Netherlands_list_of_fuels_version_January_2017_final.pdf}>.

196. M. Acuto. "Give cities a seat at the top table". In: *Nature* **537**.7622 (2016), pp. 611–613. DOI: 10.1038/537611a.

197. M. J. van der Kam, A. A. H. Meelen, W. G. J. H. M. van Sark and F. Alkemade. "Diffusion of solar photovoltaic systems and electric vehicles among Dutch consumers: Implications for the energy transition". In: *Energy Research & Social Science* **46** (2018), pp. 68–85. DOI: 10.1016/j.erss.2018.06.003.

198. B. Nykvist and M. Nilsson. "Rapidly falling costs of battery packs for electric vehicles". In: *Nature Climate Change* **5**.4 (2015), pp. 329–332. DOI: 10.1038/nclimate2564.

199. A. Ajanovic and R. Haas. "Driving with the sun: Why environmentally benign electric vehicles must plug in at renewables". In: *Solar Energy* **121** (2015), pp. 169–180. DOI: 10.1016/j.solener.2015.07.041.

200. J. Sijm, P. Gockel, J. de Joode, W. van Westering and M. Musterd. *The demand for flexibility of the power system in the Netherlands, 2015-2050, Report of phase 1 of the FLEXNET project*. Tech. rep. ECN & Alliander, 2017.

201. F. Mwasilu, J. J. Justo, E.-K. Kim, T. D. Do and J.-W. Jung. "Electric vehicles and smart grid interaction: A review on vehicle to grid and renewable energy sources integration". In: *Renewable and Sustainable Energy Reviews* **34** (2014), pp. 501–516. DOI: 10.1016/j.rser.2014.03.031.

202. S. Freitas, C. Catita, P. Redweik and M. C. Brito. "Modelling solar potential in the urban environment: State-of-the-art review". In: *Renewable and Sustainable Energy Reviews* **41** (2015), pp. 915–931. DOI: 10.1016/j.rser.2014.08.060. <https://doi.org/10.1016/j.rser.2014.08.060>.

203. B. B. Kausika, O. Dolla, W. Folkerts, B. Siebenga, P. Hermans and W. G. J. H. M. van Sark. "Bottom-up Analysis of the Solar Photovoltaic Potential for a City in the Netherlands - A Working Model for Calculating the Potential using High Resolution LiDAR Data". In: *Proceedings of*

the 4th International Conference on Smart Cities and Green ICT Systems. SCITEPRESS - Science, and Technology Publications, 2015. DOI: 10.5220/0005431401290135.

204. S. Freitas, C. Reinhart and M. C. Brito. "Minimizing storage needs for large scale photovoltaics in the urban environment". In: *Solar Energy* **159** (2018), pp. 375–389. DOI: 10.1016/j.solener.2017.11.011.

205. P. R. Defaix, W. G. J. H. M. van Sark, E. Worrell and E. de Visser. "Technical potential for photovoltaics on buildings in the EU-27". In: *Solar Energy* **86**.9 (2012), pp. 2644–2653. DOI: 10.1016/j.solener.2012.06.007.

206. J. Hofierka and J. Kaňuk. "Assessment of photovoltaic potential in urban areas using open-source solar radiation tools". In: *Renewable Energy* **34**.10 (2009), pp. 2206–2214. DOI: 10.1016/j.renene.2009.02.021.

207. K. Mainzer, K. Fath, R. McKenna, J. Stengel, W. Fichtner and F. Schultmann. "A high-resolution determination of the technical potential for residential-roof-mounted photovoltaic systems in Germany". In: *Solar Energy* **105** (2014), pp. 715–731. DOI: 10.1016/j.solener.2014.04.015.

208. L. R. Rodríguez, E. Duminil, J. S. Ramos and U. Eicker. "Assessment of the photovoltaic potential at urban level based on 3D city models: A case study and new methodological approach". In: *Solar Energy* **146** (2017), pp. 264–275. DOI: 10.1016/j.solener.2017.02.043.

209. D. Assouline, N. Mohajeri and J.-L. Scartezzini. "Large-scale rooftop solar photovoltaic technical potential estimation using Random Forests". In: *Applied Energy* **217** (2018), pp. 189–211. DOI: 10.1016/j.apenergy.2018.02.118.

210. A. Molin, S. Schneider, P. Rohdin and B. Moshfegh. "Assessing a regional building applied PV potential – Spatial and dynamic analysis of supply and load matching". In: *Renewable Energy* **91** (2016), pp. 261–274. DOI: 10.1016/j.renene.2016.01.084.

211. P. Wegertseder, P. Lund, J. Mikkola and R. G. Alvarado. "Combining solar resource mapping and energy system integration methods for realistic valuation of urban solar energy potential". In: *Solar Energy* **135** (2016), pp. 325–336. DOI: 10.1016/j.solener.2016.05.061.

212. L. Bottaccioli, A. Estebsari, E. Patti, E. Pons and A. Acquaviva. "A Novel Integrated Real-time Simulation Platform for Assessing Photovoltaic Penetration Impacts in Smart Grids". In: *Energy Procedia* **111** (2017), pp. 780–789. DOI: 10.1016/j.egypro.2017.03.240.

213. L. R. Camargo, R. Zink, W. Dorner and G. Stoeglehner. "Spatio-temporal modeling of rooftop photovoltaic panels for improved technical potential assessment and electricity peak load offsetting at the municipal scale". In: *Computers, Environment and Urban Systems* **52** (2015), pp. 58–69. DOI: 10.1016/j.compenvurbsys.2015.03.002.

214. Y. Mu, J. Wu, N. Jenkins, H. Jia and C. Wang. "A Spatial–Temporal model for grid impact analysis of plug-in electric vehicles". In: *Applied Energy* **114** (2014), pp. 456–465. DOI: 10.1016/j.apenergy.2013.10.006.

215. Y. Yamagata and H. Seya. "Community-based resilient electricity sharing: Optimal spatial clustering". In: *2013 43rd Annual IEEE/IFIP Conference on Dependable Systems and Networks Workshop (DSN-W)*. IEEE, 2013. DOI: 10.1109/dsnw.2013.6615539.

216. Environmental Systems Research Institute (Esri). *ArcGIS Spatial Analyst*. 2017. <http://desktop.arcgis.com/en/arcmap/10.3/tools/spatial-analyst-toolbox/area-solar-radiation.htm>.

217. P. M. Rich, D. R., H. W. A. and S. S. C. "Using Viewshed Models to Calculate Intercepted Solar Radiation: Applications in Ecology". In: *American Society for Photogrammetry and Remote Sensing Technical Papers* **66** (1994), pp. 524–529.

218. P. Fu and P. M. Rich. "A geometric solar radiation model with applications in agriculture and forestry". In: *Computers and Electronics in Agriculture* **37**.1-3 (2002), pp. 25–35. DOI: 10.1016/s0168-1699(02)00115-1.

219. Het kadaster. *Basisregistraties Adressen en Gebouwen (BAG)*. 2016. <https://www.kadaster.nl/bag>.

220. Actueel Hoogte Bestand Nederland. *Wijk- en buurtkaart 2016*. 2016. <http://www.ahn.nl/index.html>.

221. Centraal Bureau voor de Statistiek. *Wijk- en buurtkaart 2016*. 2016. <https://www.cbs.nl/nl-nl/dossier/nederland-regionaal/geografische\%20data/wijk-en-buurtkaart-2016>.

222. Stedin Holding N.V. *Stedin Verbruiksgegevens*. 2016. <https://www.stedin.net/zakelijk/open-data/verbruiksgegevens>.

223. Centraal Bureau voor de Statistiek. *Verkeersprestaties personenauto's, leeftijd uitgebreid, brandstof*. 2016. <http://statline.cbs.nl/StatWeb/publication/?VW=T\&DM=\&PA=83702NED\&D1=a\&D2=0\&D3=a\&D4=a\&HD=171009-0949\&HDR=T,G3\&STB=G1,G2>.

224. J. Munkhammar, J. D. K. Bishop, J. J. Sarralde, W. Tian and R. Choudhary. "Household electricity use, electric vehicle home-charging and distributed photovoltaic power production in the city of Westminster". In: *Energy and Buildings* **86** (2015), pp. 439–448. DOI: 10.1016/j.enbuild.2014.10.006.

225. Sociaal-Economische Raad. *The Agreement on Energy for Sustainable Growth*. Tech. rep. Sociaal-Economische Raad (Social and Economic Council), 2015. <{https://www.energieakkoordser.nl/\textasciitilde{}/media/files/energieakkoord/publiciteit/agreement-on-energy-policy-in-practice.ashx}>.

226. C. Catita, P. Redweik, J. Pereira and M. C. Brito. "Extending solar potential analysis in buildings to vertical facades". In: *Computers & Geosciences* **66** (2014), pp. 1–12. DOI: 10.1016/j.cageo.2014.01.002.

227. K. Sinapis, C. Tzikas, G. Litjens, M. van den Donker, W. Folkerts, W. G. J. H. M. van Sark and A. Smets. "A comprehensive study on partial shading response of c-Si modules and yield modeling of string inverter and module level power electronics". In: *Solar Energy* **135** (2016), pp. 731–741. DOI: 10.1016/j.solener.2016.06.050.

228. L. Beurskens and J. Lemmens. *Advies SDE+ Zon-PV najaar 2018*. Tech. rep. 2018, pp. 1–15. <https://www.rvo.nl/sites/default/files/2018/07/Notitie_advies_najaar-sde-plus-2018-zon-PV.pdf>.

Acknowledgement / Dankwoord

In the last four years, I spend a lot of time on research and creating this dissertation. I would like to thank everyone who supported and helped me in these past years. Speciale dank aan vrienden en familie die naast mijn promotie mij hebben geholpen om het werk even los te laten en met een frisse blik weer op te pakken.

Zonder mijn promotoren had ik nooit kunnen promoveren. Wilfried, dank voor je dagelijkse begeleiding en alles wat daarbij hoort. Ondanks dat je altijd druk was, kon ik altijd binnenlopen voor goede raad. Je adviezen waren kort, maar zeker krachtig! Ernst, jij gaf mij de mogelijkheid om mijn promotie te doen binnen het NWO project "Transitioning to a More Sustainable Energy System", waarvoor veel dank. Jouw geruststelling rondom de drukke afrondingsfase van mijn promotie waardeer ik enorm.

Big thanks to all colleagues of Team PV. Boudewijn P, als oud studiegenoot en eerste kamergenoot maakte jij mij wegwijs op de universiteit. Bhavya, I really enjoyed working with you together on our paper, and also the humorous moments when we were room buddies. Atse, dank voor de altijd open vraagbaak die je was en voor de latex code om mijn proefschrift te maken. Boudewijn E, bedankt voor het toevoegen van extra wiskundige achtergrond en uitleg. Ik vond het een grote eer om een van je paranimfen te zijn! Anne, je had altijd goede ideeën en inzichten om data in figuren beter te visualiseren. Wouter, samen aan hetzelfde onderwerp werken heeft mij zeer geïnspireerd. Als geen ander was jij de sparringpartner tijdens mijn promotie! Marte, fijn hoe jij openstaat en altijd bereid was om even te helpen met de tekst, vooral in de drukke laatste maanden. Mart, Odysseas, Panos, Ioannis, Tarek, Sara, Nick, Eelke, and Lennard, thanks for all the help, from python questions to feedback on presentations!

Thanks to all other colleagues. Aisha, veel dank voor alle ondersteuning en hulp, vooral in het laatste half jaar van mijn onderzoek. Siham en Fiona, dank voor jullie assistentie. Maurits, dank voor je support met de rekenserver. I really enjoyed the nice non-scientific conversions with the lunchgroup. Also the coffee breaks or the brief stops in the corridors made my time at the UU very pleasant. Marnix, Marc, Anna, Lotte, Sierk, Will, Ric, Martin, Vincent, Gert Jan J, Machteld, Anne-Sjoerd, Niels, Carina, Cathelijne, Gijs, Ana, Anand, Hu Jing, Vinzenz, Steven, Blanca, Pita, Floor, Evert, Jesús, and many others, thanks for making the university a great place to work!

I also would like to thank people outside the university who assisted me with the research. My former colleagues at SEAC: Corry, Menno, Kostas, Roland, Wiep, Guus, Chris and Burkhard. Thanks for inspiring me to pursue a PhD and helping me writing my PhD proposal. Daphne, dank voor het regelen van data vanuit Enexis en het organiseren van onderzoeksessies met andere PhDers. Tim, jouw masterthesis en het artikel dat daarop volgde kon ik goed gebruiken als basis voor een van mijn artikelen, waarvoor dank.

Jeroen, de tijd bij Fraunhofer ISE met jou was een van de belangrijkste inspiratiebronnen om een PhD te gaan doen. Ook je enthousiasme rond zonne-energie is voor mij altijd een vooraanstaande reden geweest om in deze richting onderzoek te doen. Hubert, dank voor het geven van data en voor je vernieuwende blik die je hebt op de energiemarkt. Friso, als iedereen zo gedreven was als jij dat bent, waren we nu al klaar met de energietransitie. Roel, jouw non-stop babbel zorgde voor leuke discussies en waren een goede positieve afleiding. Ook Remco, Esther, Nina, Kendall, Luuk en Ruud dank voor jullie enthousiasme om de wereld te verbeteren. Veerle en Gijs, dank voor jullie gezelligheid, levensdiscussies en open kijk op de wereld. Hamza, I really enjoyed our philosophical talks about life and society. Judith, bedankt voor de leuke gesprekken over reizen en leven in het buitenland. Myrthe, dank voor de goede diepgaande conversaties over het leven en de leuke feestjes door de jaren heen. Nynke en Max, thanks for brainstorming with me about a perfect thesis title and other random checks. I hope to be the number one someday in our never ending cow trade game. Stephanie, dank voor de leuke tijd in Overvecht en het positivisme dat je altijd uitstraalt. Erik, door de jaren heen zijn we echt volwassen geworden, maar de chill factor blijft altijd. Edwin, onze tijd in Finland heeft mijn persoonlijkheid doen groeien. Thijs, Arthur en Jasper, jullie stonden altijd klaar voor leuke borrels en andere uitjes. Ook Sabine, Kathi, Ida, Annemieke, Thao, Tamara, Vivian, Linette, Niels, Arie, Maaik, Rosanne, Jelte, Aranka, Agatha, Rob, Lisa, Soufiane, en alle anderen, dank voor de leuke en relaxte tijden.

Sander, dank voor het ontwerpen van mijn cover en de ontelbare kookkunsten en etentjes die mij steeds opnieuw verrassen. Je was altijd wel te porren voor een heerlijke koffie of gewoon doelloos de dag doorbrengen. Dank ook voor het opnemen van het paranimfschap. Koos, dat jij ging promoveren was voor mij een reden om het ook te doen. Door tegelijk te promoveren kon ik bij jou altijd terecht voor de ups en down tijdens het promotietraject. Ik vond het een eer om paranimf te zijn bij jou, en ben blij dat jij dat ook wilt zijn bij mij.

Joni en Wilbert, op de boerderij tussen de koeien werken is voor mij altijd een moment om er helemaal tussenuit te zijn. Ik hoop er nog vele jaren rond te kunnen lopen en te genieten van de natuur. Marlies, dank voor alles, speciaal voor de leuke politieke discussies en de ontspannende tijden in Puiflijk. Papa en mama, dank voor alle steun in de afgelopen jaren, in welke vorm dan ook. Het ondernemerschap wat ik van jullie heb meegekregen heeft uiteindelijk gezorgd voor dit proefschrift.

Helen, allereerst, dankjewel voor het nakijken van al mijn artikelen. Ondanks de complexe materie heb je het toch duidelijker gemaakt. Dank voor het monitoren en mede bepalen van mijn werk privé balans. Ook je relativerende vermogen heeft mijn motivatie zeer geholpen om een proefschrift te maken binnen 4 jaar. Ik heb grote bewondering voor de manier waarop jij in het leven staat. Er zijn nog veel dingen die ik hier kan opnoemen, maar jouw bijdrage aan mijn proefschrift is van onschatbare waarde. Ik ben je enorm dankbaar en kijk uit naar een toekomst met jou samen.

About the Author

Geert Litjens was born on June 15th 1987 in Druten, the Netherlands. He studied Operational Technology with a specialization in energy technology at the University of Applied Sciences Utrecht. After receiving his Bachelor of Engineering, he started his Master in Energy Science at Utrecht University in 2011. He graduated on a research project at Fraunhofer ISE investigating the influence of spectral effects on PV performance in 2013. After he obtained his MSc degree, Geert started working at the Solar Energy Application Centre on performance modelling, assessment and optimization of Building Integrated PV applications. He joined the Energy & Resources Group of the Copernicus Institute of Sustainable Development of Utrecht University as a PhD candidate in 2014. There he worked on the NWO project "Transitioning to a More Sustainable Energy System". His research focused on the technical, economic and environmental benefits from using solar PV power in buildings. This resulted in five peer-reviewed publications and one conference publication. Geert won two poster awards and gave five oral conference presentations in the United States, Germany and The Netherlands.

Journal publications

- G.B.M.A. Litjens, B.B. Kausika, E. Worrell and W.G.J.H.M. van Sark. "A spatio-temporal city-scale assessment of residential photovoltaic power integration scenarios". in: *Solar Energy* **174** (2018), pp. 1185-1197. DOI:10.1016/j.solener.2018.09.055
- G.B.M.A. Litjens, E. Worrell and W.G.J.H.M. van Sark. "Lowering greenhouse gas emissions in the built environment by combining ground source heat pumps, photovoltaics and battery storage". in: *Energy and Buildings* **180** (2018), pp. 51-71. DOI:10.1016/j.enbuild.2018.09.026
- G.B.M.A. Litjens, E. Worrell and W.G.J.H.M. van Sark. "Economic benefits of combining self-consumption enhancement with frequency restoration reserves provision by photovoltaic-battery systems". in: *Applied Energy* **223** (2018), pp. 172-187. DOI:10.1016/j.apenergy.2018.04.018
- G.B.M.A. Litjens, E. Worrell and W.G.J.H.M. van Sark. "Assessment of forecasting methods on performance of photovoltaic-battery systems". in: *Applied Energy* **211** (2018), pp. 358-373. DOI: 10.1016/j.apenergy.2018.03.154
- G.B.M.A. Litjens, E. Worrell and W.G.J.H.M. van Sark. "Influence of demand patterns on the optimal orientation of photovoltaic systems". in: *Solar Energy* **155** (2017), pp. 1002-1014. DOI:10.1016/j.solener.2017.07.006

- T.W. Hoogvliet, G.B.M.A. Litjens and W.G.J.H.M. van Sark. "Provision of regulating- and reserve power by electric vehicle owners in the Dutch market". in: *Applied Energy* **190** (2017), pp. 1008-1019. DOI:10.1016/j.apenergy.2017.01.006
- K. Sinapis, C. Tzikas, G. Litjens, M. van den Donker, W. Folkerts, W. G. J. H. M. van Sark and A. Smets. "A comprehensive study on partial shading response of c-Si modules and yield modeling of string inverter and module level power electronics". in: *Solar Energy* **155** (2016), pp. 731-741. DOI:10.1016/j.solener.2016.06.050
- K. Sinapis, G. Litjens, M. van den Donker, W. Folkerts and W. van Sark. "Outdoor characterization and comparison of string and MLPE under clear and partially shaded conditions". in: *Energy Science & Engineering* **3** (2015), pp. 510-519. DOI:10.1002/ese3.97

Conference publications

- T. AlSkaif, W. Schram, G. Litjens and W. van Sark. "Smart charging of community storage units using Markov chains". In: *2017 IEEE PES Innovative Smart Grid Technologies Conference Europe (ISGT-Europe)* (2017), pp. 1-6. DOI:10.1109/isgteurope.2017.8260177
- G. Litjens, W. van Sark and E. Worrell. "On the influence of electricity demand patterns, battery storage and PV system design on PV self-consumption and grid interaction". In: *2016 IEEE 43rd Photovoltaic Specialists Conference (PVSC)* (2016), pp. 2021-2024. DOI:10.1109/pvsc.2016.7749983
- K. Sinapis, T.T.H. Rooijakkers, C. Tzikas, G.B.M.A. Litjens, M.N. van den Donker, W. Folkerts and W.G.J.H.M. van Sark. "Annual Yield Comparison of Module Level Power Electronics and String Level PV Systems with Standard and Advanced Module Design". In: *32nd European Photovoltaic Solar Energy Conference and Exhibition* (2016), pp. 2011-2015. DOI:10.4229/eupvsec20162016-5bv.2.49
- K. Sinapis, C. Tzikas, G.B.M.A. Litjens, M.N. van den Donker, W. Folkerts, W.G.J.H.M. van Sark and A. Smets."Yield modelling for micro inverter, power optimizer and string inverter under clear and partially shading shaded conditions". In: *31st European Photovoltaic Solar Energy Conference and Exhibition* (2015), pp. 1587-1591. DOI:10.4229/eupvsec20152015-5ao.8.4
- M.N. van den Donker,B. Hauck, R. Valckenborg, K. Sinapis, G.B.M.A. Litjens, W. Folkerts,R. Borro and W. Passlack."High Throughput Roof Renovation Using Prefabbed and Prewired Watertight PV Insulation Elements ". In: *29th European Photovoltaic Solar Energy Conference and Exhibition* (2014), pp. 3545-3548. DOI:10.4229/eupvsec20142014-6do.5.1
- K. Sinapis, G.B.M.A. Litjens, M.N. van den Donker and W. Folkerts."Outdoor Characterization of Three PV Architectures under Clear and Shaded Conditions". In: *29th European Photovoltaic Solar Energy Conference and Exhibition* (2014), pp. 2249-2254. DOI:10.4229/eupvsec20142014-5ao.9.6
- K. Sinapis, M.N. van den Donker, G.B.M.A. Litjens, P.P. Michiels, E.J.M.G. Philipse, A. van Hese and W. Folkerts."The Glass-Glass Aesthetic Energy Roof: Thermal Behavior for Various Ventilation Levels". In: *28th European Photovoltaic Solar Energy Conference and Exhibition* (2013), pp 4351-4356. DOI: 10.4229/28theupvsec2013-5cv.7.5